



University
of Glasgow

McGonigal, Rhona (2009) *Anti-GD1a antibody targeted disruption of the node of Ranvier in a mouse model of acute motor axonal neuropathy*.
PhD thesis.

<http://theses.gla.ac.uk/1453/>

Copyright and moral rights for this thesis are retained by the author

A copy can be downloaded for personal non-commercial research or study, without prior permission or charge

This thesis cannot be reproduced or quoted extensively from without first obtaining permission in writing from the Author

The content must not be changed in any way or sold commercially in any format or medium without the formal permission of the Author

When referring to this work, full bibliographic details including the author, title, awarding institution and date of the thesis must be given

Anti-GD1a antibody targeted disruption of the node of Ranvier in a mouse model of acute motor axonal neuropathy

Rhona McGonigal MSci (Hons)

A thesis submitted in fulfilment of the requirements of the University of Glasgow for the degree of Doctor of Philosophy

Division of Clinical Neuroscience
University of Glasgow
October 2009

Abstract

Guillain-Barré syndrome (GBS) is a peripheral neuropathy characterised by acute flaccid paralysis. The axonal variant is associated with anti-GD1a ganglioside antibody-dependent, complement-mediated injury to the peripheral axon with conduction block. The blood-nerve barrier (BNB) relatively protects axons from factors in the extra-neural environment; however, it does not extend over the neuromuscular junction, leaving this terminal portion of the axon unprotected. It is here that susceptibility to antibody attack in a mouse model of GBS has previously been demonstrated. It was the aim of this thesis to determine to what extent more proximal portions of the distal axon are at risk from circulating antibody and what exogenous protection can be provided therapeutically.

GD1a is expressed at the nodes of Ranvier (NoR) of intramuscular axons. To investigate the injury caused by anti-GD1a antibodies in relation to BNB permeability, anti-GD1a antibodies were applied to mice genetically engineered both to over-express GD1a and to express cyan fluorescent protein (CFP) in the cytoplasm of axons. Endogenous fluorescence allowed identification of intramuscular nerve bundles and their terminal branches, which were categorized depending on bundle size. Within these categories, IgG and the final product of the complement pathway (membrane attack complex, MAC) deposition were quantified after an acute injury, alongside the deleterious effects on NoR protein's. Nerve conduction studies were also performed to better elucidate the pathological pathway.

IgG and MAC were localized in a gradient-dependent manner, with significantly more deposition at NoR as the bundles progressively branch to a single terminating fibre. Furthermore, MAC deposition was associated with the loss or disruption to immunostaining for nodal protein's including voltage gated sodium channel and ankyrin G. This is indicative of targeted injury to this region of the distal axon in an acute model. The loss of nodal protein staining is associated with the activation of complement and the Ca²⁺-dependent protease calpain as determined by the protection of staining by the complement inhibitor Eculizumab and the calpain inhibitor AK295. A similar disruption to nodal protein staining is also shown at the proximal NoR of the desheathed phrenic nerve.

Extracellular nerve recordings demonstrate a detrimental effect on function as there is a decrease in the peak of the compound nerve action potential over time, which can be associated with Nav channel staining loss.

This study is suggestive of a resilient proximal barrier that becomes more permeable towards the nerve terminal. Therefore, it is not only the axon at the terminal that can be a target of injury, but also the distal axons at their nodes of Ranvier, resulting in disruption at this site. Prevention of staining loss by Eculizumab and AK295 exemplify the route of injury and identify a potential point of therapeutic intervention in human disease.

I dedicate this thesis to my mum- a true inspiration.

Acknowledgements

It would not be possible to make it through a PhD without the help of many people, and I am grateful to each and every one of them.

First and foremost, thanks is due to all of the wonderful people in the Willison lab group both past and present who have assisted me through this scientific adventure. Initially, I would like to thank Prof Hugh Willison for his approachability and his guidance through all of the highs and lows. I am honoured to be the first in the group to be given the task of travelling up the nerve to the node of Ranvier and I hope my investigations have proven successful enough that you don't want to retreat to the terminal! Next I would like to acknowledge Peter Humphrey's and Dr Sue Halstead for setting me off on the right path with their advice and encouragement and arming me with the required technical skills. Great times were had in office B333 of the GBRC with my fellow colleagues, whom I now consider friends, Drs Kay Greenshields, Kate Townson, Katie Brennan and Simon Rinaldi. At some point or another you all encouraged, motivated, and made me smile and I couldn't have asked for a better bunch to be in a tiny office with!

Dr Eddie Rowan at Strathclyde University is due thanks for the many days spent trying to progress my dissecting technique from an anatomist's to that of an electrophysiologist. Also, many others played a crucial role to the completion of my thesis even if it involved only a phonecall or the loan of an antibody- Dr Julia Edgar, Dr Mark McLaughlin, Robert Kerr, Jennifer Barrie, Prof Peter Brophy and Dr Diane Sherman.

And finally, special thanks to the three most important people in my life. To my sister Lindsey, I cannot thank you enough for all of the occasions you have patiently listened to my science chat without even a hint of your eyes glazing over. And let's not forget all of the presentation practice you had to endure- you gave me confidence to do what I do. Andy- thank you for bearing with me through all of the ups and downs that are part and parcel of a PhD. I am eternally grateful for your absolute faith in my abilities even though you do not know the first thing about science! I hope I can offer the same kind of support to you in years to come. And finally to my mum whom I dedicate this thesis. Quite simply I would not be where I am today if it was not for your endless words of encouragement, support and love.

Declaration of authorship

All experiments are the work of the author unless specifically stated otherwise.

Rhona McGonigal, MSci (Hons)

University of Glasgow

October 2009

Contents

Abstract.....	ii
Dedication.....	iii
Acknowledgements.....	iv
Declaration of authorship.....	v
Contents.....	vi
List of figures.....	xii
List of tables.....	xiii
Abbreviations.....	xiv
1 Introduction	1
1.1 Guillain-Barré syndrome	1
1.1.1 Characterization and diagnosis.....	1
1.1.2 GBS subtypes	2
1.1.2.1 Acute inflammatory demyelinating polyradiculoneuropathy (AIDP)	2
1.1.2.2 Miller Fisher syndrome (MFS)	2
1.1.2.3 Acute motor axonal neuropathy.....	4
1.1.2.4 Acute motor and sensory neuropathy (AMSAN)	5
1.1.3 Associated infections	5
1.1.4 Molecular mimicry.....	6
1.2 Gangliosides	7
1.2.1 Biosynthesis and nomenclature	7
1.2.2 Localisation.....	8
1.2.3 Ganglioside function and animal models	12
1.3 Blood-nerve barrier.....	13
1.3.1 Structural protection of the nerve	14
1.3.2 Vasculature.....	14
1.3.3 Permeability.....	15
1.3.4 Importance to GBS	17
1.4 Myelinated axons and the node of Ranvier	17
1.4.1 The axon	18
1.4.2 The myelin sheath.....	18
1.4.3 Node of Ranvier.....	19
1.4.3.1 Nodal gap.....	20
1.4.3.2 Paranode	22
1.4.3.3 Juxtaparanode.....	23
1.4.4 Nodal Proteins	24
1.4.4.1 Voltage-gated sodium channel.....	24

1.4.4.2	The cytoskeletal protein ankyrin G	29
1.4.4.3	Cell adhesion molecules Neurofascin and NrCAM.....	32
1.4.4.4	Paranodal proteins Caspr and contactin	34
1.4.4.5	Juxtaparanodal proteins Kv1.1, Caspr 2 and Tag 1.....	37
1.4.5	Clustering at the NoR	38
1.4.5.1	Modelling of the nodal gap proteins	39
1.4.5.2	Formation of the axo-glial junction.....	43
1.4.5.3	Juxtaparanodal development	44
1.4.5.4	Importance of correct nodal protein localisation.....	46
1.4.6	Nodal Pathology associated with GBS	46
1.4.6.1	Electrophysiological studies using anti-ganglioside antibodies	47
1.4.6.2	Disruption to nodal proteins in response to anti-ganglioside antibodies.....	48
1.5	Animal models of AMAN.....	49
1.5.1	Rabbit models of AMAN.....	49
1.5.2	Mouse model of AMAN	50
1.5.2.1	Use of ganglioside transgenic mice in a murine GBS model....	50
1.5.3	Transgenic mice expressing fluorescent proteins	52
1.6	Complement and GBS	54
1.6.1	Complement cascade	54
1.6.1.1	Complement components.....	55
1.6.1.2	Membrane attack complex	55
1.6.1.3	Role of complement	57
1.6.2	Complement inhibitors	58
1.6.2.1	Endogenous complement inhibitors.....	58
1.6.2.2	Synthetic complement inhibitors in animal models	59
1.7	Calpain.....	60
1.7.1	Structure and activity of calpain	60
1.7.2	Axonal proteins as calpain substrates.....	61
1.7.3	Calpain inhibitors.....	62
1.8	Aims.....	63
2	Materials and Methods.....	64
2.1	Reagents & Buffers	64
2.1.1	Reagents	64
2.1.1.1	Antibodies.....	64
2.1.1.2	Labelling reagents	64
2.1.1.3	Toxins.....	66
2.1.1.4	Miscellaneous reagents.....	66
2.1.2	Buffers	67
2.2	Animals	68
2.2.1	Transgenic mice	68
2.2.2	Genotyping	68
2.2.3	Ultrastructure.....	69
2.3	Antibody production.....	70
2.3.1	Anti-GD1a antibody cell-lines	70

2.3.2	Antibody purification	71
2.3.3	Enzyme-linked immunosorbent assay (ELISA).....	72
2.4	Muscle and nerve preparations	72
2.4.1	Triangularis sterni ex vivo preparation	72
2.4.2	Phrenic, sciatic and sural nerve	74
2.4.3	Muscle sectioning.....	74
2.5	Permeability studies.....	75
2.5.1	GD1a localisation and binding-gradient.....	75
2.5.2	Ubiquitous GD1a expression	76
2.5.3	Sheath permeability	77
2.5.4	Specific GD1a localisation at NoR	77
2.6	Complement mediated injury to NoR.....	77
2.6.1	Ex vivo complement deposition	77
2.6.2	Complement mediated effect on neurofilament and CFP	78
2.6.3	Complement-mediated effect on nodal proteins/ion channels.....	79
2.6.4	α -latrotoxin effect on nodal proteins	79
2.7	Route of injury	80
2.7.1	Use of calcium indicators in PC12 cells.....	80
2.7.2	Protection by complement and calpain inhibition	81
2.7.3	Ultrastructure.....	82
2.7.3.1	Ultrastructural comparison of transgenic mice NoR to <i>wild-type</i>	82
2.7.3.2	Ultrastructural study of experimental tissue.....	83
2.8	Fate of nodal proteins	83
2.8.1	Electrophysiology.....	83
2.8.2	Tetrodotoxin labelling	86
2.8.3	Nav Western blots	87
3	Permeability of peripheral nerve to circulating antibody	89
3.1	Introduction.....	89
3.2	Results	91
3.2.1	Mouse strain dependent GD1a localisation.....	91
3.2.1.1	Wild type versus GD3/CFP: MOG35 binding.....	91
3.2.1.2	GD1a localisation	91
3.2.1.3	Nodal sub-region localisation of GD1a.....	94
3.2.2	BNB permeability.....	95
3.2.2.1	<i>Ex vivo</i> gradient dependent binding of MOG35.....	95
3.2.2.2	<i>In vivo</i> gradient dependent binding of MOG35	97
3.2.2.3	Uniform GD1a expression.....	97
3.3	Discussion	98
4	Characterisation of antibody-mediated axonal injury.....	101
4.1	Introduction.....	101

4.2	Results	102
4.2.1	Injury to the distal axon.....	102
4.2.1.1	Neurofilament loss.....	102
4.2.1.2	Real-time loss of CFP in distal axon	103
4.2.1.3	Comparison of α -latrotoxin induced loss of CFP compared to antibody-mediated injury	105
4.2.2	Complement deposition at NoR	105
4.2.3	Nodal protein disruption	108
4.2.3.1	Nodal gap.....	109
4.2.3.2	Paranode	112
4.2.3.3	Juxtaparanode.....	115
4.2.3.4	Targeted nodal disruption	116
4.2.3.5	Phrenic nerve protein disruption	116
4.3	Discussion	120
5	Complement and calpain mediated injury to distal axons.....	125
5.1	Introduction.....	125
5.2	Results	126
5.2.1	Calcium influx due to MAC deposition	126
5.2.2	Complement inhibition protects ex vivo preparations	129
5.2.2.1	CFP	129
5.2.2.2	Nav1.6	131
5.2.2.3	Ankyrin G.....	132
5.2.2.4	Caspr	132
5.2.2.5	Antibody and MAC.....	132
5.2.3	Calpain inhibition protects ex vivo preparations.....	134
5.2.3.1	Calpeptin	134
5.2.3.2	Protective effects of AK295	136
5.2.3.3	MAC and neurofilament	136
5.2.3.4	Nav1.6	137
5.2.3.5	Ankyrin G.....	140
5.2.3.6	Caspr	140
5.2.4	AK295 protection in Phrenic nerve	143
5.3	Discussion	144
6	Fate of the sodium channel at NoR after injury	148
6.1	Introduction.....	148
6.2	Results	149
6.2.1	Effect of injury to binding of alternative Nav antibody.....	149
6.2.2	Alteration to Nav channel staining at early time-points	151
6.2.3	Western blotting.....	151
6.2.3.1	Suitability of nerve	152
6.2.3.2	Fodrin/all spectrin as a marker of calpain activity	153
6.2.3.3	Nav channel immunoblots	153
6.2.4	Extracellular nerve recordings	154
6.2.4.1	Conduction of the sciatic nerve after 1h NHS incubation	154
6.2.4.2	Conduction of the sciatic nerve after 3h NHS incubation	155

6.2.4.3	Differential IgG deposition and injury at sensory and motor nerves.....	157
6.2.4.4	Effect of pathology on phrenic nerve versus sural nerve conduction.....	161
6.2.4.5	Tetrodotoxin staining	163
6.3	Discussion	164
7	Conclusions	170
7.1	Permeability of peripheral nerve to circulating antibody.....	170
7.2	Characterisation of antibody-mediated axonal injury	171
7.3	Complement and calpain mediated injury to distal axons	174
7.4	Fate of the sodium channel at NoR after injury	177
7.5	Future directions.....	179
	Appendix 1.....	186
	Appendix 2.....	188
	List of abstracts.....	191
	References	192

List of figures

Figure 1.1	Pathology of AIDP	3
Figure 1.2	AMAN patient autopsy tissue	4
Figure 1.3	Biosynthetic pathway of gangliosides	9
Figure 1.4	GM1 and GD1a at the NoR	11
Figure 1.5	Structure of the nerve barrier	15
Figure 1.6	Axons and subdomains	21
Figure 1.7	Nav channel structure	26
Figure 1.8	Ankyrin G structure and localisation at NoR	31
Figure 1.9	Neurofascin structure and localisation at NoR	33
Figure 1.10	NrCAM structure and localisation at NoR	35
Figure 1.11	Caspr structure and localisation at paranode	36
Figure 1.12	Caspr2 structure and co-localisation with Kv1	37
Figure 1.13	Tag1 structure and localisation at NoR	38
Figure 1.14	Initial formation and clustering at NoR	43
Figure 1.15	Mechanism of clustering at juxtaparanode	45
Figure 1.16	Disruption at NoR in a rabbit model of AMAN	48
Figure 1.17	Ganglioside expression in transgenic mouse strains	53
Figure 1.18	Complement cascade	56
Figure 2.1	WT vs GD3/CFP nodal ultrastructure	70
Figure 2.2	Trangularis sterni muscle schematic	73
Figure 2.3	Electrophysiological recording set-up	84
Figure 3.1	GD1a at NMJ and NoR of WT and GD3/CFP mice	92
Figure 3.2	GD1a localisation in GD3/CFP mouse	93
Figure 3.3	Sub-localisation of GD1a at NoR	94
Figure 3.4	IgG permeability gradient	96
Figure 3.5	IgG deposition at sectioned diaphragm NoR	97
Figure 4.1	Distal axon neurofilament loss in response to injury	103
Figure 4.2	Live-imaging of distal nerve CFP loss	104
Figure 4.3	Distal axon CFP loss in injured and α -LTx treated TS	106
Figure 4.4	MAC deposition at NoR	107
Figure 4.5	Nav1.6 staining at NoR in response to injury	110
Figure 4.6	Ankyrin G staining at NoR in response to injury	111
Figure 4.7	Caspr staining at NoR in response to injury	113
Figure 4.8	Neurofascin staining at NoR in response to injury	114
Figure 4.9	Kv1.1 staining at NoR loss at NoR in response to injury	115
Figure 4.10	α -LTx injury does not lead to loss of Nav1.6 staining	116
Figure 4.11	Staining at phrenic nerve NoR in response to injury	118
Figure 4.12	Reclassification of phrenic nerve nodal staining	119
Figure 5.1	Rhod 2-AM in PC12 cells	127
Figure 5.2	Rhod 2-AM at NMJ	128
Figure 5.3	CFP protection by Eculizumab	130
Figure 5.4	Nav1.6 protection by Eculizumab	131
Figure 5.5	Ankyrin G protection by Eculizumab	133
Figure 5.6	Caspr protection by Eculizumab	134
Figure 5.7	MAC prevention by Eculizumab	135
Figure 5.8	AK295 optimal concentration	136
Figure 5.9	AK295 does not prevent MAC deposition	137

Figure 5.10	AK295 protection of neurofilament	138
Figure 5.11	AK295 protection of Nav1.6	139
Figure 5.12	AK295 protection of ankyrin G	141
Figure 5.13	AK295 protection of Caspr	142
Figure 5.14	AK295 protection of phrenic nerve nodal proteins	143
Figure 6.1	Potential Nav channel calpain cleavage sites	150
Figure 6.2	Stages of Nav1.6 loss	152
Figure 6.3	Nav Western blotting	154
Figure 6.4	Sciatic nerve extracellular recordings	156
Figure 6.5	Comparison of 1h and 3h NHS incubation to SN conduction	158
Figure 6.6	IgG at sural and phrenic nerve NoR	159
Figure 6.7	Nav1.6 staining loss at sural and phrenic nerve NoR	160
Figure 6.8	Sural and phrenic nerve extracellular recordings	162
Figure 6.9	Tetrodotoxin staining at NoR	163
Figure 7.1	Model of nodal injury	185
Figure A1	Perineural recordings	187
Figure A2	<i>In vivo</i> IgG and MAC deposition	189

List of tables

Table 1.1	Transgenic mouse strains	41
Table 2.1	Primary antibody dilutions and source	65

Abbreviations

a.a.	amino acids
AK295	α -keto amide [Z-leu-Abu-(CH ₂) ₃ -4-morpholinyl]
AIDP	acute inflammatory demyelinating polyradiculoneuropathy
AMAN	acute motor axonal neuropathy
AMSAN	acute motor and sensory axonal neuropathy
ANOVA	analysis of variance
APES	3-aminopropyltriethoxysilane
BBB	Blood-brain barrier
BBG	bovine brain gangliosides
BCA	bicinchoninic acid
BNB	Blood-nerve barrier
bp	base pairs
BSA	bovine serum albumin
BTx	bungarotoxin
CAM	cell adhesion molecule
CAP	compound action potential
Caspr	contactin-associated protein
CFP	cyan fluorescent protein
CNS	central nervous system
C-terminal	carboxyl terminal
CTx	cholera toxin
Cy-5	cyanine-5
DAF	decay accelerating factor
dH ₂ O	distilled water
DIC	differential interference contrast
ELISA	enzyme-linked immunosorbent assay
EM	electron microscopy
FCS	Foetal calf serum
FITC	fluorescein isothiocyanate
FNIII	fibronectin type 3
FA	Freunds adjuvant
GalNAcT	GalNAc transferase
GBS	Guillain-Barré syndrome
GD3s	GD3 synthase
GFP	green fluorescent protein
GPI	glycophosphatidylinositol
HRP	horse-radish peroxidase
IHC	Immunohistochemistry
Ig	immunoglobulin
i.p.	intra-peritoneal
kDa	kilodalton
KLH	keyhole limpet hemocyanin
KO	knock-out
Kv	voltage-gated potassium channel
LOS	lipooligosaccharide
LTx	latrotoxin
LM	light microscopy
M	molar
m-calpain	millimolar-calpain
mAb	monoclonal antibody
MAC	membrane attack complex

MAG	myelin-associated glycoprotein
<i>med</i>	motor endplate disease
MFS	Miller Fisher syndrome
MW	molecular weight
Nav	voltage-gated sodium channel
NF	neurofascin
NHS	normal human serum
NMJ	neuromuscular junction
NoR	node of Ranvier
N-terminal	amino terminal
NgCAM	neuron-glia CAM
NrCAM	NgCAM-related CAM
OD	optical density
O/N	overnight
P1	prime position
PBS	phosphate buffered saline
PCR	polymerase chain reaction
PDZ	PSD95, DlgA, zo-1
PFA	paraformaldehyde
PLL	poly-L-lysine
PN	phrenic nerve
PNS	peripheral nervous system
PSD	post-synaptic density protein
PVDF	polyvinylidene fluoride
RNAi	interference RNA
rpm	revolution per minute
RT	room temperature
S1	segment 1
SN	sciatic nerve
SuN	sural nerve
Tag	transient axonal glycoprotein
TRITC	tetramethylrhodamine isothiocyanate
TS	triangularis sterni
TTX	tetrodotoxin
WB	Western blot
WT	wild type
μ-calpain	micromolar-calpain

1 Introduction

1.1 Guillain-Barré syndrome

Guillain-Barré syndrome (GBS) is the name given to a group of disorders that result in peripheral neuropathy and acute flaccid paralysis. Since it was first described in the early 20th century, the clinical symptoms, mechanism of disease process and many other factors have been the source of debate. It was not until 1978 that diagnostic criteria were laid down, and even then these were reassessed for relevance in 1990 (Asbury & Cornblath, 1990). Thus, there is still much to elucidate on the many aspects of GBS, but there has been great progress in the last few decades.

1.1.1 *Characterization and diagnosis*

The standard feature of GBS is a progressive, predominantly ascending, motor weakness of at least two limbs, and areflexia (Asbury & Cornblath 1990). Symptoms can occur over a period of days to weeks, with the peak of illness at 2-4weeks. Recovery will occur over weeks to months and will not always be complete- it is dependent on the extent of the injury in each individual. If respiratory difficulties are encountered, which result in the need for artificial ventilation, a poorer outcome is likely.

A rise in cerebrospinal fluid protein levels and electrophysiological features such as prolonged distal and F-wave latencies, and reduced conduction velocities have also been used to aid diagnosis. Electrophysiology particularly is often used to determine variants of the general syndrome. However, depending on criteria set, a different percentage of patients fall into specific categories (Hadden et al. 1998). Therefore, electrophysiological diagnosis can be supportive, but not conclusive alone. For example, it is useful as a predictor of progression concerning the risk of respiratory failure (Durand et al. 2006).

1.1.2 GBS subtypes

The four most common subtypes of GBS are as follows- acute inflammatory demyelinating polyradiculoneuropathy (AIDP), acute motor axonal neuropathy (AMAN), acute motor and sensory axonal neuropathy (AMSAN) and Miller Fisher syndrome (MFS).

The prevalence of each subtype differs throughout the world. AIDP is the most common variant in Europe and North America while AMAN only makes up about 5% of cases (Hadden et al, 1998). AMAN is much more common in Asia, and there are even known yearly epidemics in some regions (McKhann et al., 1993). The symptoms at onset can be similar for AIDP, AMAN and AMSAN, however the pathophysiology is what sets these subtypes apart. Each subtype is described in more detail below. These subtypes are often characterised serologically by the antibody titres present to gangliosides (described in more detail in section 1.5.2.1).

1.1.2.1 Acute inflammatory demyelinating polyradiculoneuropathy (AIDP)

The pathological changes that occur during disease were first described as inflammatory demyelination of roots and nerves (Asbury 1969). This 'classical' subtype of GBS is known as acute inflammatory demyelinating polyradiculoneuropathy (AIDP) where the Schwann cells undergo an inflammatory autoimmune attack resulting in degradation of the myelin (Asbury 1969). As reviewed by Hughes & Cornblath (2005), the inflammatory attack could be due to macrophage denuding of the myelin sheath or complement fixation and destruction of myelin due to bound antibodies. Secondary 'bystander' damage to axons can occur in severe cases (Figure 1.1).

1.1.2.2 Miller Fisher syndrome (MFS)

More closely related to AIDP, MFS is characterised by ophthalmological abnormalities, ataxia and areflexia (Fisher 1956). It is commonly associated with prior *Campylobacter jejuni* infection and anti-GQ1b antibodies are detected in more than 90% patients. This association of anti-GQ1b antibodies in MFS patients

was first reported by Chiba *et al* (1992), who later went on to show that the oculomotor, trochlear and abducens cranial nerves have a relatively higher concentration of this ganglioside at their paranodal myelin (Chiba et al. 1997), which would explain the specificity of the symptoms. No other subtype has been shown to so closely correlate with particular anti-ganglioside antibodies.

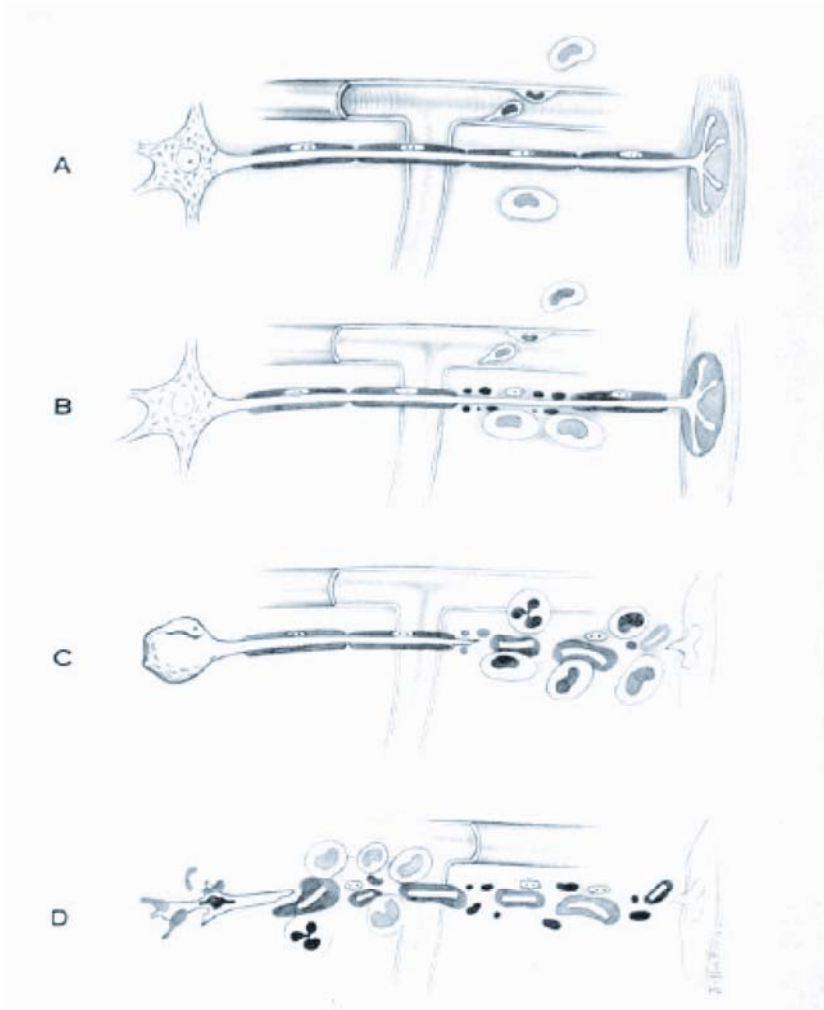


Figure 1.1: Process of segmental demyelination in AIDP.

This diagram, taken from Asbury (1969), shows the sequence of events suspected to occur in AIDP. Initially the myelin undergoes attack (B), which in severe cases can lead to damage and severing of the axon (C,D).

1.1.2.3 Acute motor axonal neuropathy

More recently, in an attempt to develop a method for predicting severity and recovery outcome, another subtype that has a motor axonal neuropathy was discovered (Feasby et al. 1986). This was controversial as GBS was considered to have a pathophysiological mechanism that primarily involved demyelination (Chowdhury & Arora 2001; Triggs et al. 1992). In this subtype, now known as acute motor axonal neuropathy (McKhann et al. 1993), motor nerves are inexcitable and axonal degeneration occurs at spinal roots and peripheral nerves with no demyelination, and little or no inflammation (Feasby et al., 1986). In distal nerve there is a conduction block not found in AIDP (Kuwabara et al. 2002). The myelin sheath remains intact as the pathological process involves binding of antibodies to gangliosides located on the axolemma, resulting in infiltration of macrophages at nodes of Ranvier (NoR) (Griffin et al. 1996a; Hafer-Macko et al. 1996).

The studies by McKhann and colleagues suggest that recovery after AMAN is rapid, but other studies indicate severity associated with this subtype (Yuki et al. 1992). There could be other contributing factors such as preceding infection and the immunogenic history of patients.

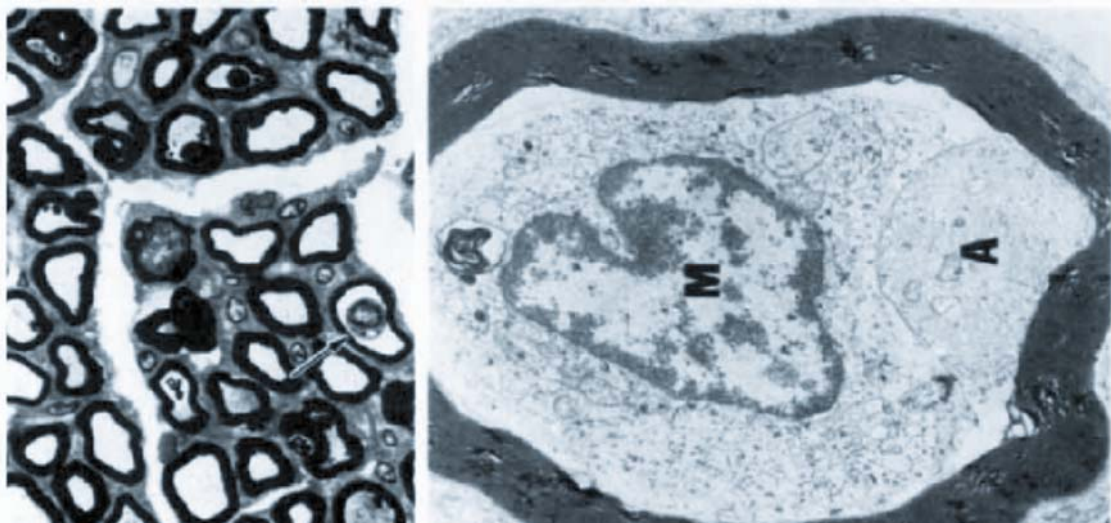


Figure 1.2: AMAN patient autopsy tissue.

Left: A transverse section through the ventral root of an AMAN patient shows Wallerian degeneration of the axons and the unaffected intact myelin sheath. **Right:** A higher power image details the infiltration of a macrophage (M) under the myelin sheath.

1.1.2.4 Acute motor and sensory neuropathy (AMSAN)

This subtype is similar to AMAN, but sensory axons are also affected. It was first proposed by Griffin *et al* (1996a) that AMAN and AMSAN could be part of a spectrum of a subtype where the target epitope is axonal. It would seem that they share a common immunological profile in regard to what anti-ganglioside antibodies are found in patient sera, which differs to those common to AIDP (Yuki *et al*. 1999). It is unclear why the sensory axons are only affected in a proportion of cases.

1.1.3 Associated infections

GBS has been associated with an antecedent infection, common in patients before onset of symptoms, for many decades, but as there is such a wide range of implicated agents, there has been trouble elucidating a specific causative agent. These agents include bacterial infections, viral infections, inoculations, surgery and *Mycoplasma* infections. One particular bacterial infection that has captured the interest of many is that of *Campylobacter jejuni* (*C. jejuni*, first associated with GBS by Rhodes & Tattersfield 1982). The sub-type and severity of GBS linked to *C. jejuni* infection has long been discussed mainly with the hope that this may aid diagnosis or predict outcome.

In a study of North American and European GBS patients by Hadden *et al* (1998), it was found that 60% of AMAN patients had preceding diarrhoeal illness (indicative of some form of bacterial enteritis such as *C. jejuni*, although not directly determined in this study) while only 18% of AIDP patients shared this complaint. McKhann *et al* (1993) found that most of the AMAN cases under investigation in the group of patients in China had elevated levels of antibodies to *C. jejuni*. These cases showed good recovery. In addition, another Chinese group reported that 76% of AMAN patients and 42% AIDP patients had *C. jejuni* infection. These results could be indicative that *C. jejuni* infection is more common in China and in AMAN cases. This is a sensible postulation as summer epidemics in rural children have been associated with *C. jejuni* infection which is more prevalent in this region, plus the fact that AMAN is more common to these regions. However, this does not explain why there are still a large proportion of

AIDP cases with the same prior infection. The fact that the quite different pathophysiologies of two subtypes can be preceded by the same infection suggests that there is not one disease causing mechanism and patients may have differing immune responses.

1.1.4 Molecular mimicry

An interesting finding relating to the involvement of *C.jejuni* in GBS was that a particular serotype (O:19) could be found in many patients. It had already been determined that O:4 serotype showed similarities with GD1a ganglioside (Aspinall et al. 1993). Subsequently it was shown that O:19 also had structures similar to GM1 and GD1a (Aspinall et al., 1994). It has long been documented that anti-ganglioside titres can be increased during disease (Illa et al. 1995; Ilyas et al. 1988), which resulted in the realisation that if molecules on the bacterial coat mimicked self-antigens, an autoimmune response would be mounted. A plethora of molecules can be found on the bacterial coats. Therefore, each strain has molecules that can mimic specific human ganglioside which probably explains the diversity of symptoms to a common preceding *C.jejuni* infection.

When it was recognised that plasmapheresis aided in the recovery of a number of GBS patients (The Guillain-Barre Syndrome Study Group * 1985), it was speculated that antibodies might play a role in pathogenesis. The link between gangliosides and GBS was made after studies showed that some patients with paraproteinemic neuropathies had monoclonal antibodies that reacted with gangliosides of the peripheral nerve (as reviewed by Willison & Yuki 2002). In addition, the injection of GM1 gangliosides to treat stroke or sciatica resulted in some patients developing AMAN (Illa et al., 1995). All of those who developed neuropathy had anti-GM1 antibodies, whereas patients who were similarly injected but did not develop AMAN, had no detectable antibodies against GM1 (Illa et al., 1995).

A study that compared the titres of anti-GM1 and anti-GD1a antibodies in AMAN and AIDP patients of Chinese and American origin found that GM1 could be present in both sub-types, whereas in Chinese patients GD1a was only present in 4% of AIDP cases (Ho et al. 1999). The American group only had two cases of

AMAN out of 38 patients, one of which had anti-GD1a antibodies, so it is difficult to draw any conclusions from such a small number. However, it is interesting that the reason the association between GD1a and GBS may have been overlooked is because AIDP populations are more common in the west, therefore more often studied.

1.2 Gangliosides

Gangliosides, first named by Ernst Klenk in 1942, are glycosphingolipids that contain sialic acids. The various gangliosides and their component parts are depicted in Figure 1.3. These molecules are found on cell membranes (Miller-Podraza et al., 1982) throughout the body but are at particularly high levels in nervous tissue (Ledeen 1978). More specifically gangliosides present in the membrane are often sequestered in lipid rafts containing cholesterol (Sonnino et al. 2007). This localisation accounts for their role in cell adhesion, growth and motility. The most common gangliosides are GM1, GD1a, GD1b and GT1a. Since the 1980's it has been documented that GBS patient sera has had high titres of anti-ganglioside antibodies (Illa et al., 1995; Ilyas et al., 1988). Antibodies against the various glycosphingolipids have been associated with different manifestations of GBS. Therefore, it has become of interest to elucidate their expression profile and to potentially correlate this information with particular disease phenotype.

1.2.1 Biosynthesis and nomenclature

Figure 1.3 illustrates the various gangliosides, their component parts, and the pathways down which they are synthesised. As reviewed by Kolter *et al* (2002), gangliosides are formed at intracellular membranes before transport to the plasma membrane. Lactosylceramide is formed by the addition of a galactose residue, from UDP-galactose, onto glucosylceramide by membrane bound galactosyltransferase I in the Golgi apparatus. Sugars including sialic acids are added in a step-wise pattern to the newly formed chains by substrate specific sialyltransferase enzymes, i.e. GM3 is produced by α -2,3-sialyltransferase and

GD3 by α -2,8-sialyltransferase. These derivatives (GM3 and GD3) form the basis for the production by GalNAc transferase enzymes of the complex ganglioside a- and b-series, respectively. The letter represents the number of sialic acids (a=1, b=2) linked to the inner galactose moiety.

To easily identify gangliosides without writing out the entire structure, a shorthand nomenclature was devised where G stands for ganglioside, the number of sialic acid residues are denoted by M-, D-, T etc (mono-, di-, tri-) and the number characterizes the order of migration in thin-layer chromatography (Svennerholm 1994).

1.2.2 Localisation

To begin with, many researchers used indirect, non-specific methods of showing the localization of gangliosides such as investigation of tissue homogenates and localisation of known ligands. For example, in the human peripheral nerve, a study of ganglioside composition showed that GD1a and GM1 were more enriched in the axonal fractions than the myelin fractions, and the ceramide structure of these gangliosides were different in sensory nerves compared to motor nerves (Ogawa-Goto et al. 1990). A later study showed that motor nerve myelin had a higher concentration of GM1 and GD1a compared to sensory nerves (Ogawa-Goto et al. 1992). This could explain why in AMAN there is only motor involvement, as although the gangliosides are present in sensory nerves, they are at a lower concentration and in a different conformation meaning antibodies may not so easily bind. However, what these studies do not elucidate is if gangliosides are expressed homogeneously or at specific sites. It was realised that this would be invaluable in explaining the variety of phenotypes.

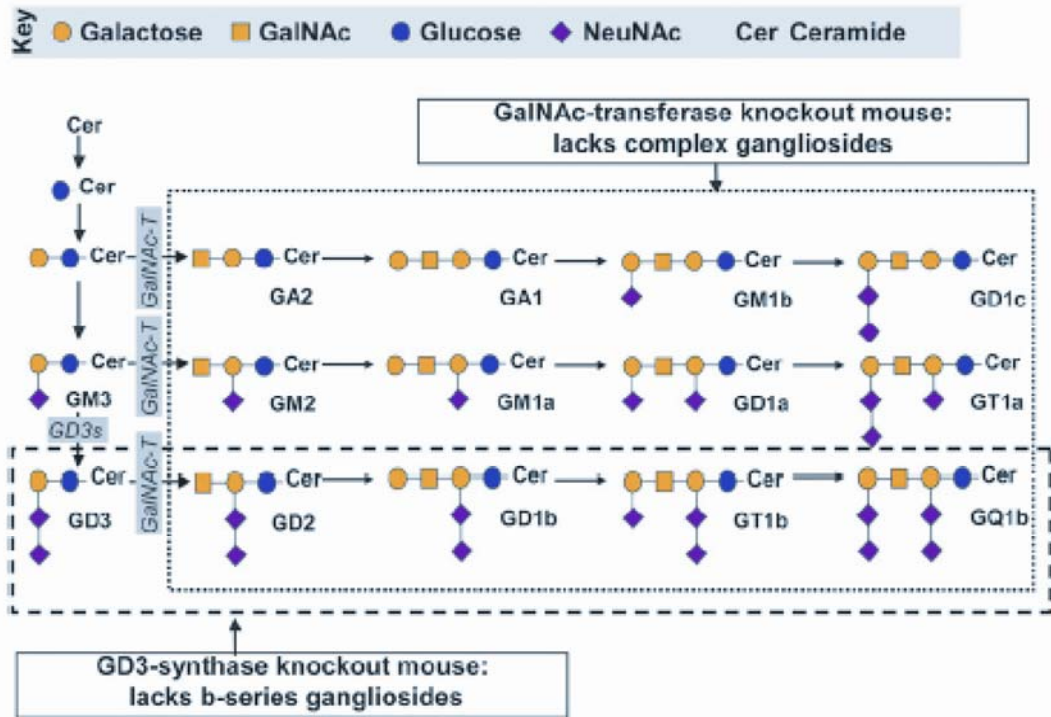


Figure 1.3: Biosynthetic pathway of gangliosides.

Gangliosides are synthesised from a ceramide with an added glucose and galactose group (known as lactosylceramide). α -sialyltransferases add sialic acids, while GalNAc transferases result in the addition of GalNAc. The boxed area represents complex gangliosides of the nervous system which are not expressed in GalNAcT^{-/-} mice, while the area boxed by dashed lines represent the b-series gangliosides which are not expressed in mice where the α -2,8-sialyltransferase enzyme has been knocked out (i.e. GD3s^{-/-}), described in section 1.2.3 in more detail. (Willison et al., 2008)

Cholera toxin (CTx) is known to bind GM1 (Cuatrecasas 1973), and therefore it can be used to localise this ganglioside in tissue. In this way GM1 has been located at the node of Ranvier in sciatic nerves of the mouse Figure 1.4 (Ganser et al., 1983). Focus was often on the GM1 ganglioside as the possible antigen of GBS until Lugaresi *et al* (1997) isolated anti-GD1a antibodies from serum of AMAN patients who had suffered a recent *C. jejuni* infection. GD1a was later identified at nodes of Ranvier in human spinal root motor nerves by co-localization with botulinum toxin B subunit that binds in this region Figure 1.4 (De Angelis et al. 2001). In the rat nerve, tetanus toxin binding was localised to the NoR (Sheikh et al. 1999a) and as GD1a is a known ligand of this toxin (Staub et al. 1986), the inference is that GD1a is expressed here along with GM1. However, aside from the study by Lugaresi *et al* (1997), a preference for motor

nerve binding as observed clinically has not been shown. Using various monoclonal antibodies (mAb) raised against GM1 and GD1a, Gong *et al* (2002) demonstrated that the specificity of binding in the rat peripheral nerve could vary between fibre populations. One anti-GD1a antibody bound preferentially to motor nerve, while others were not as specific and would also bind at NoR in sensory nerve, albeit to a lesser degree than motor nerve. The authors support the possibility that the antibodies are more partial to binding to the motor nerve due to an altered conformation of GD1a at this site, and also suggest a differential susceptibility of particular fibre populations. The same group later confirmed this observation with further experiments involving the manipulation of GD1a moieties and found that ganglioside orientation in the tissue contributed to recognition by antibodies (Lopez *et al.* 2008). Another possible source of variation is the new concept of ganglioside masking and complex formation. Recently, the masking of GM1 epitope by GD1a ganglioside was described to occur in the membrane (Greenshields *et al.* 2009). The interactions of various molecules in the membrane could perhaps account for the differential binding between antibodies as they can be inhibited by certain ganglioside complexes.

As sodium channels have sialic acids, it has also been suggested that anti-ganglioside antibodies would target these molecules, thus representing a mechanism of disruption (Waxman 1995). Consequently, there is a great interest in determining the exact site of gangliosides in the peripheral nerve and if antibodies directed at them could somehow interfere with ion channels and therefore conduction. In a bid to determine the site of action of GM1, a more detailed study was carried out to elucidate the specific site of binding at the nodes of Ranvier (Sheikh *et al.*, 1999a). Electron and light microscopy (EM & LM, respectively) revealed that cholera toxin (and therefore anti-GM1) labelled the axolemma at the node of Ranvier and the paranode in sections, and the paranodal Schwann cell and node of Ranvier in teased sciatic nerve of mice. Interestingly, demyelinated mice showed cholera toxin staining the entire length of the axon, but these sites are presumably masked under physiological circumstances. Attempts to study human tissue are hampered by the difficulty in acquiring reasonably fresh post-mortem tissue, and even then only fatal cases can be studied, which are presumably more severe than most cases.

Immunoglobulin (IgG) deposits have been shown, predominantly at nodes, in tissue from fatal cases of AMAN (Hafer-Macko et al., 1996).

Other methods can be used to investigate anti-ganglioside antibody binding in human instead. Sera from rabbits inoculated with *C.jejuni* has illustrated the possibility of cross-reactivity of anti-ganglioside antibodies, as IgG deposits at NoR were observed on application to normal human nerve (Moran et al., 2005).

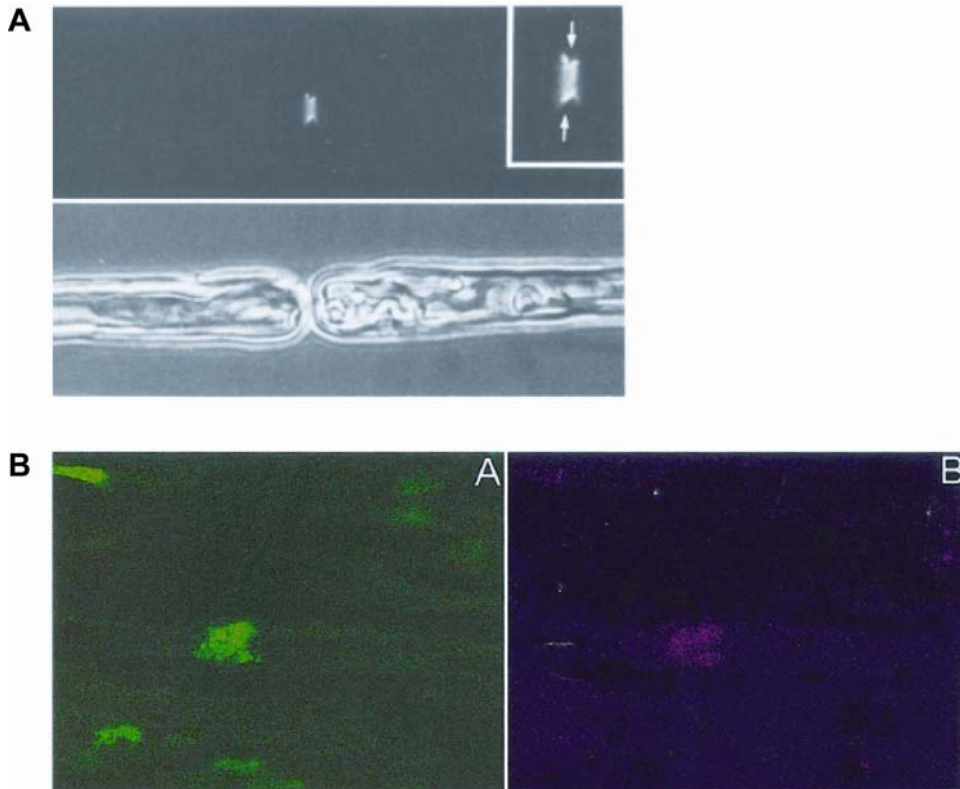


Figure 1.4: Localisation of GM1 and GD1a at the NoR.

A) GM1 is indirectly localised to the nodal gap by cholera toxin staining (arrows)(Ganser et al., 1983). **B)** D'Angelis et al (2001) were the first to demonstrate anti-GD1a antibody binding (A, green) at the NoR of motor root co-localised with botulinum toxin (B, red).

Additionally, AMAN patient sera can be applied to normal tissue to determine ganglioside localization by its binding pattern. In this way, GM1 presence at the nodes of Ranvier has been demonstrated in human (Illa et al., 1995).

1.2.3 Ganglioside function and animal models

The development of transgenic mice where enzymes of ganglioside biosynthesis can be eliminated, has not only progressed the understanding of the function of gangliosides, but also has been convenient for the study of localisation and disease (described later in 1.5.2.1).

It was presumed that gangliosides were involved in the development of the nervous system, therefore Takamiya *et al* (1996) sought to prove this by creating a mouse lacking all complex gangliosides. This was achieved by disrupting the β 1,4-*N*-acetylgalactosaminyltransferase gene and selectively excluding all complex gangliosides beyond GM3 and GD3 to create what is known as the GalNAcT^{-/-} mouse. On investigation of behaviour and nerve morphology this mouse appeared essentially normal (aside from a modest reduction in conduction velocity between the tibial nerve and somatosensory cortex). Therefore it was presumed that complex gangliosides were not crucial for essentially normal development. It is possible that GM3 and GD3 can compensate for the complex gangliosides absence as the levels of the former were elevated. Two more groups developed a GalNAcT^{-/-} mouse strain, but instead studied the nervous system of older mice. The reasoning behind this was to investigate the potential role of complex gangliosides as a ligand of myelin-associated glycoprotein (MAG) considered to mediate axon-glial interactions (Fruttiger *et al.* 1995). In these MAG deficient mice, they too develop normal myelin sheaths, but this becomes disrupted with age resulting in the degeneration of both axon and myelin. Therefore it was the intention of Sheik *et al* (1999b) to determine if aged GalNAcT^{-/-} mice developed a similar phenotype and thus reinforce the possibility that complex gangliosides play an important role in maintaining the axo-glial junction. Their results were markedly different from those obtained in the study of younger GalNAcT^{-/-} mice, instead showing axonal degeneration of the optic and sciatic nerve (Sheikh *et al.* 1999b). This was reinforced by comprehensive neurobehavioural studies demonstrating a variety of progressive behavioural neuropathies (Chiavegatto *et al.* 2000). To confirm that any deficits may be associated with the role of ganglioside as a MAG ligand, the GalNAcT^{-/-} mouse was directly compared to the MAG^{-/-} mouse (Pan *et al.*, 2005). The similarities in central and peripheral nervous system (CNS and PNS, respectively) axon degeneration between these transgenic mice suggest a role for complex

gangliosides and MAG in the stabilisation, post-development, of the axo-glial junction and myelin.

The disruption of the gene encoding the α -2.8-sialyltransferase enzyme that synthesises GD3 (i.e. $GD3s^{-/-}$), was developed to examine the role of b- and c-series gangliosides (Kawai et al. 2001). Not only did these mice develop normally, but they also achieved a normal life span. Where Kawai *et al* presumed a redundancy in ganglioside requirement, Okada *et al* (2002) discovered an impaired regeneration of transected nerve in this transgenic mouse suggesting a role for b-series gangliosides in repair or growth rather than development of the nervous system.

On crossing the two transgenic mice described above to create a mouse only expressing GM3, development to adulthood can still occur, albeit with some defects such as fatal audiogenic seizures. This suggests that to a degree this simple ganglioside can basically replace the function of complex gangliosides. However, more recently Susuki and colleagues (2007a) have shown by EM and immunohistochemistry that the $GalNACT^{-/-}$ mouse does have ultrastructural abnormalities that include the disruption of paranodal loops and nodal proteins such as Caspr and neurofascin (NF), which become progressively worse with time. They also found that $GD3s^{-/-}$ mice did not differ significantly from wild type (WT) in these respects, perhaps representing more specifically a role for a-series gangliosides in axo-glial stability. It must be kept in mind however that this is far from a natural system as this group of gangliosides are highly over-expressed in this particular knock out (KO) mouse.

1.3 Blood-nerve barrier

If the pathology of Guillain-Barré syndrome is mediated by antibodies targeting the axon and myelin sheath, there must be access from the blood to these sites. The blood-nerve barrier (BNB) is a physiological barrier of axons against factors in the external environment. However, it is known that this barrier is not as complete as the blood-brain barrier of the CNS and that there are regions of susceptibility.

1.3.1 Structural protection of the nerve

The nerve is surrounded by a dense outer connective tissue coat known as the epineurium, a layer of flattened cells called the perineurium surrounds each fascicle within the nerve, and each fibre is surrounded by the endoneurium (Figure 1.5), the fine structure of which were investigated in detail with the advent of EM (Burkel 1967).

Starting from the innermost level of protection, the endoneurium, surrounds individual fibres. Within this layer are axons, their associated Schwann cells, and a few capillaries, and it is involved in support of the axon and ultrafiltration (Thomas 1963).

The perineurium surrounds all the axons of one fascicle. It is a sheath formed by concentric layers of flattened cells. The larger the fascicle, the more layers (Thomas & Jones 1967), the number of which decreases closer to the terminal, eventually leaving only one layer, by gradual loss or termination of the innermost sleeves. There are predominantly tight junctions between the perineurial cells, and not generally any connections between the layers. There are no fenestrations and only a small number of pinocytotic vesicles. This sheath acts as a diffusion barrier preventing access of substances to the endoneurium from the surrounding tissue.

1.3.2 Vasculature

There are blood vessels within the fascicles alongside nerve fibres. Schwann cells require nutrients from the blood and this is supplied by the extracellular fluid of the PNS which communicates with these blood vessels. The vessels in the epineurium pierce the perineurium to access the endoneurial vascular network of capillaries. When this happens, the vessel is coated in a sleeve of perineurial cells (as reviewed by Olsson 1990). It is the endothelial cells of these capillaries in the endoneurium that form the barrier between blood and the axons.

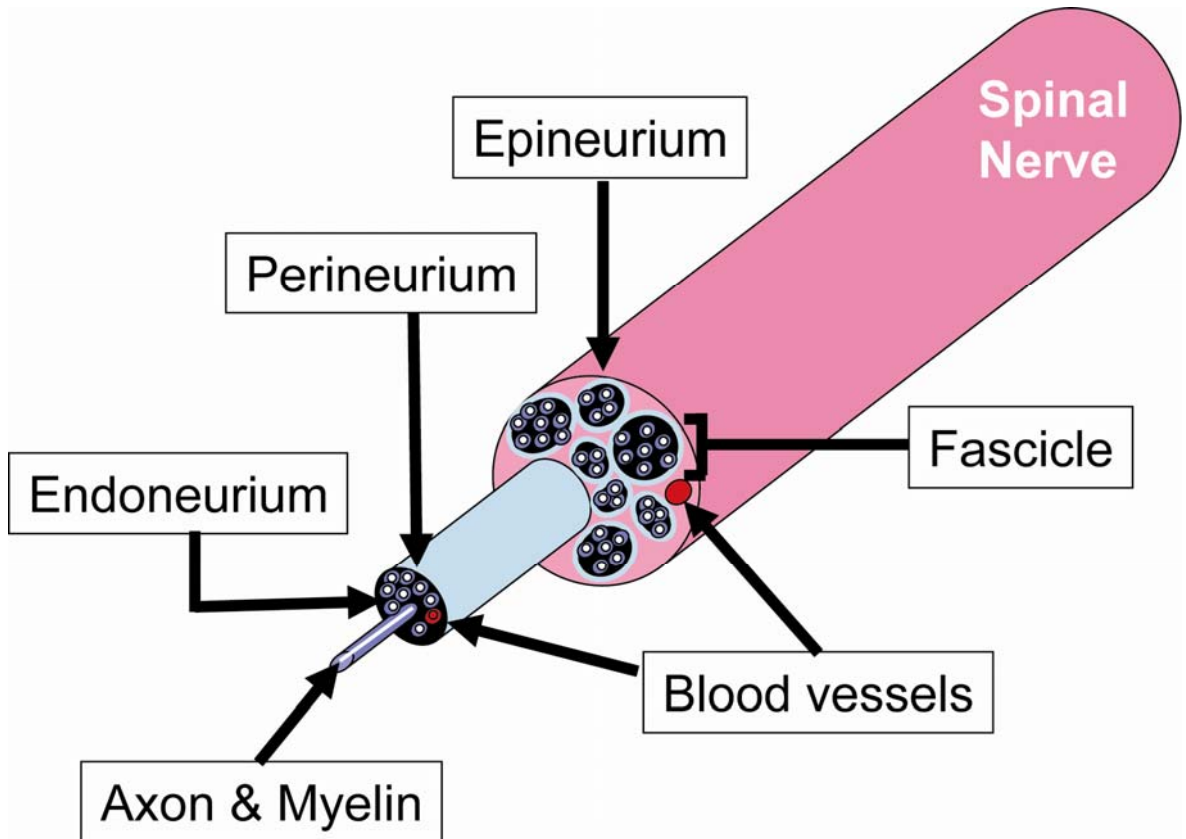


Figure 1.5: The structure of the protective barriers surrounding the nerve.

The nerve is protected by the epineurium that surrounds the fascicles coated by the perineurium, which in turn protects the nerves surrounded by the endoneurium. The blood-nerve barrier exists at the level of the endothelium between the endoneurial capillaries and the axons.

1.3.3 Permeability

Three regions exist where the continuity of the BNB is breached: blood vessel and reticular fibre entry, at the terminal, and at the nerve roots.

Injection of tracers and dyes was the primary vehicle for studying permeability of the BNB. In the early 1900's it was shown that water-soluble dyes injected into the peripheral vasculature stained all of the organs of the body but did not stain the brain or spinal cord. In the mouse a trace amount of Evans-blue labelled albumin can be detected outwith the endoneurial vessels in the endoneurium after intravenous injection, but some leakage can occur in different species (Olsson 1990). Mouse sciatic nerve endoneurial vessels are also impermeant to horse-radish peroxidase (HRP) and prevent its movement into the

endoneurium, probably due to tight junctions (Olsson & Reese 1971). More specific studies investigating the permeability of many compounds find that only low molecular weight compounds such as ions and glucose can reach the endoneurium after a delay. Additionally, Malmgren *et al* (1980) found that while sodium fluorescein rapidly penetrated the epineurium and perineurium, it was only after excessive time and doses it could be found in the endoneurium, and still only at low concentrations. When compared to the penetration of Evans blue (M.W. 69kDa), the penetration of the 376Da sodium fluorescein molecule was markedly quicker and more extensive. As some tracers have been found in vesicles and the basal lamina, it is possible that as the number of layers of the perineurium are reduced, and the smaller the molecule, the more likely it is that a compound will eventually penetrate the barrier.

How do proteins cross this barrier? Vesicular transport is a form of vascular leakage. Serum proteins can be found in the endoneurial fluid although it was thought that the barriers were impermeable to these compounds (as reviewed by Olsson 1990). The flow of endoneurial fluid is expected to be along the nerve to the terminal. At the nerve terminal of peripheral nerve branches, the BNB is often open-ended and lacks a perineurial sheath (Burkel 1967;Malmgren & Olsson 1980;Saito & Zacks 1969). The purpose of this open-end could be to remove the excess endoneurial fluid as there is no lymphatic system in the nerve fascicles. However this could also result in an access point of compounds to travel up into the nerve. Furthermore, at small nerve terminal branches there are no endoneurial vessels and instead the perineurial sheath is permeable to compounds in the epineurium (Malmgren & Olsson 1980;Oldfors 1981).

Seitz *et al* (1985) studied the permeability of the mouse BNB to IgG as this could offer a relationship of antibodies to disease processes. The concentration injected was that which would approximately mimic physiological circulating IgG levels. After one day post-injection, IgG was detected in the perineurium and endoneurial blood vessel lumina, but was absent in axons and myelin sheath. Even after four days myelinated fibres remained negative for IgG deposition but the endoneurial space was now positive. This reflects a partial permeability of the mouse BNB to IgG.

It would seem that the breakdown of the BNB can cause leakage and increased permeability. This has been demonstrated in association with inflammatory neuropathies (Neuen et al. 1987) and Wallerian degeneration in the frog sciatic nerve (Weerasuriya et al., 1980). More recently, Seitz *et al* (2004), conducted a study to investigate the effect of crush and transection on the permeability of the mouse sciatic nerve. The authors found that the BNB had a prolonged leakiness to IgG, complement components C3 and C5 after transection and Wallerian degeneration and suggest the purpose of this breakdown could be to enhance the repair process by allowing the exchange of trophic factors that would normally be of too large a size to cross the barrier.

1.3.4 Importance to GBS

IgG permeability, small nerve branches with permeable perineurium, and open-ended terminals all predominantly predispose distal axons to attack by circulating pathogenic antibodies. This could explain the prevalence of injury in the PNS as opposed to the CNS even though gangliosides are highly localised here too. Furthermore, if Wallerian degeneration does begin distally, the breakdown of the BNB allowing further antibodies access to nerve could further exacerbate the pathology and continue to progress the injury proximally along the nerve.

1.4 Myelinated axons and the node of Ranvier

Vertebrates owe the evolution of a more complex nervous system to the development of the myelin sheath. Unfortunately with this increasing complexity also arises opportunity for damage and disruption. There are many diseases associated with the nerve generally, and some that can more specifically target its component parts- the axon and myelin sheath. It is therefore imperative to understand the fine detail of the anatomy of the nerve in an attempt to correlate structure with function and ultimately provide intervention to pathological conditions. GBS has both been associated with disruption to the myelin and the axon, but as the current study primarily concerns the axonal

variant AMAN, a focus will be placed on the axon and more specifically the node of Ranvier.

1.4.1 The axon

The axon consists of mitochondria, microtubules, neurofilaments, endoplasmic reticula and vesicular bodies. The structural neurofilaments and microtubules are lined up in parallel longitudinally within the axon and are essential to maintaining cytoskeletal structure (reviewed by Peters et al., 1991).

Neurofilaments are more spaced out in the internode while at NoR they are more compact. Interactions with the overlying myelin sheath appear to cause an increase in phosphorylation of neurofilament which in turn leads to greater spacing between the filaments in the internode. NoR are likely to be more constricted as the neurofilament is not in a phosphorylated state and there are also less filaments present (Hsieh et al. 1994).

As the axon can extend many centimetres (or even metres) they have developed specialised modifications to enable rapid conduction, namely the myelin sheath and NoR.

1.4.2 The myelin sheath

The myelin sheath enables a more rapid and efficient conduction of action potentials compared to unmyelinated fibres, due to its properties of insulation. One of the major benefits of the myelin sheath is that a larger number of myelinated smaller calibre fibres can replace larger calibre unmyelinated fibres with the same conduction velocity, thus saving space. Additionally, the metabolic consumption is reduced as action potentials only need to be generated at the node of Ranvier rather than along the entire membrane (Crotty et al., 2006; Poliak & Peles 2003). Conduction velocity is dependent on axon diameter and myelin sheath thickness (Waxman 1980).

Myelin, first described by Virchow in 1854, is a multilamellar membrane made up of lipids and proteins. Myelin is formed by the glial cells closely associated with the axon- Schwann cells in the peripheral nervous system and oligodendrocytes in the central nervous system. These cells enwrap the axons in segments known

as internodes, which are separated by unmyelinated regions known as NoR. It is via these NoR that saltatory conduction can occur, where the current can 'jump' to the excitable membrane from node to node allowing for the increase in speed of transmission of action potentials (Huxley & Stampfli, 1949). There are similarities and differences between the CNS and PNS- as GBS is a peripheral neuropathy the emphasis will be placed on the PNS.

In the PNS, axons designated to become myelinated (those over 1 μ m) become enveloped by what begins as a furrow in the Schwann cell surface. The edges of the furrow join to form a mesaxon that lengthens to wrap round the axon several times. When more than three layers are complete, the cytoplasm is lost and the end result is what is known as compact myelin. The diameter of the axon correlates to the number of myelin lamellae, although it is not a linear relationship (Friede & Samorajski 1967). The myelin along the internode is compact, which is achieved by one of the integral myelin protein P₀ tetramers interacting in *cis* and *trans* (Shapiro et al. 1996). The entire peripheral nerve is covered by a basal lamina, plus the nodal axolemma is additionally covered by Schwann cell microvilli that extend into the space filled with filamentous matrix (Landon & Langley 1971). Each ensheathing Schwann cell is separated from other axons by this basal lamina and its endoneurium.

1.4.3 Node of Ranvier

As mentioned above, the NoR are the gaps between the internodes formed by myelin (Figure 1.6A). They are essential to the initiation and propagation of action potentials and thus are highly specialised domains. The NoR is typically 1 μ m in length or greater, becoming longer with increasing calibre (as reviewed by Waxman 1978). During development the axons and glia communicate to develop these highly specialised domains, which themselves consist of several subdomains, discussed below. Nodes are found at intervals ranging from 100 μ m to 1mm (Jaros & Jenkison 1983). The length of internodes increases with the length of the nerve, i.e. internode number does not increase but its length does, therefore this will approximately correspond to about 100x the diameter of the axon (Peters et al., 1991). Ramón y Cajal (1928) was first to describe the

extensive branching of nerves towards the terminal and the reduction in internode length at this location:

“...internodes become shorter and shorter in proportion to the number of divisions and proximity to the ending.”

This can be reduced to as little as 10µm towards the nerve terminal (Quick et al., 1979). The purpose of this shortening was speculated to increase the safety factor and the number of available NoR to contribute to transmission and facilitate conduction into unmyelinated terminals (later reviewed by Khodorov & Timin 1975).

The NoR can be divided into three regions (node proper, paranode and juxtaparanode) based on specialisations and expression of particular proteins, described in more detail below (Figure 1.6).

1.4.3.1 Nodal gap

The axon remains a fairly constant calibre except for at the NoR where it approximately halves (Reles & Friede 1991). At this narrowing in the peripheral nervous system, the outer collars of the two adjacent internodal Schwann cell project microvilli into the gap, which is filled with filamentous matrix (Landon & Langley 1971).

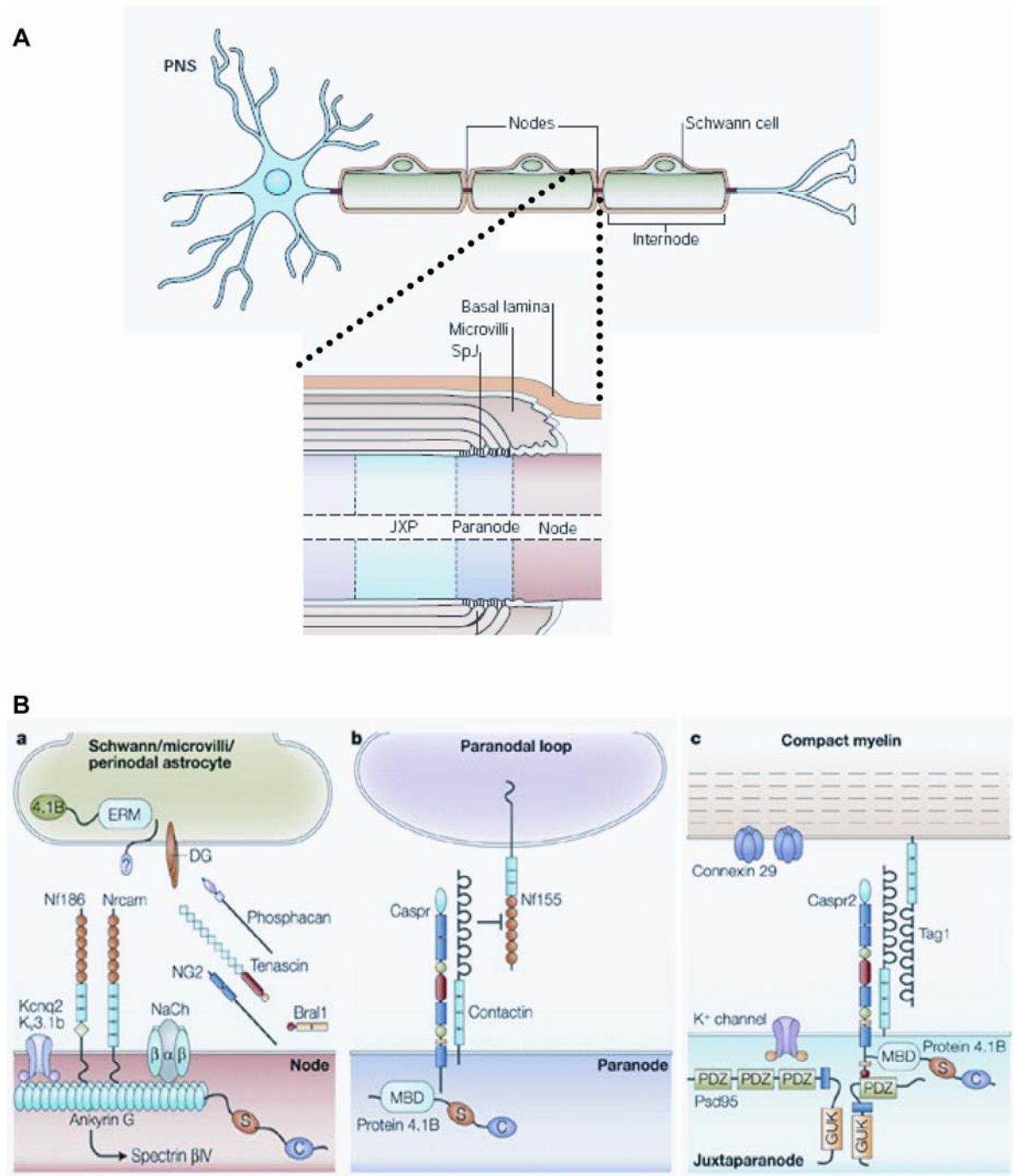


Figure 1.6: Schematic of the axon and its specialisations.

A) Axons of the PNS are myelinated by Schwann cells, which are separated by NoR. An example of the basic components of the NoR is depicted in the enlargement. **B)** A representative diagram of the nodal proteins and their associations at the (from left to right) nodal gap, paranode and juxtapanode. Modified from Poliak & Peles, 2003.

The most prominent and important protein found at the nodal gap is the voltage-gated sodium channel (VGSC or Nav) due to its role in conduction (Chiu 1980; Hildebrand et al. 1993; Salzer 1997). It has been estimated that Nav channels cluster here at a density of more than 1200 channels per square μm^2 of

axolemma (Ritchie & Rogart 1977), which enables the propagation of the action potential. Potassium channels are also localised here, notably the KCNQ2 involved in the slowly activating current of the action potential (Devaux et al. 2004). In fact, the whole nodal zone is geared towards an increased level of activity as there are also many more mitochondria, five times more than in the internodes (Waxman 1978). This is not to say that sodium channels do not also exist along the internodes, the density is simply far less ($<80/\mu\text{m}^2$).

Many other important proteins are found at this region including the cell adhesion molecules NrCAM and NF186 (Davis et al., 1996; Tait et al. 2000), and cytoskeletal proteins ankyrin G (Kordeli et al., 1995) and β IV spectrin (Berghs et al. 2000), which are discussed in more detail below.

1.4.3.2 Paranode

The nodal gap is flanked by the paranodal loops of the Schwann cell. These occur when the layers of compact myelin open out, beginning with the outermost, and become filled with cytoplasm, before forming specialised contacts with the axolemma, known as axo-glial junctions. The formation of periodic intracellular densities, the transverse bands, occur between the loops and axon and have been compared to septate-like junctions in invertebrates (as discussed by Poliak & Peles 2003). As these form after loop attachment, this is an indicator of a mature junction (Tao-Cheng & Rosenbluth 1983). Not all lamellae reach the axolemma, but where they do they cause depressions in the surface. There are many more loops for larger calibre fibres, which could explain the increased level of constriction at the nodes relative to that seen in smaller calibre fibres. Disruption of these junctions severely interferes with the conduction of action potential, exemplifying the importance of this structure (see below). It was suggested that the paranode was responsible for the concentrating effect of proteins at the NoR (Rosenbluth 1976). On recording sodium and potassium currents after deliberate demyelination of myelinated axons, Chiu and Ritchie (1981) proposed that paranodal junctions create a high resistance barrier to the flow of ionic current. The axo-glial junction is not completely impermeant as dyes injected into the extracellular space can cross

into internode, but this diffusion is sufficiently slow to ensure propagation of action potentials (Girault et al. 2003). Caspr and contactin are the major transmembrane constituents of the junction, while NF155 is the glial component (Charles et al. 2002; Einheber et al. 1997; Tait et al., 2000), discussed in more detail below. In summary, the major functions of the paranodes are to anchor myelin to the axon, create a barrier isolating the juxtaparanode from the electrical activity at the NoR, and to act as a physical barrier to prevent molecules moving laterally from the nodal axolemma.

1.4.3.3 Juxtaparanode

This portion of the axon is found just lateral to the innermost paranodal loop, identified by the gradual increase in cross-sectional area from the node. There is a higher concentration of molecules at the membrane here that then dissipate into the internode, as first observed in the frog by Rosenbluth *et al* (1976). The juxtaparanode is often characterised by the presence of heteromultimers of voltage-gated potassium channels Kv1.1 and Kv1.2, plus the Kvβ2 subunit (Arroyo et al. 1999; Chiu 1980; Mi et al. 1995; Rhodes et al. 1997; Wang et al. 1993). The purpose of these channels is likely to stabilise conduction and maintain resting potential of the internode (Chiu & Ritchie 1984; Vabnick et al. 1999; Zhou et al. 1998b). This proposed function is reinforced by the fact that while Kv1 clustering is lost in Caspr2^{-/-} mice, the overall amount of Kv1 channels is the same and there is little effect on conduction (Poliak et al. 2003; Traka et al. 2003). Although Nav channels are distributed in the correct location by the first postnatal week, voltage-gated potassium channels (Kv1) are found aberrantly localised in the nodal gap and paranode until they are finally redistributed to their functional destination at the juxtaparanode (Vabnick et al., 1999).

Kv1 channels at the juxtaparanode associate with Caspr2 (Poliak et al. 1999) and Tag1 (transient axonal glycoprotein), a glycosylphosphatidylinositol (GPI)-anchored cell adhesion molecule (CAM) known to be a constituent of both Schwann cells and axons at the juxtaparanode (Traka et al. 2002). The interaction of these three proteins will be discussed below.

Connexin 29 is found in the innermost layer of myelin at the border of the axon and internode in peripheral nerve (Li et al. 2002). Connexins form intercellular communicating channels for exchange of ions and metabolites from cell to cell (Goodenough et al., 1996) and have been implicated in a so-called “axoglial synapse” between axon and Schwann cell at the juxtaparanode (Fields & Stevens-Graham 2002).

1.4.4 Nodal Proteins

1.4.4.1 Voltage-gated sodium channel

The sodium channel is an integral membrane protein that conducts sodium ions through the membrane. Sodium channels can be classed as voltage-gated (focus of this study) or ligand-gated, depending on what triggers their activation. In excitable cells, depolarisation causes movement of Na^+ into the membrane and is responsible for the rising phase of the action potential (Hodgkin and Huxley 1952). Three distinct functional states exhibited by the sodium channel during action potential are as follows: resting (closed), activated (open), and inactivated (closed). Electrophysiology highlighted many of the properties of the sodium channel, while the molecular mechanisms behind its function were determined subsequently. Several neurotoxins are known to bind and block the activity of the sodium channel specifically, and thus this binding property could be exploited to serve as a probe during purification. This was the technique used by Barchi *et al* (1983) and Hartshorne *et al* (1984) to identify that the mammalian sodium channel consists of a complex formed by a larger membrane traversing α -subunit (M.W.= ~260kDa), and one or more auxiliary β -subunits (M.W.=~39kDa and ~37kDa). Two more β -subunits have since been identified. The significance of these β -subunits to the functioning of the channel were initially thought to be quite minimal, as it was shown that the injection of only the α -subunit mRNA into *Xenopus* oocytes was sufficient to result in a functional sodium channel (Goldin et al. 1986;Noda et al. 1986). However, the β -subunit is now known to contribute to regulation of channel gating, binding of other proteins, and the modulation of channel expression.

The β -subunits are also transmembrane proteins, but with an extracellular N-terminus and intracellular C-terminus. All four isoforms are structurally homologous to the Ig superfamily that includes cell adhesion molecules (Catterall 2000). The C-terminal has a role in α -subunit affinity (Meadows et al. 2001) and possibly recruiting the cytoskeletal protein ankyrin (Malhotra et al. 2000), while the extracellular N-terminus can be involved in binding to the CAMs NF186 and contactin, and also to extracellular matrix molecules (Kazarinova-Noyes et al. 2001; Ratcliffe et al. 2001; Srinivasan et al., 1998; Xiao et al. 1999).

The sodium channel from the electric eel, *Electrophorus electricus*, electroplax membrane was the first to have its cDNA cloned and its sequence and primary structure determined (Noda et al. 1984a). This was followed soon after by the cloning of rat brain cDNA by the same group (Noda et al., 1986). The electroplax sodium channel protein α -subunit is composed of 1820 amino acids (a.a). From the sequences, it was established that there were four homologous repeats, that each consisted of five hydrophobic segments and one segment with strong positive charge (Figure 1.7). It has since been confirmed that there are indeed four identical domains (denoted I-IV) that assemble and join to form the pore of the α -subunit (Greenblatt et al., 1986). Each one of these domains consists of six segments (S1-S6) that fully traverse the membrane as α helices and are connected by short extracellular loops to the next, with a re-entrant loop between the helices of S5 and S6 (Yu & Catterall 2003). The intracellular loops connecting each of the domains, and the amino- and carboxy-terminal tail domains that both project into the cytoplasm, are much larger. The fourth segment of each domain is the voltage sensor due to positive arginine (predominantly) and lysine amino acids in every third position, with non-polar residues in between (Guy & Seetharamulu 1986; Noda et al. 1984b; Stühmer et al. 1989). The helix-coil transition model proposes that during depolarisation the S4 segment α -helices become unstable and expand resulting in the breakage of the hydrogen bonds with adjacent helices (Leuchtag 1994). In addition there is a proline near the cytoplasmic end of this segment that adds a kink in the peptide. Stühmer et al (1989) were the first to provide evidence that the fourth segment is involved in voltage sensing and gating of the channel by investigating site-directed mutations. By altering positively charged amino acids, mainly in domain I (where there are the fewest of these residues, which would presumably result

in the largest effect due to charge alteration), into neutral or negatively charged residues, there was a decrease in the steepness of the voltage dependence of activation.

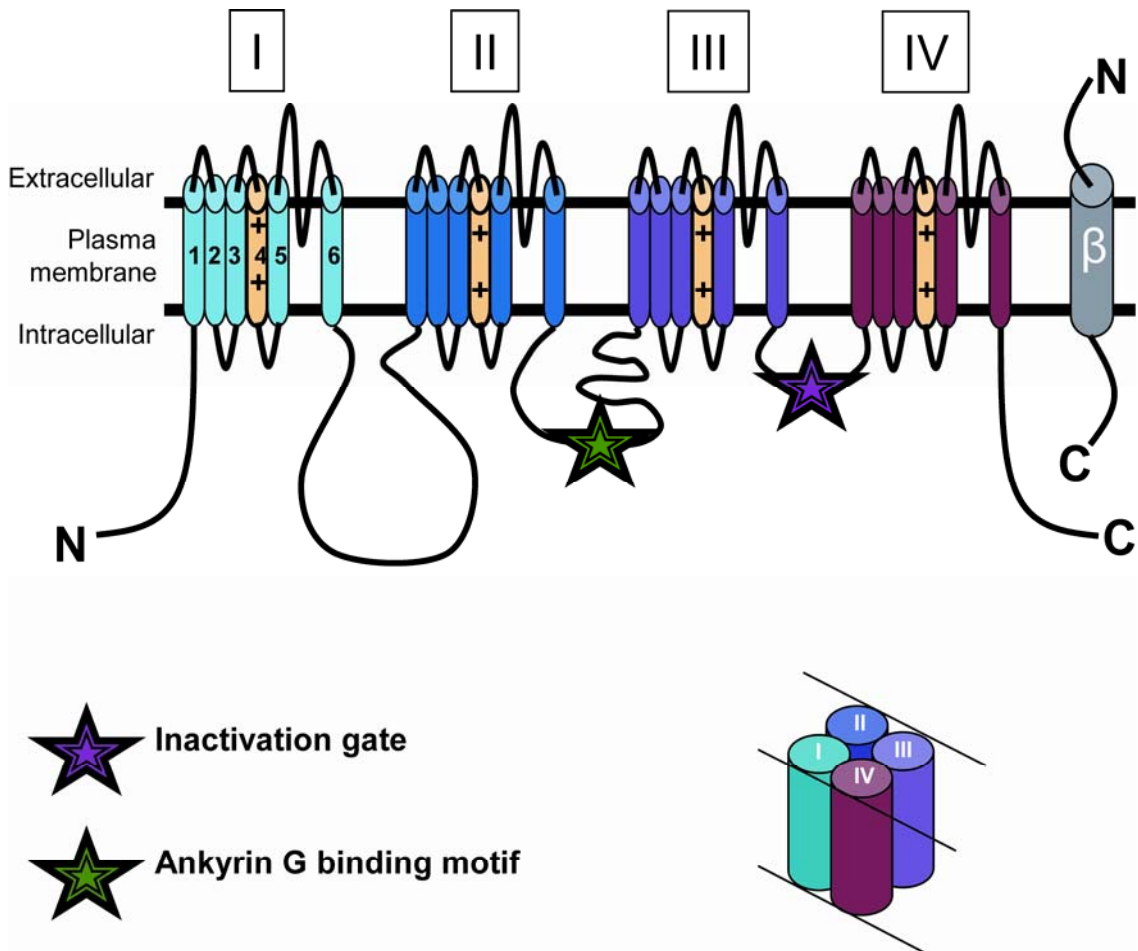


Figure 1.7: Diagrammatic representation of basic Nav channel α - and β -subunit structure.

The Nav channel alpha-subunit is made of four domains (I-IV) each of which consists of six segments. The fourth segment of each domain is the voltage sensor (marked by +) due to positively charged amino acids at every third position. The pink star on the third cytoplasmic loop represents the location of the channel inactivation gate, while the green star on the second cytoplasmic loop is the location of the ankyrin G binding motif. The β -subunit consists of one transmembrane domain with a cytoplasmic C-terminal and extracellular N-terminal. At the bottom of the figure is an image that represents the conformation of the channel in its native state.

Additionally, this study suggested the region involved in inactivation of the channel, which had been investigated in more general terms previously. An initial study into the effect of the proteolytic enzyme pronase after its internal perfusion into squid axons, showed that the inactivation of the sodium channel was destroyed, even though gating was unaffected, indicating that the site of inactivation was in the cytoplasmic loops of the sodium channel (Armstrong et al., 1973). This was confirmed by other studies using various proteolytic reagents (Eaton et al. 1978; Oxford et al., 1978; Rojas & Rudy 1976). In the article by Stuhmer (1989) discussed above, it was shown that by more specifically cleaving or deleting a portion of the cytoplasmic linker between domains III and IV, the inactivation rates become much slower than those of normal sodium channels. Interestingly, the cleavage of other cytoplasmic linkers did not affect the functionality of the sodium channel, although all four transmembrane domains are essential. Other methods used to examine the location responsible for inactivation used site-directed antibodies. Vassilev *et al* (1988) used antibodies targeting each of the intracellular domain linkers to show that only those binding the III-IV linker reduced inactivation. Furthermore, the antibody against this portion did not effect activation of the channel. Most importantly, antibody only bound at negative potentials implying a conformational change to the area during depolarisation as binding was diminished. It was proposed that the cytoplasmic III-IV linker would move into a position to occlude the movement of sodium ions due to conformational change. In the III-IV linker, there is a cluster of three hydrophobic amino acids (isoleucine, phenylalanine and methionine) that are essential for fast inactivation (West et al. 1992). These are adjacent to a region of positive charges, and together form a structural motif related to inactivation (McPhee et al. 1998). A suggested model by Miller *et al* (2000) is that the positive charges of both the linker and S4 segment repel each other in the closed state but when S4 moves on activation the linker can 'relax' towards the opening of the pore. This was determined primarily by the removal of positive charges in the linker that led to quicker inactivation and the weakening of activation-inactivation coupling, which would be expected if there was no longer such a strong electrostatic repulsion.

Use of the pore-blocking toxins tetrodotoxin and saxitoxin has helped to elucidate the amino-acid residues in the extracellular pore that are involved in

ion selectivity. The outer pore is formed by the re-entrant loops of the linker between S5 and S6 and two particular amino acids are located here in each domain to form a negatively charged ring. These are suspected receptors to the pore-blocking toxins. A mutation of one of these residues (glutamic acid to glutamine- E387Q) was shown to cause insensitivity to tetrodotoxin and saxitoxin binding (Noda et al. 1989). Other mutagenesis studies have shown the involvement of residues in the selectivity of the channel to certain ions. These include the discovery of certain negatively charged residues (384 and 387) that when mutated reduced single-channel conductance (Pusch et al. 1991), followed by transformation of a sodium channel into a calcium-selective channel by mutating these inner ring residues to those normally found in the calcium channel (Heinemann et al. 1992; Terlau et al. 1991). These studies identify that the outer pore confers permeability and the sodium ion selectivity. The conformation of the channel is expected to be bell-shaped with a narrow extracellular portion at the top that widens towards the cytoplasmic surface (Sato et al. 2001). It follows that the pore will be at its most narrow at the exterior due to the overall reduction to the width at this region, and additionally the large S5-S6 re-entrant loops. The sodium ion is expected to move through one at a time as the pore is only about 35Å (3.5nm) wide. Furthermore it will not follow a straight path as the cryo-electron microscopy of Sato *et al* (2001) was suggestive of several orifices at the extracellular domain that connect to a larger internal cavity before connecting to four narrow, peripheral regions within the transmembrane domain. It is thought that the ions jump from one free site to the next as the hydrogen bonds of the α -helices break in a zipper-like motion from the exterior due to depolarisation and expansion of the S4 segment (Leuchtag 1994).

The discovery that there was more than one sodium channel isoform came originally from a study that identified two distinct mRNAs from the rat brain (Noda et al., 1986). It is now known that at least ten genes encode the various α -subunits (named Scn1a-9 and x), while four genes (Scn1b-4) encode the β -subunits (Lai & Jan 2006; Yu & Catterall 2003). The nomenclature for voltage-gated sodium channels, e.g. Nav1.1, represents the chemical symbol (Na) of the ion, the trigger of activation (voltage) in subscript (Na_v), the gene subfamily (1) and the specific channel isoform after the decimal (.1) (Goldin et al. 2000). Each

of the sodium channels can not only be discriminated by their differing sequences, but also their kinetic and expression profiles.

On the examination of distribution of Nav channels in the PNS, it has been reported that clustering begins within the first postnatal week (Vabnick et al. 1996). Although the NoR express Nav1.2 during development, this predominantly switches to Nav1.6 in the adult (Boiko et al. 2001;Kaplan et al. 2001). This transition appears to be under the control of myelin formation and paranodal junction formation, as *Shiverer* mice lacking compact myelin, and Caspr KO mice with disrupted paranodes, respectively, fail to make this switch at CNS NoR, and it is delayed in the PNS (Boiko et al., 2001;Rios et al. 2003). Nav1.6 is expressed in various brain areas, spinal cord, dorsal root ganglia and peripheral nerve (Tzoumaka et al. 2000). Particularly, Nav1.6 is the only isoform expressed at adult NoR (Caldwell et al. 2000). The importance of the Nav1.6 isoform is shown by the motor endplate disease (*med*) mouse that suffers from a loss of expression of this isoform leading to severe muscle atrophy and hind limb paralysis, ultimately resulting in death (Burgess et al. 1995;Porter et al. 1996). This expression is particularly important to development of normal function as shown in a study of postnatal induction of Nav1.6 expression (Garcia et al. 1998). Furthermore, in *Xenopus* oocytes it was shown that those expressing Nav1.6 seemed to maintain a higher firing rate and be more resistant to inactivation than those expressing Nav1.2 (Zhou & Goldin 2004). This would be important for the rapid conduction of action potentials and explains the particular expression pattern of Nav1.6 at NoR. Thus differing functional roles of Nav channels can account for their particular expression patterns.

1.4.4.2 The cytoskeletal protein ankyrin G

Ankyrin G, also found enriched at the NoR (Kordeli et al. 1990;Kordeli et al., 1995), is a cytoskeletal protein considered to be an adaptor as it links integral membrane proteins to the spectrin cytoskeleton (Bennett & Baines 2001). Ankyrin was first discovered in human erythrocytes, before other isoforms were uncovered. There are three members of the ankyrin family: Ank1, Ank2 and Ank3 (AnkG) (Kordeli et al., 1995;Lambert et al. 1990;Lux et al., 1990;Otto et al.

1991). It was shown that an isoform of ankyrin was localised to the NoR and axon initial segment that was not of the erythrocyte origin by using erythrocyte ankyrin deficient mice (Kordeli & Bennett 1991), but it was not until later that it was identified specifically to be ankyrin G (Kordeli et al., 1995). All ankyrins are composed of three conserved domains: a membrane-binding domain, a spectrin-binding domain and a death domain, followed by a regulatory sequence (Figure 1.8). Additionally, specialised domains can be inserted, or regions removed in splice variants. Ankyrin G was so named as it has a large addition of up to 2100 a.a. between the spectrin-binding domain and death domain making it a giant ankyrin of either 270 or 480kDa (Kordeli et al., 1995). It is unknown what the function of this extra sequence could be, but it may be involved in axonal targeting as isoforms lacking this region are found neuronally. Also although antibodies react to both splice variants and seem to localise to the same areas, there could be a divergence in function as the 480kDa is expressed earlier in development (Bennett & Lambert 1999). It is a 46kDa domain rich in serine/threonine that distinguishes the nodal isoform from other ankyrins (Zhang & Bennett 1996).

The membrane-binding domain consists of a 33-residue repeat, known as ANK, copied 24 times. Each ANK repeat is organised into four subdomains of 6 repeats. These subdomains have distinct binding properties and not only allow ankyrin to bind many diverse proteins with unrelated primary sequences, but also to bind several proteins simultaneously (Michaely & Bennett 1995).

Ankyrin was first associated with Nav channel binding when they were found to co-purify on isolation of the channel (Srinivasan et al. 1988). Ankyrin G anchors Nav channel to the NoR (Kordeli et al., 1990;Kordeli et al., 1995), and also interacts with neurofascin and NrCAM (Davis et al., 1996;Zhang et al. 1998). Binding to the cytoskeleton is via the protein BIV spectrin that itself is anchored by protein 4.1B (Becker et al. 1990). A new variant of spectrin, BIV spectrin, was found to co-localise in rat brain and sciatic nerve with ankyrin G at NoR and axon initial segments (Berghs et al., 2000). Originally it was expected that the binding of ankyrin G to Nav channel could be via the N-terminal membrane-binding domain of ankyrin, to either the α - or β -subunit of Nav channels (Malhotra et al., 2000). Recently it has been identified that it is more specifically via a sequence of nine amino acids in loop 2 of the α -subunit, a

sequence conserved in all Nav isoforms (Lemaitte et al., 2003). This motif was also shown to localise neurofascin/sodium channel complexes to the initial segment of hippocampal neurons in culture. Binding of ankyrin G to the CAM family is through a conserved FIGQY sequence in their cytoplasmic tails.

Although ankyrin G and BIV spectrin are classically associated with the nodal axolemma, recently Ogawa *et al* (2006) demonstrated the necessity of further scaffolding proteins, namely ankyrin B, all spectrin and BII spectrin to form a cytoskeletal protein complex associated with paranodal junctions.

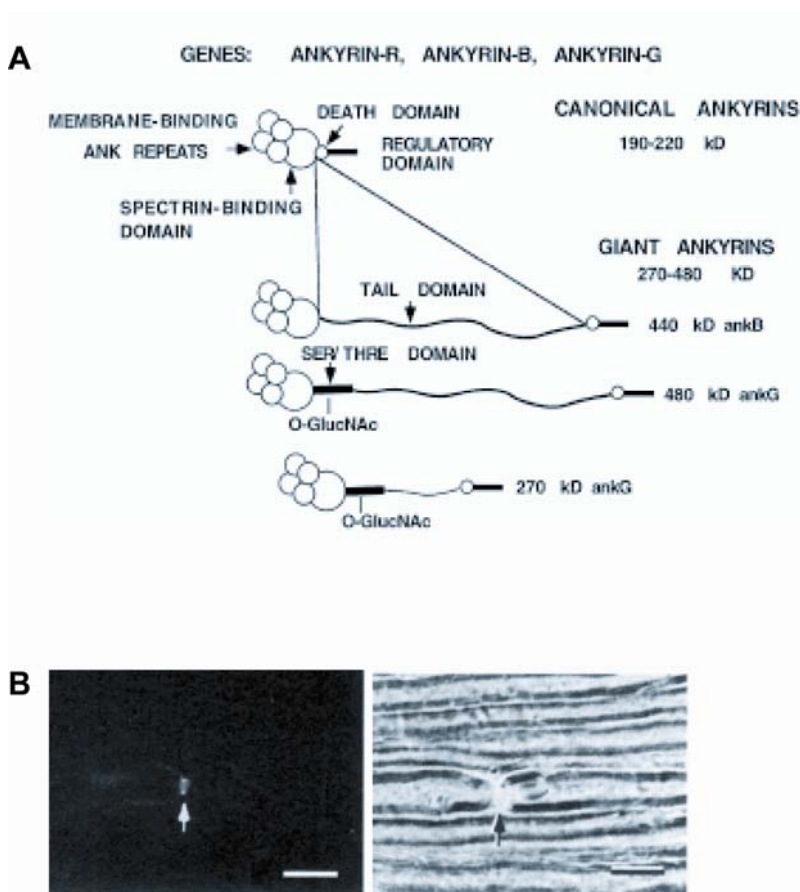


Figure 1.8: Structure and staining pattern of ankyrin.

A) The ankyrin family generally consists of a membrane-binding domain made of ANK repeats, a spectrin-binding domain, a death domain and finally a C-terminal regulatory domain. Giant ankyrins, including ankyrin G, have insertions between the spectrin-binding and death domains. **B)** An example of ankyrin G localisation at the nodal gap of rat sciatic nerve (arrow). Modified from Bennett *et al*, 1999.

1.4.4.3 Cell adhesion molecules Neurofascin and NrCAM

Neurofascin (NF) and NrCAM belong to the immunoglobulin/fibronectin type 3 (Ig/FNIII) family of cell surface glycoproteins known as cell adhesion molecules (CAMs). Together they account for 1% of total membrane protein in the mature brain (Davis et al., 1996). These proteins both display ankyrin-binding activity in their cytoplasmic domains and are associated with the NoR. Other adhesive and signalling activities displayed by these proteins involve specific localisation to regions of the membrane, which accounts for their necessity to interact with ankyrin G and the cytoskeleton.

More specifically, neurofascin has two isoforms, NF155 and NF186, which relates to their molecular weight and is due to alternative splicing. The configuration of both isoforms, first established by Davis *et al* (1996), are represented in Figure 1.9. The molecules are characterised by an intracellular ankyrin-binding domain, and an extracellular domain composed of six Ig domains and 3-5 FNIII domains (Davis & Bennett 1994; Davis et al., 1996; Tait et al., 2000). The NF186 isoform contains a 173 a.a. serine, threonine and proline rich domain, similar to mucin, and lacks the third FNIII domain. The NF155 isoform does not express a mucin-like domain. Both have inserts at the amino-terminal. It has been established that NF 186 (i.e. the mucin-like domain expressing isoform) can be co-localised with ankyrin G and Nav channels at NoR and axon initial segments. There is a conserved FIGQY sequence that binds to ankyrin G, but this interaction can be attenuated by phosphorylation of the tyrosine residue (Garver et al. 1997). Therefore it is reasonable that the tyrosine-phosphorylated neurofascin is located at the paranode, while the isoform at the NoR that associates with ankyrin G is not. More recently it has been shown that NF186 associates with the extracellular domains of $\beta 1$ and $\beta 3$ subunits of the Nav channel, resulting in targeting and maintenance of channels at developing and mature NoR (Ratcliffe et al., 2001). NF186 also binds other proteins to maintain nodal architecture necessary for conduction (Sherman et al. 2005). The NF155 isoform that lacks the mucin-like domain was originally reported to be expressed in unmyelinated axons (Davis et al., 1996), and later found to be an important feature of the axo-glial junction (Charles et al., 2002; Sherman et al., 2005; Tait et al., 2000). In NFasc null mice the amount of nodal and paranodal proteins expressed are the

same, but as they do not localise correctly, it is suggestive of a role for neurofascin in the assembly of protein complexes (Sherman et al., 2005).

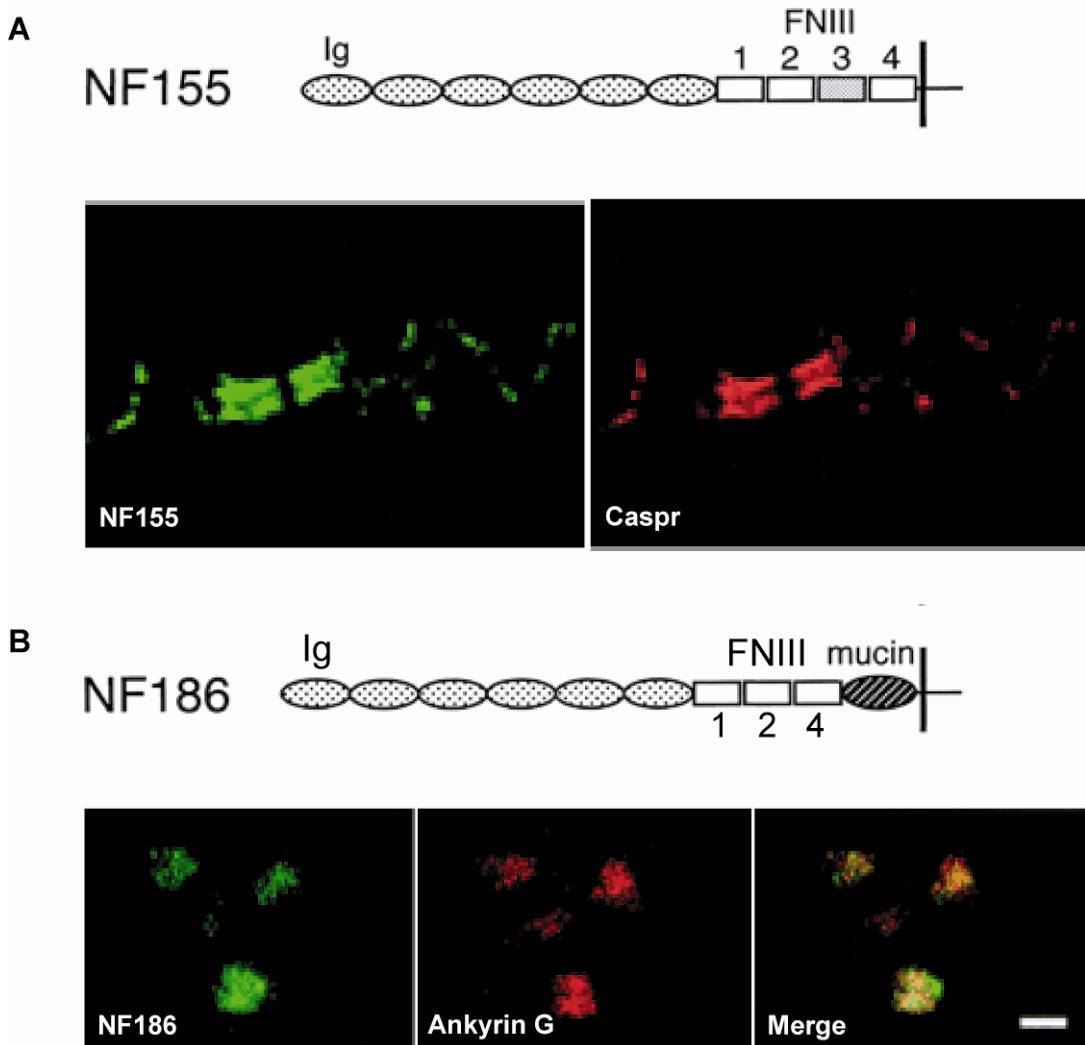


Figure 1.9: Structure and localisation at NoR of two neurofascin isoforms.

A) NF155 (green) consists of six immunoglobulin (Ig) domains and four FNIII domains extracellularly and can be found co-localised with Caspr (red) at the paranodes. **B) NF186 (green)** shares the same structure as NF155 except for the omission of the third FNIII domain and the insertion of a mucin-like domain. It is found to co-localise with ankyrin G (red) at the nodal gap. Images modified from Tait *et al*, 1999.

On screening a rat brain cDNA library with a neurofascin antibody, Davis *et al* (1996) identified and cloned for the first time mammalian NrCAM. The neuron-glia CAM (NgCAM) related CAM, NrCAM, was first characterised in the chicken (Grumet *et al.* 1991; Kayyem *et al.* 1992). Its structure encompasses six Ig domains, four FNIII domains, a transmembrane domain and a short cytoplasmic domain (Figure 1.10). It possesses more than 70% sequence identity with the NF cytoplasmic domains. As described for neurofascin, the cytoplasmic domain of NrCAM binds to ankyrin G (Davis & Bennett 1994) via a FIGQY sequence that is conserved in other members of the Ig/FNIII CAM family. Staining initially identified NrCAM at the surface of cells in culture, but later it was localised in the nervous system particularly at NoR (Davis *et al.*, 1996) where in the peripheral nerve it co-localises with Nav channels, neurofascin and ankyrin G. Binding studies have identified the interactions of NrCAM with various other CAMs and extracellular matrix proteins (as reviewed by Grumet 1997). Particularly, Volkmer *et al* (1996) demonstrated the heterophilic binding between neurofascin extracellular Ig domains and NrCAM. Contactin and NrCAM appear to interact laterally *in vivo* as they can be co-precipitated from brain extracts (Sakurai *et al.* 1997). The cytoplasmic tail of NrCAM is the only member of the L1 CAM family to contain PDZ binding motifs and has been shown to interact specifically with the PDZ domains of PSD95 proteins that can cluster receptors and channels in specific regions (Dirks *et al.*, 2006).

1.4.4.4 Paranodal proteins Caspr and contactin

Contactin is a member of the immunoglobulin superfamily and is a GPI-anchored protein, which means it does not have a cytoplasmic domain. It is expressed by neurons of the PNS and CNS (Einheber *et al.*, 1997). Contactin has high homology with the Nav channel β -subunit and it is likely that the interaction between these proteins aid in the targeting of Nav channels to the NoR during development (Kazarinova-Noyes *et al.*, 2001). Caspr was discovered to be the binding partner of contactin when it was postulated that contactin would likely interact with another protein with the capacity for signalling via a cytoplasmic domain (Peles *et al.*, 1997).

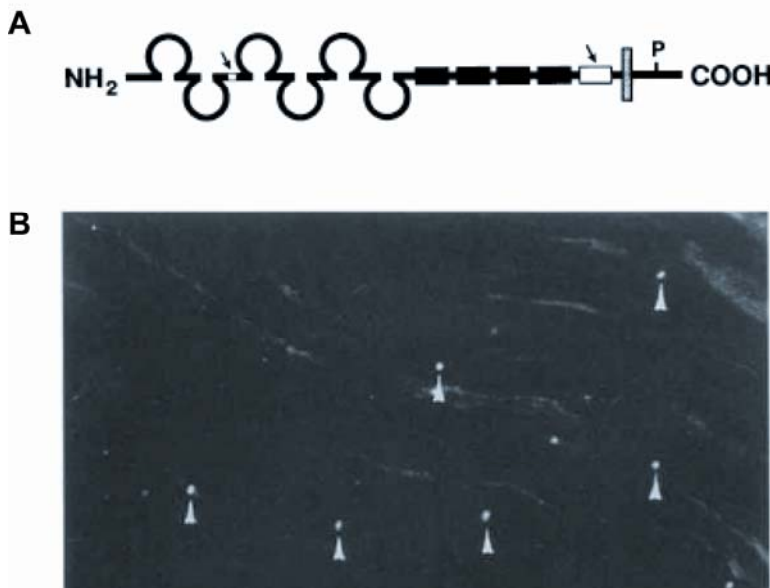


Figure 1.10: NrCAM structure and binding at NoR.

A) Like neurofascin, the extracellular region of NrCAM is comprised of six immunoglobulin domains (represented by loops) and four FNIII domains (black boxes) with a cytoplasmic tail. The white boxes indicate possible splice variants, and P indicates a possible phosphorylation site (modified from Grummet *et al*, 1991). **B)** NrCAM can be localised to the nodal gap (arrows) of rat sciatic nerve NoR (modified from Davis *et al*, 1996).

Contactin and Caspr form a complex in *cis* found at the paranodal junction (Einheber *et al.*, 1997; Menegoz *et al.* 1997; Peles *et al.* 1997; Rios *et al.* 2000). The importance of these proteins to normal paranodal formation are revealed by deficient mice (Bhat *et al.* 2001; Boyle *et al.* 2001), described in more detail below. NF155 also found at the paranode acts as the glial receptor for the axo-glial junction.

Contactin-associated protein, Caspr, is a type I transmembrane proteins (i.e. consists of one transmembrane domain) that belongs to the neurexin family known to be involved in cell adhesion and intercellular communication. As Caspr is a homolog of Neurexin IV found at septate junctions in *Drosophila*, it is perhaps not surprising that it can be found at paranodal junctions that are known to be septate-like (Bellen *et al.* 1998). As reviewed by Poilak and Peles (2003), there are several Caspr proteins and they can bind many CAMs. A number

of domains in the extracellular region are involved in protein-protein interactions (Figure 1.11). Furthermore a 4.1B protein binding domain can be found in the cytoplasmic domain, which links the Caspr/Contactin complex to the cytoskeleton. It has been shown that Caspr acts essentially as a “transmembrane scaffold” by the internalisation of the Caspr/contactin complex caused by the removal of this protein 4.1B binding sequence (Gollan et al. 2002).

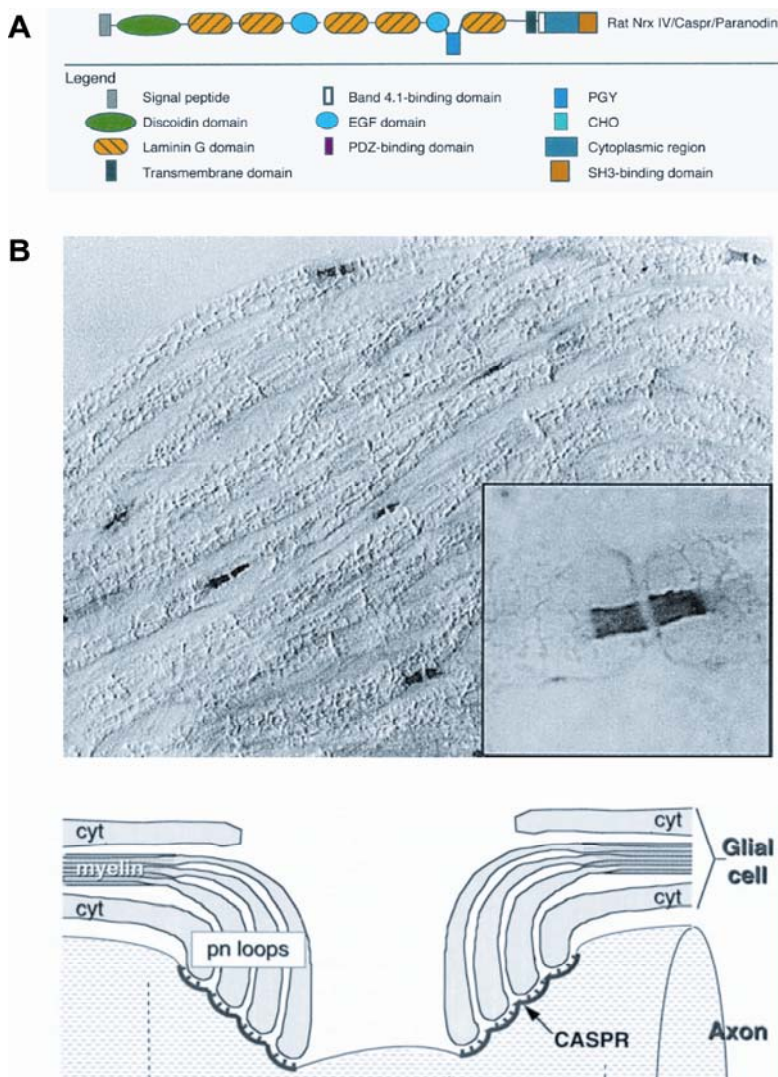


Figure 1.11: Caspr structure and localisation at the paranode.

A) Caspr is a homolog of Neurexin IV molecule of *Drosophila* and is composed of a variety of domains extracellularly as depicted with a 4.1B-binding and SH3-binding domain in the cytoplasmic tail (Bellen *et al*, 1998). **B)** Caspr can be localised in nerve at the paranode as shown immunohistochemically (top) and schematically (bottom, modified from Peles *et al*, 1997).

1.4.4.5 Juxtaparanodal proteins Kv1.1, Caspr 2 and Tag 1

Potassium channel α -subunits consist of only one domain (of six segments similar to Nav channels) that assembles with other α -subunits to form heteromultimeric channels, allowing for a great diversity in these channels. The potassium channels Kv1.1 and Kv1.2 have been localised to the juxtaparanode (Arroyo et al., 1999; Wang et al., 1993). Although the α subunit of Kv1 channels can associate with 2 different β -subunits, it is specifically with the Kv β 2 subunit at juxtaparanodes (Rhodes et al., 1997).

While Caspr is localised to the paranode, Caspr2 is located at the juxtaparanode (Poliak et al., 1999). It consists of a mosaic of domains extracellularly including discoidin, fibrogen-like domains, two epidermal growth factor repeats and four domains similar to a region in laminin A, referred to as the G domain. Caspr2 is co-localised with Kv1.2 immunohistochemistry at the juxtaparanode and its presence in development parallels that of Kv1.2.

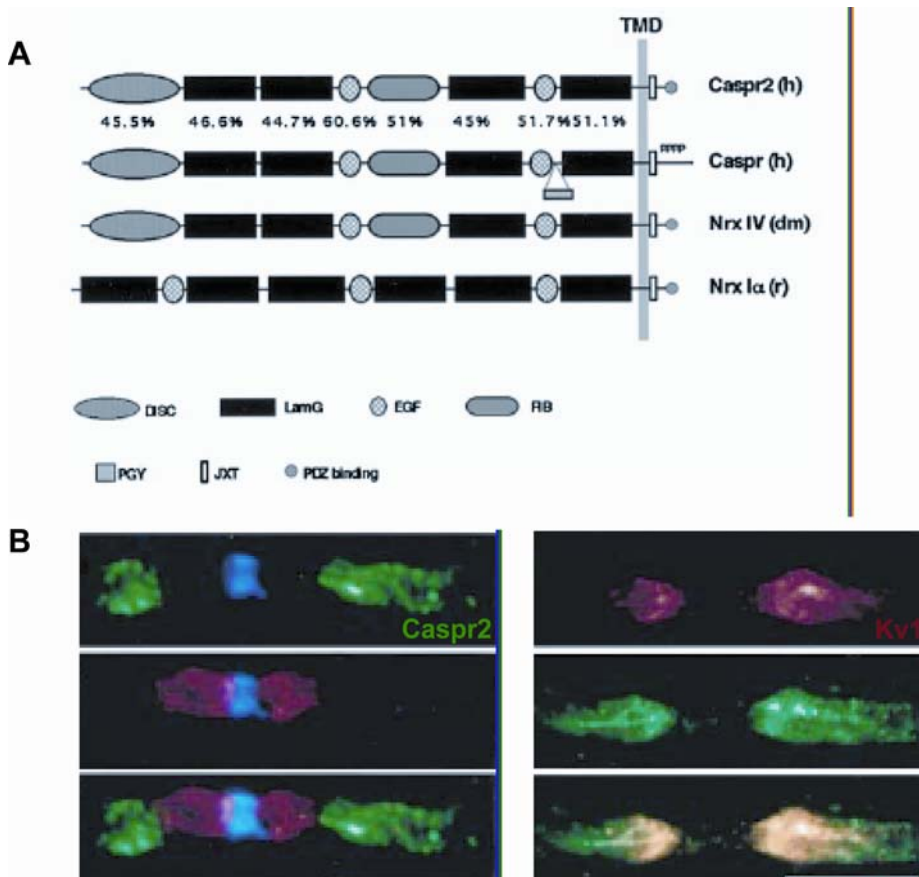


Figure 1.12 (Previous page):Structure of Caspr2 and co-localisation with Kv1 at juxtaparanodes.

A) The various domains of Caspr2 as compared to Caspr and Neurexins. **B)** Caspr2 is similar in structure to Caspr, however staining shows that while Caspr can be identified at the paranode (red), Caspr2 (green) is localised to the adjacent juxtaparanode (*left panel*). Co-localisation occurs with Kv1.2 (red), although Caspr2 staining is more extended (*right panel*). (Modified from Poliak *et al*, 1999).

Tag 1 is a GPI-anchoring member of the Ig superfamily. It is not only expressed by neurons, but by glia as well, and more particularly at the juxtaparanodal axolemma and adjacent Schwann cell membrane (Traka *et al.*, 2002).

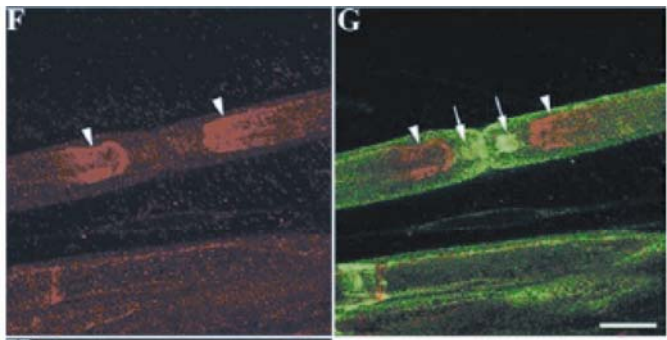


Figure 1.13: Localisation of Tag1 (red) at juxtaparanodes of axons compared to MAG (green) at paranodes. (modified from Traka *et al*, 2002)

1.4.5 Clustering at the NoR

Although it is well known what proteins are expressed at the NoR, until recently it was unclear exactly in what order these specific complexes form. In addition, even though axon initial segments and NoR possess the same protein profile, they do not assemble in the same sequence or to the same cues. An example of this is the requirement of glial signals for NoR formation (Kaplan *et al.* 1997; Melendez-Vasquez *et al.* 2001). A specific series of events are now considered to occur for the formation of the NoR:

1. glia initiate clustering
2. membrane domains are organised via protein-protein interactions

3. all of the proteins present form a complex that maintains the molecules in the correct conformation.

Interestingly this clustering does not seem to be restricted to the axon, but Nav channels, ankyrin G and β -spectrin are also found co-localised in the post-synaptic folds of the neuromuscular junction (NMJ)(Wood & Slater 1998).

As transgenic mice have been highly informative when investigating the importance of ganglioside to nervous system function, the same is true for the study of nodal proteins. Many mutant mice have been created (Table 1.1) and will be discussed below in relation to the information provided about certain protein interactions of the nodal subdomains.

1.4.5.1 Modelling of the nodal gap proteins

Nav channels first accumulate at the end of adjacent myelin sheaths, which on elongation cause the two clusters to fuse and form a node (Lambert et al., 1997;Vabnick et al., 1996;Vabnick & Shrager 1998). Originally, it was thought that intrinsic axonal factors mobilised Nav channels to the NoR as clustering can develop without myelination (Ellisman 1979;Wiley-Livingston & Ellisman 1980). However, glial cells also seem to have a role as shown in several models, the first of which involved the use of Schwann cell-sensory neuron co-cultures developed by Joe *et al* (1992). Vabnick *et al* (1996) demonstrated the necessity of Schwann cells to the development of Nav channel clustering by observing a significant reduction in clusters associated with the attenuation of glial cell proliferation using an antimitotic agent. Rasband *et al* (1999) show that in the CNS, axo-glial contact is required for clustering as not only did Nav clusters become reduced and aberrantly localised, but so did ankyrin G in the *Shiverer* mouse that lack compact myelin and normal axo-glial junctions. Another mutant, the hypomyelinating claw paw (*clp*) mouse, further strengthens the argument for myelin involvement in Nav channel clustering, as in this mutant clustering is delayed in parallel with delayed myelination (Koszowski et al., 1998). England and colleagues (1996) postulate that glial cell contact could

refine structure at the NoR and suppress expression of nodal proteins along the axolemma it ensheaths.

Ankyrin G is also involved in the clustering of Nav channels to the NoR and initial segment. Berghs *et al* (2000) found BIV spectrin at axon initial segments as early as embryonic day 19, and thus proposed a role for this protein known to interact with ankyrin G in the clustering of Nav channels at NoR. At the initial segment Jenkins & Bennett (2001) showed that ankyrin G and BIV spectrin were present 7 days prior to Nav1.6 and the L1 CAMs, NrCAM and neurofascin. Further to this, in mice lacking ankyrin G, Nav channels and neurofascin did not cluster appropriately, and there was an impaired ability to generate action potentials (Zhou *et al.* 1998a), providing evidence that ankyrin G is essential to the correct co-ordination of this complex of molecules at the initial segment. While this is true of the initial segment, ankyrin G presence at the NoR seems to be more dispensable, although it is likely to promote stabilisation after formation (Dzhashvili *et al.* 2007). It is probable that ankyrin G and BIV spectrin mutually co-localise to form an anchor for Nav channels, as clustering of the above mentioned nodal proteins in BIV spectrin null mice does not occur and conduction is impaired, as is the case for an ankyrin G^{-/-} mouse (Komada & Soriano 2002). This complex, however, is preceded by neurofascin and NrCAM at the NoR (Lambert *et al.*, 1997).

A study addressing the issue of whether ankyrin G or neurofascin promote clustering demonstrated that NF is essential to establish PNS NoR as shown by the loss of clustering of all nodal proteins in NFasc-null mice, and death less than a week after birth, a time coincident with the commencement of saltatory conduction in normal mice (Sherman *et al.*, 2005). It was expected that NF186 is the vital nodal isoform as an attempt to save the NF-null mice by expressing NF155 in glial cells did not improve the loss of clustering at the nodal gap. A later report confirmed that NF186 is critical for nodal assembly (driven by Schwann cell signals as clustering did not occur in unmyelinated fibres) and recruits ankyrin G that then localises Nav channels (Dzhashvili *et al.*, 2007). This is in contrast to what occurs at the axon initial segment that develops independently of neurofascin clustering, and is instead reliant on ankyrin G accumulation.

Transgenic name	Manipulation	Phenotype related to node of Ranvier	References
<u>Ganglioside Tg mice</u>			
<i>GalNACT^{-/-}</i>	Prevention of complex gsl synthesis	Normal development, age-related degeneration of myelin, breakdown of axo-glial junction	Takamiya 1996 Sheikh 1999 Chiavegatto 2000 Susuki 2007 Pan 2005
<i>MAG^{-/-}</i>	Myelin-associated glycoprotein deficient		
<i>GD3s^{-/-}</i>	Attenuation of b- and c-series gsl production	Normal except for impaired regeneration after transection	Kawai 2001 Okada 2002
<u>Nodal protein and myelin Tg mice</u>			
<i>Ankyrin G^{-/-}</i> <i>BIV spectrin^{-/-}</i>	Deficient for ankyrin G Deficient for BIV spectrin	Failure for nodal protein clustering and impaired conduction	Komada & Soriano 2002 Zhou 1998
<i>Claw paw (clp)</i>	Unknown mutation	Delay of myelination and appropriate nodal clustering	Kosowski 1998
<i>Motor end-plate disease (med)</i>	Mutation of Nav1.6/ <i>Scn8A</i> gene	Severe muscle atrophy, hind limb paralysis, death	Burgess 1995 Porter 1996
<i>Dystroglycan^{-/-}</i>	Deficient in dystroglycan	Abnormal nerve conduction, microvilli organisation and Nav clustering at the NoR	Saito 2003
<i>NrCAM^{-/-}</i>	Deficient in NrCAM	Delay to nodal Nav channel clustering, normal thereafter	Custer 2003
<i>Caspr^{-/-}</i> <i>Shiverer (Shi)</i>	Caspr deficient Natural mutation to myelin gene	Disruption/loss of axo-glial junction. Failure to switch nodal Nav isoform	Rasband 1999 Rios 03 Boiko 2001
<i>Contactin^{-/-}</i>	Contactin deficient	Disruption of transverse bands and axo-glial junction clustering	Boyle 2001
<i>Neurofascin^{-/-}</i>	Deficient in neurofascin	Loss of nodal clustering, death by P7	Sherman 2005
<i>Caspr2^{-/-}</i> <i>Tag1^{-/-}</i>	Caspr2 deficient Tag1 deficient	Mislocalisation of Kv1 channels at juxtaparanode	Poliak 2003 Traka 2003

Table 1.1: Transgenic mouse strains

This study also demonstrated that the sequence responsible for initial segment targeting of NF186 is found on the cytoplasmic domain, as omission of this sequence or substitution with non-polarised proteins attenuated clustering. Conversely, this effect was not repeated for NoR, which suggests that the extracellular domain is sufficient at this location. It was confirmed that the Ig domain specifically is required for NF186 targeting to the NoR by various deletions to the Ig, FNIII or mucin domains. A specific FIGQY sequence found in the cytoplasmic domain that binds ankyrin G, had previously been speculated to affect distribution of NF186 to cell membranes (Zhang et al., 1998). Concentration of proteins at the NoR coincides with a down-regulation along the internode (Dzhashvili et al., 2007).

NrCAM is also involved in node formation (Custer et al. 2003; Lambert et al., 1997). However, while NFasc-null mice are not viable past birth, NrCAM-null mice have essentially normal nodes aside from a delay in clustering of Nav channels (Custer et al., 2003). This suggests that NrCAM is not as critical for NoR clustering and that it can not compensate for a loss of NF186 even though both bind ankyrin G. Once it had been established that NF186 was the first axonal protein to cluster at the NoR, attention turned to what caused this to occur. Eshed *et al* (2005) have found a Schwann cell binding partner for NF186 in the form of gliomedin, which could mediate the formation of proteins at the NoR. Gliomedin was shown to be present at the edges of myelinating Schwann cells during development, while in mature axons it is found in Schwann cell microvilli that project into the nodal gap. When interference RNA (RNAi) was used to attenuate gliomedin expression, myelin sheaths form but Nav channels do not cluster. This represents the possible requirement of gliomedin and/or Schwann cell microvilli for NF186 to cluster correctly and recruit Nav channels to the NoR (Figure 1.14). Additionally, a dystroglycan^{-/-} mouse has been used to show that this protein, also expressed by Schwann cells, is essential to normal nerve conduction, microvilli organisation and nodal sodium channel clustering (Saito et al. 2003). The authors propose that this is due to its role in maintaining the nodal architecture via interactions between the SC microvilli and axolemma, reinforcing the importance of this structure.

1.4.5.2 Formation of the axo-glial junction

Although *Caspr*^{-/-} and *contactin*^{-/-} mice show that these proteins and normal transverse bands are not required for initial Nav channel clustering at the NoR, they are essential for creating a barrier that maintains Kv1 channels at the juxtaparanode (Boyle et al., 2001). Mice that have been modified to lack enzymes that produce galactolipids of the myelin sheath have strikingly similar paranodal phenotypes to the aforementioned KO mice. This can be explained by the requirement at the paranode of *cis*-interactions between NF155 and galactolipids to stabilise this junction (Schafer & Rasband 2006). *Shiverer* mice that lack myelin associated glycoprotein (MAG) have abnormal paranodal junctions, *Caspr* and NF155 localisation (Rasband et al. 1999; Tait et al., 2000). NF155 extracellular domain binds to the *cis* interacting *Caspr*/contactin complex in cells transfected with both, but doesn't bind cells transfected with contactin alone (Charles et al., 2002). As some NF155 has still been detected at paranodal loops in *Caspr* and *contactin* null mice, it is possible that these proteins do not target the neurofascin to this location, but neurofascin instead has a role in recruiting them (Sherman et al., 2005). Recently it has been reported that *Caspr* clustering occurs after myelination in the PNS and that NF155 is required for this to occur (Eisenbach *et al*, 2009, Epub ahead of print).

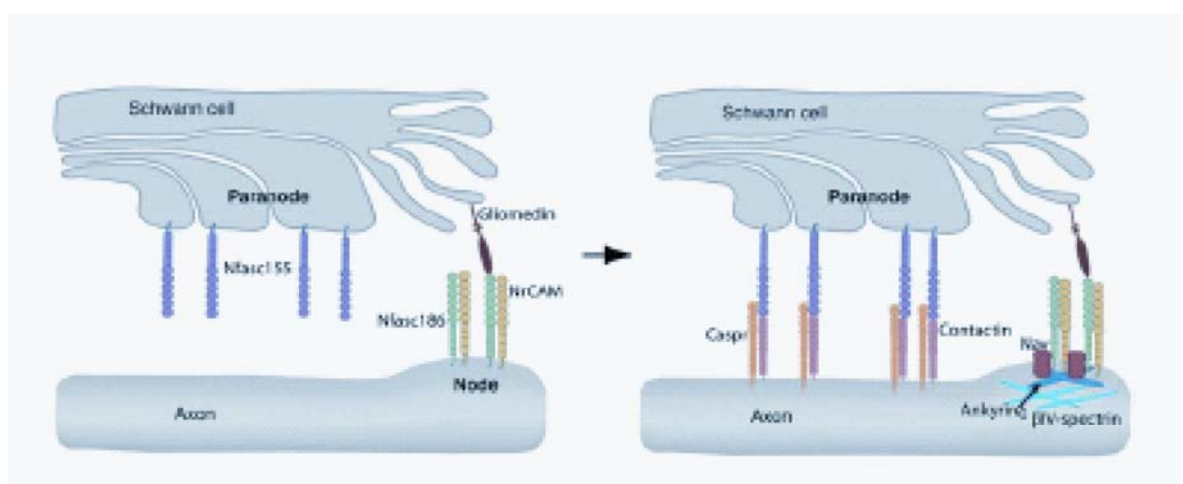


Figure 1.14: Schematic representing the possible role of gliomedin and NF interactions to the initial formation and clustering of proteins at the PNS NoR (taken from Sherman *et al*, 2005).

A further study highlighting the importance of myelin to the formation of the axo-glial junction is that of Ishibashi *et al* (2004). CD9 is a membrane glycoprotein found in myelin and appears concomitantly with Caspr at the latter stage of myelination during development. KO mice for this protein show diffuse labelling through internode and a disruption of axo-glial junction.

At the paranode and juxtaparanode, the protein 4.1B is likely to be responsible for the anchoring of Caspr and Caspr 2, respectively, as it is highly enriched here (Denisenko-Nehrbass *et al.* 2003). Binding, is via a common intracellular GNP motif, as this is prevented by deletion of this sequence.

The importance of the axo-glial complex as a sieve for the prevention of bilateral movement of ion channels and other molecules at the NoR is discussed in more detail by Pedraza and colleagues (2001). All of the above studies emphasise the importance of this complex and the reason behind such a severe phenotype of the neurofascin knock-out mice, as without this complex, which is initially formed by neurofascin, function is lost.

1.4.5.3 Juxtaparanodal development

Although Caspr2 and Kv1 channels are co-localised to the juxtaparanodal membrane, their association is not direct. Caspr2 antibodies were used to detect proteins with which it would co-immunoprecipitate and it was found that association was with Kv1.2 and the Kv β 2 subunit, but not Kv2.1. However, as these proteins did not seem to form a complex in cell culture, it was suspected their may need to be a common binding protein. Similarly to Caspr, Caspr2 possesses a protein 4.1B binding domain in its cytoplasmic tail, therefore it could link the potassium channel/Caspr2 complex to the juxtaparanodal cytoskeleton (Gollan *et al.*, 2002). Thus, Caspr2 association with the juxtaparanode has been linked to its PDZ binding sequence in its C-terminal tail and interaction with cytoskeletal protein 4.1B. An investigation into Kv1 channel localisation strongly implicated binding to PDZ domains on PSD95 as well. Using the C-terminal tail of shaker Kv1.4 channel as 'bait', Kim *et al* (1995) revealed that these channels are anchored by the association of their carboxy-terminus

with PDZ domains 1 and 2 of the PSD95 protein. Particularly, the final 4 a.a. were essential for binding as shown by progressive deletion analysis. These results could be repeated for Kv1.1, 1.2 and 1.3. To further confirm their association, Kv1 channels and PSD95 were expressed individually or together in cell culture. There was a striking difference in distribution, both were diffuse at the membrane or through the cytoplasm when alone, but co-clustered to the cell surface in distinct patches when together. However, more recently contradictory studies by Rasband *et al* (2002) and Horresh *et al* (2008) have shown that although the potassium channel and PSD95 protein can be co-localised at the juxtaparanode, mutant mice lacking this cytoskeletal protein do not suffer a loss of Kv1 or Caspr2 clustering. As it had been expected that PSD95 mediated the indirect interaction of the clustering of the Kv1 channels and Caspr2 to this particular site, instead another molecule in the form of Tag1 is required (Figure 1.15).

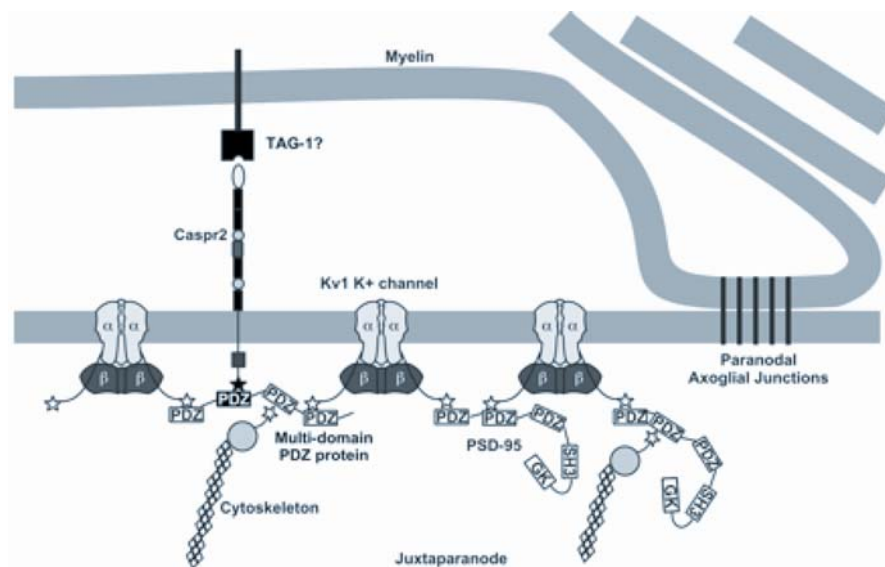


Figure 1.15: Proposed mechanism of clustering of Kv1 at the juxtaparanode via a Caspr2 and Tag-1 complex (Rasband *et al*, 2002).

Kv1 channels require a Caspr2/Tag1 scaffold for correct localisation as demonstrated by mislocalisation of the ion channel in Caspr2 KO and Tag1 KO mice (Poliak *et al.*, 2003; Traka *et al.*, 2003). The conformation for this is proposed to be a glial Tag1 molecule forming a juxtaparanodal complex with an

axonal Caspr2/Tag1 heterodimer. There is no detectable interaction between Tag1 and Kv1.2 alone, suggesting the requirement of both Tag1 and Caspr2 and possibly other adaptor proteins to complex with Kv1 channels. Mutants for paranodal proteins contactin and Caspr show the importance of the barrier between paranode and juxtaparanode to the appropriate placement of Kv1 channels and Caspr2 (Bhat et al., 2001;Boyle et al., 2001).

1.4.5.4 Importance of correct nodal protein localisation

The above studies demonstrate the similar yet unique interactions between molecules in each specific nodal domain. Mutant mice show the importance of each of the proteins to developing and maintaining the correct nodal architecture. Interestingly it would seem that the key structure is that of the paranode, as disruption of this structure causes mislocalisation of proteins from all domains, whereas transgenic mice lacking proteins from the other domains manage to develop normally aside from their direct interactions.

1.4.6 Nodal Pathology associated with GBS

As NoR are not ensheathed they are more vulnerable to circulating antibody. As discussed above, GM1 and GD1a have been localised to the NoR and therefore it is of interest to determine what injury occurs at this region in response to anti-ganglioside antibodies and if it could be linked to that observed under pathological conditions in patients. Many electrophysiological studies were undertaken to establish whether antibodies binding to gangliosides could directly effect conduction by this route. Under certain conditions, anti-GM1 antibodies appear to increase potassium current or reduce sodium current in the sciatic nerve (Takigawa et al. 1995).

Further studies have attempted to determine the role gangliosides have in nodal stability, and ion channel disruption at nodes in models of AMAN (Susuki et al. 2007b;Susuki et al. 2007a). There are two routes in which gangliosides can cause conduction failure, and therefore paralysis, in AMAN patients- conduction block

and axonal Wallerian-like degradation. Conduction block is reversible and explains rapid recovery that is not consistent with remyelination or regeneration (Kuwabara et al. 1998). Axonal degradation is most likely due to complement-mediated attack of the axons (Hafer-Macko et al., 1996). It is possible that in some cases both mechanisms are occurring. Conduction failure would be due to distal axonal degeneration and also antibody binding and complement activation at nodes, which would explain conduction failure and paralysis, yet rapid recovery (Ho et al. 1997). A mouse model of GBS has been used to show that the nerve terminal at the NMJ undergoes severe damage and massive exocytosis of vesicles rendering it non-functional (Bullens et al. 2000; O'Hanlon et al. 2001). This too could perhaps explain paralysis in patients that could result in rapid recovery, or not depending on whether injury proceeds further along the axon.

1.4.6.1 Electrophysiological studies using anti-ganglioside antibodies

Electrophysiological data regarding the effect of anti-ganglioside antibodies on conduction in animal models has been quite contradictory. Thomas *et al* (1991) injected rabbits with GM1 or with Gal(β1-3)GalNAc-BSA, and reported the development of antibodies to the immunizing antigens in association with a fall in the ratio of the amplitudes of the compound muscle action potential evoked by proximal versus distal stimulation of the sciatic nerve. Mild axonal degeneration was also observed in the peripheral nerve and immunoglobulin deposits were prominent at nodes of Ranvier. Therefore it was expected that anti-ganglioside antibody binding at the NoR would result in conduction block.

Several other *in vitro* studies supported these results showing block of conduction in rat sciatic nerves exposed to patient sera with high anti-ganglioside antibody titres (Arasaki et al. 1993; Arasaki et al. 1998; Santoro et al. 1992). However, Harvey *et al* (1995) found that the intraneural injection of patient sera into rat nerve did not cause conduction block or histological changes even though antibody deposits could be found bound to the nodal axolemma and sometimes the paranodes. This was also true for mouse nerve treated *in vitro* with anti-ganglioside antibodies (Paparounas et al. 1999).

1.4.6.2 Disruption to nodal proteins in response to anti-ganglioside antibodies

The disruption to nodal proteins under GBS conditions has best been described in a rabbit model of AMAN with high anti-GM1 antibody titres (Susuki *et al.*, 2007b). In this model Nav channel clustering disappeared or was disrupted, as were the other structures (paranode, Schwann cell microvilli, nodal cytoskeleton) that normally maintain the ion channel localisation. As this disruption was coincident with complement product deposition (Figure 1.16), it followed that use of a complement inhibitor prevented these effects (Phongsisay *et al.* 2008).

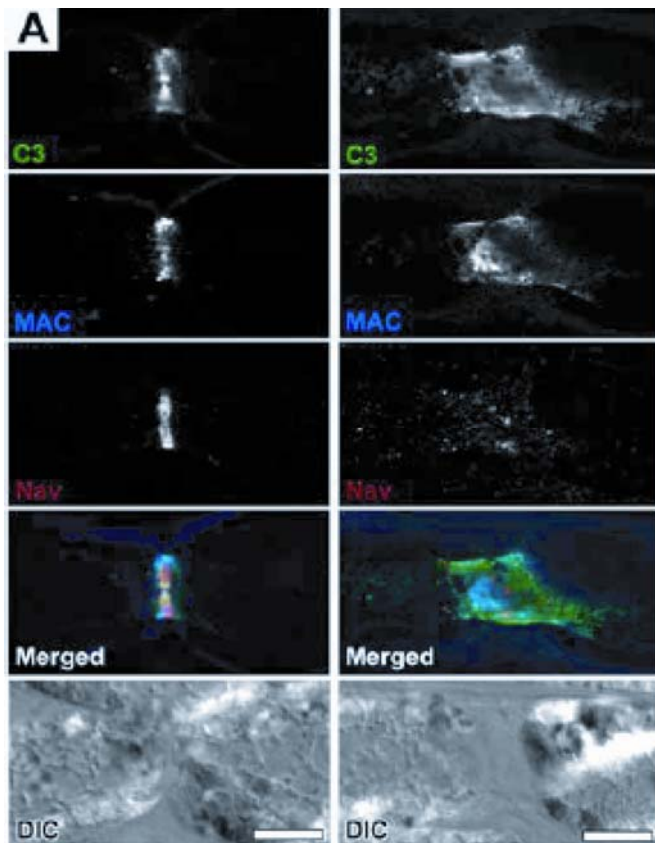


Figure 1.16: Disruption of Nav channel staining at ventral root NoR of AMAN rabbits coincides with extended complement deposition (taken from Susuki *et al.*, 2007).

Similarly, disruption to certain nodal proteins has been reported in models of the demyelinating variant AIDP. Lonigro and Devaux (2009) recently showed that

neurofascin and gliomedin disruption preceded demyelination, which would explain conduction block considering that complement was not associated with injury to the NoR.

1.5 Animal models of AMAN

1.5.1 Rabbit models of AMAN

The first animal model that resembled GBS was experimental allergic neuritis (EAN), which was created by injecting rabbits with peripheral nerve homogenate (Waksman & Adams 1955). Rabbits developed an inflammatory disease of the peripheral nerves, therefore it is akin to AIDP rather than AMAN. This model will not be further discussed due to the focus of this study on the the non-inflammatory AMAN subtype.

Developing a model to AMAN was first successful with the repeated injection of either bovine brain gangliosides (BBG, a mixture consisting of 21% GM1, 40% GD1a, 16% GD1b and 19% GT1b), or GM1 ganglioside alone into Japanese White (JW) rabbits with Freund's adjuvant (FA) and keyhole limpet hemocyanin (KLH) (Susuki et al. 2003; Susuki et al. 2004; Yuki et al. 2001). Rabbits showed limb weakness and flaccid paralysis, and inspection of tissue revealed Wallerian-like degeneration of sciatic nerves (not spinal roots), macrophage infiltration of endoneurial-perivascular areas, and anti-GM1 antibody titres. As there was no effect on the central nervous system, it would seem that antibodies are able to cross the blood-nerve barrier (BNB) but not the BBB.

Other groups have not been so successful when trying to recreate rabbit models of AMAN. When Ang *et al* (2001) immunised New Zealand white (NZW) rabbits with LPS from three strains of *C. jejuni* with FA the animals produced titres high for anti-GM1 antibody but did not develop flaccid paralysis or show signs of neuropathy or inflammation on examination of the sciatic nerve. On the addition of KLH to the above immunization protocol, Caporale *et al* (2006) were successful in recreating disease in NZW rabbits as observed by Yuki *et al* (2001,

2004) and Susuki *et al* (2003) in JW rabbits. They attribute this to the action of KLH, which seems to play a crucial role although the specific mechanism is unclear. KLH is usually used to enhance an immune response, but it has also been shown to produce low titres of anti-GM1 antibodies itself, probably owing to the fact it possesses oligosaccharides with Gal(β 1-3)GalNAc groups (Wirguin *et al.* 1995). Wirguin and colleagues (1997) later predicted that as gangliosides are poor immunogens, a glycoprotein antigenic stimulus (as found in KLH) can induce B-cells reactive to ganglioside but which were not activated. From all of the studies mentioned above an interesting observation is that anti-ganglioside antibodies can indeed be induced, but only under certain circumstances do they result in pathology, by an as yet undefined mechanism.

1.5.2 Mouse model of AMAN

There have been problems in transferring the AMAN model into rats and mice, as injection of gangliosides or antibodies does not lead to paralysis. It could be that rodents have a less permeable BNB. However, studies performed to test the permeability of the mouse BNB to various molecules have shown that small molecules such as sodium fluorescein permeate with ease (Malmgren & Olsson 1980), whilst larger IgG molecules take longer, but can still partially cross into the endoneurium (Seitz *et al.* 1985). Implantation of an anti-GD1a/GT1b antibody producing hybridoma into mice resulted in the development of a mild peripheral neuropathy with similar features to AMAN (Sheikh *et al.* 2004). The BNB became leaky and antibody could be found in the endoneurium, which was thought to be due to a systemic inflammatory response to the hybridoma. This led to the postulation that a good mouse model requires circulating antibodies *and* access to the gangliosides.

1.5.2.1 Use of ganglioside transgenic mice in a murine GBS model

Genetic modification has also proven a useful tool in progressing an AMAN-like lesion in mice. Injection of gangliosides or epitopes from ganglioside mimicking strains of *C. jejuni* into mice may have proven unsuccessful due to the problem

of evolutionary conservation across species, and tolerance (Bowes et al. 2002). As gangliosides are present from birth the body develops tolerance to their structures in order that the immune system will not attack them. In addition, there is also a difficulty in developing mouse monoclonal antibodies against gangliosides as their injection does not elicit a normal response and antibody production (Kawashima et al., 1992; Kotani et al. 1992). To circumvent this problem, mice engineered to lack complex gangliosides (see Figure 1.3) (Liu et al. 1999; Takamiya et al. 1996) have been used to develop high affinity antibodies against injected gangliosides (Lunn et al. 2000).

Subsequently much work has been carried out using these antibodies in mice to establish localisation of gangliosides, and the effect of antibody binding to nerve. High affinity antibodies against GQ1b have been used to cause a lesion of the axon and perisynaptic Schwann cells at motor nerve terminals in the diaphragm of mice in *ex vivo* preparations or after intra-peritoneal (i.p.) immunization with normal human serum as an additional source of complement (Halstead et al. 2004). However, antibodies against other complex gangliosides do not have the same effect in wild-type mice. Conveniently, a mouse developed to uncover the role of b- and c-series gangliosides by disrupting the gene encoding α -2,8-sialyltransferase enzyme, concomitantly resulted in the over-expression of a-series gangliosides (see Figure 1.3) (Okada et al. 2002). This model seems to overcome the problem of tolerance, probably due to such a high expression of antigen. Consequently this GD3s^{-/-} mouse has enabled the creation of an experimental paradigm where a robust reaction develops in response to antibodies against a-series gangliosides GM1 and GD1a Figure 1.17 (Goodfellow et al. 2005; Greenshields et al., 2009). More specifically the hemidiaphragm preparation has been used to study IgG and membrane attack complex (MAC) deposition, and neurofilament loss at the nerve terminal produced by application of anti-ganglioside antibody and complement. Electrophysiological recordings made under the same conditions show a massive increase in asynchronous spontaneous neurotransmitter release at the NMJ, ultimately ending in a block to synaptic transmission. Development of the mouse model of AMAN by injection of antibodies is yet to be achieved, although it is possible to cause injury to the diaphragm by the i.p. injection of anti-GD1a

antibody and complement into a transgenic mouse over-expressing gangliosides and lacking complement inhibitors (JA Goodfellow, unpublished observation).

1.5.3 Transgenic mice expressing fluorescent proteins

Although the models described above are useful, staining requires the tissue to be exposed to toxic agents, antibodies and permeabilising solutions. This fact, along with general unreliability of some cell labelling, has resulted in the production of mice engineered to have intrinsic fluorescence of certain structures.

Green fluorescent protein (GFP) is a polypeptide chain that is intrinsically fluorescent. Prasher and colleagues (1992) were the first to sequence the green fluorescent protein found naturally in jellyfish. The possibility that transferring this cDNA sequence into eukaryotic cells would cause GFP expression and could be a marker of gene expression was first demonstrated by Chalfie *et al* (Chalfie *et al.* 1994). Therefore if it is coupled to cell-specific promoters it can be expressed in any cell type. The importance of this discovery to the advancement of science has since been recognised by the award of the Nobel prize in Chemistry for 2008 to the researchers involved.

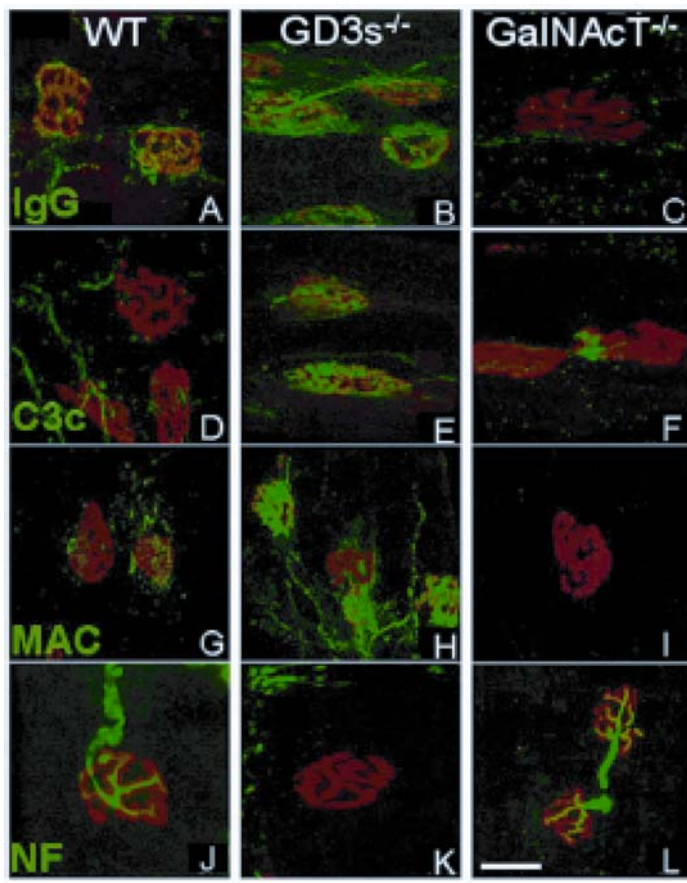


Figure 1.17: Anti-ganglioside antibody binding at the NMJ of *wild type* mice compared to those genetically modified to over-express ($GD3s^{+/-}$) or completely lack complex gangliosides ($GalNAcT^{-/-}$).

Alteration of ganglioside expression in mice affects the binding ability of anti-ganglioside antibodies, and in turn the development of complement-dependent neurofilament injury at the nerve terminal (modified from Goodfellow *et al*, 2003).

It is advantageous for cells to endogenously express fluorescence as no disruption of the cell membrane is necessary to visualise the desired cell in live or processed tissue. Furthermore, characterisation of development, degeneration, or regeneration of the nervous system can be improved as the same tissue can be imaged at different stages in the same live mouse as the tissue does not need to be removed and processed. Mice have been engineered to express a variant of GFP, CFP, in axons (coupled to the *thy-1* promoter) (Feng *et al.* 2000), and GFP in their Schwann cells (coupled to the S100B promoter) (Zuo *et al.* 2004). These so-called CK mice, have been used to follow the reinnervation of muscle guided by terminal Schwann cells after nerve injury, by imaging terminals at several time-points (Kang *et al.*, 2003). Currently much work at the NMJ utilises the post-synaptic marker bungarotoxin that binds acetylcholine receptors localised here. This is extremely convenient for

identifying this region as its staining profile does not change under injurious conditions. In the future, the fluorescent model could be put to use to better localise and study axons proximal to the terminal during degeneration in AMAN models.

1.6 Complement and GBS

From the previous sections it is apparent that anti-ganglioside antibodies tightly correlate with GBS. Further to this, complement is also a key component of the injury pathway. Where antibodies have been detected in animal models and human tissue, complement products are also present and associated with pathology (Goodfellow et al., 2005; Hafer-Macko et al., 1996; Halstead et al., 2004; Koski 1990; Lu et al. 2000; Putzu et al. 2000; Sanders et al. 1986; Susuki et al., 2007b; van Sorge et al. 2007). The work of Halstead *et al* (2004) underscored the activation of complement via the classical pathway (i.e. antibody-dependent pathway) to induce injury in a mouse model of anti-GQ1b antibody associated nerve terminal degeneration. The necessity for complement in turn highlighted the possibility of therapies that interfere with this pathway. In order to determine potential targets it is important to first understand the components of the complement cascade.

1.6.1 Complement cascade

The body possesses an innate and an acquired immune system that work together to eliminate invading pathogens. The complement system was originally named because it supported and interacted with (i.e. complemented) the acquired immune system when an antigen was recognised by antibody. It is now known to interact with the innate pathway as well. There are many antibody isotypes of which the IgG1 and 3 isotypes are most effective at activating the classical pathway, while of the IgG subclass IgG2 better activates the alternative pathway (Valim et al., 1991). The density of epitope also contributes to the activation of complement by antibody binding.

1.6.1.1 Complement components

The complement system consists of serum glycoproteins, regulatory proteins and complement receptors. C3 is considered to be the critical component of the complement system, as its conversion into C3b by C3 convertase, is the point from which many essential immunological processes occur (as reviewed by Morgan 2000). The activation of C3 by the classical pathway begins with the binding of C1q to antibody that produces the serine protease C1r to cleave C1s. The complex of these three molecules splits C2 and C4 so that their component parts make a C4b2a complex- also known as C3 convertase (Figure 1.18, shaded area). This is where the classical pathway ends and the alternative pathway begins, ultimately resulting in the membrane attack complex lysis of the target cell.

1.6.1.2 Membrane attack complex

MAC is the terminal stage of the complement cascade. Five hydrophobic serum glycoproteins (C5b, C6, C7, C8 and C9) associate to form the MAC pore. This begins with the cleavage of C5 by C5 convertase to form C5b which forms a complex with soluble C6. This complex then binds C7 resulting the membrane-binding capacity of this molecule to be revealed. C8 also develops the ability to insert into the membrane on binding to the C5bC6C7 complex. The C5b-8 complex recruits ten or more C9 molecules that complete the pore. All molecules that are of the right size can freely diffuse through the pore, especially water courtesy of the hydrophilic inner pore surface, which disrupts the internal milieu resulting in rapid cell lysis.

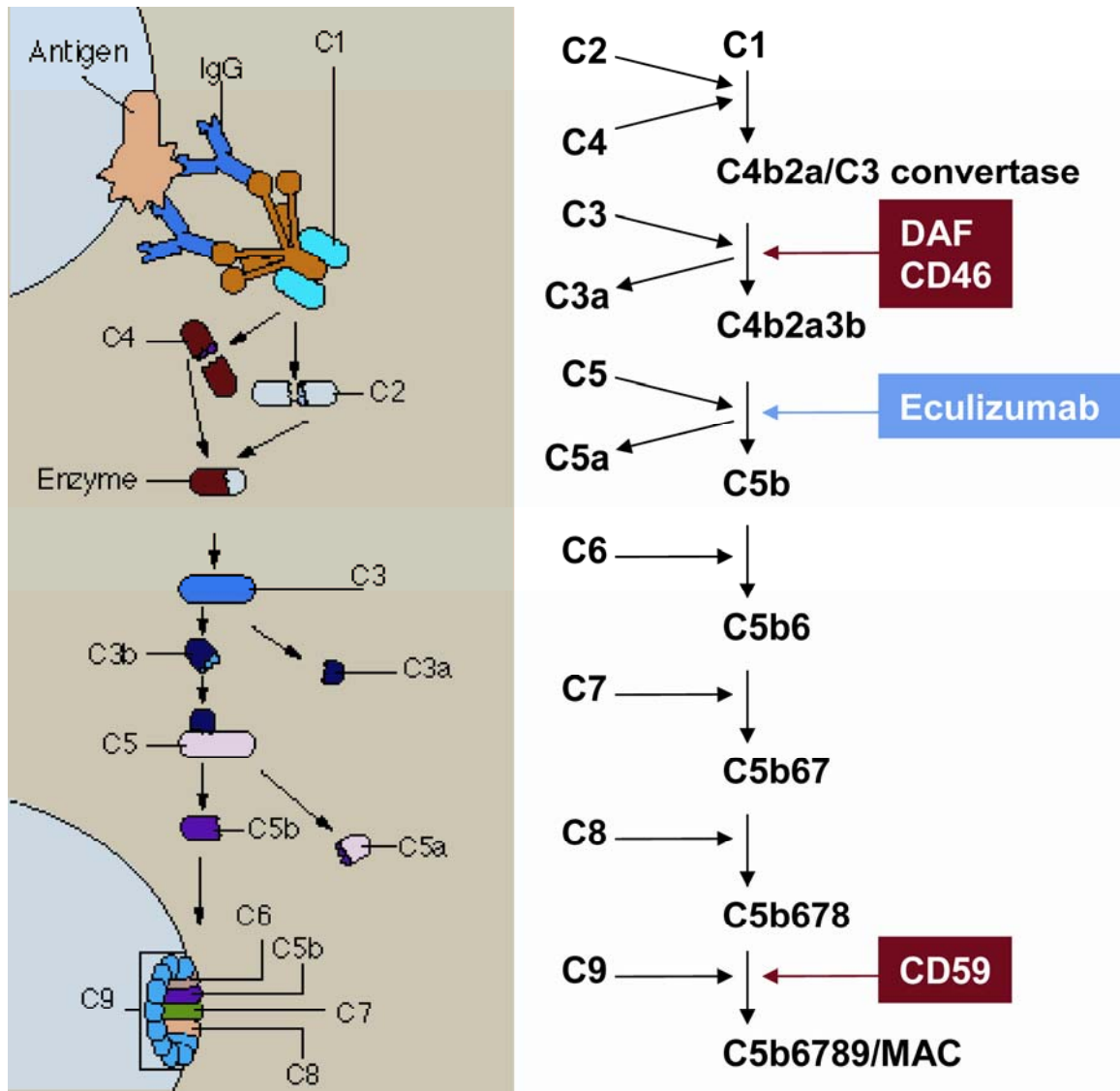


Figure 1.18: Classical pathway of the complement cascade.

The pathway components and their step-wise addition and interactions are represented on the right. The points of intervention of the endogenous inhibitors DAF, CD46 and CD59 (red) and the synthetic inhibitor Eculizumab (blue) are shown. The events of the pathway culminating in MAC pore insertion into a cell membrane are illustrated to the left (Image taken from the National Cancer Institute website).

The complement system has a role in host defence via processes such as phagocytosis, antibody response, inflammatory response and cell lysis. To circumvent damage by over-activation, certain regulatory molecules are also present, discussed below. Keeping the complement system in check is very important as dysregulation and deficiencies can manifest themselves in the form of many diseases. Consequently, the regulation of complement therapeutically is a major focus of research (Morgan & Harris 2003).

MAC pore mediated lysis was first demonstrated in sheep erythrocytes, where as little as one could cause osmotic swelling and cell lysis. Nucleated cells are far more resilient and require many complexes for cell lysis (Koski et al. 1983). However these complexes are transient and are continually removed by exocytosis and endocytosis in a partly calcium dependent manner (Carney et al., 1986).

1.6.1.3 Role of complement

Complement can be beneficial as, for example, it is essential to the activation of macrophages during Wallerian degeneration after peripheral nerve injury that normally clear away the debris and promote axonal regeneration (Dailey et al. 1998). This correlates to macrophages observed in GBS patient post-mortem tissue (Griffin et al., 1996a). A review by Morgan *et al* (1986), discusses the concept that there is a threshold of MAC injury. Below this threshold, the Ca^{2+} influx due to mild complement attack activates inflammatory mediators involved in the inflammatory response allowing for recovery. However, severe complement attack and MAC formation above this threshold overwhelms the cell's recovery processes resulting in death.

It was hoped by Uetz-von Allmen *et al* (1998) that a correlation could be made between peripheral neuropathy, antibodies and complement in order to use MAC binding of antibodies as a diagnosis. However, although some GBS patient sera had high complement binding capacity, there were some that did not, so this method could not be used for accurate diagnosis.

MAC pore formation is essential to pathogenesis observed in mouse injury models, as described by Willison *et al* (2008). It is however, possible that there is a role for the other components of the complement pathway to injury in the long term.

1.6.2 Complement inhibitors

The complement system is very effective at targeting and destroying invaders to the host, however there is also the potential for damage to self cells. To prevent this occurring, self cells are protected by the expression of a variety of membrane regulators that can inhibit complement activation. It is debateable whether these inhibitors are species specific or not (Morgan 1999;Rollins et al. 1991). The three membrane regulators important to complement activity attenuation are membrane cofactor protein (MCP; CD46), decay accelerating factor (DAF; CD55) and CD59, described in more detail below.

1.6.2.1 Endogenous complement inhibitors

CD59 is a membrane glycoprotein with a GPI anchor that specifically protects cells from lysis by the MAC pore (Davies et al. 1989;Meri et al. 1990a;Meri et al. 1990b;Rollins & Sims 1990). CD59 regulates complement by inhibiting the formation of MAC by binding both C8 α , and C9 to prevent C9's association with the C5b678 complex Figure 1.18 (Davies et al., 1989;Huang et al. 2006;Ninomiya & Sims 1992;Rollins & Sims 1990). Initially described on erythrocytes and lymphocytes, it is present on a variety of self cells to prevent their damage by MAC (Meri et al., 1991). CD59 present on compact myelin lipid rafts in peripheral nerve (Erne et al. 2002).

DAF regulates complement by preventing the assembly of C3 convertase, or accelerates the disassembly of already formed C3 convertase, and thus blocks the development of MAC (Fujita et al. 1987). Similarly, CD46, a type I transmembrane protein, regulates complement by inactivating the C3b and C4b components of the complement pathway (Liszewski et al., 1991). Both are depicted in Figure 1.18.

As discussed by Chrast *et al* (2004), mouse peripheral nerve not only has the potential to activate the classical pathway by expressing C3 one of the initial components, but also to attenuate the reaction by the expression of complement inhibitors DAF, CD59. KO mice for these regulators have been very informative as to their function (Turnberg & Botto 2003). Particularly to GBS,

the use of CD59 KO mice in a mouse model of anti-ganglioside antibody mediated injury at the NMJ demonstrated the importance of this regulator in the control of MAC (Halstead et al., 2004). This transgenic mouse has also shown exacerbation of neuronal cell death in a mouse model of traumatic brain injury further illustrating a role for this inhibitor in protection against injury (Stahel et al. 2009).

1.6.2.2 Synthetic complement inhibitors in animal models

In the murine nerve terminal disease model of GBS, great success has been achieved in attenuating injury by way of various complement inhibitors (as reviewed by Willison et al. 2008). Recently similar results in the rabbit model of AMAN have been reported (Phongsisay et al., 2008).

APT070 is a C3/C5 convertase inhibitor modelled on the endogenous CR1 regulator and is effective at abolishing MAC deposition at the nerve terminal in a model of MFS (Halstead et al. 2005). More recently, Eculizumab a humanised mAb which neutralises the C5 component (Figure 1.18), and rEV576 a C5 inhibiting recombinant protein from tick saliva have also been used to prevent MAC pore formation in this model (Halstead et al. 2008a; Halstead et al. 2008b).

A confounding issue with the mouse model is the requirement for an exogenous source of complement to induce pathology. Antibodies used are capable of fixing mouse complement, therefore it was suspected that inhibitory factors must be present. Mouse complement regulators include complement receptor-1 related gene/protein Y (Crry), CD59a, decay accelerating factor 1 (DAF1, CD55) and Factor H. CD59a has been detected at the nerve terminal, but as the regulation of human complement by murine regulators has not been established, the significance of this is unclear (Willison et al., 2008). However, there is a benefit of using a human source of complement- inhibitors intervening with complement activation that would be applied to human cases can be directly tested for their efficacy in the mouse (e.g. Eculizumab, a humanised mAb).

1.7 Calpain

It was suspected that MAC pores and the influx of calcium ions would activate calpains resulting in injury to the terminal via this route (O'Hanlon et al. 2003). Therefore, it is of interest to know more about calpains and possible blocking agents.

Calcium plays a vital role in mediating complement and in cell death. Calcium ionophores when inserted into the cell membrane cause an influx of calcium that results in cell death. It is known that calcium and not the ionophore is responsible as insertion in a calcium free media does not result in death. One of the routes of calcium mediated injury is likely via calpain.

Calpains are ubiquitously expressed Ca^{2+} -activated neutral cysteine proteases first described in the rat brain by Guroff (1964). There are two major isoforms of calpain that *in vitro* require either micromolar (μ -calpain/calpain I) or millimolar (m-calpain, calpain II) concentrations of calcium to be activated. They are best associated with regulatory processes. Calpains are ubiquitously expressed, largely cytosolically, and are regulated by the endogenous inhibitor calpastatin.

1.7.1 Structure and activity of calpain

As summarised by Goll *et al* (2003), both μ - and m-calpain consist of two subunits (28kDa and 80kDa), of which the large proteolytic subunit differs between the two calpains, while the small regulatory subunit is the same. The active site cysteine is found in the large subunit in domain II and domain IV is the region responsible for Ca^{2+} binding. The small subunit consists of an N-terminal and C-terminal domain linked by a proline rich sequence, which are involved in membrane association and calcium ion binding, respectively. Both calpains are widely distributed, but their abundance differs from tissue to tissue. Calpain undergoes autolysis of the small subunit in the presence of calcium ions, but only large subunit of μ -calpain and not m-calpain is autolysed (Saido et al. 1994). In fact, the subunits are resistant to any kind of proteolysis until they are activated, at which time they are quickly degraded.

As the first calpain studies showed that m-calpain required 400-600 μ M concentrations of calcium ions to be activated, which well exceeds the natural concentration found in cells, it was expected that a molecule existed that would reduce the required activating concentration. One study by Thompson *et al* (2000) proposed that μ -calpain could fill this role on account of the fact that it is able to self-autolyse and the large subunits share 50% homogeneity. However, the conformation must be sufficiently different as μ -calpain was unable to activate m-calpain. It is still unclear what the mechanism for altering calcium ion activation properties of calpain is. Hyperactivation of calpain associated with altered Ca^{2+} homeostasis is now considered to contribute to a number of pathologies, including ischaemia, and traumatic brain injury. However it is important to clarify that it is not an increase in calpain activity that is the injurious factor *per se*, but an unregulated influx of calcium ions that causes proteolysis of intracellular proteins, mediated through calpain.

1.7.2 Axonal proteins as calpain substrates

Calpain targets many different proteins, and this property can be very useful for indirectly determining calpain activation. For example, spectrin is targeted by calpain and therefore the detection of spectrin breakdown products is useful as a marker for calpain activity in the absence of suitable antibodies (Roberts-Lewis *et al.* 1994). This method has been used to demonstrate the activity of m-calpain in the peripheral nerve during neuropathy (Castejon *et al.*, 1999)

There is functional significance to the breakdown of certain proteins. Ca^{2+} -dependent breakdown of neurofilament leading to Wallerian degeneration has been linked to m-calpain activity (Glass *et al.* 2002;Kamakura *et al.* 1983).

Other integral cytoskeletal proteins known to be degraded by calpain include ankyrin, protein 4.1 and PSD95 (Boivin *et al.*, 1990;Doctor *et al.*, 1993;Harada *et al.* 1997;Lu *et al.*, 2000;Yoshida & Harada 1997). This is significant as these proteins have roles in anchoring and positioning other proteins and ion channels at specific locations (refer to section 1.4.5). More recently sodium channels themselves have been described to undergo proteolysis under models of traumatic brain injury *in vitro* (Iwata *et al.* 2004;von Reyn *et al.* 2009).

The desire to uncover an optimal calpain cleavage sequence is to create a calpain substrate that can be used to identify calpain activity. This would also presumably be extremely useful to the identification of susceptible proteins. Cleavage specificity to particular a.a. sequences has not been elucidated, however, it seems that elements of tertiary structure of protein substrates may influence activity. According to a study on μ -calpain cleavage specificity, most often small, hydrophobic a.a. such as leucine, valine and isoleucine are targeted when adjacent to a large hydrophobic a.a. like phenylalanine and tyrosine (Cuerrier et al., 2005). However, another study by Tompa *et al* (2004) suggests the position adjacent to the prime position, P2, is commonly filled by leucine, threonine and valine, while P1 is usually a lysine, tyrosine and arginine. The latter study reinforced previous findings by Sasaki and colleagues (1984) that tyrosine, methionine or arginine at the prime position were often preceded by Leu or Val, and also suggested there was no real difference in specificity between μ - and m-calpain cleavage sites.

1.7.3 Calpain inhibitors

Similar to complement, calpain is very closely regulated so as not to have detrimental effects. Calpastatin is the endogenous inhibitor of both μ - and m-calpain once they have been activated by calcium (Murachi 1989). As calpain mediates the proteolysis found in many degenerative diseases, the production of calpain inhibitors for therapeutic use could be very beneficial. *In vivo* models of brain injury and nerve transection have shown encouraging neuroprotective effects by the administration of calpain inhibitors (Bartus et al. 1994; Saatman et al. 1996). Synthetic cell-permeable calpain inhibitors, calpeptin and calpain inhibitor V, were the first used to show protection at the nerve terminal in the mouse model of GBS (O'Hanlon et al., 2003). ALLM is a calpain II inhibitor that protects against nerve terminal degeneration *in vitro* (Gyls et al., 2002). More recently the synthetic reversible calpain inhibitor AK295 (Li et al. 1996) has shown effective protection of sensory nerves against neuropathy *in vivo* (Wang et al. 2004) and protection in models of ischaemia (Bartus et al., 1994; Saatman et al., 1996). If nodal proteins do indeed undergo calpain cleavage during

antibody-dependent, complement-mediated pathology of the nerve, calpain inhibitors such as AK295 may well be a useful therapeutic tool.

1.8 Aims

Data from animal models and human studies point towards a disturbance of architecture at the node of Ranvier in the axonal variant of GBS, AMAN. This in turn is likely to interfere with conduction and play a role in resulting paralysis. Although the route of injury almost certainly involves anti-ganglioside antibody activation of complement initially, it is unclear what follows. It would also seem that accessibility may play a role in sites targeted during neuropathy. The hypothesis of the following study is that calpain is activated and cleaves proteins at the NoR resulting in reduced conduction due to the disruption of the Nav channel clusters and the axo-glial junction.

Therefore the broad aim of my thesis is to characterise the axonal injury, and the route by which it occurs, in a mouse model of AMAN with a particular focus on distal fibres and nodes of Ranvier. Antibodies to GD1a were chosen as high titres of antibodies against this ganglioside have been found in AMAN patients, GD1a is localised at the NoR, and antibodies against this ganglioside has been shown to initiate a complement-mediated lesion at the mouse nerve terminal.

To achieve these aims I will investigate;

1. Binding of anti-GD1a ganglioside at NoR and the effect of accessibility due to the BNB
2. Complement activation and resulting effect on various axonal and nodal proteins
3. The consequence of complement and calpain inhibition
4. Functional outcome of any disturbances

2 Materials and Methods

2.1 Reagents & Buffers

2.1.1 Reagents

2.1.1.1 Antibodies

Table 2.1 provides the details of the primary antibodies used throughout this work.

Goat anti-IgG2a and 2b, FITC and Rhodamine labelled were all purchased from Southern Biotech, (Birmingham, AL, supplied at 1mg/ml). Donkey anti-Rabbit IgG-Cy5 was purchased from Jackson ImmunoResearch Labs (Baltimore Pike, PA, supplied at 1.5mg/ml). All secondary antibodies were used at a dilution of 1:200 for whole-mount muscle, and 1:300 for sections and teased nerve.

Donkey anti-rabbit IgG-HRP (Santa Cruz, Europe) and goat anti-mouse IgG-HRP (Sigma, Aldrich) for western blot (WB) were used at 1:4000.

2.1.1.2 Labelling reagents

α -bungarotoxin (BTx) Alexa Fluor 488 and 647 conjugates (Molecular Probes), 1mg/ml stock used at dilutions of 1:500 for whole-mount muscle and 1:750 for sectioned tissue to label postsynaptic ACh receptors.

FluoroMyelin Green (Molecular Probes), 1ml stock diluted to 1:300 for identification of myelin.

Rhod 2-AM and Fluo-4 (Molecular Probes), cell-permeant calcium indicators, effective concentration- 1-5 μ M.

Pluronic acid (Molecular Probes) assists in dispersion of Ca²⁺ indicator.

Antigen	Host	Isotype	Dilution		Acetone?	Source
			IHC	WB		
Ankyrin G	Ms	IgG1	1:100		Y	Zymed Labs San Francisco, CA
Caspr	Rbt	IgG	1:1000		N	Kind gift from E. Peles, Israel
B actin	Rbt	IgG		1:1000	-	Novocastra Newcastle, UK
Dystrophin	Ms	IgG1	1:200	-	N	Sigma Missouri, USA
Fodrin	Ms	IgG1		1:1000	-	BIOMOL Int Europe
FluoroMyelin green	-	-	1:300	-	N	Molecular Probes Paisley, UK
Kv1.1	Rbt	IgG	1:200	-	Y	Alomone Labs Israel
MAC (C5b-9)	Hu	IgG2a	1:50	-	N	Dako Glostrup, Denmark
MAG	Ms	IgG1	1:40	-	Y	Chemicon Int Europe
Moesin	Ms	IgG1	1:100	-	Y	BIOMOL Int Europe
Nav1.6	Rbt	IgG	1:100	1:100	N	Sigma Missouri, USA
pan Nav	Ms	IgG1	1:100	1:100	N	Sigma Missouri, USA
pan Neurofascin	Rbt	IgG	1:1000	1:2000	N	Kind gift from P. Brophy, Edinburgh
Neurofilament	Rbt	IgG	1:200	-	Y	Chemicon Int Temecula, CA
Nf186 (MNF2)	Rbt	IgG	1:100	-	N	Kind gift from P. Brophy, Edinburgh
NrCAM	Ms	IgG1	1:100	-	N No Triton	Abcam Cambridge, UK
NrCAM	Rbt	IgG	1:100	-	N	Kind gift from P. Brophy, Edinburgh
Radixin	Rbt	IgG	1:400		N	Kind gift from D. Sherman, Edinburgh
Tetrodotoxin	Rbt	IgG	1:200	-	-	Advanced Targeting Systems, San Diego, CA

Table 2.1 (previous page): Primary antibody dilutions. Abbreviations as follows: Ms, Mouse; Rbt, Rabbit.

2.1.1.3 Toxins

α -Latrotoxin (LTx, Alomone Labs, Israel), used at 12nM to cause huge increase in spontaneous neurotransmitter release that is mimicked by anti-ganglioside antibodies injurious to the terminal.

Tetrodotoxin (TTX) with citrate (Biotium Inc, USA)

2.1.1.4 Miscellaneous reagents

AK295 (Georgia Institute of Technology), calpain inhibitor used at 100 μ M

Eculizumab and ALXN3300 (Alexion Pharmaceuticals, USA), humanised anti-human C5 mAb and non-specific isotype-matched control, respectively, used at 100 μ g/ml

Calpeptin (Calbiochem, UK), calpain inhibitor used at 100 μ g/ml

Normal human serum (NHS), from a single donor stock

Ionomycin (Alomone Labs), an antibiotic acting as a Ca²⁺ ionophore used at 0.1-2 μ M

Araldite for EM embedding was made up in the fume-hood as follows:

CY 212	10ml
DDSA	10ml
D. Butyl phthalate	1ml
DMP 30	0.5ml

For staining of EM grids:

Uranyl acetate- add to 50% ethanol until saturated, filter

Lead citrate- Dissolve 1.33g lead citrate in ~30ml water then add 1.76g sodium citrate. Allow to stand for 30mins with occasional

agitation. Add 8ml 1N sodium hydroxide and water up to 50ml

2.1.2 Buffers

For all *ex vivo* preparations and electrophysiology, the tissue was sustained in pre-gassed Ringer's, recipe as follows:

Ringer's (10X stock solution)

NaCl	66g (1.13M)
KCl	3.36g (0.045M)
NaHCO ₃	21g (0.25M)
NaH ₂ PO ₄ .2H ₂ O	1.56g (0.01M)
Glucose	21.86g (0.12M)
1M MgCl ₂	10ml (0.01M)

Made up to 1L with distilled water (dH₂O). Diluted 1 in 10 for use followed by addition of 1M CaCl₂ to a final concentration of 2mM.

Phosphate buffered saline (PBS, 10X stock solution)

NaCl	80g (1.4M)
KH ₂ PO ₄	2g (0.015M)
KCl	2g (0.027M)
Na ₂ HPO ₄ .2H ₂ O	29g (0.19M)

Made up to 1L with dH₂O, diluted 1 in 10 for use.

Lysis buffer

Tris	1.211g (10mM)
NaCl	5.844g (100mM)
EDTA	0.29g (1mM)
10% glycerol	
2% SDS	

Made up to 1L in dH₂O. One Roche protease inhibitor cocktail tablet added to every 10ml before homogenisation.

Blocking solution

1% Lysine	3.62g (0.025M)
0.5 or 1% Triton	
1% Normal goat serum (NGS)	

Made up to 50ml in PBS

2.2 Animals

2.2.1 Transgenic mice

All mice used were of the GD3s^{-/-} background, unless otherwise stated. Male or female mice (15-30g) were killed by a rising concentration of carbon dioxide following UK laws and Glasgow University guidelines.

A new variety of GD3s^{-/-} transgenic mouse that has endogenously fluorescent axons was developed for the purposes of this study by breeding GD3s^{-/-} mice with B6/Cg-TgNxDBA mice (also known as CK mice). Although the parent CK strain has fluorescence to axons and Schwann cells, only the fluorescence to axons was selected. The reasoning for this is that CFP and GFP have very similar excitation spectra and thus CFP can bleed-through into the GFP channel on imaging. To avoid this occurring and possibly interfering with results, I chose the axonal fluorescence as it is more useful to this study. Interestingly, the more appropriate partner for CFP would ideally be YFP as discussed by Lippincott-Schwartz and Patterson (2003). This new strain would be termed GD3s^{-/-} x B6.Cg-TgN(Thy1-CFP) by the international naming nomenclature, but for simplicity will be referred to as GD3/CFP throughout this study. The CK strain will be considered the WT partner to the GD3/CFP strain as it is assumed to possess a ganglioside expression akin to WT. PCR was used to genotype the mice for GD3 synthase expression. However, as fluorescent proteins are fused to Thy1 protein, which retains normal expression, it was necessary to phenotype rather than genotype the mice to monitor fluorescence. This consisted of splitting an ear punch and using a Zeiss Axio Imager Z1 with ApoTome attachment and appropriate filters to identify an emission wavelength of 474nm for CFP positive axons in the skin.

2.2.2 Genotyping

DNA extraction was performed on ear punches taken from transgenic mice using a Puregene kit from Flowgen Bioscience (Ruddington, UK). Ear punches were added to 300µl of the kit cell lysis solution plus 0.1mg/ml proteinase K for a minimum of 1h at 55°C. After the samples were cooled to room temperature (R.T.), 100µl protein precipitation solution was added before vortexing. Samples

were spun at 12,500rpm for 3mins to pellet the protein. Supernatant was added to 100% isopropanol (2-propanol) to precipitate the DNA before repeating centrifugation. 70% ethanol was added to the DNA pellet before a final centrifugation. The pellet was left to dry after removal of the alcohol before rehydration in 50µl DNA hydration solution. This was stored at -20° C or used immediately for PCR.

Specific primers were created to identify the wild-type (490bp), heterozygous (380 & 490bp) and knock-out (380bp) GD3 synthase transcripts produced from PCR.

2.2.3 Ultrastructure

To ensure that the genetic modifications did not have an adverse affect on nerve ultrastructure, electron microscopy was employed. See section 2.7.3 for protocol.

Ultrastructural examination was not suggestive of any consistent abnormalities between WT and KO strains at the NoR (Figure 2.1). Generally, the cytoskeletal integrity looked unaffected, there was no unnatural accumulation of organelles, and the paranodal loops appeared to be intact. Along the internode the compact myelin appeared normal, as did many Schmidt-Lanterman incisures.

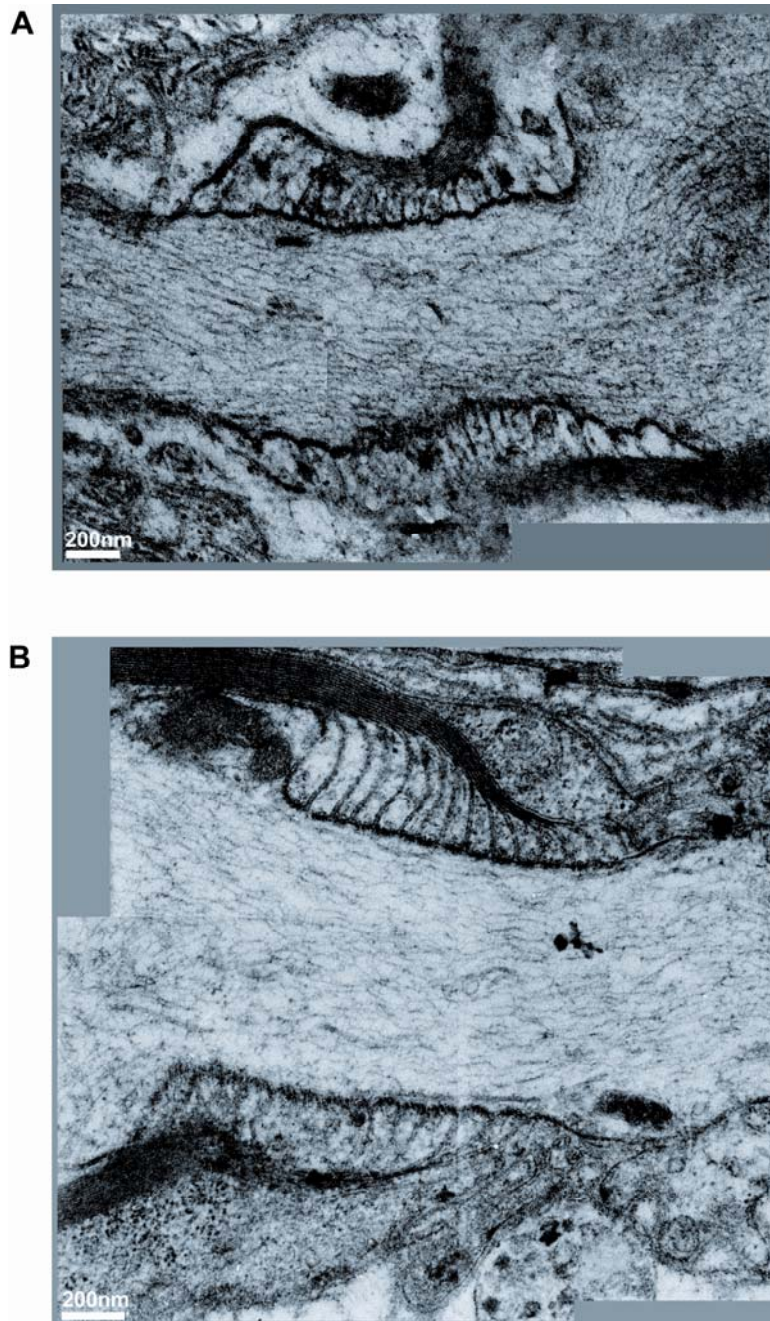


Figure 2.1: Ultrastructural comparison of wild type and GD3/CFP mouse nerve.

Montages of several electron micrographs assembled to illustrate comparable axonal integrity and normal paranodal loop formation between wild type (A) and GD3/CFP (B) heminodes. Scale bar= 200nm.

2.3 Antibody production

2.3.1 Anti-GD1a antibody cell-lines

The GD1a mimicking lipooligosaccharide (LOS) strain O:19 was previously injected into ganglioside deficient $\text{GalNAcT}^{-/-}$ mice to create high affinity anti-

GD1a antibodies. MOG35 is the established anti-GD1a antibody producing cell-line of which stocks are kept in liquid nitrogen.

To produce antibody, cells were suspended in flasks of RPMI 1640 media with 10% foetal calf serum (FCS) and 5% L-glutamine and maintained in an incubator at 37°C. Media was removed twice weekly and spun down at 1000rpm for 5mins. Cells were resuspended in fresh media while supernatant was collected and stored at -20°C until there was a large enough volume for purification.

When the flasks reached a high confluence, it was possible to transfer the cells to an Integra Cell line (Integra Bioscience, Zizers, Switzerland) that allowed for a more efficient production of antibody. In this instance, cells were maintained in RPMI 1640 media plus 20% FCS, were passaged once a week, and supernatant collected once weekly as above.

2.3.2 Antibody purification

To purify monoclonal antibodies, the supernatant was centrifuged in a Sorvall RC5C centrifuge at 10 000rpm for approximately 30mins before filtration through a 0.22µm membrane. Overnight dialysis at 4°C allowed supernatant to adjust to 1:10 binding buffer (20mM sodium phosphate). Ten column volumes of binding buffer were applied to a HiTrap Protein G affinity column (Amersham Pharmacia Biotech, UK), followed by supernatant. Flow-through was collected and stored at -20°C. IgG that was eluted off the column with glycine (pH2.8) was neutralized with 1M Tris-HCl at pH9. Eluted fractions and flow-through were assayed by ELISA for IgG. Antibody was concentrated to 0.5mg/ml for *ex vivo* preparations and 1.5mg/ml for passive transfer, desalted using PD10 columns (Amersham Pharmacia Biotech, UK) and stored at -70°C. Concentration of the sample in mg/ml was calculated by dividing the absorbance measured at A280nm by 1.43, which represents 1mg/ml of protein.

2.3.3 Enzyme-linked immunosorbent assay (ELISA)

ELISA's were used to either confirm that cell-lines were producing antibody, or to ensure that antibody was administered to and was present in treated tissue/animals. The following protocol can be used for both purposes.

Alternate rows in a ninety-six well plate were coated with 100µl methanol (from which background optical density at 492nm [OD] readings were subtracted) and 2µg/ml GD1a (Sigma, Missouri, USA) and allowed to dry for 2-3h. After storage at 4°C for at least 1h, plates were blocked with 200µl 2% bovine serum albumin (BSA) in PBS for 1h at 4°C. A dilution series for each supernatant was generated, ranging from 1 in 10 to 1 in 10 240 with appropriate controls, and incubated for 4h at 4°C. Plates were thoroughly washed in PBS and dried before addition of 100µl 1:3000 HRP-conjugated anti-mouse IgG antibody (Sigma) in 0.1% BSA in PBS to every well for 1h at 4°C. Plates were washed as before and dried, then incubated in 100µl of substrate buffer (14ml 0.1M citrate, 16ml 0.2M Na₂HPO₄, 30ml d.H₂O, one OPD tablet [Sigma] and 20µl H₂O₂) in the dark for 20mins. The reaction is terminated by the addition of 50µl 4N H₂SO₄ (54ml to 500ml d.H₂O) to each well before reading plates on a Labsystem Multiskan for OD (492nm).

2.4 Muscle and nerve preparations

2.4.1 *Triangularis sterni ex vivo preparation*

The triangularis sterni (TS) is a thin muscle, only a few fibres thick, which is located on the inner surface of the ribs. It is innervated by branches of the 3rd, 4th and 5th intercostal nerves. Innervation occurs in a well defined region, with the endplate band running parallel to the sternum, and the nerves lying in plane with the muscle. Both the thickness and the innervation pattern make the TS ideal for following axons to their termination in whole-mount preparations and sections.

To dissect the TS, the entire ribcage is first removed and pinned out into a Sylgard (Dow Corning, Michigan, USA) lined dish containing Ringer's, ventral side up. The intercostal muscles between the ribs 3 to 6 are carefully cut to reveal the TS underneath. The ribs are then removed to create a window (depicted in

diagram 2.2). To separate the two sides the sternum is divided leaving half on the lateral edge of each window, which allows the muscle to be more easily kept under a natural tension. The rest of the unwanted ribcage is removed, only leaving the adjacent ribs on the rostral and caudal edges of the TS and a border of muscle on the distal edge.

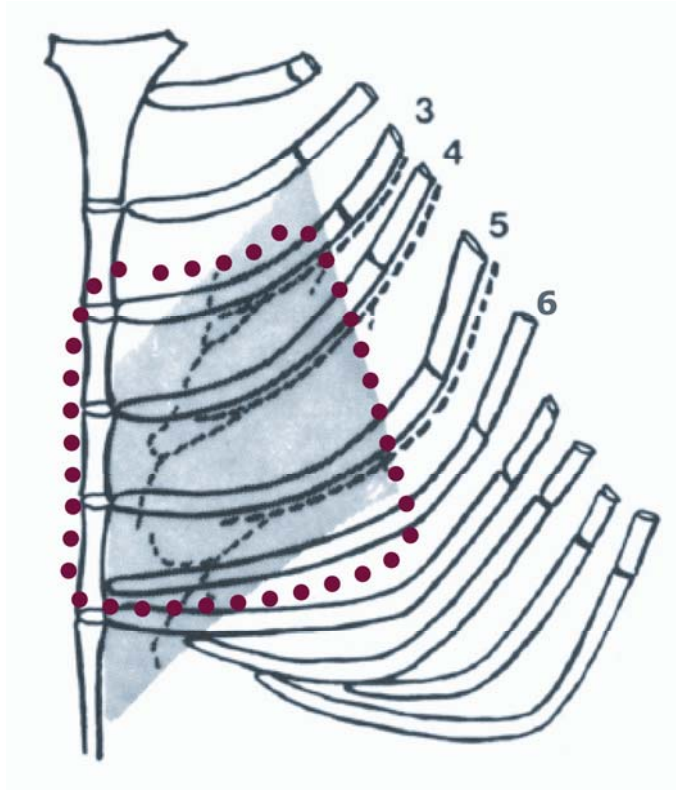


Figure 2.2: Schematic of the triangularis sterni (TS) muscle in the right hemithorax of the mouse. Black dashed lines depict the branches of the intercostal nerves innervating the TS (shaded grey). The region surrounded by the red dotted line illustrates the area removed for *ex vivo* preparations. (Modified from McCardle, 1981)

At this stage, the whole-mount is maintained in Ringer's and is considered an '*ex vivo*' preparation as, although it has been removed from the animal, it is maintained in a viable state for up to 8h. As described in more detail below, this preparation was used to study blood-nerve barrier permeability, antibody-mediated pathology to nodes of Ranvier, and the prevention of this pathology by various inhibitors.

2.4.2 Phrenic, sciatic and sural nerve

The phrenic nerve was an ideal candidate for many experiments as it consists entirely of motor axons, whereas the sciatic nerve is mixed and the sural purely sensory.

In order to isolate the phrenic nerve, the ribcage was carefully removed by first making an incision along the line of the sternum from the neck to the final rib, before cutting laterally and finally down either side to create a cavity. The nerves can be identified on either side of the heart. Fine forceps were used to separate the nerve from surrounding connective tissue before it could be tied off with thread as close to both the apex of the thorax and the insertion into the diaphragm as possible. The nerve was removed and transferred to a Sylgard dish where it was kept taught by pins through the knots. At this stage it was useful to desheath the nerve using a 0.3ml insulin syringe to drag away excess fat cells and the outer epineurium. The success of desheathment could be determined by the ability to visualise axons bulging out behind the path of the syringe. From this stage, nerve could now be used for experiments on nodal disruption, electrophysiology and ultrastructural studies, as described below.

Similarly, sciatic nerve was located by removal of the overlying leg muscles, tied off distally before the branch point, and proximally as close to the sciatic notch as possible, pinned out, and desheathed ready for experimental use. The sural nerve had to be dissected with extreme care as it is very delicate and inserts into the muscle normally removed to reveal the sciatic nerve. The sural nerve branches from the sciatic nerve a short distance proximally to the bifurcation into tibial and peroneal nerves. Once identified it is similarly tied off and desheathed (often it was easier to tie off the proximal end of the entire sciatic nerve before carefully separating the distinctive fascicle of the sural nerve).

2.4.3 Muscle sectioning

The TS and diaphragm were routinely sectioned to optimise the number of staining protocols possible and thus data collected, and for use in dilution series, respectively. When using muscle from endogenously fluorescent mice it was

essential to fix in 4% paraformaldehyde (4% PFA) before sectioning in order to retain fluorescent signal, otherwise tissue could be snap-frozen.

10µm sections were cut using a freezing cryostat (Bright Instruments, Cambridgeshire, England) and collected on 3-aminopropyltriethoxysilane-coated (APES) slides. Slides could be stored at -20°C until required, or immunostained once air-dried.

2.5 Permeability studies

2.5.1 GD1a localisation and binding-gradient

To investigate the localisation of the GD1a ganglioside and the permeability of the blood-nerve barrier in intramuscular nerve bundles to antibody, TS from GD3/CFP and WT mice (i.e. CK mice, as discussed above) were incubated *ex vivo* with the anti-GD1a antibody MOG35. For each treatment group, three TS preparations were examined and 20-40 NoR per bundle category, per mouse, analysed. The exact protocol was as follows:

1. Incubation of TS with 100µg/ml MOG35 in Ringer's (or Ringer control) plus 1:500 BTx-FITC for 2h at 32°C, 30mins at 4°C, 10mins at R.T.
2. Rinse in Ringer's, fix in 4% PFA for 20min at R.T.
3. 10min washes in PBS, 0.1M glycine, and PBS
4. 1:200 goat α-mouse IgG2b-TRITC plus 1:1000 rabbit α-NFC2 in blocking serum with 1% Triton overnight at 4°C
5. Rinse in PBS, 1:200 donkey α-rabbit IgG-Cy5 in PBS for 3h at R.T.
6. Rinse in PBS, mount in Citifluor (Citifluor, Canterbury, UK)

Images of sectioned or whole-mount tissue were captured using a Zeiss Pascal confocal laser scanning microscope with a 40x oil-immersion Plan NeoFluor

objective lens, or under epi-fluorescence on a Zeiss Axio Imager Z1 with ApoTome attachment with a 63x oil-immersion Plan Fluor Aplanachromat objective lens, using Zeiss LSM and AxioVision LE version 4.5 software, respectively. Slides were imaged blind and with set levels throughout the analysis. Measurements were made using ImageJ analysis software.

Initially binding of antibody over the endplate was investigated. NMJ were identified by FITC-labelled BTx that binds post-synaptic acetylcholine receptors, and the fluorescence intensity of TRITC-labelled IgG was measured over this region.

The intramuscular bundle was categorized into single fibres, small (<15µm), medium (15-35µm), and large bundles (>35µm). For each bundle size IgG2b fluorescence intensity was measured at NoR, identified by NFC2 and CFP, using ImageJ software. Background fluorescence intensity due to the excess scatter of light often found in epi-fluorescent imaging was always subtracted during quantification.

Statistical analysis was carried out using Minitab software, with data considered significant when $p < 0.05$ using the Mann-Whitney U test (used due to the non-parametric nature of the data). Measurements were plotted as box and whisker plots to represent the spread of data.

This was repeated *in vivo* by passive transfer of antibody. 3mg MOG35 was injected i.p into three mice (also three PBS i.p. injected controls) and animals left overnight. The TS was removed and the above protocol was followed from step 2. To assay the level of antibody found in the serum, blood was removed and clotted at R.T. for 1-2h. Centrifugation at 10 000rpm for 10mins resulted in cells forming the pellet so that serum could be removed and frozen for ELISA.

2.5.2 Ubiquitous GD1a expression

Diaphragm sections were incubated with 50µg/ml MOG35 for 4h at 4°C, rinsed then treated as from step 4 above. Images were taken as superficially as possible to ensure that only MOG35 intensity at NoR that had been sectioned through, and thus would not have an intact barrier to the antibody, was measured.

2.5.3 Sheath permeability

Phrenic nerve (n=6) was pinned out and the sheath was either left intact or removed prior to incubation with 100µg/ml MOG35 to study the necessity of desheathment for antibody binding. The nerve was then fixed, stained and analysed as above.

2.5.4 Specific GD1a localisation at NoR

To determine the sub-regional expression of GD1a at the NoR, co-localisation studies were prepared using the Schwann cell microvilli marker radixin, and the paranodal marker myelin associated glycoprotein (MAG). Z-stacks of distal intramuscular axons and phrenic nerve were captured using the Zeiss Axio Imager Z1 with ApoTome attachment.

2.6 Complement mediated injury to NoR

2.6.1 Ex vivo complement deposition

To elucidate the terminal complement complex, MAC (C5b-9), activation at NoR associated with MOG35 deposition, the same protocol as for GD1a localisation was used with some additions as follows:

1. TS from GD3/CFP mice only
2. From step 1, rinse in Ringer's, incubate with 40% normal human serum (NHS) as a source of complement for 3h at R.T.
3. Rinse in Ringer's, fix in 4% PFA for 20min at R.T.
4. 10min washes in PBS, 0.1M glycine, and PBS
5. Cryosection at 10µm
6. 1:50 mouse α-human MAC plus 0.5% Triton in blocking solution overnight at 4°C

7. Rinse in PBS, 1:150 α -mouse IgG2a-TRITC in PBS for 3h at R.T.
8. Rinse, 1:300 fluoromyelin-green for 20min at R.T.
9. Rinse thoroughly in PBS, mount in Citiflour

Fluoromyelin green is a stain that is selective for myelin due to its lipophilic nature. It is therefore useful in identifying NoR in different bundle categories as it is most apparent in the lipid-rich paranodal loops. As there is often background fluorescence due to the labelling of all lipids to a degree, localisation of NoR was confirmed by immunostaining for dystrophin, which labels the Schwann cell sheath and appears strongly at the NoR. The MAC intensity was measured and quantified as for MOG35.

2.6.2 Complement mediated effect on neurofilament and CFP

The fluorescence intensity of labelled antibody binding to the structural protein neurofilament was measured along the distal axon after MOG35 antibody and complement-mediated injury. The axon was divided into the first two internodes and NoR for measurements. ImageJ software was utilised and background fluorescence was subtracted from the epifluorescent images taken of the nerves.

The TS was imaged live using a 40x water-immersion Achromplan objective lens on the Zeiss epifluorescent microscope to investigate loss of CFP after a complement lesion. Muscle was incubated *ex vivo* with antibody as normal. Ideal areas of endplates for live imaging were located and then NHS serum was added (at 10% so as not to interfere with the image quality). The area was reimaged at set time-points with set-levels in an attempt to identify an alteration to CFP fluorescence. Ideally NoR should have been identified by primary labelled CTx, but this was quite irregular and thus not very useful.

2.6.3 Complement-mediated effect on nodal proteins/ion channels

The staining patterns of several proteins and ion channels were studied after antibody-mediated injury to determine pathology at specific sites of the node of Ranvier. Proteins specific to the nodal axolemma (Nav1.6, Ankyrin G, NrCAM), Schwann cell microvilli (moesin), paranode (Caspr, NF155) and juxtaparanode (Kv1.1) were identified in TS sections and/or teased phrenic nerve. The protocol for complement-mediated injury was followed with the addition of primary antibodies overnight (specific dilutions of antibodies shown in table 2.1). Secondaries were Cy5 labelled as a further means of blinding the sections due to this particular fluorophore not being visible by eye.

To quantify the presence of the immunostaining of a protein- and where necessary the normality of the staining motif- positive/negative counts were made and statistically analysed using the Chi-squared test of independence, when $df=1$ and the level of significance was 0.5% when $\chi^2 > 7.87$. NoR were identified by IgG deposition, which also showed there had been successful desheathment, and/or fluoromyelin-green or dystrophin.

2.6.4 α -latrotoxin effect on nodal proteins

To ensure that the loss of nodal protein immunostaining and endogenous CFP signal was due to targeted injury to the node and not a progression of injury from the terminal proximally up the nerve, the terminal specific toxin α -latrotoxin (α -LTx) was employed.

The TS was exposed to MOG35 and complement ($n=3$), or 12nM α -LTx ($n=3$), fixed and incubated with α -Nav1.6 antibody. Nav1.6 was identified at NoR in blinded samples while CFP fluorescence at the terminal and 100 μ M along axons was measured and plotted. CFP intensity after antibody and complement treatment or α -LTx treatment was then compared to control levels.

2.7 Route of injury

2.7.1 Use of calcium indicators in PC12 cells

To investigate the movement of calcium, PC12 cells were used initially. These cells were grown and made ready for use in the following way:

1. Poly-L-Lysine (PLL) is added to flasks at 13.3 μ g/ml in dH₂O and left for 10min, before removal and washes with PBS
2. After air-drying, incubate flasks at 37°C O/N and store at R.T.
3. PC12 cells are grown in DMEM with 7.5% foetal calf serum (FCS) and 7.5% horse serum (HS)
4. To remove cells for transfer onto coverslips, medium is removed and cells washed with PBS
5. Add 2.5mg/ml trypsin in PBS and flick to dissociate cells (check under microscope)
6. Add cell solution to Falcon tube containing medium with 10% serum to neutralise trypsin
7. Centrifuge at 1000rpm for 5mins
8. At this point cells can be resuspended in media and transferred to PLL coated coverslips located in 12 well tissue culture plates. After 12h at 37°C, coverslips were ready for experimental use.

PC12 coated coverslips were incubated with antibody and the calcium indicators Fluo 4-AM or Rhod 2-AM. Fluo 4-AM was the initial choice for use with the Zeiss Axio Imager epifluorescent microscope. However, distinguishing specific areas with a high amount of scattered light was not possible. Therefore Rhod 2-AM was more convenient for use with a confocal laser scanning microscope whose lasers diminish high background.

The protocol for measuring fluorescence from calcium indicator activation in cells was as follows:

1. Incubate PC12 cells with 1 μ M Rhod 2-AM in Ringer's plus 100nM Ca²⁺Cl⁻ for 5min in dark at R.T. (Cells may have been incubated with 20 μ g/ml MOG35 for one hour at R.T prior to this)
2. Rinse thoroughly, find cells with phase contrast, image with a 40x objective water immersion lens and set levels
3. Add 1 μ M ionomycin or 5% NHS to well and image cells at set time-points (i.e. every five minutes for 60 minutes)

Quantification was not performed as cells were used chiefly to establish a working protocol for calcium indicators before transferring the experiment to tissue to examine the movement of calcium at NoR after injury. Unfortunately, Rhod 2-AM was never successfully imaged in *ex vivo* muscle preparations for reasons discussed in chapter 5.

2.7.2 Protection by complement and calpain inhibition

The above protocol to identify the effect of antibody and complement on nodal proteins was used to study the protective effects of complement and calpain inhibitors (n=3 per treatment group and counts performed as above).

10mins prior to the stage at which complement is added to the *ex vivo* preparations, the complement inhibitor Eculizumab (100mg/ml) or its non-specific isotype-matched control antibody ALXN3300 (100mg/ml) were incubated with the NHS at R.T. This concentration was utilised as it has successfully prevented MAC deposition and neurofilament loss at the nerve terminal in similar *ex vivo* preparation (Halstead et al., 2008b).

In other experiments the calpain inhibitor AK295 was added to the NHS at 100 μ M (DMSO control). This was determined to be the optimal concentration by quantifying the level of protection of Nav1.6 in single fibres at AK295

concentrations of 200 μ M, 100 μ M and 50 μ M compared to control and unprotected nerve. The level of protection afforded to the nodal proteins affected by antibody and complement injury were quantified in a similar way to the control versus antibody studies.

2.7.3 Ultrastructure

2.7.3.1 Ultrastructural comparison of transgenic mice NoR to *wild-type*

For electron microscopy (EM), mice (3xWT, 3xGD3/CFP) were vascularly perfused with 2% paraformaldehyde plus 2.5% glutaraldehyde in PBS. Perfusion was followed by the removal and immersion of desired tissue in the same fixative overnight at 4°C. Fixed tissue was cut into squares, no larger than 5mm², rinsed several times with PBS and stored at 4°C until embedding. Samples were post-fixed with Osmium tetroxide (OsO₄), which doubles as an electron stain, dehydrated and embedded in araldite for sectioning. The specific protocol was as follows:

1. Post-fixation in fume-hood with 1% OsO₄ for 45min
2. 3x 10min PBS washes
3. 10min in 25% ethanol, then drain
4. 10min in 50% ethanol, then drain
5. 10min in 75% ethanol, then drain
6. 2x 15min in 100% ethanol, then drain
7. 2x 15min propylene oxide, then drain
8. 2-4h on rotating mixer immersed in propylene oxide/araldite 1:1
9. Overnight on rotating mixer immersed in propylene oxide/araldite 1:3

10. Block out in fresh araldite in moulds for several hours at R.T.

11. Cure overnight at 60° C

Semi-thin (~500nm) and ultra-thin (~90nm) sections were cut on an ultramicrotome using glass knives. Semi-thin sections were stained with toluidine blue and used to determine areas of interest. Ultra-thin sections were mounted on copper grids and stained with uranyl acetate for 10mins and Reynolds lead citrate solution for 2min prior to viewing with the electron microscope.

Negatives of images captured using a Phillips C10 electron microscope were scanned and digitised for processing with Adobe photoshop software. Appropriate levels were set and applied to subsequent images.

2.7.3.2 Ultrastructural study of experimental tissue

Preparations were prepared as per normal experimental conditions before following the above protocol. As the experimental protocol required tissue to be *ex vivo* for over four hours, the ultrastructure suffered severely and it was difficult to identify any particular structures or indeed make a comparison between treatment groups. Therefore the decision was made that EM was not possible under these conditions.

2.8 Fate of nodal proteins

2.8.1 Electrophysiology

Electrophysiology was carried out on desheathed nerve following treatment with antibody, as per normal experimental procedures. The nerve was mounted in a custom made Perspex recording chamber consisting of 3 chambers (Figure 2.3) for non-invasive extracellular recordings of nerve potential changes along the nerve.

The chambers were isolated by vacuum grease and were supplied by a stimulating electrode, earth, and recording electrode, respectively.

1. Nerves (sciatic, sural or phrenic) were removed, desheathed and incubated for 2h in 100 μ g/ml MOG35 at 32 $^{\circ}$ C, before removal to 4 $^{\circ}$ C for 30mins
2. The nerve was mounted traversing all three wells of the recording chamber before the middle chamber was sealed off with grease
3. Ringer's was added to each chamber as were the electrodes
4. A steady baseline compound action potential (CAP) was recorded before the addition of 40% NHS to the middle chamber for 2h.
5. 100 μ M AK295 could be added with NHS if desired

On the completion of the experiment, tetrodotxin (TTX, 5 μ M) was added to the middle chamber to block sodium channels and confirm that the nerve was indeed functional.

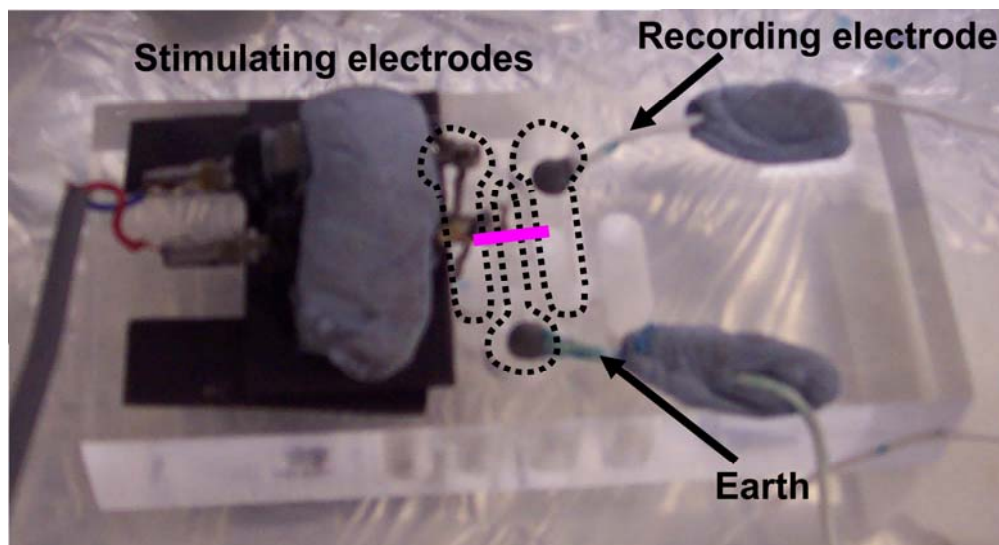


Figure 2.3: Electrophysiological recording chamber.

Photograph of recording block with three chambers (outlined by dashed lines) supplied by various electrodes. The nerve traverses the three chambers (solid pink line) before being sealed in with vacuum grease.

It was expected that reagents could be added to the middle chamber holding the experimental nerve segment. This was suitable for finer calibre phrenic and sural nerve, but unfortunately for sciatic nerve there was no MAC deposition (as determined by subsequent immunohistochemistry, section 6.2.4). Therefore, the following amendments were made to establish the effect of complement on sciatic nerve conduction. A steady baseline was recorded before the nerve was removed from the chamber and placed in a well of NHS. It was then returned to the recording chamber to record for the final half an hour. It was determined by immunohistochemistry that 3h of NHS incubation was sufficient to cause MAC activation in the nerve.

Although for studies assessing loss of Nav staining due to injury only those NoR with good IgG deposition were included, for electrophysiology every NoR identified in differential interference contrast microscopy (DIC) was counted, as all would contribute to conduction.

Nerve stimulation was performed with a Grass S88 stimulator, delivering pulses at a frequency of 1Hz through a CED 1902 amplifier. Recordings were captured and analysed using WinWCP version 4.1.0 software. A representative graph of the positive peak value of CAP over time was plotted to convey conduction. 200 peak values from the beginning of the final half an hour of recording in the case of sciatic nerve, and from the point of addition of NHS to phrenic and sural nerve preparations, were averaged and acted as the starting value from which the final averaged 200 recorded peak values before tetrodotoxin addition could be compared. Absolute values were not used as these were extremely varied, so instead the percentage of the starting peak value was calculated for each preparation then averaged for each group. A paired t-test was used to identify significant differences between sciatic nerve treatment groups (n=6 per treatment group), and a straight-forward 2-sample t-test for comparison of phrenic and sural nerve (n=3-5 per nerve group). Significance was set at $p < 0.05$.

Post-experiment, the nerve was fixed and stained for IgG, MAC and Nav1.6.

2.8.2 Tetrodotoxin labelling

Staining for tetrodotoxin (TTX) was carried out in an attempt to determine the structural integrity of the extracellular portion of the Nav1.6 channel after antibody-dependent complement-mediated injury. The protocol was as follows:

- Phrenic nerve/sciatic nerve treated as per electrophysiological recording experimental procedures
- TTX added at 5 μ M
- Nerve was fixed for 12mins in 2.5% glutaraldehyde plus 4% PF in PBS at 4 $^{\circ}$ C
- Transfer into 4% PFA O/N at 4 $^{\circ}$ C
- Rinse in PBS 3x 10mins, block in 10% NGS plus 0.3% Triton X-100 for 20mins
- Primary antibody 1:100 O/N at 4 $^{\circ}$ C
- Rinse in PBS 3x 10mins
- 1h 1:200 α -Rbt IgG-biotinylated in PBS at R.T
- Rinse in PBS 3x 10min
- 1h 1:1000 avidin-biotin-peroxidase complex (Sigma)
- Rinse in PBS 3x 10min
- Add H₂O₂ to 3,3'-diaminobenzadine (DAB) at 0.025M to react with the HRP conjugated antibody
- Rinse in PBS 3x 10min

- Dehydrate through alcohol series and clear in HistoClear before mounting using Histomount (both from Flowgen Bioscience, Ruddington, UK)

2.8.3 Nav Western blots

Nerves were collected after completion of experimental procedures and snap-frozen. Nerves (at least ten) were pooled and homogenised for 3mins at RT using a mortar and pestle in a 1.5ml eppendorf in 100µl lysis buffer containing a Roche proteinase inhibitor cocktail tablet (1 per 10ml). The protein was spun at 13,000rpm for 20mins at RT. The Western blot protocol was as follows and used the Invitrogen Novex XCell SureLock Mini-cell gel tank and NuPAGE reagents:

- 20µg protein (as determined by BCA assay) was added to 1x LDS Sample buffer with 1x sample reducing agent to a final volume of 10µl and heated at 50°C for 10mins
- Load 20µg protein in a 3-8% Tris-Acetate gel (1mm x 12well) and run at 200V for 50mins in 1X Tris-Acetate SDS Running Buffer with 1X sample reducing agent. Novex sharp prestained markers (Invitrogen, Paisley, UK) were loaded for identification of molecular weights.
- Transfer protein onto PVDF membranes overnight at 100mA at 4°C. Retain a portion of the gel and stain with SimplyBlue safe stain (Invitrogen) for 1h before destaining O/N on a rocker in several changes of dH₂O to reveal protein bands.
- Block membrane in 2% Marvel + 0.1% Tween-20, 3x 10mins.
- Incubate membrane with primary antibody (for dilutions see Table 2.1) for 1h at R.T.
- Rinse membrane in 2% Marvel + 0.1% Tween-20, 3x 10mins
- Incubate membrane in secondary for 1h at R.T.

- Rinse membrane in 2% Marvel + 0.1% Tween-20, 3x 10mins
- ECL Western blotting detection system (Amersham) for 5mins in dark, following manufacture's instructions
- In a light-proof cassette, expose membrane to Kodak medical X-ray film for appropriate length of time to reveal bands

The optical density of the band in each lane was measured five times for each of three runs using ImageJ software. These values were averaged and the background subtracted, before analysis by ANOVA. Significance was set at <0.05 .

3 Permeability of peripheral nerve to circulating antibody

3.1 Introduction

The purpose of this chapter is to discuss the experiments employed to assess the localisation of GD1a in a suitable mouse model, prior to experiments described in subsequent chapters that characterise injury related to antibody raised against this ganglioside. This target was chosen as it has been associated with acute motor axonal neuropathy in humans.

The monoclonal antibody MOG35 has high affinity for GD1a (Boffey et al. 2002) and consequently has been used to demonstrate abundant GD1a expression at the nerve terminating in the neuromuscular junction of GD3s^{-/-} mice (Goodfellow et al., 2005), which have been modified to over-express a-series gangliosides (Okada et al., 2002). Binding of MOG35 at the nerve terminal could also be associated with MAC pore formation and loss of neurofilament in the presence of an external source of complement (Goodfellow et al., 2005). This is likely a consequence of the NMJ being exposed to circulating factors since it resides outwith the BNB. Ventral roots are also minimally protected by the BNB. Therefore, it is perhaps unsurprising that the ventral roots of AMAN patients had disrupted myelinated axons, specifically at the gaps in the myelin sheath known as NoR (Griffin et al. 1996b;Hafer-Macko et al., 1996). As the perineurial sheath becomes thinner towards the terminal of the axon it ensheaths, it is highly likely that the distal axon, particularly at the NoR, will also be susceptible to damage from circulating antibody. Therefore I sought to demonstrate MOG35 binding upstream from the NMJ at the NoR of intramuscular axons, with a view to creating a model and investigating injury targeted at this site. I focused on identifying binding of MOG35 in intramuscular nerve bundles of the Triangularis Sterni (TS) muscle, and also used diaphragm sections and phrenic nerve (all preparations outlined in more detail in section 2.4).

Primarily, it was important to be able to unequivocally locate NoR. The GD3/CFP strain was developed by crossing the GD3s^{-/-} strain (Okada et al., 2002) with the CK strain, which has endogenously fluorescent axons and Schwann cells (Zuo et

al., 2004). The reason for this cross was to create a mouse that not only would bind MOG35, but would also allow for easy identification of NoR. Axons could be followed from the terminal by the expression of endogenous cytoplasmic CFP, just as BTx was utilised to identify NMJ in previous studies. To ensure the cross did not diminish the effect of antibody binding, measurements of the intensity of deposition at endplates were compared between strains. The GD3s^{-/-} mice are on a C57BL/6-CBA background, while the CK mice have a C57BL/6-DBA background. As the ganglioside profile of CK mice has not previously been investigated, it was important to verify MOG35 binding in this strain as unpublished observations have shown that there can be variations between strains, as there can be for other anti-ganglioside antibodies (Halstead et al., 2004; Halstead et al., 2005). To confirm transgenic modifications did not alter normal nodal architecture, ultrastructural comparisons were carried out (section 2.2.3) before use of the GD3/CFP strain in experiments.

In some experiments it was necessary to use phrenic nerve as opposed to TS, therefore a study of permeability was necessary to determine under what conditions MOG35 would bind. This is important as previously it has been shown that anti-ganglioside antibodies cannot penetrate the intact perineurial sheath (Arasaki et al., 1993; Arasaki et al., 1998; Paparounas et al., 1999). Intraneural injection of antibodies has successfully resulted in deposition of antibody and would thus circumvent the necessity to desheath (Harvey et al. 1995; Ortiz et al. 2009; Santoro et al., 1992), but I felt desheathment was adequate for the purpose of my experiments.

Finally, as permeability of antibody is known to be an issue in nerve, I had to consider the possibility that the blood-nerve barrier would be detrimental to antibody binding in intramuscular bundles as well.

3.2 Results

3.2.1 *Mouse strain dependent GD1a localisation*

3.2.1.1 Wild type versus GD3/CFP: MOG35 binding

IgG deposition at the nerve terminal of GD3/CFP and WT mice was determined by measuring fluorescence intensity over the endplate, outlined by the post-synaptic binding of BTx. In the TS, deposition was significantly increased in GD3/CFP mice compare to WT (Figure 3.1A&C, $p < 0.001$).

Phrenic nerve showed a similar pattern with significantly greater levels of IgG deposition at NoR after desheathment compared to WT (Figure 3.1B, $p=0.001$). Nerve with an intact sheath had deposition comparable to WT.

3.2.1.2 GD1a localisation

The localisation of GD1a was first qualitatively assessed in the TS and SN of GD3/CFP mice by incubating the tissue with MOG35. The antibody binding was selective to the nerve terminal and at the NoR (Figure 3.2A) as seen previously for GD3s^{-/-} mice. NoR were easily identified in the GD3/CFP mouse due to the indicative narrowing of endogenous cytoplasmic CFP, followed by a central bulge (Figure 3.2C, top right).

The distribution of GM1 and GD1a across the NoR was compared by measuring the spread of CTx and MOG35 immunostaining, respectively. The length of staining was significantly longer for CTx (Figure 3.2B, $p < 0.001$). CTx deposition was on average more than double the length, measuring 3.5 μ m, while MOG35 deposition showed an average length of 1.5 μ m. MOG35 antibody seemed to be more focused to the nodal gap, while CTx appeared to bind more strongly at the paranodes (Figure 3.2C). This is indicative of a specificity of GD1a to the axolemma.

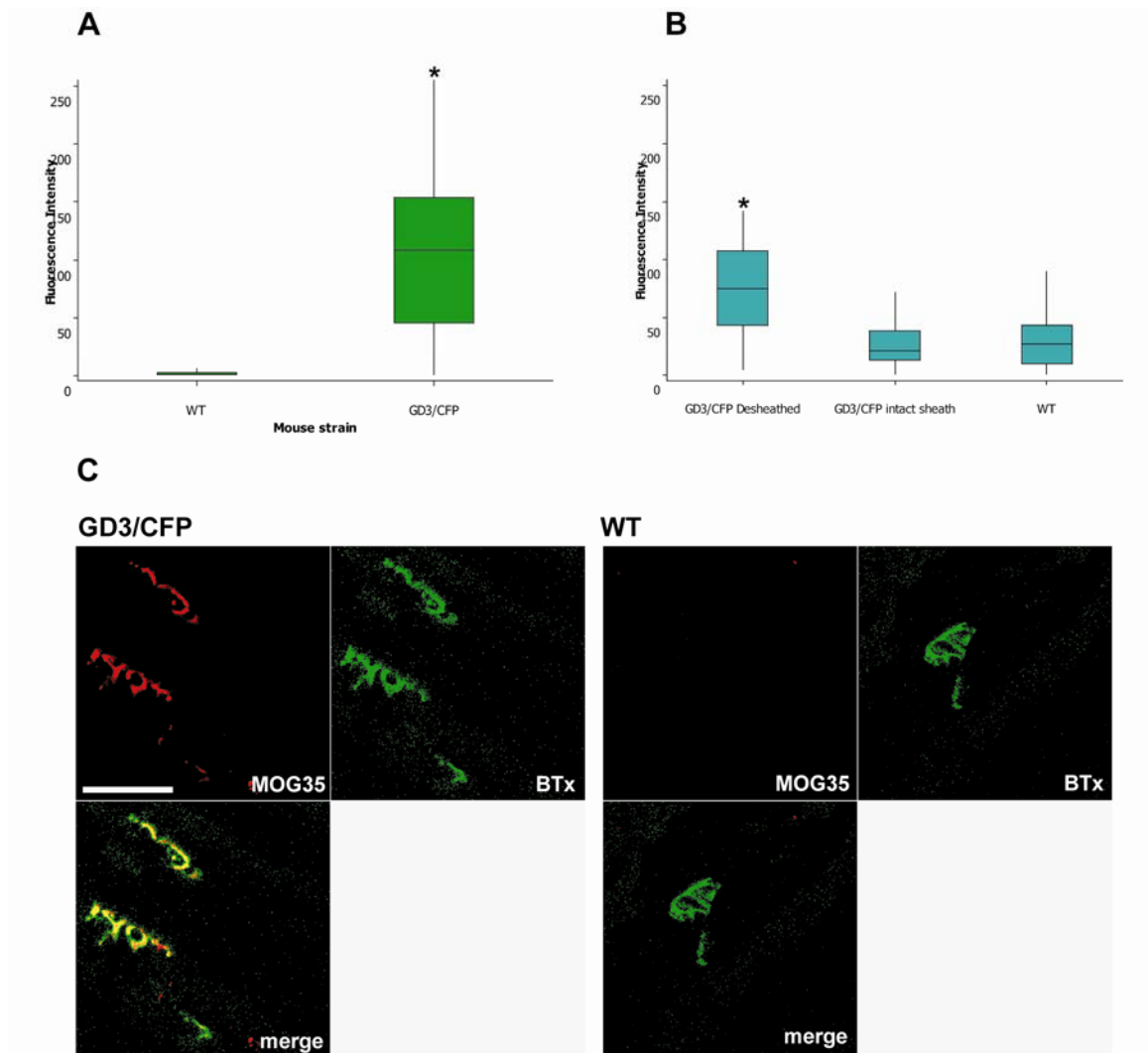


Figure 3.1: MOG35 binding at the NMJ of wild type (CK) and GD3/CFP mouse TS whole-mount and phrenic nerve.

A) Quantitative analysis of the TS demonstrates that there is minimal binding of MOG35 at the NMJ of the WT CK mouse, whereas binding is very strong in the GD3/CFP mouse. B) Quantitative analysis of phrenic nerve MOG35 binding indicates the requirement for the nerve to be desheathed before MOG35 binding is possible. C) Illustrative examples of confocal images of MOG35 (red) binding at the NMJ delineated by BTx (green). * indicates significance where $p < 0.05$ compared to CK wild type using the Mann-Whitney U test scale bar = $50\mu\text{m}$.

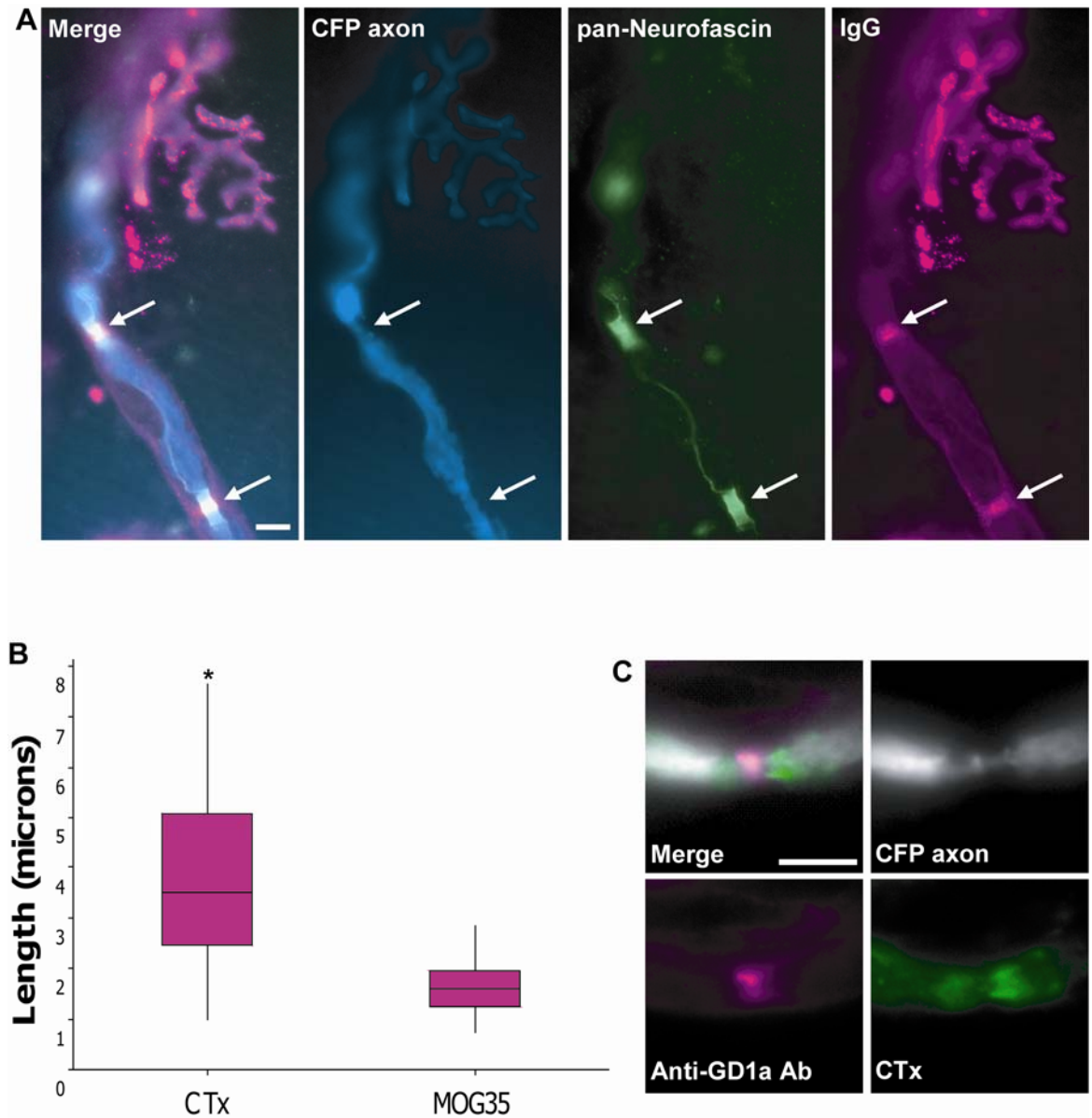


Figure 3.2: GD1a localisation in GD3/CFP mice.

A) GD1a (purple) is located on the nerve terminal and at the NoR (arrows) which can be identified by a narrowing in the CFP axon (white) and antibody against the nodal protein neurofascin (green). B) The length of staining measured along the NoR is significantly more extensive for CTx, a marker of GM1 ganglioside, than MOG35 the antibody against GD1a. C) The expression of GD1a appears to be more specific to the axolemma as intensity of fluorescence to MOG35 (purple) is greater at the nodal gap than fluorescently labelled CTx (green) that identifies the GM1 ganglioside. This ganglioside is more prominent at the paranodal loops than GD1a. * indicates significance where $p < 0.05$ compared to the length of MOG35 staining using the Mann-Whitney U test, scale bar = 5 μ m.

3.2.1.3 Nodal sub-region localisation of GD1a

In order to further elucidate the specific location of GD1a at the NoR, co-localisation studies were carried out using the Schwann cell microvilli marker radixin, and the paranodal loop marker myelin associated glycoprotein (MAG).

It emerged that GD1a immunostaining does not strongly co-localise with radixin, but there can be a partial overlap on occasion (Figure 3.3A and 3.3B, respectively). Anti-GD1a antibody deposition was strongest at regions flanking radixin staining, possibly at the paranodes. Co-localisation studies were then performed with MAG and this marker plus anti-GD1a staining did appear to overlap. Thus anti-GD1a antibody does not only bind to the axolemma at NoR, but also at the innermost paranodal loops.

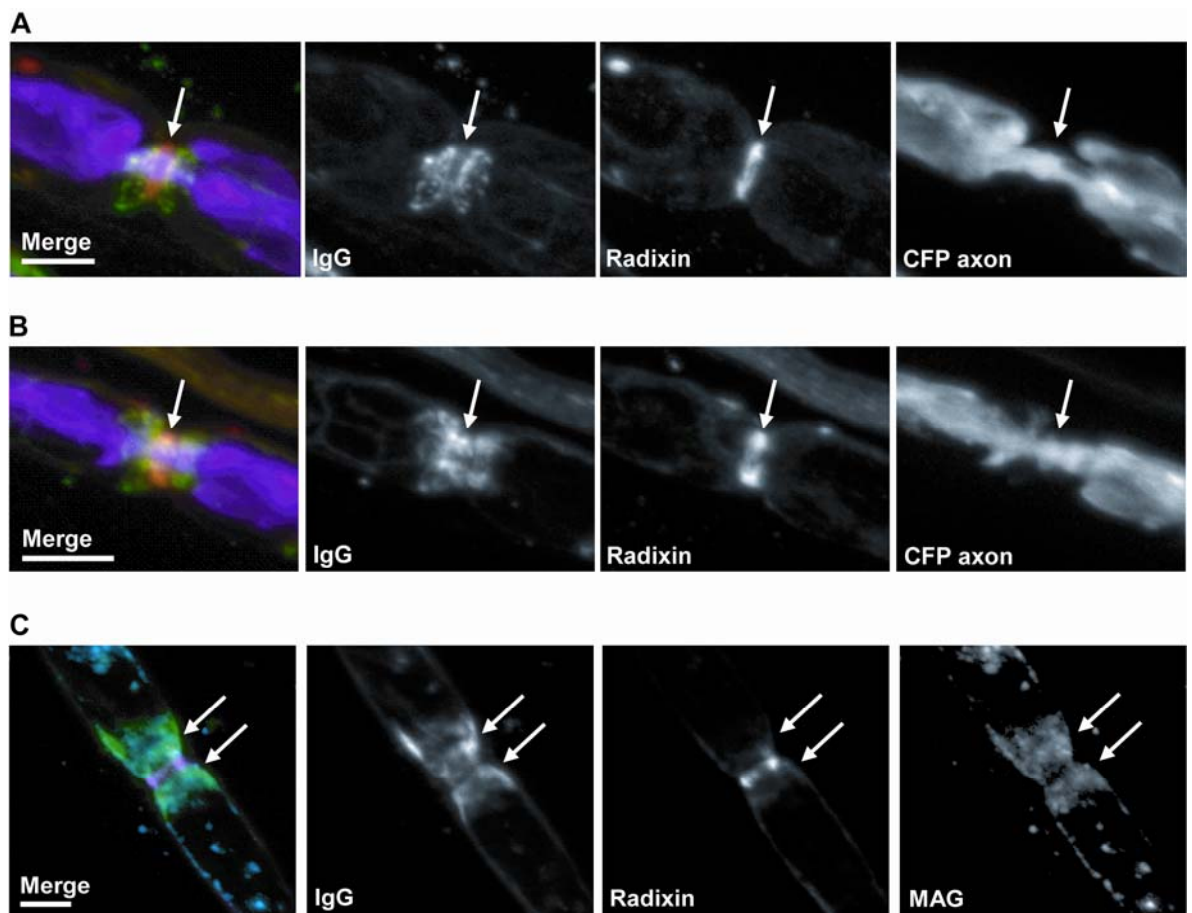


Figure 3.3: anti-GD1a localisation at sub-domains of the NoR.

Anti-GD1a antibody binds most strongly at regions flanking radixin (indicated by single arrow) expressed at the Schwann cell microvilli (A), although overlap can occur (B). Co-localisation of anti-GD1a antibody with MAG (indicated by arrows) is suggestive of a GD1a expression in the paranodal loops as well as the axon. Scale bars= 5µm.

3.2.2 BNB permeability

3.2.2.1 Ex vivo gradient dependent binding of MOG35

Whole-mount TS was used to study the BNB gradient dependent binding effect of MOG35 as intramuscular nerves could be followed with no interruptions caused by sectioning. Nerve bundles were arbitrarily categorised as follows (example illustrated in Figure 3.4A);

1. Single fibre
2. Small bundle <15 μ m
3. Medium bundle 15-35 μ m
4. Large bundle >35 μ m

Using this categorisation, NoR were identified for each group and the fluorescence intensity of antibody binding to MOG35 measured (Figure 3.4B). Single fibres have a significantly increased IgG deposition in comparison to all other bundle categories ($p<0.001$). In turn, small bundles had a significantly higher IgG deposition than medium and large bundles ($p<0.001$), and medium bundles compared to large ($p=0.0023$). Large bundles showed a level of IgG deposition comparable to untreated control, suggesting no permeability to antibody for this specific period of incubation or antibody concentration.

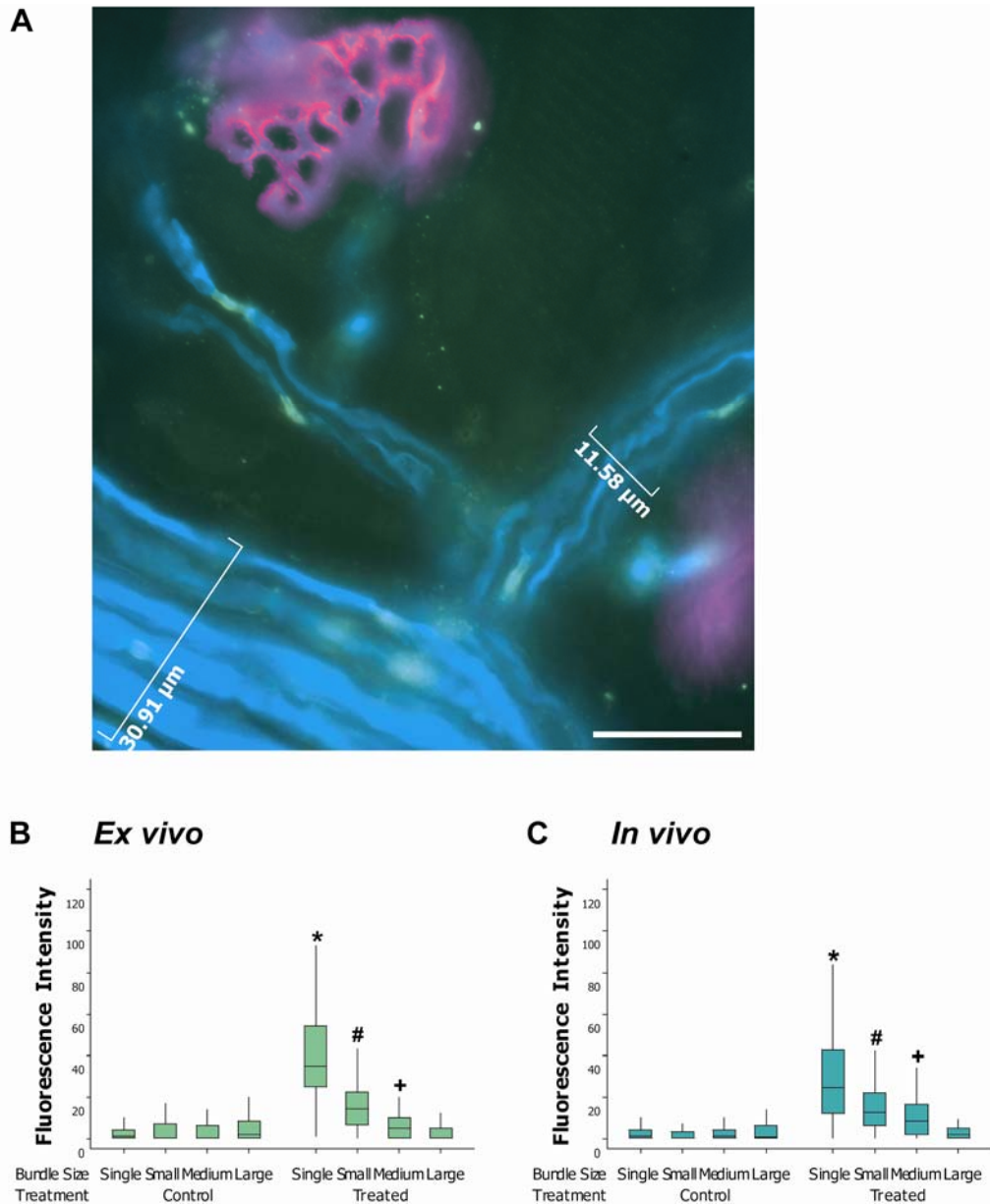


Figure 3.4: Categorisation of intramuscular nerve bundles to aid the quantification of MOG35 binding at NoR.

A) Epifluorescent image illustrating a portion of the intramuscular nerve bundle (cyan axons) of the TS branching from a medium sized bundle, to a small bundle and ultimately a single fibre that terminates at an NMJ. **B)** Fluorescence intensity of antibody deposited at NoR in single fibres is significantly greater than small bundles, and in small and medium bundles compared to large bundles and control. This demonstrates a reduction in permeability of the BNB to MOG35 *ex vivo*. **C)** The same pattern of permeability occurs *in vivo*. * signifies significance where $p < 0.05$ compared to the fluorescence at small, medium and large bundle and control NoR, # compared to medium and large bundles and control NoR, and + compared to large bundle and control NoR, using the Mann-Whitney *U* test, scale bar = $20\mu\text{m}$.

3.2.2.2 *In vivo* gradient dependent binding of MOG35

To clarify that this gradient dependent binding was caused by the permeability of the BNB in a natural system and not merely the result of topical antibody application, GD3/CFP mice were injected i.p with MOG35 antibody and left for 16h. A similar effect was demonstrated (Figure 3.4C).

3.2.2.3 Uniform GD1a expression

Sectioned diaphragm was incubated with MOG35 and IgG deposition measured for all bundle categories. This was intended to rule out the possibility that a change in intensity was due to a decrease in expression further upstream from the terminal, and was indeed an issue of BNB permeability. Antibody deposition was not significantly altered between the different bundle sizes (Figure 3.5).

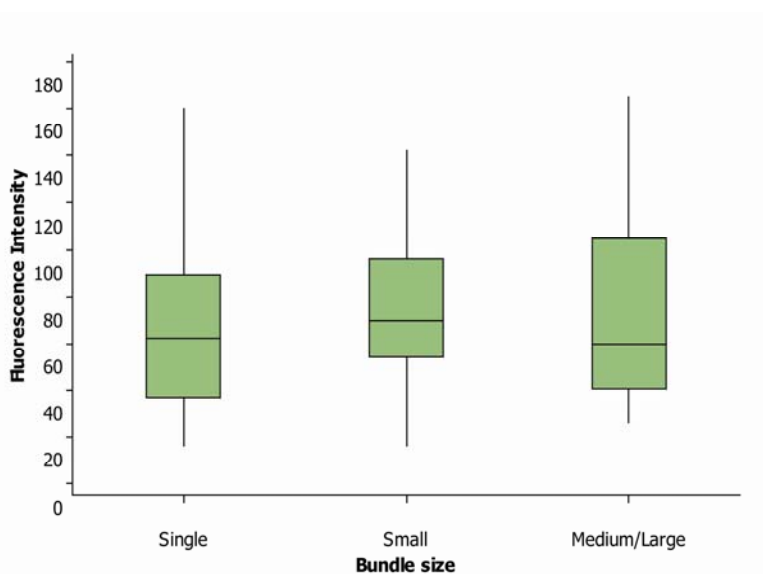


Figure 3.5: Quantification of antibody deposition at NoR in sectioned diaphragm.

When images of sectioned nerve are taken superficially to ensure the BNB no longer effects permeability, there is no significant difference in fluorescence intensity at NoR when comparing single fibres, small, medium and large bundles. This suggests that gangliosides are expressed ubiquitously and the binding gradient shown in the previous figure is indeed due to the permeability of the BNB.

3.3 Discussion

Taken together, the results of the WT versus GD3/CFP MOG35 binding assay and the ultrastructural examination are both supportive for use of this new transgenic mouse strain to create a model of injury concerning the GD1a ganglioside. It is preferable to have high expression of GD1a ganglioside for the MOG35 antibody to bind. This is true of the GD3s^{-/-} strain and the new GD3/CFP strain as crossing the former with the CK strain did not affect MOG35 binding. However, previously it has been shown that alterations to the ganglioside profile can have adverse effects. A decrease in complex ganglioside expression can cause disassembly of the nodal ultrastructure (Susuki et al., 2007a), axonal degeneration and myelination defects (Sheikh et al., 1999b), and reduced central conduction velocity (Takamiya et al., 1996) so it was important to determine whether over-expression would also unfavourably affect ultrastructural organisation of the NoR. GD3s^{-/-} mice have no complex b-series gangliosides, therefore this may have interfered with the development of the nervous system. However, it has already been shown that these animals are virtually behaviourally and morphologically normal (Okada et al., 2002). Fortunately, this change in ganglioside profile does not appear to be detrimental to the composition of the nerve, specifically the NoR, either.

As WT nerve demonstrated minimal antibody binding, it could be argued that the development of this transgenic mouse shows a bias towards positive results and may not be relevant to normal animals, or indeed humans. However, as it is the purpose of this study to assess the disease process as a result of anti-ganglioside antibody binding it was essential to produce a model where this occurred. Furthermore, the development of the GD3/CFP strain has proven indispensable to the identification of NoR. Axons are extremely difficult to track using external markers that can be unreliable- endogenous fluorescence overcomes this obstacle.

The localisation of anti-GD1a antibodies to the nodal gap, Schwann cell microvilli and first paranodal loops in distal axons, and the shorter spread of staining compared to CTx described in this study, has not been shown before. Furthermore, a possible difference in GD1a expression between distal and proximal nerves has not previously been examined. GM1 has been localised in

human nerve to the nodal gap and the surface of the paranodal myelin sheath (Illa et al., 1995). Similar staining has also been reported for mouse and rat nerve (Ganser et al., 1983; Sheikh et al., 1999a). GD1a has also apparently been localised to both of these regions in human motor root (De Angelis et al., 2001), but as there was no double-staining for a nodal gap protein, or for paranodal myelin in this study, it is difficult to be certain. In the study by Sheikh *et al* (1999a), tetanus toxin was reported to bind specifically to the axolemma. GD1a is a known ligand of tetanus toxin (Staub et al., 1986), therefore this would correspond to the axolemmal binding described here. However, spread of staining across the NoR with tetanus toxin does look wider than the axon itself, and although this was not investigated further, this could well have been microvilli staining as recognised here. The co-localisation of GD1a with MAG at the paranodal loops demonstrated in this study is possibly associated with the role of these two molecules in the stabilisation of the axo-glial junction (as discussed in section 1.2.3). Use of monoclonal antibodies to GD1a showed axonal binding in both human and rodent nerve (Gong et al. 2002), but this was in nerve cross-section and not specifically at the NoR itself. It is important to investigate specific antibody binding patterns when considering new experiments as antibodies seemingly raised to the same ganglioside can have very varied points of deposition (O'Hanlon et al. 1996).

Given that MOG35 binds to NoR, just as it was previously shown to bind the nerve at the NMJ, then presumably a similar injury will be identified further upstream on the addition of a source of complement. However, antibody binding at the NoR is more complicated than at the nerve terminal as there is an issue concerning the permeability of the BNB. As the branches of the intramuscular nerve move proximally and become wider in diameter and thus more protected by the increasing number of layers of the perineurial sheath (Olsson 1990), antibody binding diminishes. On following the nerve from the terminal proximally into the bundles I realised that it became more difficult to identify staining at NoR and decided it would be important to quantify this effect. By measuring MOG35 binding at NoR in superficial bundles that had been sectioned through we confirmed this to be an effect of permeability and not differing expression levels. As there is a distinct and significant difference to antibody binding as bundle size changes according to the categorisation used here, it is

important in all studies involving the TS preparation to consider results using the categorisation discussed above.

In some ways the use of the TS, where categorisation is required, over the sciatic or phrenic nerve, is questionable. However, these nerves require to be desheathed before the antibody is able to bind at NoR, and this did not present itself as such a natural model of injury. Having performed a passive immunisation of antibody to achieve similar antibody binding results to that of the *ex vivo* preparation, it is easy to justify use of the TS *ex vivo* preparation in most subsequent experiments. This does not completely invalidate the use of SN and PN and I found these nerves useful for several experiments described later.

4 Characterisation of antibody-mediated axonal injury

4.1 Introduction

Previous mouse models of GBS show that anti-ganglioside antibodies can cause antibody-mediated, complement-dependent injury to the motor terminals of the diaphragm (Halstead et al., 2004; O'Hanlon et al., 2001). This has also been shown using an *ex vivo* hemi-diaphragm preparation (Goodfellow et al., 2005). Injury at this site involves activation of complement, the formation of MAC pores, and loss of the integral axonal structural protein neurofilament. Injury to nerve can also be produced to a lesser degree after the implantation of an anti-ganglioside antibody-secreting hybridoma into mice (Sheikh et al., 2004). More recently, the disruption of nodes of Ranvier in ventral roots, characterised by a lengthening of the NoR and MAC deposition, has been demonstrated in a rabbit model of AMAN (Susuki et al., 2007b). As this study in rabbits mirrors pathology identified in human GBS patient spinal roots at autopsy (Griffin et al., 1996b; Hafer-Macko et al., 1996), it is clear that nodal injury specifically needs further investigation.

Initially I wanted to characterise the injury caused to the distal motor axon proximal to the nerve terminal. Injury could potentially migrate up the axon due to the damage caused to the nerve-ending, or be exacerbated due to an additional injury caused elsewhere, namely the NoR. Investigation of neurofilament integrity can be used to characterise injury as before. The characterisation of Wallerian degeneration has been enhanced using mice with endogenously fluorescent axons (Beirowski et al. 2004), and thus I could similarly investigate axonal injury by utilising the GD3/CFP mice.

Once this was established, I wished to determine if there was complement deposition and a more targeted injury at the NoR as this is where I have specifically found anti-GD1a antibody to be localised. Primarily, determining the specific localisation of MAC could be informative in that this would show if the injury is targeted at the NoR through a complement pathway, or merely a result of injury spreading from the terminal.

The NoR are found at intervals along myelinated axons where the myelin sheath forms an axo-glial junction with the axon (more detail section 1.4). This region has a very specific pattern of organisation due to its relationship with the myelin sheath and the importance of its role in conduction (Poliak & Peles 2003; Scherer 1996). As a result, discerning any alterations to the arrangement of various nodal proteins after antibody and complement treatment could reveal more about the injury found in AMAN, as has been similarly shown for various other peripheral neuropathies (Scherer & Arroyo 2002).

4.2 Results

4.2.1 Injury to the distal axon

To establish how injury develops in the distal axon due to antibody and complement-mediated attack, neurofilament loss and endogenous CFP loss were investigated. All of the experiments were carried out using GD3/CFP mice.

4.2.1.1 Neurofilament loss

After incubating the whole-mount TS preparation with complement for 3h, the intramuscular nerve bundles were examined for neurofilament immunostaining along the length of the distal axons. The axon was divided into four portions- from the terminal to the first NoR (up to 30µm), the first NoR itself, the next internode (up to 80µm) and the second NoR. Measurements were not made further along as axons would enter bundles and the additive affect of many fluorescent axons would interfere with the true intensity.

Figure 4.1 shows an example of the measurements along every axon from one muscle preparation, and then a graph of their average. Control axons (Figure 4.1A) had comparable levels of neurofilament along the first and second internode, and similarly across the first and second NoR. The levels of neurofilament immunofluorescence between internode and NoR was different presumably due to the finer calibre of the axon at this latter portion. Treated nerve showed a significant decrease in all four portions compared to the equivalent section in control nerve (Figure 4.1C, *t-test* $p < 0.001$). Furthermore,

there was an increased loss of neurofilament in the first internode and NoR compared to the second internode and NoR, respectively.

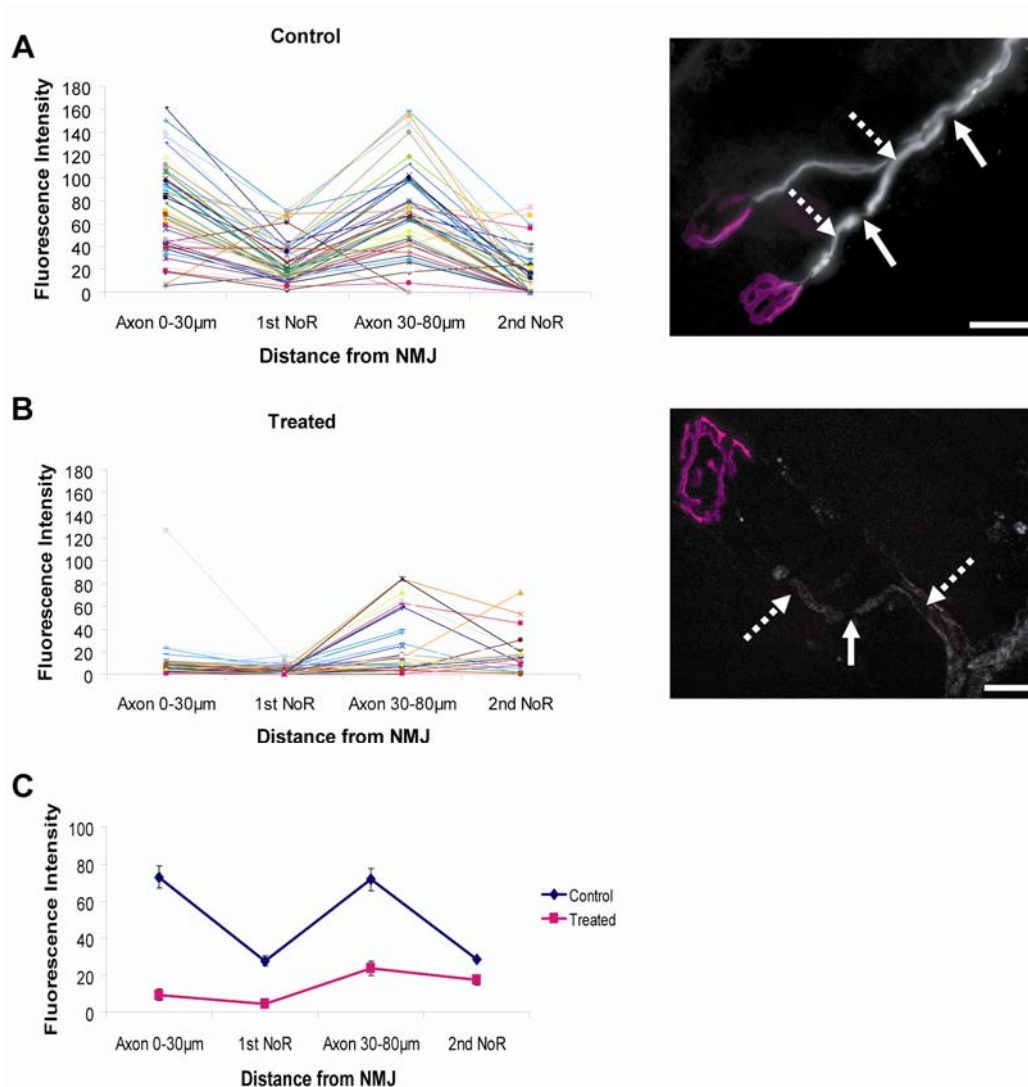


Figure 4.1: Antibody and complement mediated loss of neurofilament along the distal axons of TS intramuscular nerve.

Measurement of immunoreactivity to neurofilament along the distal axons from the NMJ was divided into four sections encompassing two internodes (broken arrows) and two NoR (solid arrows). Control axons (A) appear to have a higher level of neurofilament integrity than treated tissue (B) at both internodes and NoR. C) Average immunofluorescence along all axons from one preparation comparing treated and control. Scale bar= 20 μ m

4.2.1.2 Real-time loss of CFP in distal axon

I attempted to show loss of CFP along the distal axon in real-time by imaging live TS muscle from a GD3/CFP mouse. I used BTx to delineate the nerve terminal,

which was useful both to prevent twitching by paralysis, and to easily reimagine the same endplates. CFP was lost from the terminal within 15mins of complement addition however, it was more difficult to determine CFP loss along the distal axon. Figure 4.2 shows one of the best examples I was able to achieve of intact CFP in control tissue (Figure 4.2A) compared to loss of CFP in treated tissue (Figure 4.2B).

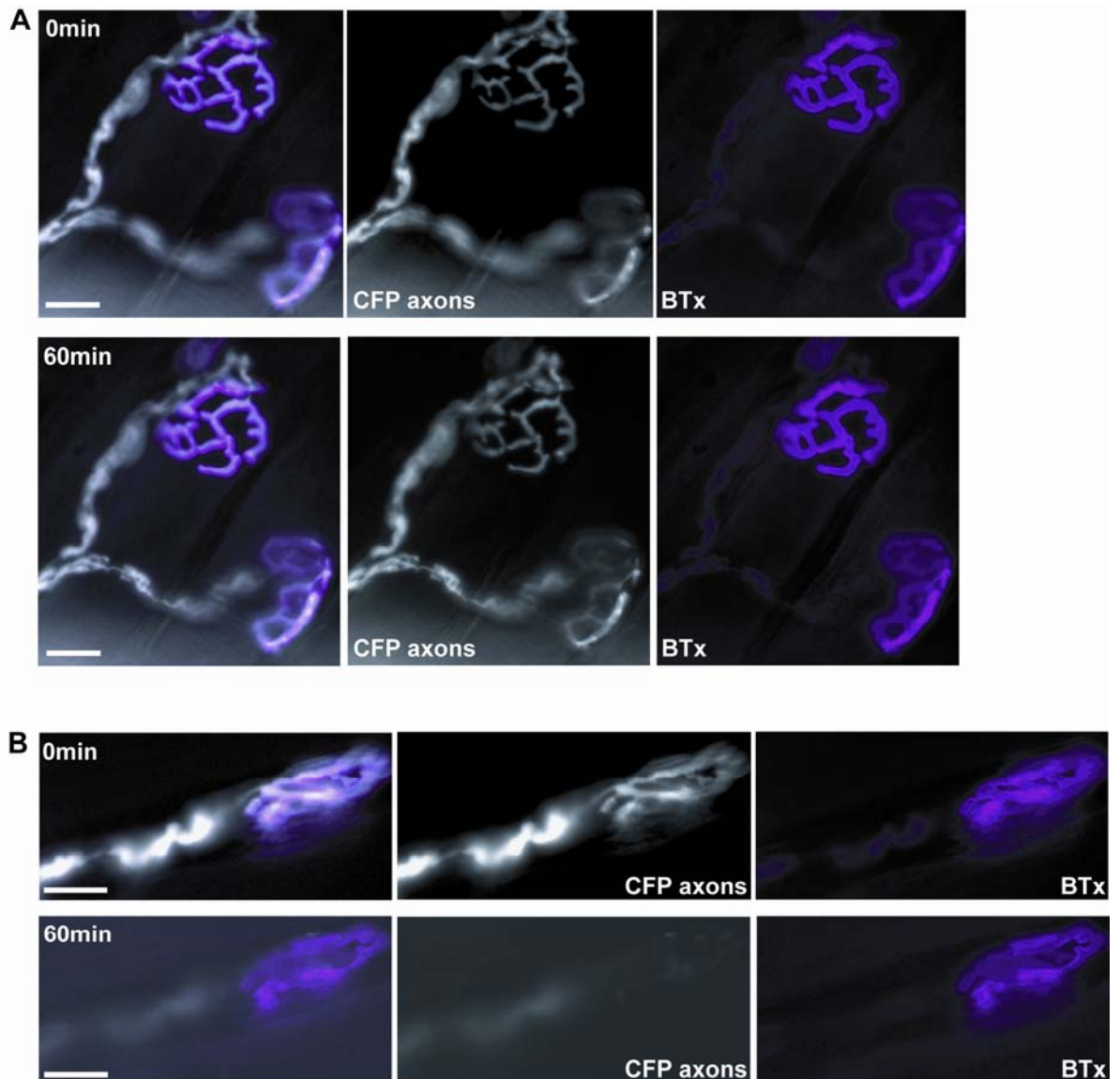


Figure 4.2 (previous page): Use of live imaging of TS preparation to determine CFP loss along distal axon in real-time as a result of antibody and complement mediated injury.

A) There is no loss of CFP (white) from axons in control tissue 60min (bottom panel) after 1st imaging. **B)** 60 mins after complement addition to treated tissue there is a loss of CFP along distal axon. BTx delineates nerve terminal (purple). Images captured with a 40x objective water immersion lens. Scale= 20 μ m.

4.2.1.3 Comparison of α -latrotoxin induced loss of CFP compared to antibody-mediated injury

To determine whether the damage to the distal axon was due to the injury ascending from the NMJ, or if antibody targeted to the NoR caused additional injury, I studied CFP loss/leakage after antibody treatment. This was compared to CFP loss after α -latrotoxin treatment that exclusively injures the nerve terminal (Rosenthal & Meldolesi 1989). There was no significant reduction to CFP intensity along the distal axon a length of 50 μ m after α -LTx treatment compared to control (Figure 4.3A,B & D, $p=0.9458$). However, after antibody treatment there was a small yet significant reduction in CFP intensity along lengths of axon up to 100 μ m from the nerve terminal compared to α -LTx treatment and control (Figure 4.3A&C, $p<0.001$). This is indicative of an additional injury at the NoR causing further CFP leakage.

4.2.2 Complement deposition at NoR

I felt it was important to show a deposition of MAC at NoR to correlate with antibody binding at this site in the TS, and to establish if this was the route of injury. However, despite following the protocol previously used to achieve MAC deposition at the nerve terminal (Goodfellow et al., 2005), I found none at the NoR. As I had established that the blood-nerve barrier could interfere with antibody binding, I presumed that this could affect exogenous complement penetration too and therefore decided to incubate the whole-mount TS preparation for 3h instead of 1h. At this time point the tissue was sectioned and stained, as it was easier to identify MAC immunoreactivity than in intact whole-mount muscle.

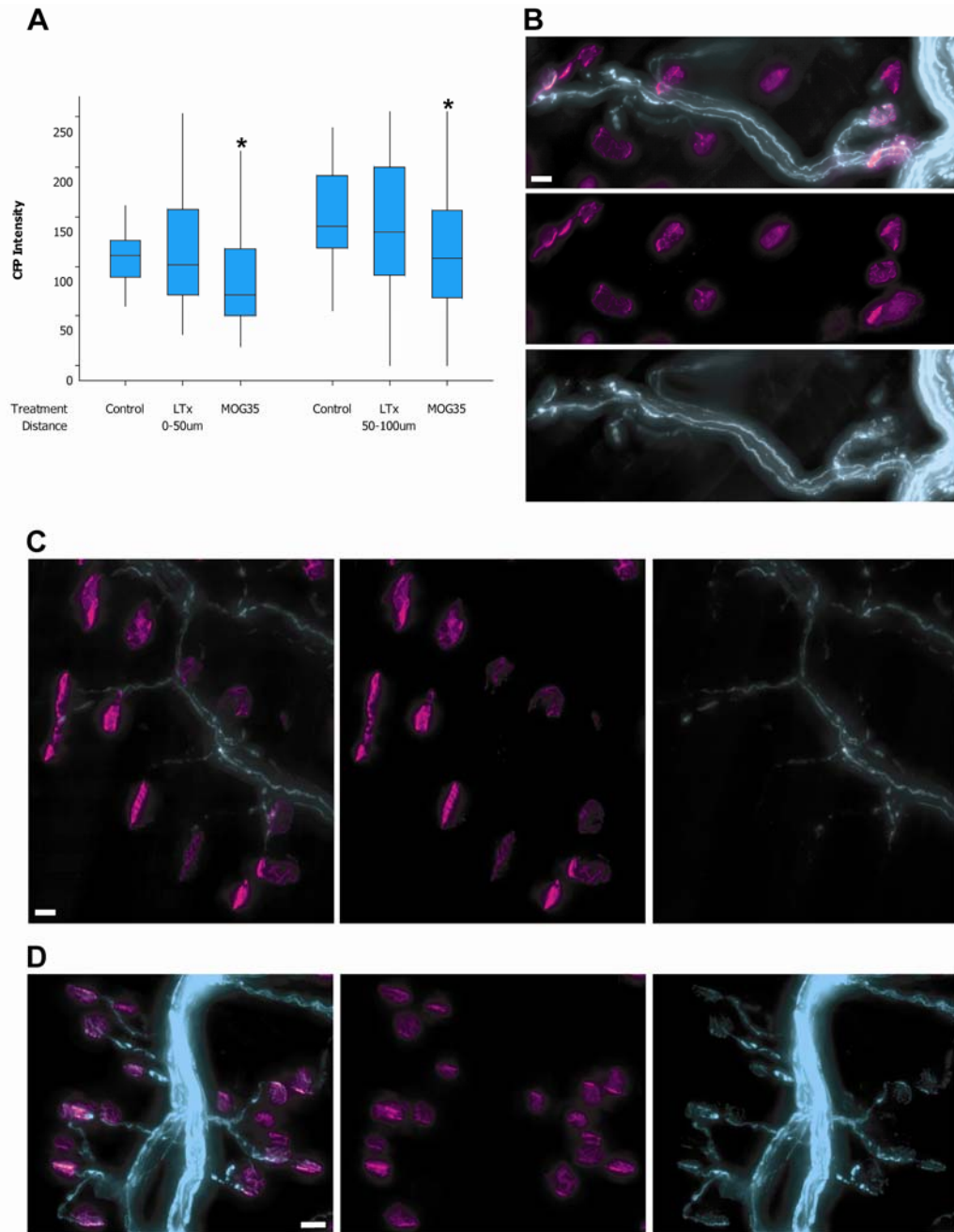


Figure 4.3: Comparison of loss of endogenous CFP along the distal axon in antibody treated and α -LTx treated intramuscular nerve from the TS compared to control.

A) Boxplot illustrating a significantly greater loss of CFP along the length of the distal axon after antibody treatment rather than the terminal specific injurious agent α -LTx. Treatment with α -LTx does not reduce CFP levels along the distal axon compared to control. **B)** Example of loss of CFP (cyan) at terminals (delineated by BTx, purple) alone after α -LTx injury, **C)** loss of CFP along axons in addition to terminals after antibody treatment, and **D)** control tissue with normal CFP fluorescent axons. * indicates significantly reduced levels of CFP compared to control or an α -LTx treated counterpart where $p < 0.05$, using the Mann-Whitney U test. Scale bar = $20\mu\text{m}$.

After treatment there was a significant increase in MAC deposition at NoR in single fibres compared to all other bundle categories, and small bundle NoR compared to those in medium and large bundles (Figure 4.4A, $p < 0.001$). Medium

and large bundle NoR had MAC deposition comparable to control. If the complement incubation time was extended to 6h, the medium bundle NoR also became more significantly enveloped with MAC depositions (Figure 4.4B, $p=0.0018$). For subsequent experiments, the time of complement exposure was 3h, unless otherwise stated, as I felt the integrity of the tissue might be compromised if it were extended. Antibody alone had no effect on nerve, and thus the appropriate control to the antibody plus complement treatment was Ringer's alone prior to complement incubation.

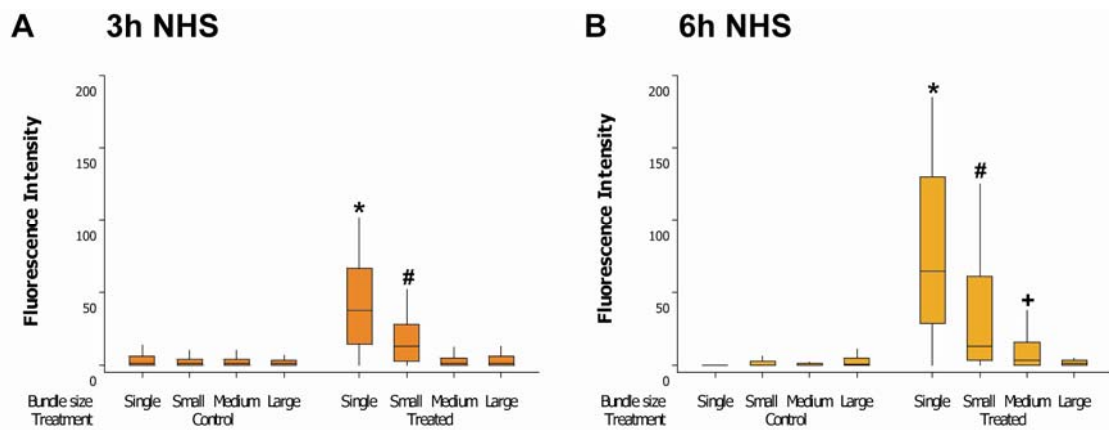


Figure 4.4: MAC deposition at the NoR of intramuscular nerve bundles of the *ex vivo* TS muscle preparation in GD3/CFP mice after treatment with antibody and complement.

A) Boxplot demonstrating that MAC deposits in treated TS are significantly higher at NoR in single fibres compared to small bundles, and small bundles compared to medium bundles, large bundles and control after 3h NHS incubation. **B)** Extending the NHS incubation to 6h also results in a significant increase to the level of MAC deposition at medium bundle NoR compared to large bundles and untreated control tissue. * indicates significance where $p < 0.05$ compared to small, medium and large bundles and control, # compared to medium and large bundles and control, and + compared to large bundles and control, using the Mann-Whitney *U* test.

4.2.3 Nodal protein disruption

To establish region-specificity of disruption to intramuscular NoR in the *ex vivo* TS preparation, I chose to look at an assortment of antibodies to different sites along the node. Essentially the NoR can be divided into three regions- the nodal gap, the paranodes and the juxtaparanodes, as outlined in section 1.4.3.

Initially I investigated the presence or absence of immunostaining to the voltage gated sodium channel, Nav1.6, which is known to form a tight cluster on the axolemma of the nodal gap of myelinated axons (Caldwell et al., 2000), and ankyrin-G the cytoskeletal protein also located at this region (Kordeli et al., 1995). Attempts were made to study another nodal gap protein, neurofascin 186, however staining was not reproducible in the whole-mount muscle preparation so I discontinued the use of this antibody for distal nerve immunohistochemistry.

At the paranode, the contactin-associated protein Caspr, is associated with the axon cytoskeleton aligning with the paranodal loops (Einheber et al., 1997). Antibody raised against this protein recognises two neat bands at the NoR, with a space inbetween staining that represents the nodal gap. The 155kDa isoform of neurofascin, Nf155, can also be found at this region (Tait et al., 2000), but it is linked to the paranodal loops rather than the axon and forms part of the axo-glial junction (Charles et al., 2002). Unlike the basic presence/absence quantification used for Nav1.6 and ankyrin-G, immunostaining to Caspr and Nf155 had to be classed as normal or abnormal/absent. This was owing to the fact that often there was still staining present after treatment, but it did not necessarily make up two neat bands delineating the paranode, as under normal circumstances. Furthermore, the antibody identifying Nf155, is a pan neurofascin antibody and therefore also recognises the Nf186 isoform found at the nodal gap (Tait et al., 2000). This made quantification quite difficult in axons of such fine calibre, and thus this antibody was not used in further studies to ensure that the quantification was accurate.

Finally, the potassium channel Kv1.1 can be found on the axolemma at the juxtaparanode flanking Caspr staining at the paranodes (Arroyo et al., 1999). Again, its disruption was less extreme than for proteins at the nodal gap and therefore classification was similar to the paranodal proteins.

4.2.3.1 Nodal gap

After antibody and complement treatment, Nav1.6 immunoreactivity at NoR in single fibres and small bundles was significantly reduced compared to their control counterparts, with only 10.3% and 10.5% positively stained, respectively (Figure 4.5A, χ^2 -test, $p < 0.001$). A similar pattern was identified for ankyrin G with only 16.7% of single fibre and 32.3% of small bundle NoR possessing positive staining (Figure 4.6A, χ^2 -test, $p < 0.001$). Immunoreactivity for these two proteins was not significantly reduced after treatment in medium and large bundle NoR compared to control.

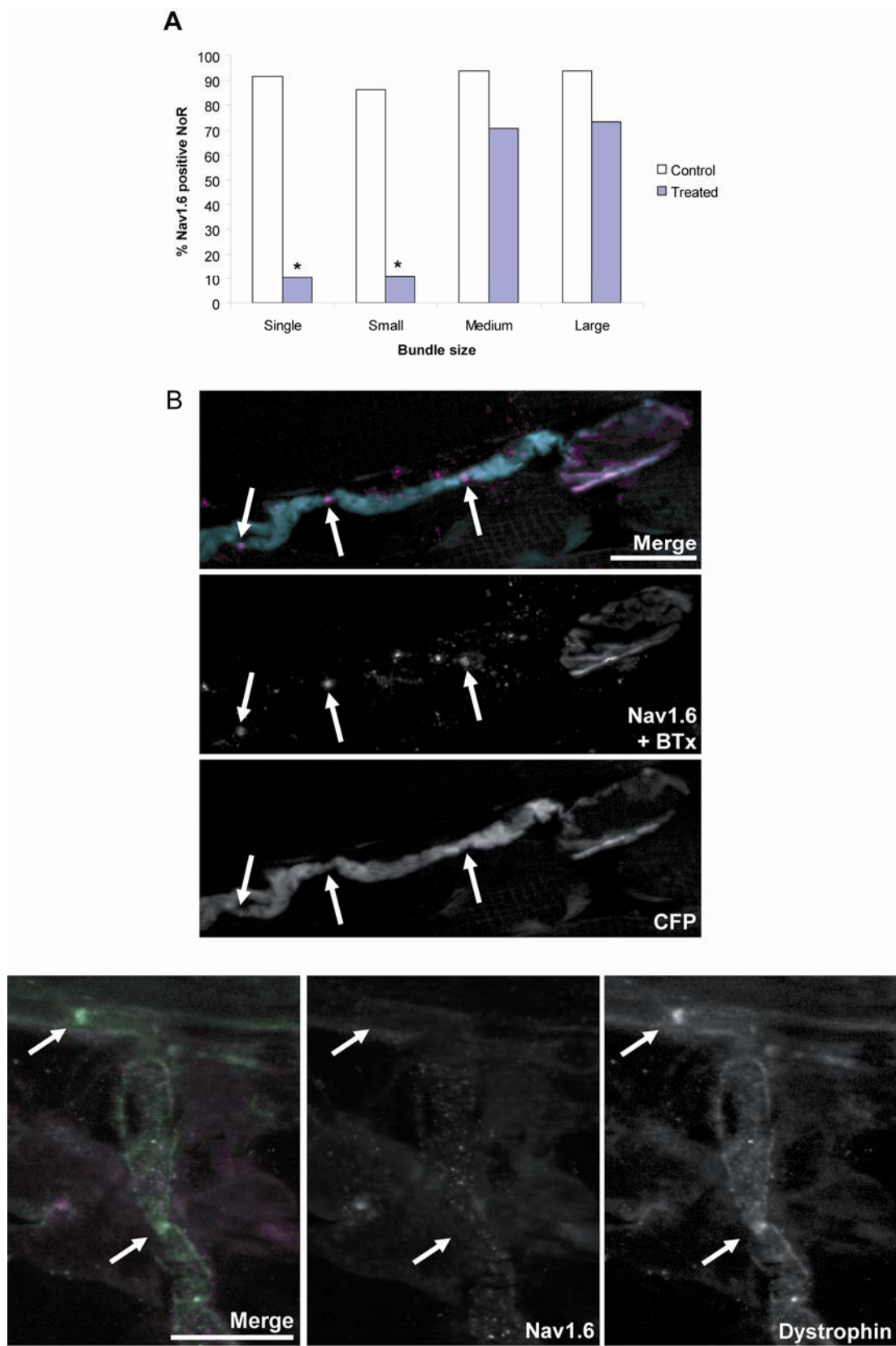
Figures for legends below on following pages

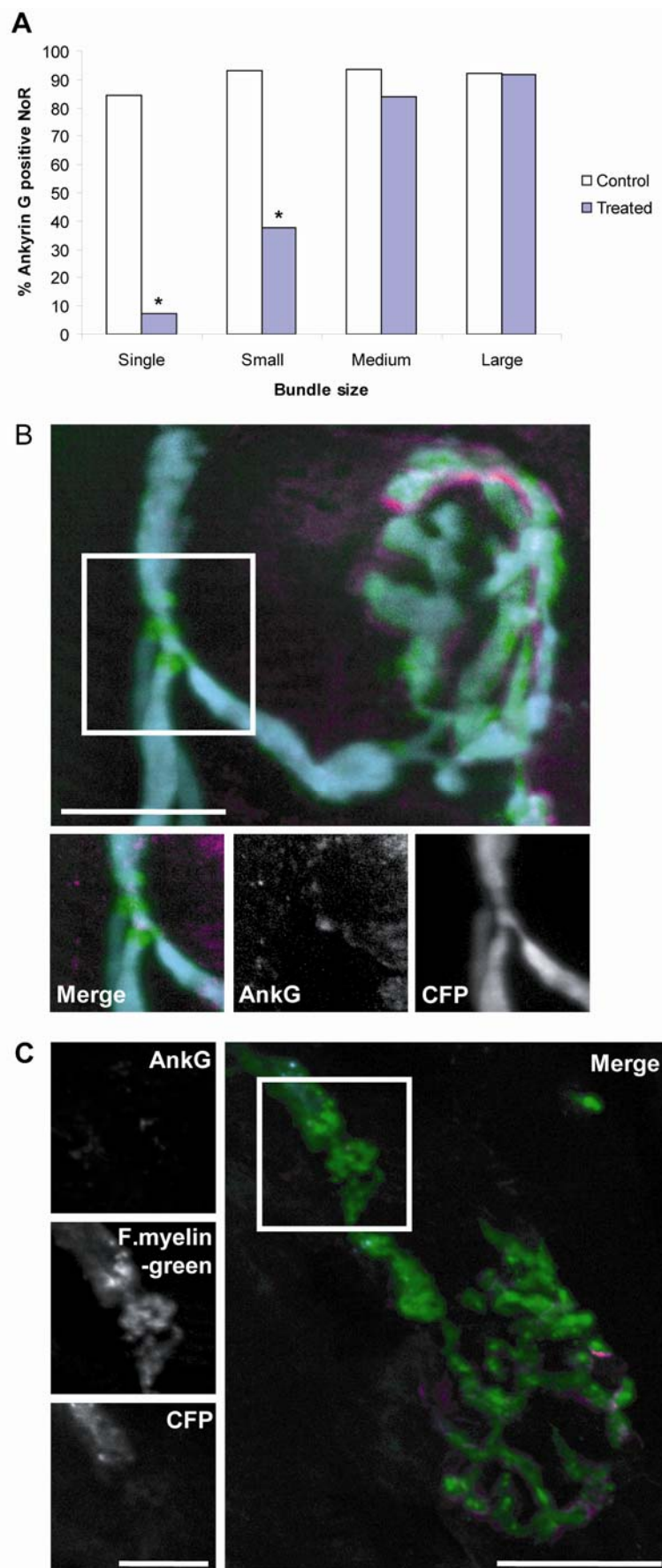
Figure 4.5: Effect of anti-ganglioside antibody plus complement treatment on the Nav1.6 channel at NoR in the TS intramuscular nerve bundle of GD3/CFP mice.

A) Single fibres and small bundles had significantly less NoR (as identified by dystrophin) with Nav1.6 channel staining compared to control counterparts. Medium and large bundle Nav1.6 staining at NoR was unaffected by treatment. B) Image showing a neat band of staining at the nodal gap representing Nav1.6 channel clustering (arrows). C) Nav1.6 channel staining is no longer present at the NoR after treatment (arrows). * indicates significance where $p < 0.05$ compared to control bundle size counterpart, using the Chi-squared test of independence. Scale bar= 20 μ m.

Figure 4.6: Effect of anti-ganglioside antibody plus complement treatment on ankyrin G at NoR in the TS intramuscular nerve bundle of GD3/CFP mice.

A) The percentage of ankyrin G positive NoR in single fibres and small bundles is significantly reduced after treatment compared to control. There is no significant change to nodal staining of medium and large bundles between treatment groups. B) Image of normal ankyrin G immunostaining at a NoR (boxed region) in control tissue. C) Example of loss of ankyrin G staining at a NoR (boxed region), depicted by fluoromyelin green. * indicates significance where $p < 0.05$ compared to control bundle size counterpart, using the Chi-squared test of independence. Scale bar= 20 μ m on large image, 10 μ m boxed region.





4.2.3.2 Paranode

Figure 4.7B and 4.8B show the normal staining configuration of Caspr and neurofascin, respectively. Antibody against Caspr forms two neat bands on either side of the nodal gap, while neurofascin staining forms a solid band due to the inclusion of staining of both the 155 and 186kDa isoforms. At the NoR in single fibres there was a significant decrease in the percent of those with normal immunoreactivity to Caspr and Nf155 after treatment compared to control fibres (83.3% and 62% reduction respectively, Figure 4.7A and 4.8A, χ^2 -test $p < 0.001$). This was also true for small bundle NoR (67.7% and 35.8% reduction, respectively), although the loss was clearly greater for single fibre NoR. Control levels of positively stained NoR for Caspr and Nf155 were the same in medium and large bundles with or without treatment.

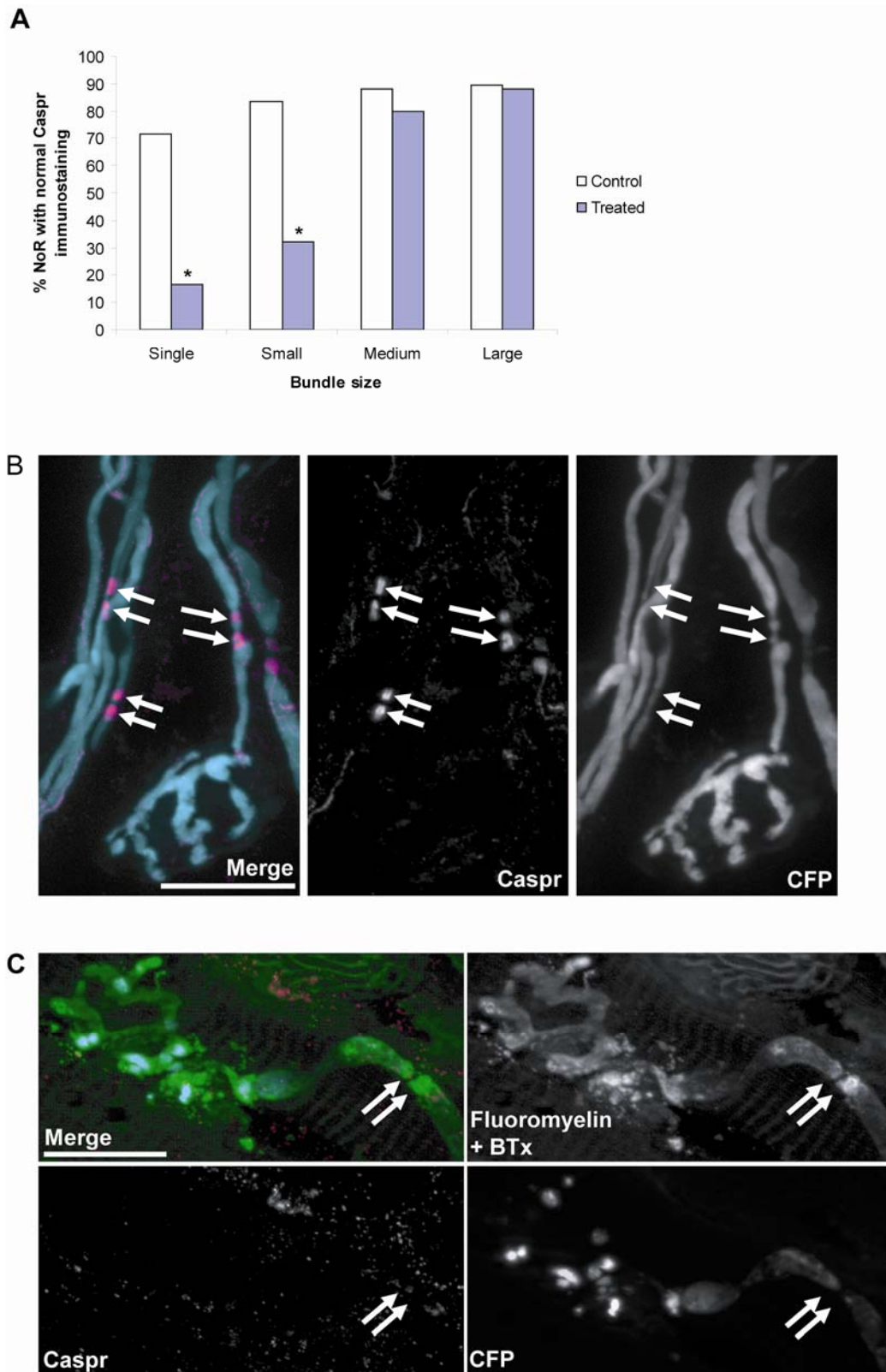
Figures for legends below on following pages

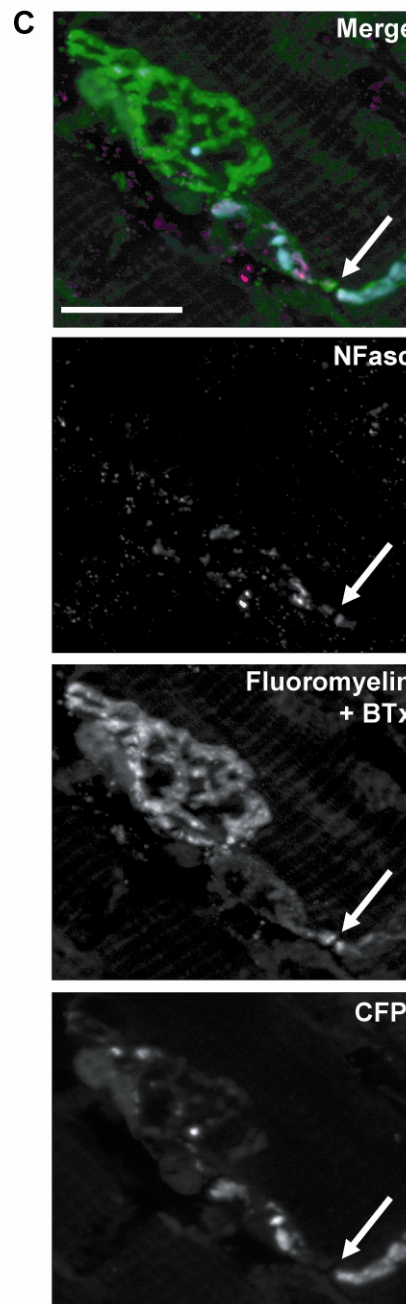
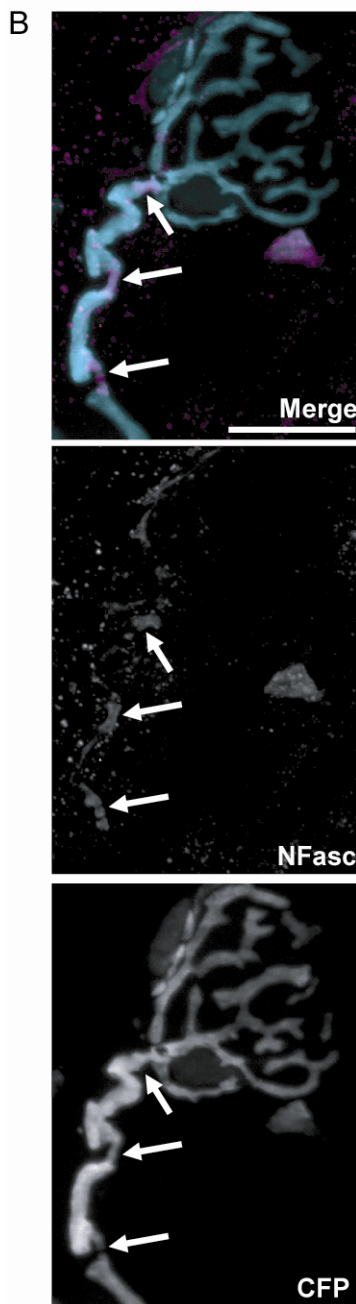
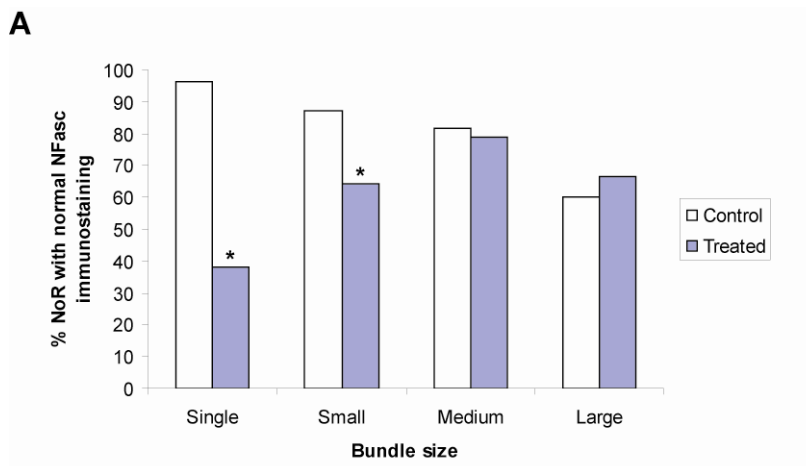
Figure 4.7: Effect of anti-ganglioside antibody plus complement treatment on the paranodal protein Caspr in the TS intramuscular nerve bundle of GD3/CFP mice.

A) Caspr immunoreactivity at NoR was significantly reduced in single and small bundles after treatment compared to control. Medium and large bundle NoR had a similar level of positively stained NoR in both treated and control groups. B) Example of normal Caspr staining forming two neat bands on either side of the nodal gap (arrows). C) A NoR identified by fluoromyelin-green staining has no apparent Caspr staining after treatment. * indicates significance where $p < 0.05$ compared to control bundle size counterpart, using the Chi-squared test of independence. Scale bar= 20 μ m.

Figure 4.8: Effect of anti-ganglioside antibody plus complement treatment on the paranodal glial protein neurofascin in the TS intramuscular nerve bundle of GD3/CFP mice.

A) The percentage of NoR with undisrupted neurofascin immunostaining is significantly reduced in single fibres and small bundles after treatment compared with control. There is no reduction to neurofascin positive NoR in medium and large bundles after treatment. B) Example of normal neurofascin staining stretching across the nodal gap and paranodes (arrows). C) A NoR identified by fluoromyelin-green staining has disrupted neurofascin staining after treatment, although it is not completely absent * indicates significance where $p < 0.05$ compared to control bundle size counterpart, using the Chi-squared test of independence. Scale bar= 20 μ m.





4.2.3.3 Juxtaparanode

The staining pattern for Kv1.1 looked the same in all bundle sizes of both treated and control tissue, therefore there was no significant difference to Kv1.1 at NoR for any bundle category between control and treated tissue (Figure 4.9A). Figure 4.9B is an example of Kv1.1 immunostaining. This was true at 3h and even when the NHS incubation was increased to 6h.

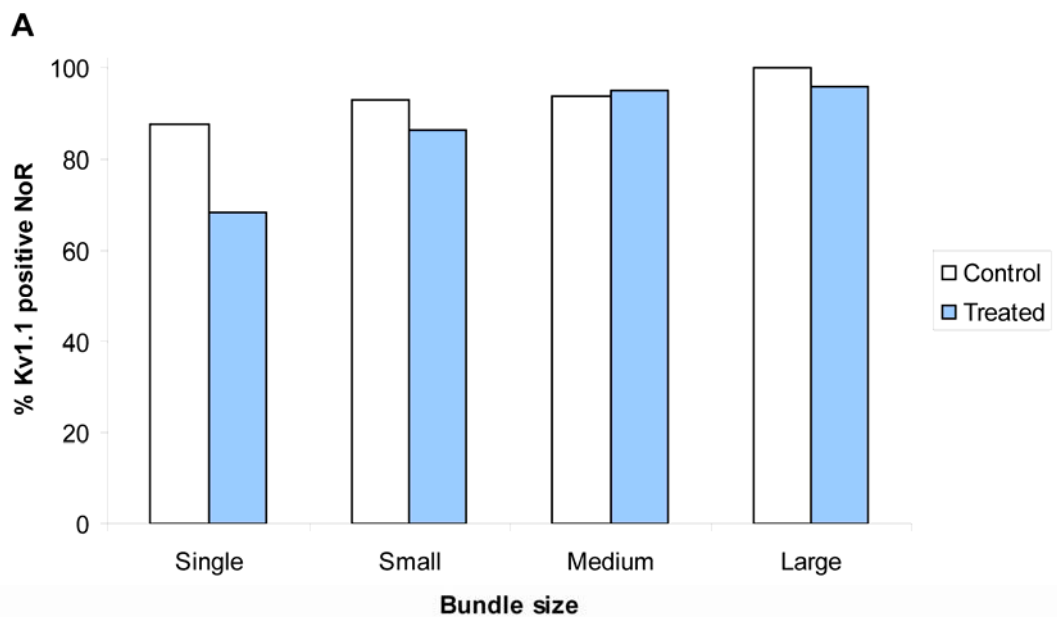


Figure 4.9: Effect of anti-ganglioside antibody plus complement treatment on the Kv1.1 channel at NoR in the TS intramuscular nerve bundle of GD3/CFP mice.

A) There is no significant change to Kv1.1 immunostaining at NoR for any bundle category between treatment and control groups. **B)** An example of normal Kv1.1 juxtaparanodal staining (green) at a node downstream from the terminal (shown by BTx, purple). Scale bar= 20 μ m.

4.2.3.4 Targeted nodal disruption

To ensure that the antibody-mediated, complement-dependent injury is indeed directed to the NoR and not merely a product of injury travelling up from the NMJ, the Nav1.6 presence/absence staining model was used after nerve terminal specific injury induced by α -LTx treatment. Figure 4.10 corroborates the data collected that shows a targeted injury to the NoR, by illustrating that Nav1.6 channel staining is still intact after an α -LTx directed insult to the nerve terminal at the NMJ.

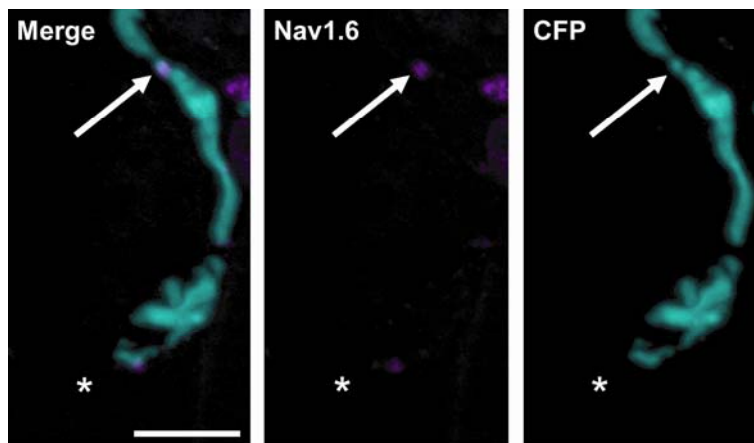


Figure 4.10: Illustration of intact Nav1.6 channel immunostaining at the NoR after an alpha-latrotoxin induced injury to the nerve terminal. Arrow indicates Nav1.6 staining at a NoR while the asterisk identifies where the nerve terminal would be. Scale bar= 20 μ m.

4.2.3.5 Phrenic nerve protein disruption

The targeting of injury specifically to the node was further explored by desheathing the purely motor phrenic nerve to expose the fibres to antibody and complement before determining nodal protein disruption.

Presence and absence of Nav1.6 and ankyrin G immunostaining was investigated and there was a significant reduction to positively stained NoR in treated nerve compared to control (Figure 4.11A, X^2 -test $p < 0.001$). This was also true for Caspr staining disruption (Figure 4.11A, X^2 -test $p = 0.05$). Interestingly, the

number of positively stained NoR after treatment for these markers was higher than observed for TS single fibres. Also, it was observed in differential interference contrast microscopy (DIC) images that the nerve fibre appeared swollen and rather bulbous at the regions flanking the nodal gap after treatment (Figure 4.10B).

In addition to the above proteins, immunostaining to the Schwann cell microvilli protein moesin, and the extracellular axonal protein NrCAM was also investigated. Staining to these proteins was similarly affected by treatment with antibody and complement, however unlike Nav1.6 and ankyrin G staining, was on the most part present, although disrupted (Figure 4.12). As the staining for NrCAM is 'spread' in such an unusual manner along what appear to be the myelin sheath, an additional antibody was tested. The results for this antibody were similar to the initial NrCAM antibody. This was further confirmed by 'spread' of NFasc 186 staining also targeted to the extracellular domain.

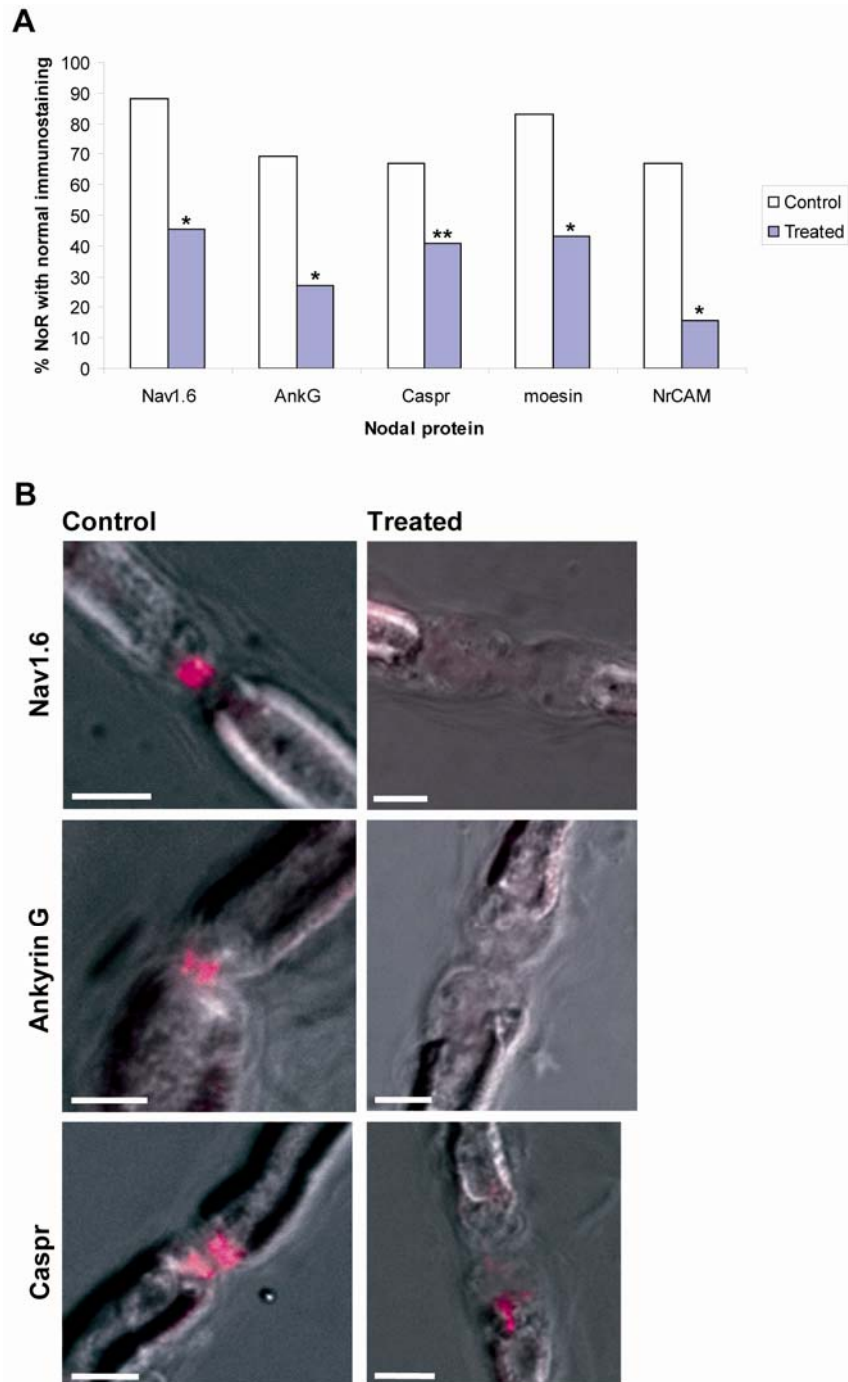


Figure 4.11: Quantification of positive staining for various proteins at the phrenic nerve NoR after anti-ganglioside antibody and complement treatment, compared to control.

A) There is a significant reduction in Nav1.6, ankyrin G, Caspr, moesin and NrCAM positively stained NoR after treatment compared to control. **B)** Images depict normal Nav1.6, ankyrin G and Caspr staining at NoR in control tissue (purple, left panel) compared to loss or disruption after treatment (right panel). The right panel also demonstrates the swollen conformation of the NoR in response to complement treatment as visualised by DIC. * indicates significance where $p < 0.05$ and ** where $p < 0.01$ compared to control, using the Chi-squared test of independence. Scale bar = $5\mu\text{m}$.

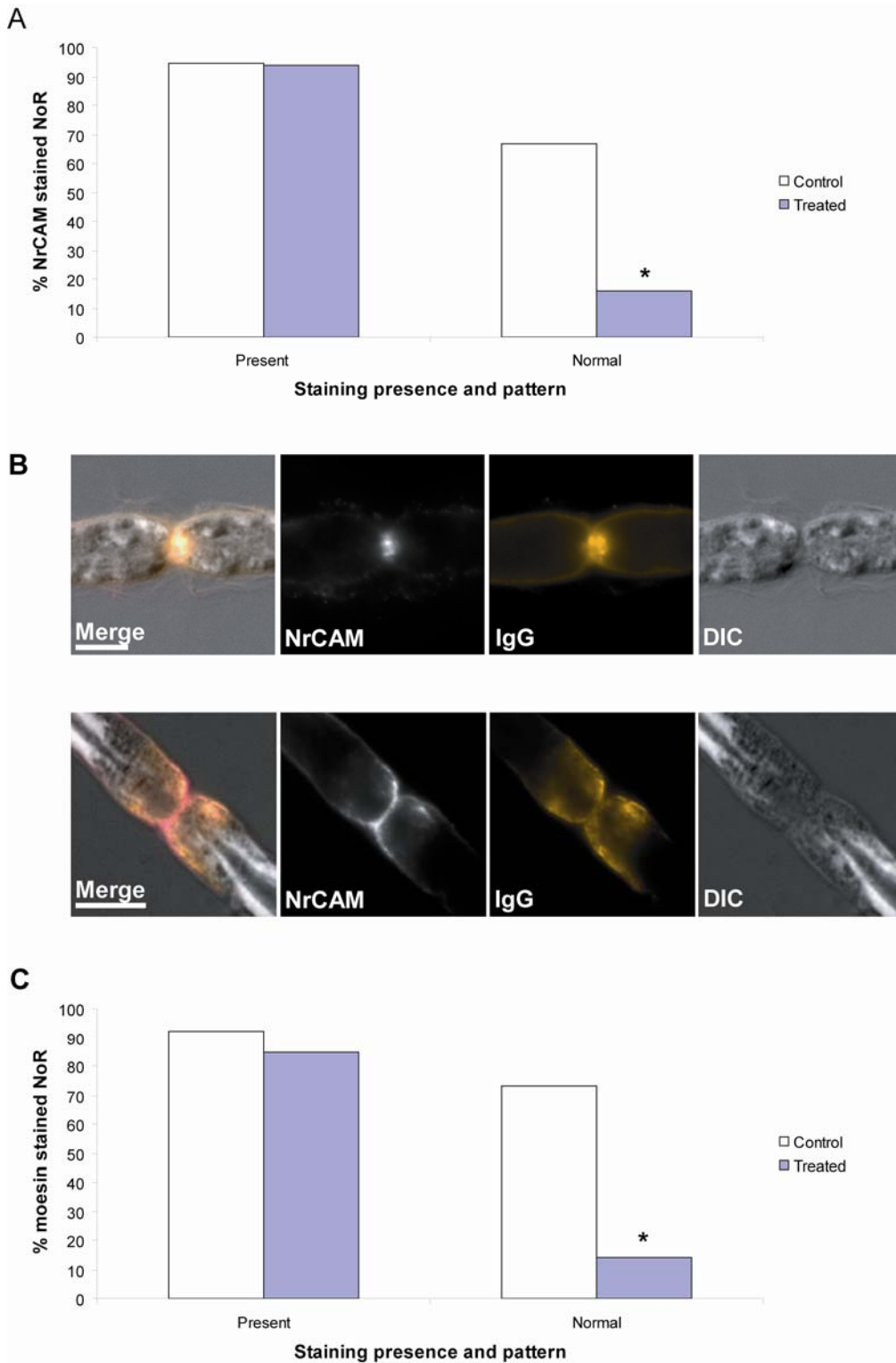


Figure 4.12: Reclassification of presence and normality of NrCAM and moesin staining at phrenic nerve NoR after anti-ganglioside antibody induced injury.

A) NrCAM staining could be classified as present or absent before further categorised into a normal or abnormal staining category. Although staining presence was not significantly reduced after treatment, the pattern became significantly disrupted compared to control. **B)** This phenomenon is illustrated with normal NrCAM at NoR (as identified by DIC) depicted in the top row of images, with an example of present but altered staining below. IgG (orange) staining is also altered around the NoR. **C)** A similar observation was made for moesin. * indicates significance where $p < 0.05$ compared to control, using the Chi-squared test of independence. Scale bar = $5\mu\text{m}$

4.3 Discussion

Previously MAC deposition and neurofilament loss have been used as indicators of injury to the nerve terminal in models of anti-ganglioside antibody-dependent complement-mediated attack (Goodfellow et al., 2005; Halstead et al., 2004; O'Hanlon et al., 2001). MAC pore formation results in the influx of many ions, including Ca^{2+} that can activate the protease m-calpain (Goll et al. 2003). This results in the breakdown of, among other substrates, the essential cytoskeletal component neurofilament, demonstrated in our model by use of calpain inhibitors for protection (O'Hanlon et al., 2003). Recent studies also show targeted disruption to the NoR by anti-ganglioside antibody and complement (Susuki et al., 2007b). As there was no effect of antibody alone on protein immunoreactivity, it appears that complement activation plays a critical role in the injury to the nerve. Therefore in the present study I found it crucial to determine MAC deposition at the NoR followed by the investigation of specific nodal injury.

Although the loss of neurofilament along the distal axon and across NoR was shown to be significant after treatment compared to control, this did not elucidate whether injury was targeted to the NoR. It does represent an injury that is more extreme distally and becomes less apparent with proximal movement along the nerve. It is feasible that the loss of neurofilament becomes less prominent more proximally as IgG deposition decreases in a gradient-dependent manner due to the blood-nerve barrier becoming less permeable (section 3.2.2.1). This in turn results in a reduced level of MAC deposition and injury where axons are less vulnerable.

As YFP labelled axons have been utilised to investigate the progress of Wallerian degeneration along nerves, I postulated that I could use the exogenous CFP in GD3/CFP in a similar manner. To follow CFP loss in real-time, I imaged live whole-mount TS preparations after the addition of NHS. Unfortunately, there were a number of caveats to this technique-

1. Bleaching. CFP is quite susceptible to photo-bleaching as the tissue was not fixed.

2. Lack of fixation also results in contortion of muscle due to injurious effect of fluorescence light. To prevent this as much as possible, only snaps were taken instead of z-stacks, however this is not as informative.
3. Small sample number. As the NHS was added to the entire preparation, only a couple of areas could be imaged to maintain a comparable injury time.
4. Difficulty in identifying NoR specifically.
5. Interference of clear optics by complement.

Ultimately, I did not find live-imaging to be a useful tool in determining injury and moved on to using fixed tissue at set time-points.

From live imaging it seemed that CFP was lost along the distal axon in a ubiquitous manner. In an attempt to separate the level of injury between the axon generally and the node itself, I compared CFP loss in the distal axon after antibody plus complement treatment, and α -LTx treatment. α -LTx targets and injures the presynaptic membrane at the nerve terminal specifically (Duchen et al., 1981) and thus extra loss of CFP in antibody treated tissue demonstrates that there must be injury elsewhere. It has previously been shown that MAC pores allow proteins of up to 35kDa to pass through (Simone & Henkart 1982) and as CFP is approximately 27kDa it is plausible that CFP from the targeted areas of injury could leak out. Alternatively it too could be a calpain substrate (discussed further in section 5.3).

Therefore, as with the neurofilament study, this could not be shown to be specific to the NoR. As neither neurofilament or CFP loss were good indicators of targeted injury to the NoR, I began to investigate the disruption to specific proteins and ion channels found in this region. Focus was placed on the *ex vivo* TS preparation as it is a more natural paradigm of injury. However, the phrenic nerve preparation was also useful to show loss of nodal protein immunostaining was not an affect of terminal damage, reinforcing the results from α -LTx experiments.

When characterising distal axonal injury, I discovered that antibodies to nodal proteins could not help me identify NoR after treatment. It was at this stage I realised staining must be disrupted due to the protein itself undergoing degradation. I tried a number of other methods to identify NoR and found success with fluoromyelin-green which labels lipids and thus not only outlines the myelin sheath along the internode, but is particularly intense at the paranodal loops of NoR. Using this marker I could follow axons to their terminals and identify whether there was antibody staining at the NoR. Localisation of nodal regions was later confirmed with anti-dystrophin antibody that also labels the myelin sheath and stains the nodal gap intensely. Loss of immunostaining to proteins at the nodal gap observed in this study may be intuitive due to the localisation of antibody and MAC deposition. The fact that there is always a more significant loss of protein immunoreactivity at single and small bundles is also in accordance with the increased level of IgG and MAC depositions at these sites. It was convenient that medium and large fibre NoR largely maintained normal staining as this was the ideal internal control to confirm staining was successful and that distal NoR truly were disrupted. On occasion staining for proteins in the medium and large bundles were not at as high a level as control single and small bundle NoR. However the treated and control levels were not different and thus I put this down to a penetration issue in very large bundles.

The fact that disruption not only occurs to proteins localised to the axon, but also those on the glial membrane, indicates a general disorder to the area rather than specific axonal damage. To explore this concept, I investigated the post-injury staining pattern of two proteins expressed at the nodal gap but whose antigenic targets are in the extracellular matrix. The first, NrCAM, is a cell adhesion molecule with a short cytoplasmic domain while the bulk of the protein extends into the extracellular matrix (Grumet et al., 1991; Kayyem et al., 1992) at the NoR (Davis et al., 1996). As the antibody to this protein binds the extracellular domain at the NoR, using Triton X-100 interfered with the staining. The result of this was that NrCAM could not be detected in the TS, presumably due to the blood-nerve barrier which would normally have been permeabilised by the Triton in most staining protocols. However, there was detectable immunostaining in the phrenic nerve and thus analysis was only carried out in this preparation for NrCAM. A similar scenario was true for the Schwann cell

microvilli protein moesin that also projects into the extracellular matrix at the nodal gap from the Schwann cell microvilli (Scherer et al. 2001). Intriguingly, unlike the axonal transmembrane protein Nav1.6 and axonal cytoskeletal protein ankyrin G whose staining 'disappeared' after treatment with anti-ganglioside antibody and a source of complement, NrCAM and moesin staining was still present. However, although it was present it was not in its normal configuration of a neat band, but instead more spread out along the Schwann cell outer surface. NoR with this abnormal staining pattern frequently displayed very swollen axons, as illustrated in DIC. As this staining was so unusual, another NrCAM antibody and an antibody to the extracellular portion of NF186 were investigated. The same pattern of spread appeared to occur in all cases. This could be suggestive that proteins within the axon are degraded, while other proteins in the immediate area are disrupted due to disorganisation of the axo-glial junction. It has not previously been shown that Nav1.6 is a calpain substrate *in vivo*, therefore this requires further investigation.

The argument for disruption specific to the axo-glial junction is strengthened due to the fact that Kv1.1 channel staining did not seem to be affected. To ensure that the Kv1.1 would not become damaged given more time for the injury to progress laterally from the nodal gap, the incubation time was increased to 6h. Kv1.1 still appeared to remain intact, which could mean it is too distant from the site of injury, or the length of incubation is still not sufficient to allow it to be affected. Paranodal protein KO mice have often shown a translocation of Kv1 from the juxtaparanodes to the paranodes (Boyle et al., 2001), but there may not have been sufficient time in this acute model for this to occur. Even in the chronic model of AMAN, Kv1 redistribution into the region of the paranode was not exceptional (Susuki et al., 2007b). As there was no apparent change I felt there was no need to use this as a marker in further experiments. Nav1.6, ankyrin G and Caspr were the preferable choices for future immunofluorescence experiments.

Susuki *et al* (2007) recognised the damage to NoR of ventral roots in a chronic rabbit model of AMAN as a lengthening and disruption to nodal proteins, followed by the reemergence of Nav channel positive heminodes that later fused to reform NoR. In my acute model, I found there was a complete loss of Nav1.6 channel and ankyrin G immunostaining at distal NoR rather than a lengthening

and separation. This could possibly explain early paralysis and the first stages of the disease process. However, it is not known that the channel and proteins are not still present or functional, it is merely known that the antigen the antibody is directed to has either been degraded or changed conformation.

In fact, as the sodium channel can undergo cleavage of its cytoplasmic loops and remain functional aside from loss of the inactivation gate (Armstrong et al., 1973; Stuhmer et al., 1989), another mechanism entirely may be at work. This will be addressed in a subsequent chapter.

5 Complement and calpain mediated injury to distal axons

5.1 Introduction

In the previous chapter it was demonstrated that immunoreactivity to several proteins and sodium ion channels was lost or disrupted at the NoR of distal axons in mouse TS intramuscular nerve after an anti-ganglioside antibody-dependent complement-mediated injury. It is the purpose of this chapter to determine what the cause of this loss and disruption might be.

The most plausible explanation is that MAC pores allow the influx of Ca^{2+} that activates the Ca^{2+} -dependent protease calpain. Prior studies at the mouse endplate have shown that MAC pore deposition and injury to neurofilament can be attenuated by complement (Halstead et al., 2005; Halstead et al., 2008b) and calpain inhibition (O'Hanlon et al., 2003), respectively.

As MAC pores form at the NoR after the aforementioned injury (section 4.2.2), it would follow that injury at this location will be similar to that described at the nerve terminal. Calpain includes ankyrin-G and neurofilament as a couple of its many substrates (Chan & Mattson 1999). In addition, several proteins that anchor other nodal molecules are also calpain substrates (more detail section 1.4.5), and could in turn result in a disruption to the protein of interest. Thus it seemed appropriate to investigate the influx of calcium and the protective effects of complement and calpain inhibitors on the staining of nodal proteins in an *ex vivo* mouse model.

Eculizumab is a humanised monoclonal antibody that binds the terminal complement component C5 to block its cleavage, and thus acts as a complement inhibitor by preventing MAC pore formation (Thomas et al. 1996). It is used clinically to treat paroxysmal nocturnal haemoglobinuria (Hillmen et al. 2006). Recently Eculizumab has been used to prevent *in vivo* injury at the nerve terminal of mice treated with anti-ganglioside antibodies in a model of Miller Fisher Syndrome (Halstead et al., 2008b). If protection is afforded to the terminal it is likely this will also apply to the NoR. If staining to nodal proteins

previously lost or disrupted are protected by this complement inhibitor then MAC pore formation is directly related to the course of injury. ALXN3300 is the non-specific isotype matched antibody that could be used as a control in all experiments. Other complement inhibitors exist but this one is so specific to human complement it seemed the most appropriate for use in this study where a source of exogenous human complement is applied to preparations.

AK295 is a synthetic reversible peptide that interferes with the activation of calpain (Li et al., 1996). Neuropathy of axons due to various injury models have all benefited from AK295 treatment (Bartus et al., 1994; Saatman et al., 1996; Wang et al., 2004). Consequently, it seemed appropriate to utilise this inhibitor to attempt to protect proteins from cleavage in our mouse model.

5.2 Results

5.2.1 Calcium influx due to MAC deposition

To begin with I used calcium indicators in PC12 cells to explore calcium influx. I first investigated the changes in calcium after treatment of the cells with the Ca^{2+} ionophore, ionomycin. This was achieved using the calcium indicator Rhod 2-AM.

10min after the addition of $1\mu\text{m}$ ionomycin, PC12 cells became brightly fluorescent, which was sustained for another 50min at least, indicating the influx and binding of calcium to Rhod 2-AM (Figure 5.1A).

I then wanted to demonstrate a similar response in cells incubated with MOG35 antibody to treatment with 10% NHS. Figure 5.1B illustrates the increased fluorescence in cells after 10mins of treatment with complement.

Unfortunately, the success witnessed in cells was not consistently replicated in whole-mount muscle preparations. Rhod 2-AM is a convenient indicator since it should be visible from the start so that you can ensure uptake has occurred, and becomes brighter with calcium ion binding. In tissue, uptake was not always a success, even with the addition of pluronic acid, which is supposed to aid movement into cells. Initially I wanted to show a change in nerve terminal

fluorescence after ionomycin treatment as the terminal are easier to identify than the NoR. Figure 5.2A and 5.2B show some examples of endplates that appeared to have an increase in Rhod 2-AM fluorescence, and some that did not, respectively. NoR were even more difficult to identify as Rhod 2-AM penetration into axons was not very successful (Figure 5.2C).

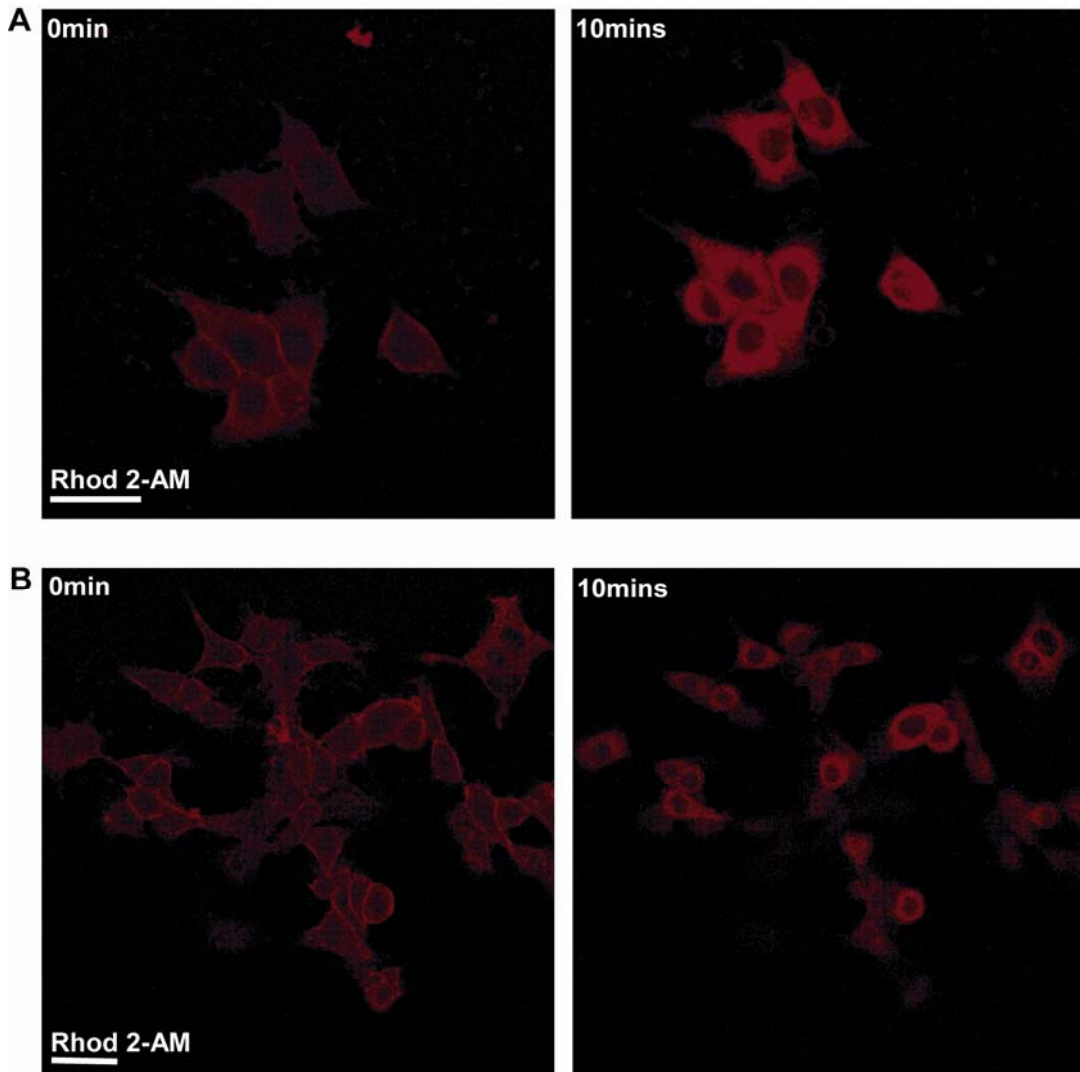


Figure 5.1: Rhod 2-AM activation by calcium ion influx into PC12 cells after treatment with the ionophore ionomycin, or anti-ganglioside antibody and a source of complement.

A) PC12 cells imaged 10mins after a treatment with 1μM ionomycin showed an increase in the fluorescence of the calcium indicator Rhod 2-AM signifying an influx of calcium. B) There was also an influx of calcium ions 10mins after the addition of complement to cells pre-incubated with anti-GD1a antibody. Scale bar= 10μm

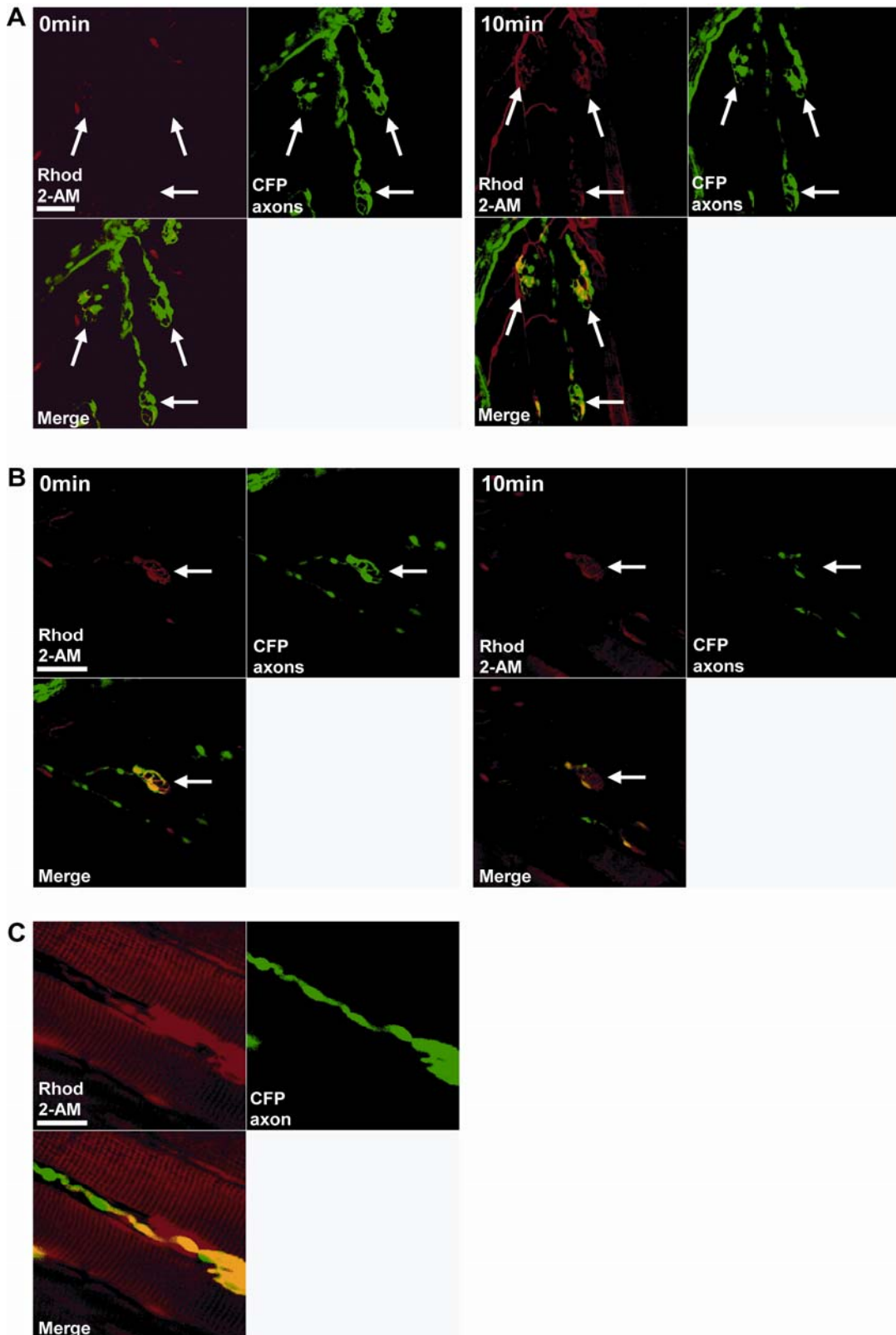


Figure 5.2: Assessment of alteration to Rhod 2-AM fluorescence at the NMJ of *ex vivo* TS preparations after treatment with ionomycin.

A) CFP axons (green) were used to identify endplates in which Rhod 2-AM (red) was also visible at a low level. After ionomycin treatment NMJs were reimaged and a stronger signal indicates an influx of calcium ions (yellow in merged image). **B)** This increase in fluorescence was not always identifiable and more often than not, the signal used to detect the endplates was lost or suffered bleaching. **C)** NoRs were virtually impossible to recognise and the Rhod 2-AM did not seem to be taken up by axons. Scale bar= 50 μ m.

5.2.2 Complement inhibition protects *ex vivo* preparations

The complement inhibitor Eculizumab was added at 100µg/ml to normal human serum 10min before application to an *ex vivo* TS preparation from a GD3/CFP mouse. The non-specific isotype-matched mAb ALXN3300 was used as control. For examples of normal nodal protein staining patterns please refer back to Figure 4.5, 4.6 and 4.7 for Nav1.6, ankyrin G, and Caspr, respectively.

5.2.2.1 CFP

CFP was the first feature to be assessed for protection by Eculizumab. Intact cytosolic CFP distribution in intramuscular nerve bundles was observed and is illustrated in a montage of apoTome images (Figure 5.3). ALXN3300 did not offer the same protection and as shown in Figure 5.3B, CFP became weaker in larger bundles and unapparent in terminals over the endplates (discriminated by BTx, purple).

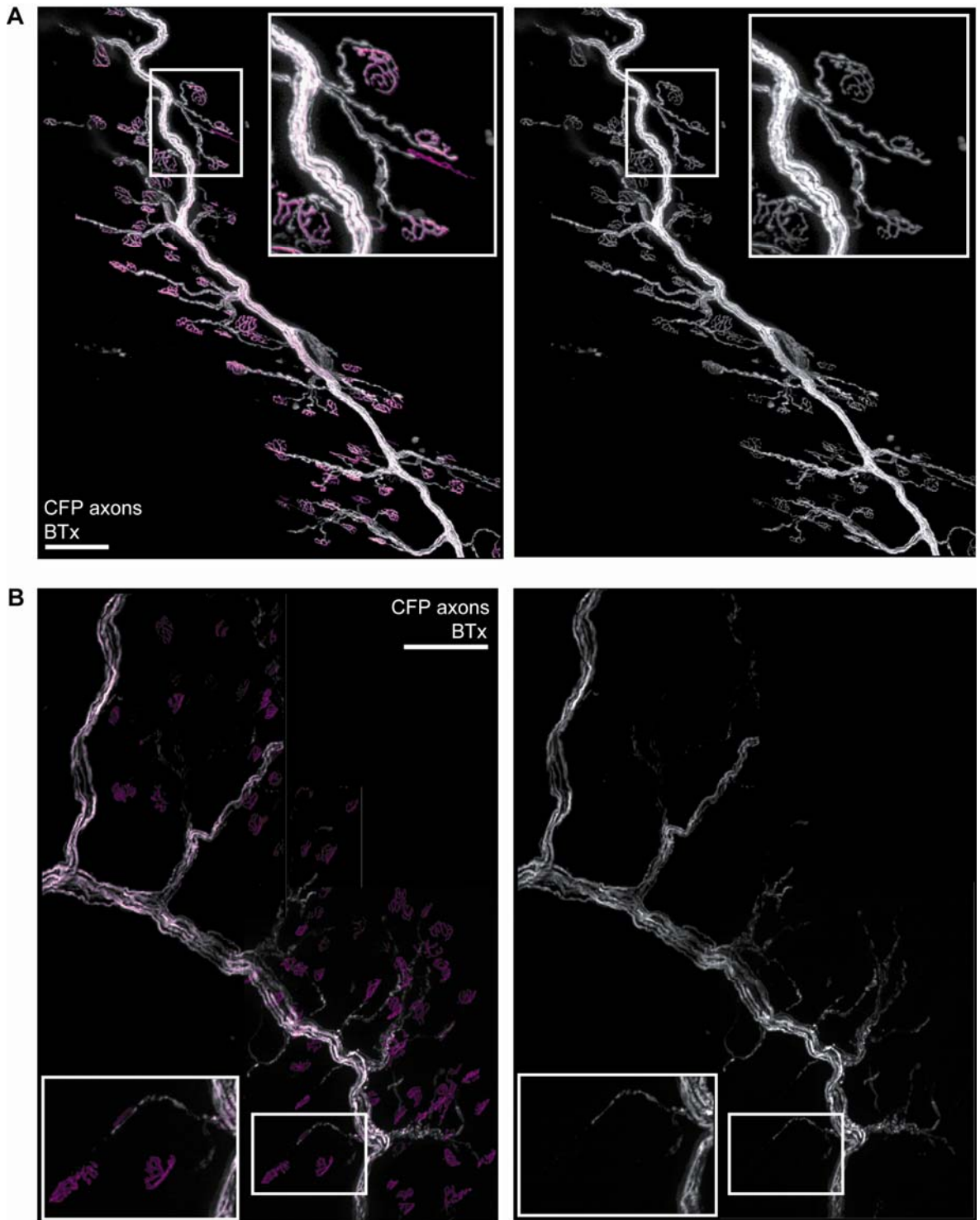


Figure 5.3: Eculizumab protection of endogenous CFP in intramuscular nerve bundles of GD3/CFP mice after exposure to antibody and complement.

A) Montage of apoTome images illustrating intact endogenous axonal CFP (white) of the intramuscular nerve bundle of the TS from GD3/CFP mice terminating at NMJ (BTx, purple) after protection from complement injury by the inhibitor Eculizumab. Right panel shows CFP axons with no BTx staining to emphasise intact CFP at nerve terminals. B) The nerve shows a reduction in fluorescence, especially in distal axons and at nerve terminals (clear in right panel with no BTx staining), when treated with the non-specific isotype-matched control mAb of Eculizumab, ALXN3300. Enlargements of boxed regions show distal axons in more detail. Scale bar= 100µm

5.2.2.2 Nav1.6

After 3h, the effect of ALXN300 was the same as that seen previously after addition of complement. An 87% loss of Nav1.6 positively stained NoR in single fibres and 70% reduction in small bundles was recorded (Figure 5.4A). There was a significant protection of Nav1.6 staining at NoR in these bundle categories after Eculizumab treatment (X^2 -test, $p < 0.001$). These levels were similar to what has previously been shown in control tissue. Additionally, the comparable staining in medium and large bundles mirrors what has previously been shown in control versus complement treated tissue.

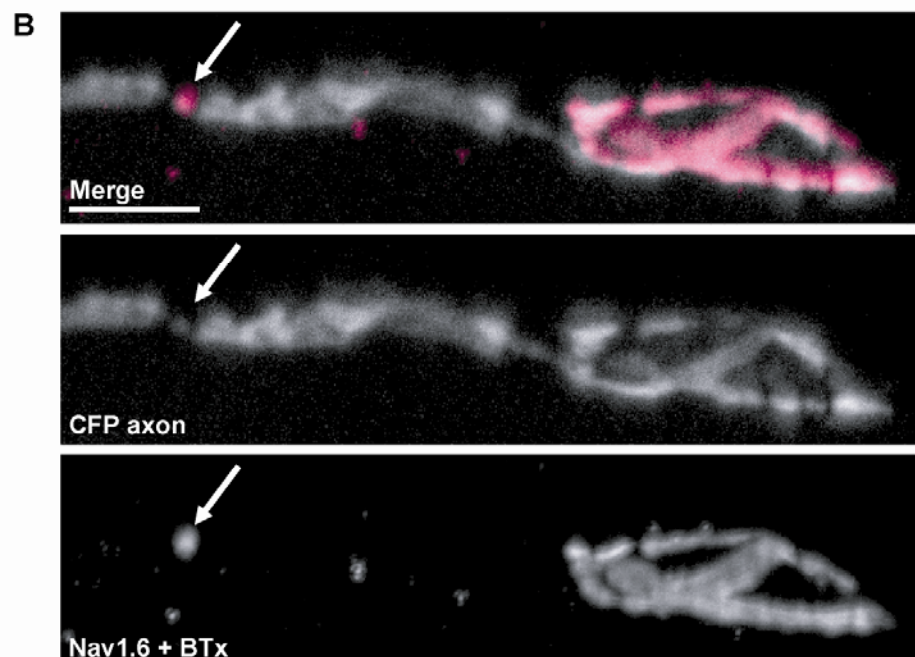
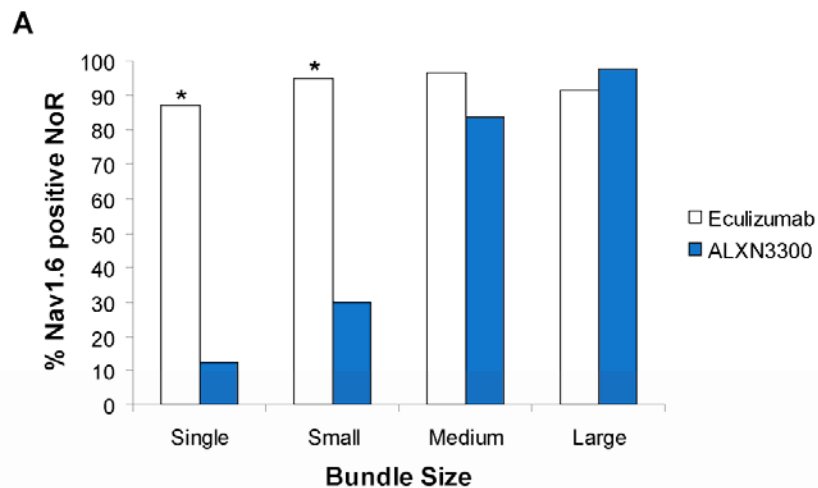


Figure 5.4 (previous page): Protection of immunofluorescence to Nav1.6 with Eculizumab in intramuscular nerve bundles of the GD3/CFP mouse.

A) Single fibres and small bundles have a significantly higher percentage of NoR with Nav1.6 staining after Eculizumab protection, compared to the non-protective isotype matched control ALXN3300, when muscle has been treated with MOG35 and complement. B) Example of protected Nav1.6 staining at a NoR (arrow) downstream from the nerve terminal (BTx, purple). * indicates significance where $p < 0.05$ compared to ALXN3300 control of the same bundle category, using the Chi-squared test of independence. Scale bar = 20 μ m.

5.2.2.3 Ankyrin G

Ankyrin G staining at NoR was similarly protected by Eculizumab compared to ALXN3300. 89% of NoR in single fibres had normal ankyrin G staining after Eculizumab treatment, while only 6% were positive after ALXN3300 treatment (Figure 5.5A, χ^2 -test, $p < 0.001$). A similar result was found for small bundle NoR, with 95% ankyrin G positive after Eculizumab, and only 39% positivity post-ALXN3300. Once again there was no significant difference in nodal staining at NoR in medium and large bundles between treatment groups (χ^2 -test, $p = 0.88$ and 0.93 , respectively).

5.2.2.4 Caspr

Caspr staining was also significantly protected by Eculizumab at single fibre and small bundle NoR (84% and 92% normal staining, respectively). Only 9.8% and 48% of NoR in single fibre and small bundles had normal undisrupted Caspr staining after ALXN3300 treatment.

5.2.2.5 Antibody and MAC

Importantly, MAC levels at NoR in all preparations were significantly increased in ALXN3300 treated tissue at single fibres and small bundles compared to Eculizumab treated (Figure 5.6A, $p < 0.001$). This demonstrates the inhibitors protective effect to complement. To ensure that lack of MAC deposition was not caused by the absence of antibody from the preparation, an ELISA was

performed that confirmed the equivalent level of antibody applied to both protected and unprotected tissue (Figure 5.7).

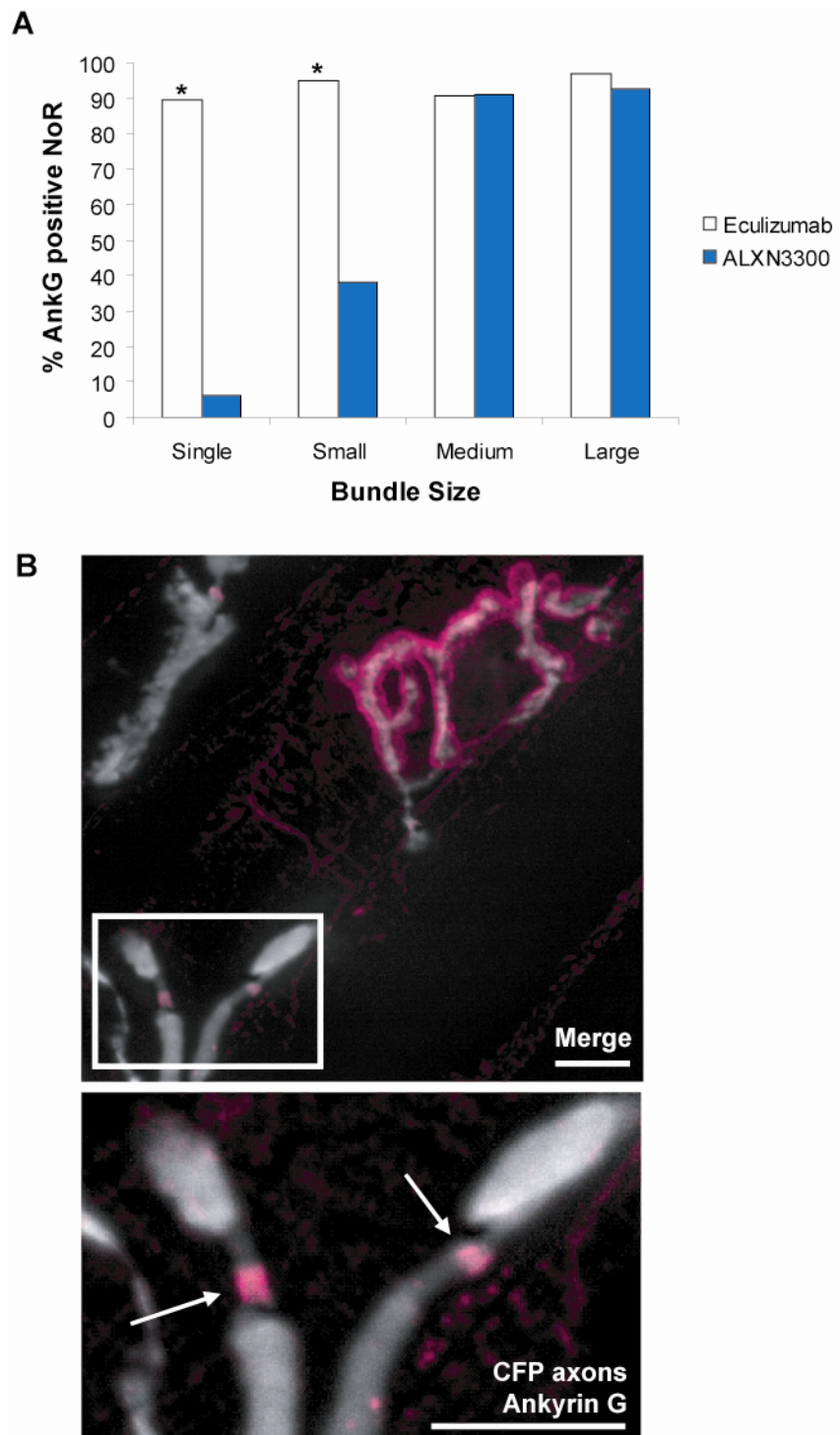


Figure 5.5: Eculizumab protects ankyrin G immunostaining at NoR in GD3/CFP mouse TS intramuscular nerve after treatment with antibody and complement.

A) Graph showing the significant protective effect of Eculizumab on ankyrin G staining at NoR in single fibres and small bundles after injury. **B)** An example of normal ankyrin G staining due to Eculizumab protection at NoR (arrows in enlarged region). Refer to Figure 4.6 for example of normal ankyrin G staining for comparison. * indicates significance where $p < 0.05$ compared to ALXN3300 incubated tissue, using the Chi-squared test of independence. Scale bar= 10 μ m.

5.2.3 Calpain inhibition protects *ex vivo* preparations

5.2.3.1 Calpeptin

The first calpain inhibitor assessed for protection of nodal protein staining was calpeptin. Results were not very reproducible, and so I elected to discontinue use of this inhibitor and instead use AK295.

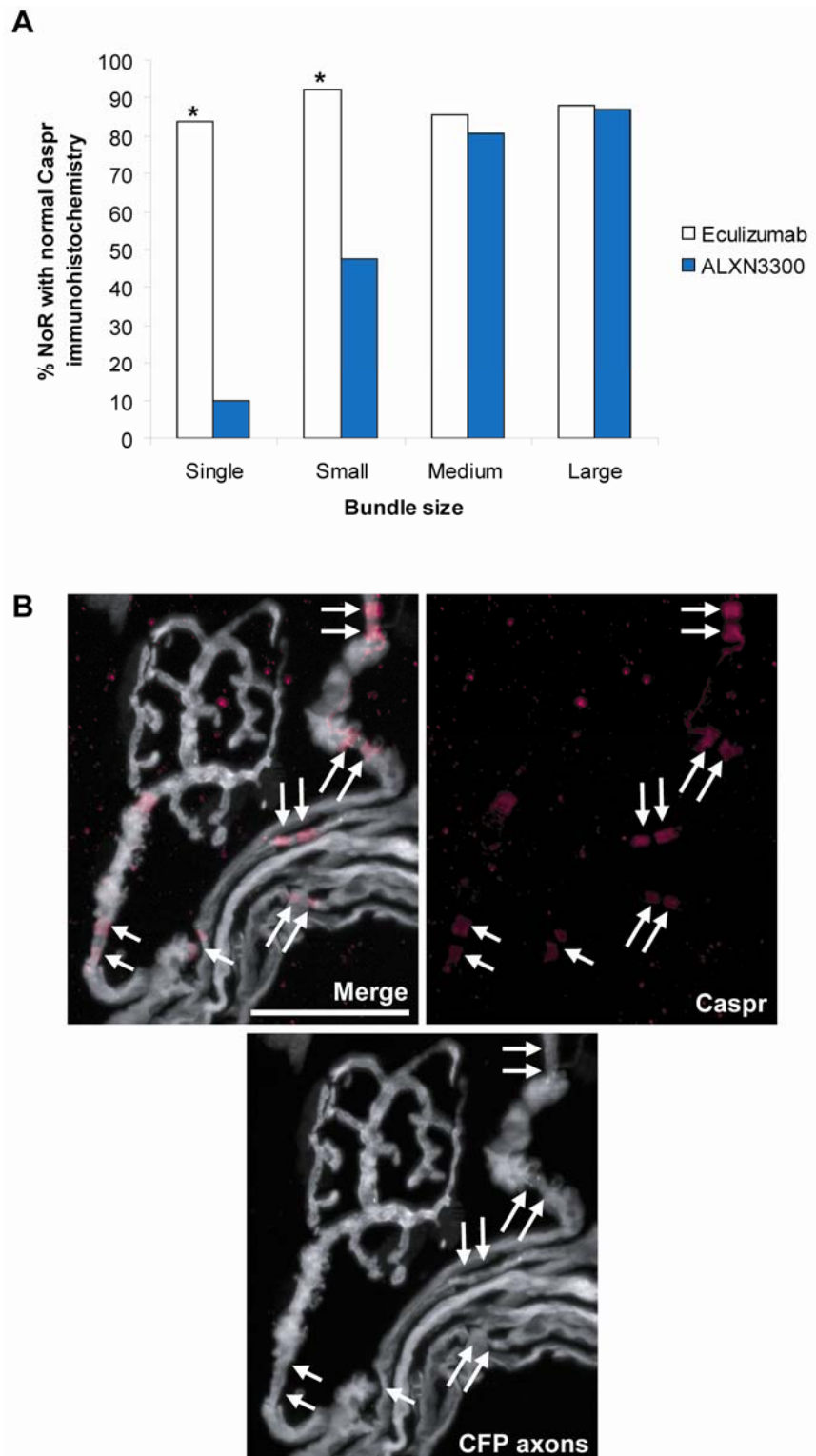


Figure 5.6 (previous page): Caspr staining is protected by Eculizumab at NoR of GD3/CFP TS intramuscular nerve bundles after MOG35 and complement treatment.

A) The percentage of NoR with a normal Caspr staining pattern is significantly higher after Eculizumab protection compared to ALXN3300. B) Normal Caspr staining motif at NoR (purple, double arrows) due to tissue protected by the complement inhibitor Eculizumab. Refer to Figure 4.7 for example of normal Caspr staining for comparison. * indicates significance where $p < 0.05$ compared to ALXN3300 incubated tissue, using the Chi-squared test of independence. Scale bar = $20\mu\text{m}$.

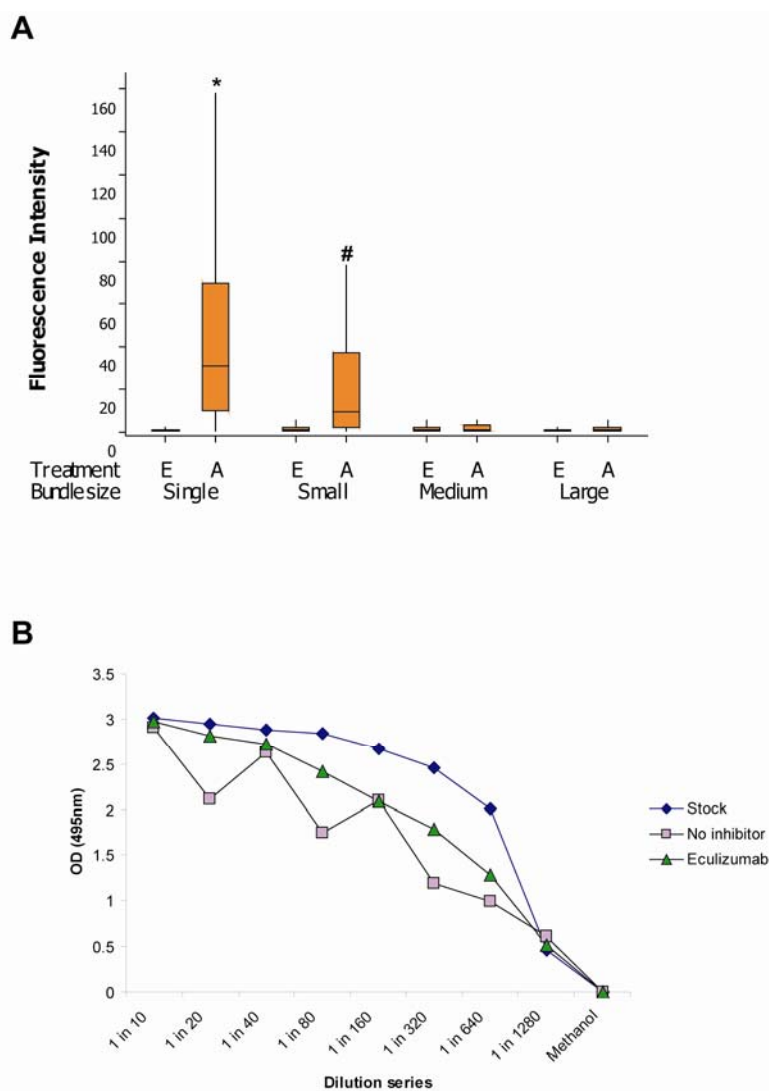


Figure 5.7: MAC pore formation is prevented by Eculizumab even in presence of antibody and complement. A) Boxplot showing that MAC deposition was not present at NoR in tissue protected by Eculizumab, compared to its isotype-matched control, ALXN3300, after antibody and complement treatment. * and # indicates significance where $p < 0.05$ compared to single and small bundle size counterpart respectively, using the Mann-Whitney U test. B) ELISA results prove that anti-GD1a antibody was applied to all TS preparations and was therefore not the reason for attenuation of MAC pore formation.

5.2.3.2 Protective effects of AK295

A dilution series of suitable concentrations of the calpain inhibitor AK295 demonstrated that 100 μ M provided a similar protection of Nav1.6 staining to 200 μ M, which was also comparable to uninjured control tissue, and significantly more protection than 50 μ M (Figure 5.8, $p=0.028$). Therefore, 100 μ M was the chosen concentration of AK295 added to TS preparations.

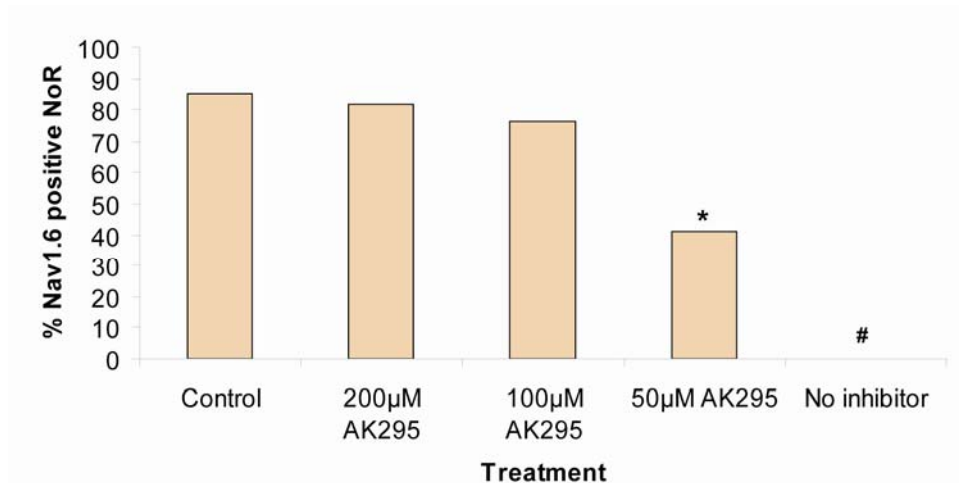


Figure 5.8: Determination of the optimal concentration of the calpain inhibitor AK295 for *ex vivo* preparations.

A dilution series of AK295 was performed to determine that 100 μ M was the optimal concentration as it had the same protective effect on Nav1.6 immunoreactivity as 200 μ M, but a significantly larger protective capacity than 50 μ M. * signifies significant reduction to Nav1.6 immunostaining where $p<0.05$ compared to control (no complement), 200 μ M AK295 and 100 μ M AK295, while # indicates significance where $p<0.05$ compared to all other categories.

5.2.3.3 MAC and neurofilament

Unlike Eculizumab, MAC pore formation was unaffected by AK295. There was no significant difference in deposition at NoR of inhibitor or non inhibitor incubated tissue for each bundle category after antibody and complement treatment (Figure 5.9).

Initially I noticed that CFP in AK295 treated nerve looked similarly weakened and disrupted as for treated tissue i.e. it was not protected as with Eculizumab.

Therefore, as neurofilament is a known calpain substrate, its protection was the first parameter investigated. A montage of confocal images show the level of protection to neurofilament provided by AK295 compared to tissue treated with no inhibitor (Figure 5.10). For quantification, the neurofilament of both AK295 and unprotected nerve was measured over the endplates and compared to control neurofilament levels. There was a significant protection to neurofilament by AK295 compared to no inhibitor (Figure 5.10C, $p < 0.001$).

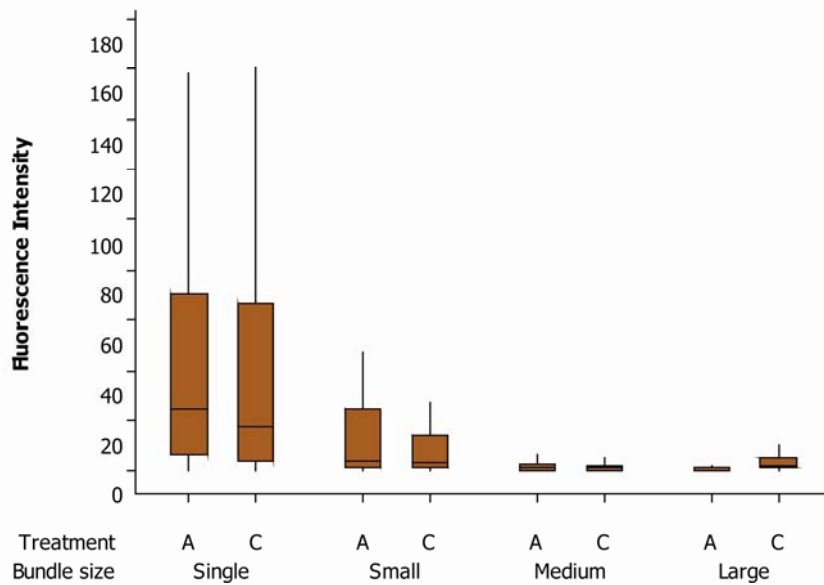


Figure 5.9: No effect of AK295 on MAC deposition at NoR of TS intramuscular nerve after antibody and complement treatment.

AK295 does not inhibit the formation of MAC pores at NoR and therefore there is no significant difference in MAC deposition between bundle categories of AK295 treated (A) and no inhibitor treated control (C) tissue.

5.2.3.4 Nav1.6

AK295 incubation resulted in 84% of single fibre NoR having normal Nav1.6 staining after antibody and complement treatment compared to a significantly reduced 9% in non-protected counterpart fibres (Figure 5.11A, χ^2 -test $p < 0.001$). This discrepancy in Nav1.6 staining also occurred at small bundle NoR with 90% positively stained after AK295 treatment, and only 37% without. The boxed region in Figure 5.11B illustrates the protection of Nav1.6 staining at a single fibre NoR with AK295 inhibition of calpain.

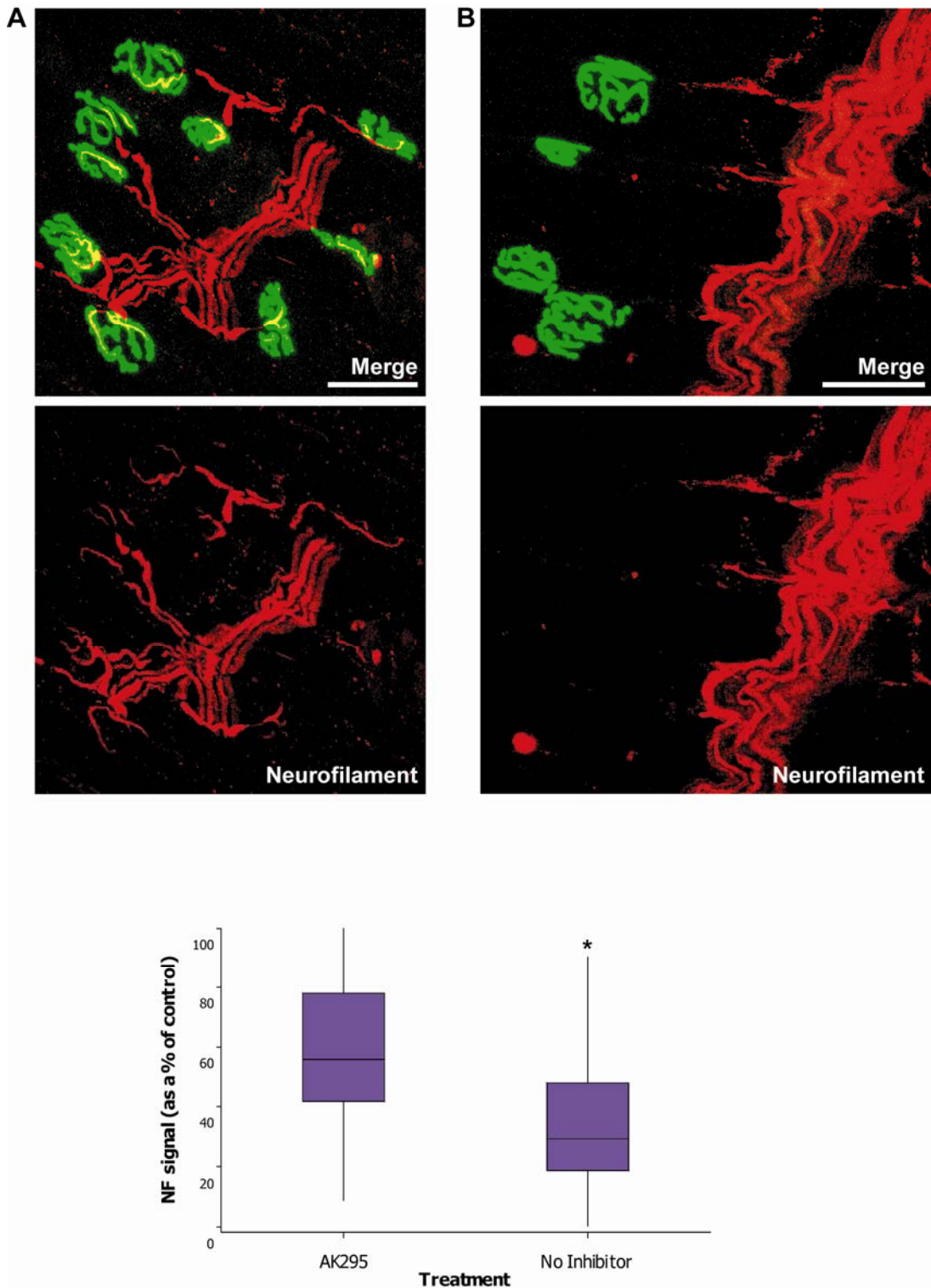


Figure 5.10: AK295 protects neurofilament at nerve terminals of GD3/CFP mouse TS treated with antibody and complement.

A) Confocal images illustrate intact neurofilament (red) at nerve terminals (appear yellow when overlaying BTx, green) after AK295 protection (left panel), compared to unprotected treated tissue (right panel). **B)** Neurofilament at the nerve terminal and along distal axons is lost after antibody and treatment when no calpain inhibitor is administered. **C)** Boxplot of neurofilament immunostaining over the endplate shows the significant reduction in unprotected tissue compared to that protected with AK295. * signifies significance when $p < 0.05$ compared to AK295 treated tissue, using the Mann-Whitney U test. Scale bar = 50 μ m.

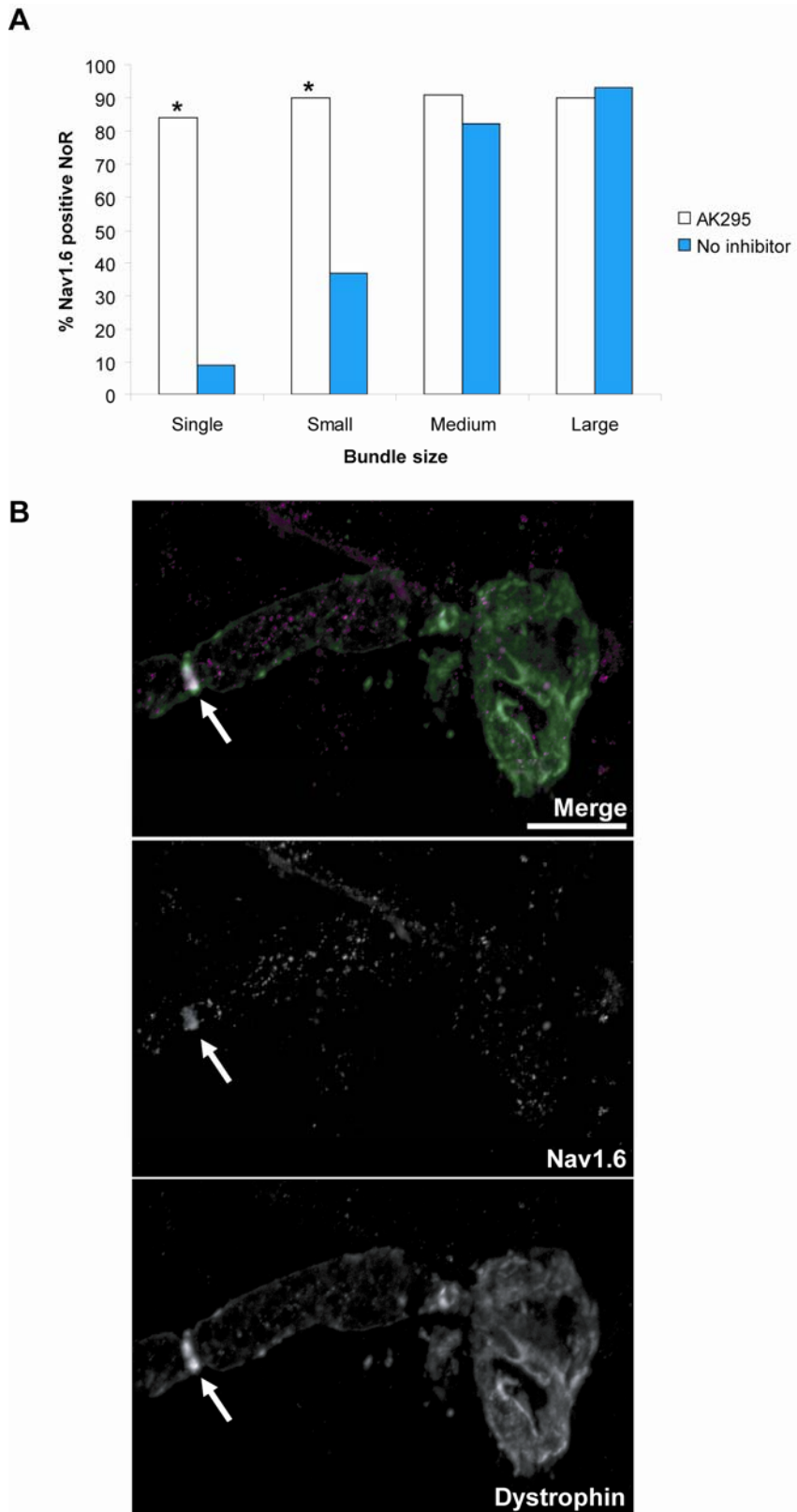


Figure 5.11: Nav1.6 immunostaining at the distal NoR in TS muscle is protected from antibody and complement disruption by AK295.

A) Single fibre and small bundle NoR have significantly more NoR with positive Nav1.6 immunoreactivity after AK295 treatment than their unprotected counterparts. **B)** Arrows indicate NoR (as identified by dystrophin) downstream from the terminal with normal Nav1.6 staining after AK295 protection. * signifies significance where $p < 0.05$ compared to matching bundle category with no inhibitor, using the Chi-squared test of independence. Scale bar = 10 μ m.

5.2.3.5 Ankyrin G

Ankyrin G exhibits a similar pattern of protection with AK295 incubation as Nav1.6. Specifically, 78.3% of single fibre NoR had normal ankyrin G staining compared to 11.3% when the tissue was not treated with a calpain inhibitor (Figure 5.12A, X^2 -test $p < 0.001$). This was also the case for small bundle NoR- 86% were protected by AK295 to have normal ankyrin G staining, while only 27%, significantly less, had normal staining with no inhibitor (Figure 5.12A, X^2 -test $p < 0.001$).

5.2.3.6 Caspr

77% of NoR at single fibres had normal Caspr staining after AK295 treatment, which is significantly greater than 26% normally stained nodes in treated tissue with no inhibitor (Figure 5.13A, X^2 -test $p < 0.001$). Similarly in small bundles, 84% of NoR had normal staining with AK295 protection compared to the significantly reduced level of 56% with no inhibitor (Figure 5.13A X^2 -test $p = 0.001$). There was no significant difference between Caspr staining at medium and large bundle fibre NoR for treatment groups.

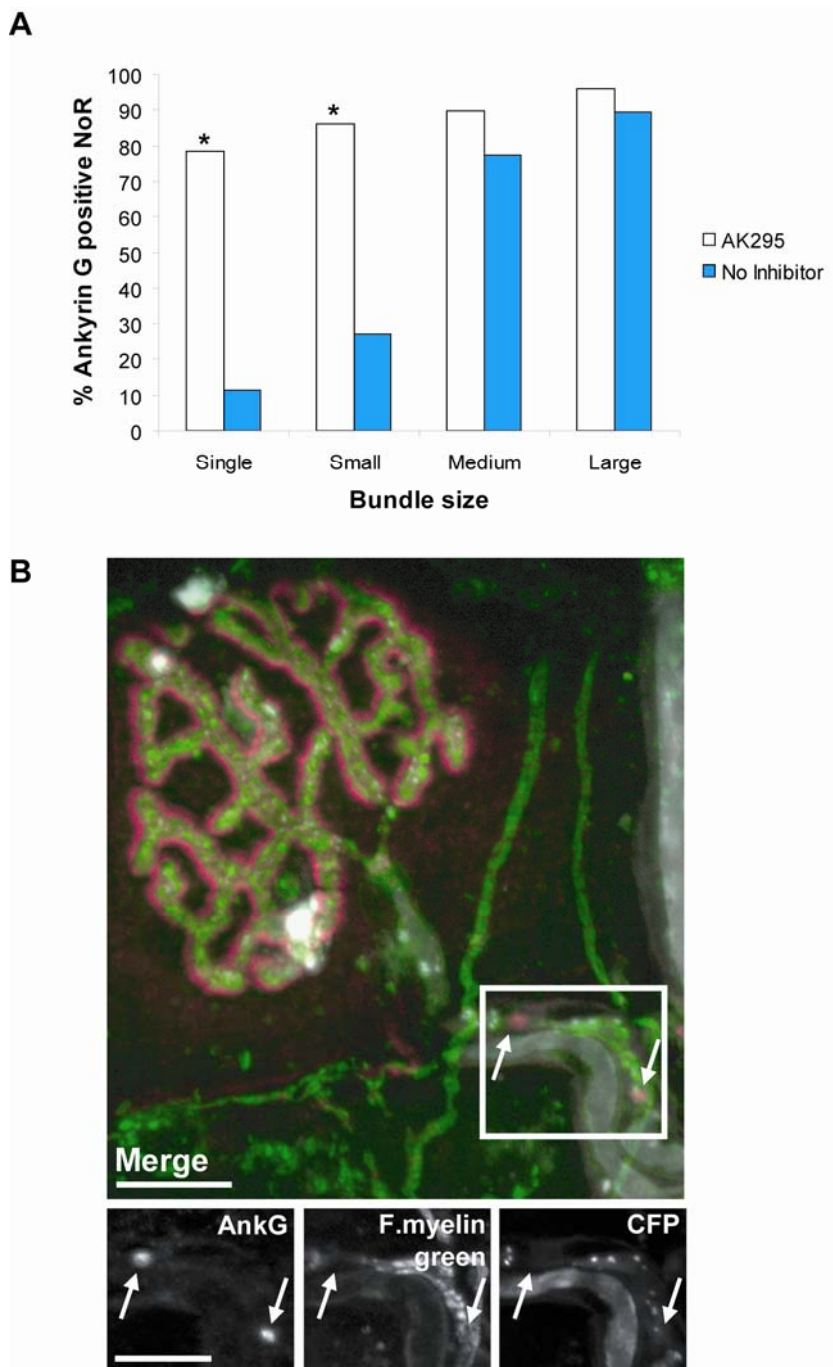


Figure 5.12: AK295 protects ankyrin G immunostaining at NoR of TS intramuscular nerves treated with antibody and complement.

A) Graph depicting the significant protection to ankyrin G at NoR of single fibres and small bundles compared to their unprotected bundle size partners. **B)** An image of normal ankyrin G staining (arrows) at single fibre NoR as identified by fluoromyelin green, downstream from the nerve terminal (BTx, purple) due to protection by AK295. *signifies significance where $p < 0.05$ compared to bundle size counterpart without protection from an inhibitor. Scale bar= 10 μ m.

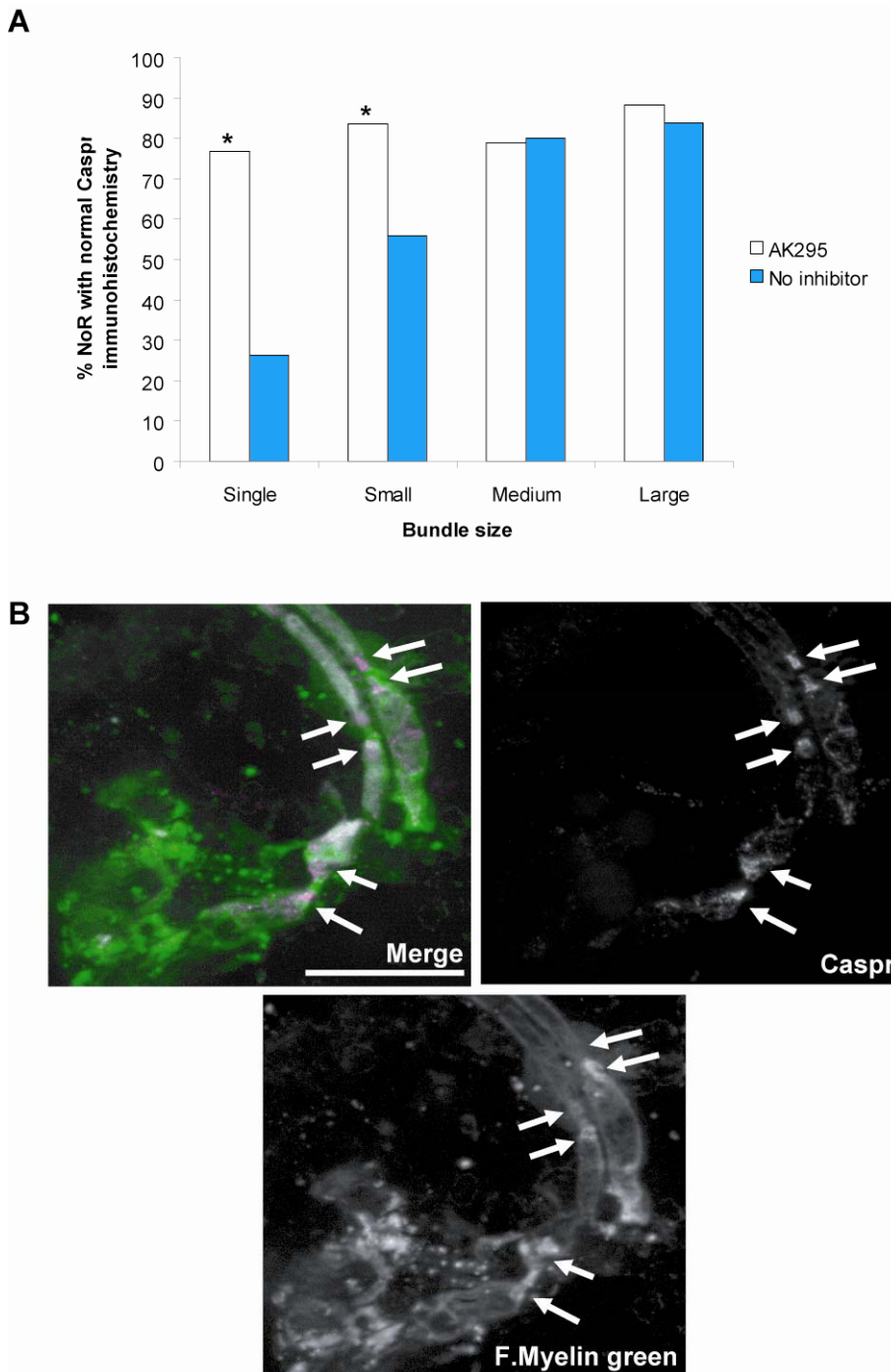


Figure 5.13: Caspr staining is protected by AK295 in TS treated with antibody and complement.

A) Single fibre and small bundle NoR have significantly more normal Caspr staining at NoR after AK295 protection compared to unprotected nerve. B) Illustration of normal Caspr staining at NoR (arrows) after antibody and complement treatment when protected by AK295. * signifies significance when $p < 0.05$ compared to bundle category matched no inhibitor control, using the Chi-squared test of independence. Scale bar = $20\mu\text{m}$.

5.2.4 AK295 protection in Phrenic nerve

Although Nav1.6, ankyrin G and Caspr immunostaining was convincingly preserved by AK295 treatment at the distal axon NoR, the same trend was not so impressive for phrenic nerve NoR. Figure 5.14 shows a plot of these three proteins comparing AK295 treatment to no inhibitor. Ankyrin G staining is not significantly protected by AK295 ($p=0.14$), while Nav1.6 and Caspr staining can be described as protected ($p=0.011$ and $p=0.009$, respectively). None reach a level higher than 40% of NoR with normal staining. On closer inspection of staining it is sometimes possible to see what looks like regions of Nav1.6 and Caspr staining that are not in a neat or normal conformation. However this is not to be confused with what was noticed for NrCAM and moesin (refer back to Fig 4.11 & 4.12). The latter proteins are labelled by antibodies to extracellular antigens and they too are not protected by AK295. The staining as before is still present, merely not of a normal configuration, but much more prominent than residual staining for the Nav1.6, ankyrin G and Caspr proteins (Figure 5.14).

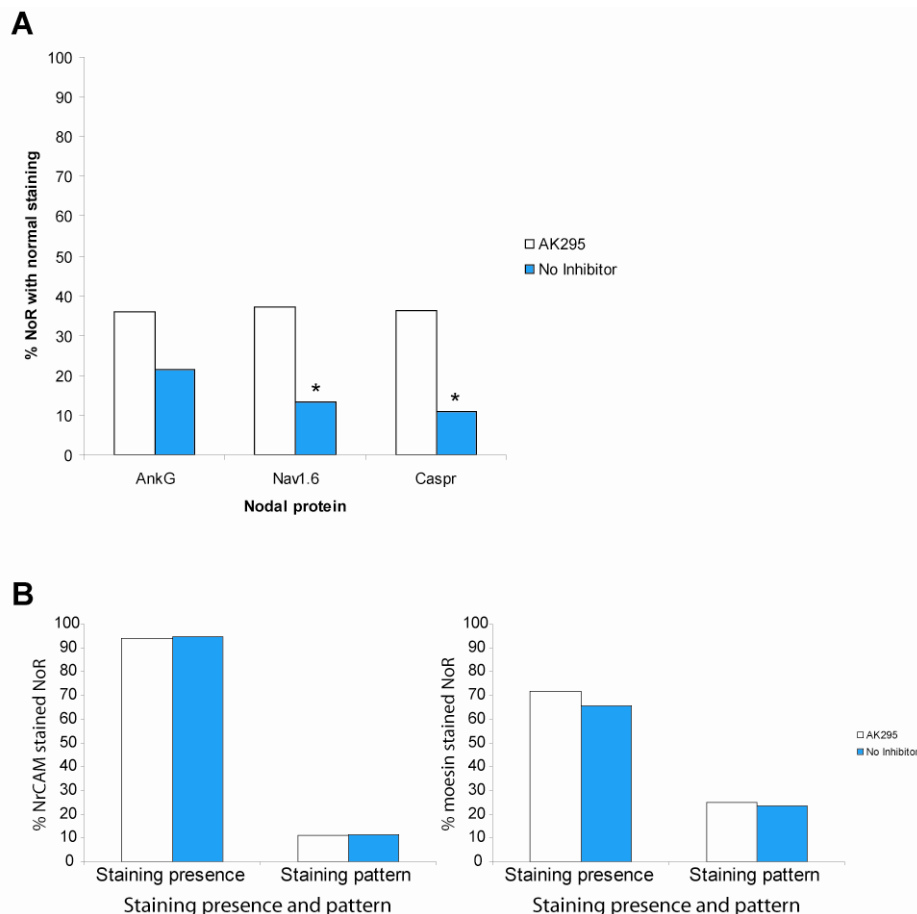


Figure 5.14 (previous page): Effect of AK295 on nodal proteins in phrenic nerve after treatment with antibody and complement.

A) Nav1.6, ankyrin G and Caspr staining is not protected by AK295. B) As previously shown, NrCAM and moesin staining is present at NoR after antibody and complement treatment but the configuration is not normal, not even on application of AK295. * signifies significance where $p < 0.05$ compared to no inhibitor control, using the Chi-squared test of independence.

5.3 Discussion

To clarify the mechanism behind loss of nodal protein staining after anti-GD1a ganglioside and complement treatment as described in the previous chapter, the route of injury was investigated. The movement of calcium through MAC pores resulting in the activation of calpain was suspected as this was the cause of loss of neurofilament at the nerve terminal in mouse model (Goodfellow et al., 2005; Halstead et al., 2004; O'Hanlon et al., 2001). Additionally, complement activation has been recognised in other models and tissue from patients (Hafer-Macko et al., 1996; Susuki et al., 2007b; van Sorge et al., 2007). Excessive calpain activation can be extremely injurious and is associated with many disease states (see section 1.7 for more detail). To prove the involvement of these processes in my model, calcium indicators were used to study calcium influx, while complement and calpain inhibitors were utilised to study their effect on protein staining at the NoR.

I initially evaluated the calcium indicator Fluo 4-AM for use in calcium influx studies. However, this indicator is only visible with FITC filters. Ultimately I felt it would be more appropriate to visualise the endogenously fluorescent axons in the FITC channel, while the calcium indicator Rhod 2-AM could be detected in the rhodamine channel. This allowed for imaging using the confocal microscope, rather than with epifluorescence, which enhances the exclusion of unwanted signal. Though the indicator was useful for studies in cells, it did not translate to whole-mount tissue preparations. This was chiefly due to what seemed to be an issue of penetration into the axon. Calcium indicators with acetoxymethyl (AM) ester groups have been developed to avoid the necessity of microinjections of calcium indicators into the desired tissue. It facilitates the permeation of the indicator into membranes due to its uncharged nature (masking of negatively charged carboxyl groups), before this portion is cleaved by non specific

esterases, resulting in its entrapment and exposure of Ca²⁺ sensing region (Molecular probes handbook). As uptake seemed unsuccessful even with the use of an AM ester derivative, I also tested the dispersing agent pluronic acid to encourage movement through the BNB. Unfortunately, this too was ineffective.

As it is likely that the route of injury at the NoR is similar to that seen at the terminal, and MAC pore formation has been established (section 4.2.2), even without evidence of calcium influx in tissue, it seemed appropriate to confirm the route of injury by ascertaining what effect complement and calpain inhibition would have on nodal protein staining.

Eculizumab proved very successful at preventing MAC pore formation. Accordingly, CFP loss did not occur and nodal protein staining was normal. The deposition of MAC is therefore directly related to the loss of staining for proteins at the NoR, which is consistent with the increase in intensity of MAC at single fibres and small bundles when this phenomenon occurs. The successful protection of protein's by Eculizumab was not such a surprising result as Halstead *et al* (2008) have shown it to be effective at inhibiting damage to the nerve terminal in a mouse model of GBS. This study provided the appropriate concentration for use in mice, but it is yet to be determined whether this drug can be as effective in human GBS patients. It could be reasoned that Eculizumab may not have much effect when administered to patients as MAC has already been activated so unlike the mouse model the damage will have already been done. However, Nishimoto *et al* (Nishimoto et al. 2004) found that intravenous immunoglobulin (IVIg) treatment improves the disease course in a rabbit model of AMAN, which suggests that complement block can also still be useful after initial injury. Furthermore, another study where the synthetic serine protease inhibitor Nafamostat mesilate was injected at disease onset to inhibit complement in a rabbit model of AMAN also demonstrated the protective effects after the initiation of the disease process (Phongsisay et al., 2008), which further justifies the interest in Eculizumab as a contender for therapy in newly diagnosed patients.

To study calpain activation I initially considered using a fluorogenic calpain substrate that could be used to reveal calpain activation. As I had encountered

several problems with live imaging as discussed above, I felt this might not be as suitable a candidate as using calpain inhibitors.

I decided to try the calpain inhibitor, calpastatin (Murachi 1989) to begin with, as this was tested in a nerve terminal injury model, previously (O'Hanlon et al., 2003). Unfortunately, the protective effects on nodal proteins were fairly inconsistent. For this reason, I began to work with the very specific calpain inhibitor AK295 which has been developed to bind calpain I, II and cathepsin B (Li et al., 1996). Once the appropriate concentration for use in TS preparations was determined, I found great success with this synthetic inhibitor. Significant protection for the known calpain substrate neurofilament was exhibited with AK295 treatment compared to non-inhibitor treated intramuscular nerve bundles, which was an excellent indicator of its efficacy. Further to this, another known substrate, ankyrin G, was protected. Nav1.6 and Caspr staining also remained intact, which is fascinating as to my knowledge Caspr has not previously been identified as a calpain substrate, while cleavage of Nav channels have only recently been described *in vitro* (Iwata et al., 2004; von Reyn et al., 2009). It is also possible of course that the substrate could be an anchoring protein (section 1.4.5 for more detail). Another intriguing discovery was that CFP was not protected suggesting that its route of loss is indeed due to increased permeability and it is not a calpain substrate itself. MAC deposition was not interfered with at all, confirming the necessity of calcium influx through these pores to activate calpain as the injurious agent.

The cause of staining loss at phrenic nerve NoR may be somewhat different to that seen at distal nerve NoR. As described in the previous chapter, staining at phrenic nerve NoR does indeed disappear after treatment. In spite of the protection provided by AK295 in distal nerve, the same level of protection of Nav1.6, ankyrin G and Caspr does not occur in phrenic nerve. As described in Chapter 3 (Figure 3.2.1.3), GD1a expression could extend to the paranodes in larger calibre phrenic nerve, and thus these extra targets could exacerbate injury. It is interesting that the level of protection by AK295 does seem to increase with lateral movement from the nodal gap, or if the protein is not purely intracellular like ankyrin G. Conversely it could be said that the level of *disruption* decreases with lateral movement and extracellular portions. Non-calpain associated damage described here is analogous to that detailed in the

study of calpeptin protection at the mouse nerve terminal exposed to α -LTx or anti-ganglioside antibody performed by O'Hanlon *et al* (2003). The authors demonstrated that although a calpain inhibitor protected neurofilament from injury, the ultrastructure showed much of the same damage as unprotected tissue.

When staining is not present after AK295 treatment in phrenic nerve, this is often coincident with an extension of IgG and MAC deposition, and swollen regions flanking the NoR as identified in DIC (described section 4.2.3.5). This might represent that a threshold of MAC deposition is required before enough calcium influx occurs for unmanageable calpain activation. It could also follow that at larger calibre axon NoR, the damage is caused by both calpain mediated degradation *and* a general disruption to the region due to an ionic and osmotic imbalance due to excess movement of water. There is no discernible change in protection of staining to the extracellularly labelled proteins NrCAM and moesin by AK295 either. The swelling described could then account for the observation that NrCAM and moesin staining are disrupted, although still present unlike the protein's with intracellular antigens, and not protected by AK295 because it is not calpain that is causing their specific disruption. It would be intriguing to stain for the Nav1.6 channel extracellularly to see if it too would still be present but disrupted. As this bulbous nodal condition has been observed in large diameter axons that are found more proximally, it is possible that such an extreme phenotype occurs in the rabbit model of AMAN where ventral nerve NoR have been studied and disruption confirmed by EM (Susuki *et al.*, 2007b).

Only complement and not calpain inhibition has been tested in models of AMAN so far, therefore the effects *in vivo* could be very interesting. As MAC will have already been activated in a real human case of GBS injury, AK295 could be very beneficial to prevent further damage. If there is a gradient dependent effect on protection to axons, it may be more useful when the disease has not yet reached a severe level of injury and paralysis.

As effective conduction requires functional sodium channels, particular attention will subsequently focus on this proteins fate at the NoR after injury. It is unclear whether Nav channel is being fully degraded, internalised, shed from the membrane, or the antigen site alone has been damaged/changed conformation.

6 Fate of the sodium channel at NoR after injury

6.1 Introduction

Sodium channel clustering at the NoR is essential for conduction of action potentials along myelinated axons (section 1.4.3). In the previous chapters, the loss of sodium channel staining at NoR has been described in response to anti-GD1a antibody-mediated complement dependent injury of the mouse distal intramuscular axons and desheathed phrenic nerve (Figures 4.5 & 4.11 respectively). Similarly, disruption of sodium channel staining at the ventral roots in a rabbit model of AMAN has been associated with GM1 pathogenicity and corresponds to my results with anti-GD1a antibody (Susuki et al., 2007b). As it has been shown in the present study that calpain inhibition strongly protects staining at distal axons of the TS muscle, and is partially protective at the phrenic nerve NoR, damage is likely to be linked to calpain-mediated injury although it is unknown if Nav1.6 specifically is a calpain substrate *in vivo*.

Two important lines of investigation concerning the fate of the sodium channel are:

1. Is the sodium channel still present although staining is not?
2. Is the sodium channel still functional?

There are several possible options to investigate the fate of the sodium channel associated with loss of staining. Firstly, using another antibody directed to a different antigenic site, the specificity of loss or cleavage of the channel could be explored. I suspected that the alpha subunit may be cleaved at the sites of antibody binding, i.e. the intracellular loops, as these are exposed to cytosolic calpain and could explain the loss of staining without establishing if the channel was still present. It has previously been shown that the intracellular loops are susceptible to cleavage due to intra-axonal injection of proteolytic compounds (Armstrong et al., 1973; Eaton et al., 1978; Oxford et al., 1978; Rojas & Rudy 1976). This proposed cleavage could result in the breakdown of the α -subunit into several fragments of protein that could later potentially be identified by Western blot analysis, as shown previously *in vitro* (Iwata et al., 2004; von Reyn

et al., 2009). In addition, proteolysis of the intracellular loops as described in the above studies only disturbed inactivation of the action potential as the inactivation gate is situated intracellularly, but no change was reported for the activation of the channel. This suggests that even if sodium channel is cleaved, it may retain its functionality.

As discussed earlier (section 1.4.6.1), many conduction studies have been carried out with contradictory results. Some studies have reported a block in conduction associated with anti-ganglioside antibodies (Arasaki et al., 1993; Arasaki et al., 1998; Santoro et al., 1992; Susuki et al., 2007b; Thomas et al., 1991), while others have reported no change (Harvey et al., 1995; Hirota et al., 1997; Paparounas, O'Hanlon, O'Leary, Rowan, & Willison 1999). Therefore it was also of interest to determine whether the channel was still functional by way of electrophysiological recordings. This could equally resolve the issue of presence. As staining to extracellular domains of proteins at the NoR has shown disruption but not loss (NrCAM section 4.2.3.5), it seemed appropriate to consider a method for labelling the portion of the Nav channel on the extracellular membrane to further prove or disprove if it remains after injury.

6.2 Results

6.2.1 Effect of injury to binding of alternative Nav antibody

The pan sodium channel (pNav) antibody has the same staining pattern (i.e. a neat band) at NoR of intramuscular nerve bundles as the anti-Nav1.6 channel specific antibody (Figure 6.1C). The binding sites of the two antibodies are illustrated in Figure 6.1A (black circles). In addition, it showed a similar pattern of loss at distal axons after treatment with antibody and complement (Figure 6.1B, D). The reduction to pan Nav channel staining at single fibre NoR after pathology compared to control is significant (15% and 87% positive, respectively, X^2 -test $p < 0.001$), as is the case for small bundle NoR (63% and 90% positive, respectively, $p = 0.002$). An example of normal and absent staining at NoR, as identified by fluoromyelin green and dystrophin, are shown in figure 6.1C and 6.1D, respectively.

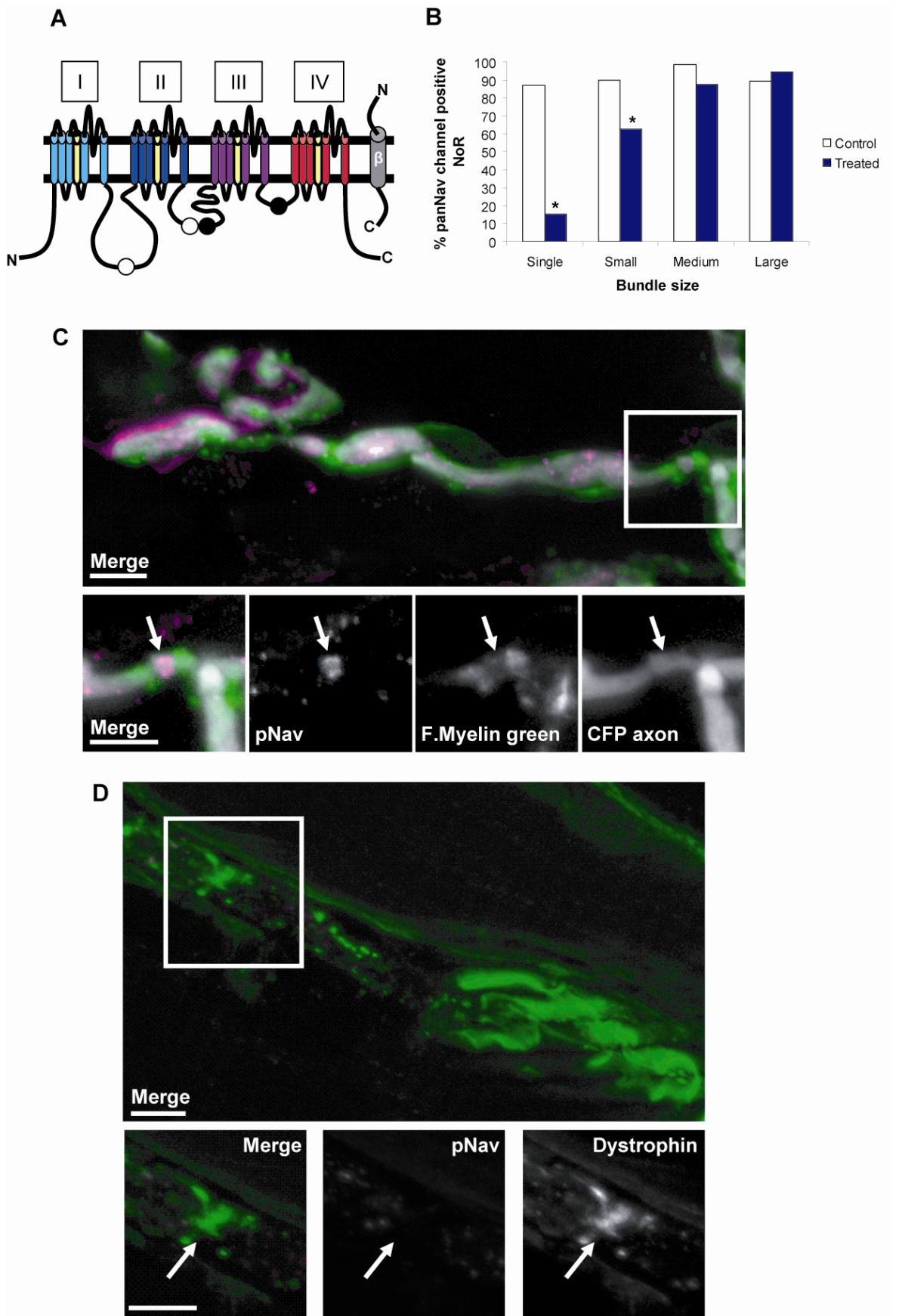


Figure 6.1 (previous page): Possible calpain cleavage sites of Nav channel and pan Nav staining at distal NoR of intramuscular nerve bundles after antibody and complement injury.

A) Illustration depicting cleavage sites of Nav channel as described by von Reyn et al (2009)(white circles), and sites of binding of antibodies used in this study (black circles). B) Graphical representation of significant reduction in pNav staining at single fibre and small bundle NoR after treatment compared to control. C) Illustration of normal pNav staining at distal axon NoR as determined by fluoromyelin green and CFP axons (white). C) pNav staining no longer forms a neat band when the axon undergoes injury. Boxed area is magnification of NoR (identified by dystrophin, green) downstream from terminal (BTx-FITC). * signifies significance where $p < 0.05$ compared to bundle size partner, using the Chi-squared test of independence. Scale bar = 5 μ m.

6.2.2 Alteration to Nav channel staining at early time-points

As it has been shown that Nav channel staining is lost, it is desirable to determine the possible stages preceding this disappearance. At the distal nerve an incubation of 3h with NHS is required for loss of staining in the TS due to issues involving the BNB, and there are only two identifiable phenotypes: present or absent. Therefore this tissue was not an ideal candidate for the study of progressive channel loss. However, in the phrenic nerve it was possible to recognise what seemed like intermediary stages of Nav channel loss, probably owing to the larger calibre of the fibre.

The alteration to sodium channel staining was investigated at NoR as little as 15min and 30mins after the addition of NHS. Although the majority of NoR had intact neatly clustered Nav1.6 channel staining at these time-points, some NoR showed what appeared to be a slight spread of the neat band or the development of punctuate-like clusters around the region after 30mins. Quantification was not possible due to the differing susceptibilities of fibres, but some of these intermediate phenotypes are illustrated in Figure 6.2.

6.2.3 Western blotting

Western blotting was used primarily to attempt to ascertain presence of protein, and then to determine if cleavage fragments could also be identified.

6.2.3.1 Suitability of nerve

It was hoped that phrenic nerve could be used for Western blot preparations to correlate the findings with the immunohistochemical results. However, PN does not yield a great deal of protein. Sciatic nerve is the next suitable choice as not only is it subsequently used in electrophysiological studies, it has often been used for Western blots of various proteins in other research. Optic nerve was valuable for developing the western blot protocol for Nav channel. A small number of nerves generated good staining (Figure 6.3A), however it was not used for actual experiments comparing injury to nodal proteins as the anti-ganglioside antibody used did not bind at this location, and it is part of the CNS therefore results would not be directly applicable to this work.

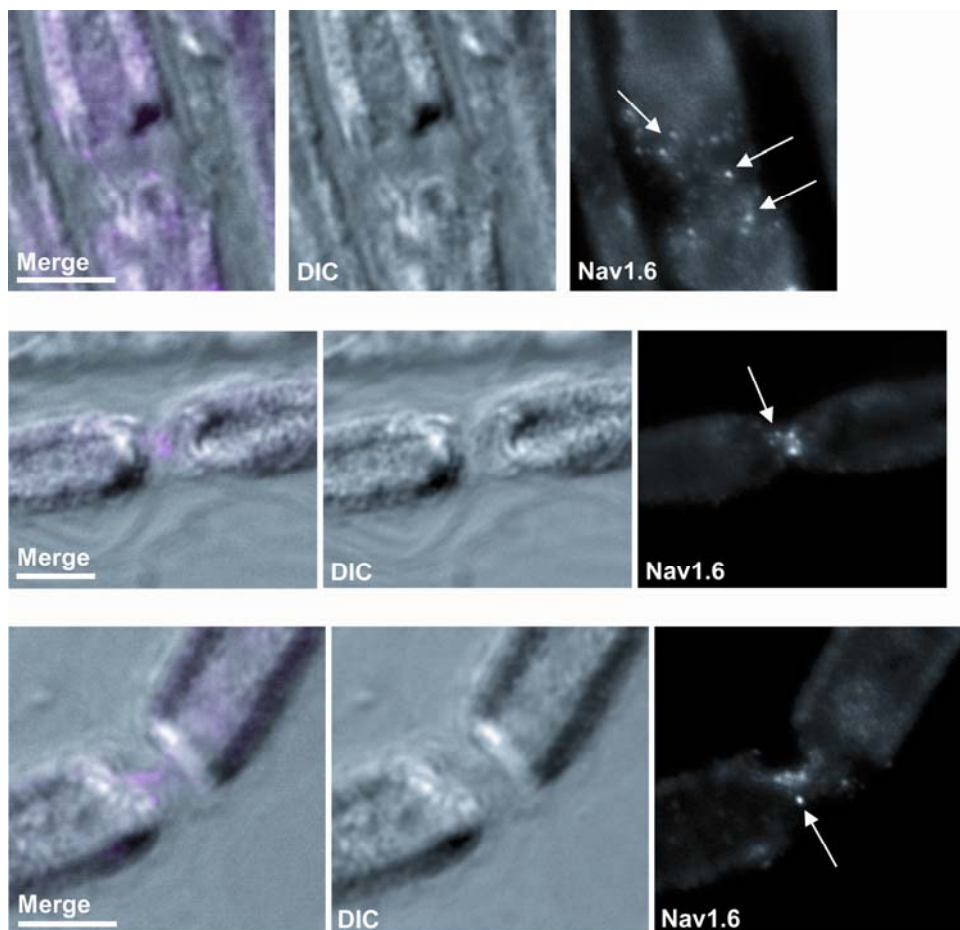


Figure 6.2: Possible preliminary stages in the injury induced loss of Nav1.6 channel staining. Unusual speckles of spread of Nav1.6 channel staining (as indicated by arrows) at the NoR of phrenic nerve (as identified by DIC) after 30mins of NHS treatment.

6.2.3.2 Fodrin/ α -spectrin as a marker of calpain activity

An anti-fodrin/ α -spectrin antibody can not only detect this protein in its intact state at 240/280kDa on a membrane, but also its breakdown products once it has been cleaved by calpain over time. Therefore it is an excellent marker of calpain activity. Regrettably this antibody detected several bands representing calpain activity in all samples including controls, thus it was not of use in this study.

6.2.3.3 Nav channel immunoblots

Several different staining protocols were attempted before the appropriate one was discovered to identify Nav channels by western blot. Staining for this protein was problematic because:

1. It is a large protein and thus is difficult to transfer
2. It is highly embedded in the membrane so is difficult to separate
3. It is susceptible to high temperatures
4. A great deal of sciatic nerve tissue is required to produce enough protein
5. Often non-specific bands were identified by the antibodies against sodium channel.

Ultimately in sciatic nerve it was not possible to detect a difference in band intensity between control, treated and AK295 'protected' tissue (Figure 6.3B, ANOVA, $p=0.284$). There was however a significant reduction in band optical density of these experimental groups compared to the intensity of staining from nerve immediately snap-frozen (Figure 6.3B, ANOVA, $p<0.001$). Rather unexpectedly, the appearance of staining at about 200kDa occurred in the lane of treated nerve, which could be a cleavage product. However as the intensity of the band at the correct size was not greatly reduced, it is perhaps an unlikely suggestion.

6.2.4 Extracellular nerve recordings

6.2.4.1 Conduction of the sciatic nerve after 1h NHS incubation

Prior to electrophysiological recordings, immunohistochemistry for MAC activation and deposition at sciatic nerve NoR was carried out when complement was added directly to the middle chamber (described in methods). As no complement activation was identified, the decision was made to apply NHS to the entire nerve in a petri dish, and subsequently return the nerve to the chamber after one hour to record for the final 30mins. 1h and 30mins was an appropriate incubation period as loss of sodium channel staining had been significant in phrenic nerve after this time. There was a reduction to conduction (as a measure of the peak amplitude of recorded compound action potentials (CAP) to 73.85% \pm 3.6% of the starting value within the final half hour after treatment (Figure 6.4). This was significant compared to control which was reduced to 98.25% \pm 4% of the starting value (*paired t-test*, $p= 0.01$). As this was not very dramatic the incubation time was reconsidered to perhaps improve the severity of the conduction block.

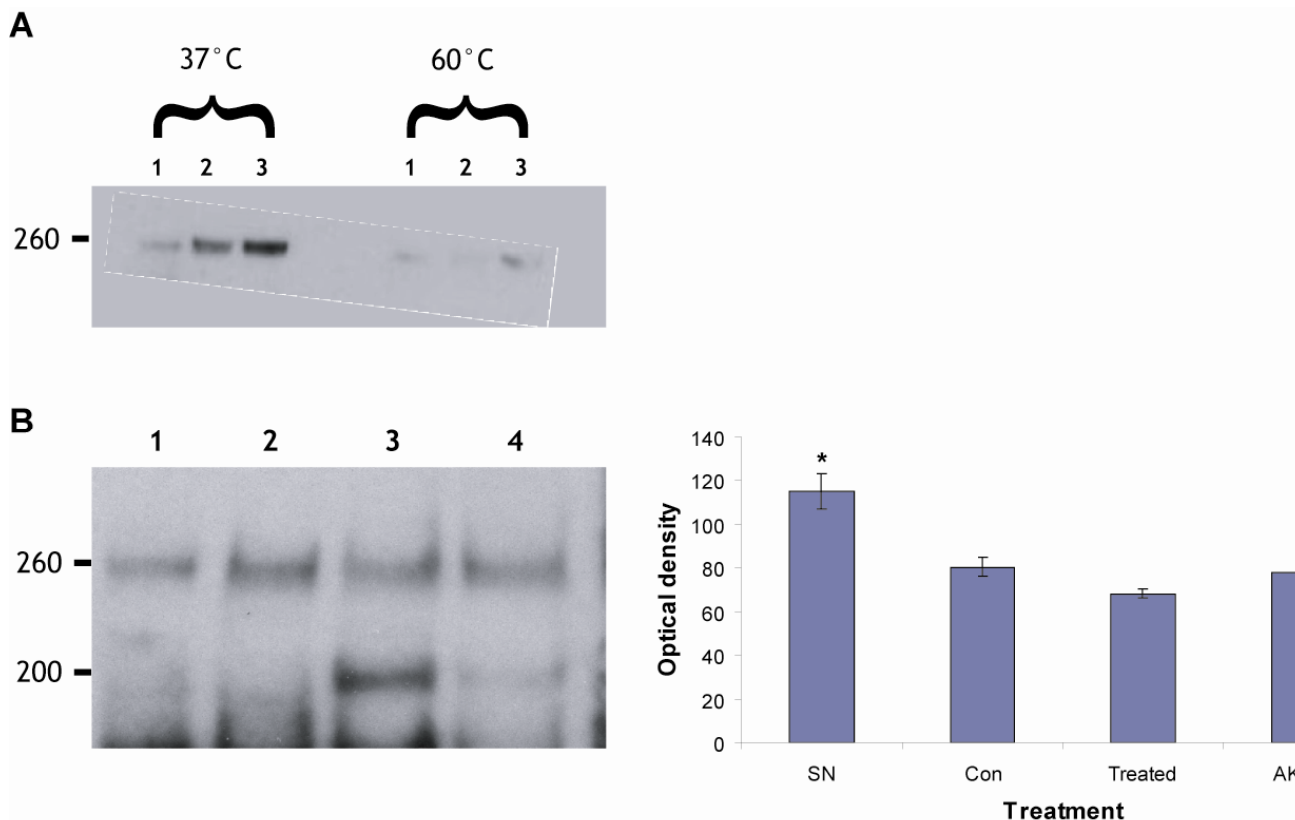


Figure 6.3 (previous page): Western blotting for Nav channel protein.

A) Western blot protocol was developed using various nerved. Staining at the correct molecular weight of 260kDa is shown for sciatic nerve (1), optic nerve (2) and PLP mice optic nerve that lack myelin (3). Samples heated at 37°C were better preserved than those heated to 60°C, and non-myelinated nerve showed the best level of staining. B) Lanes 1-4 were loaded with 20µg sciatic nerve that had either been immediately snap frozen (1), antibody treated no complement (2), antibody and complement treated (3), or AK295 treated (4), respectively. There was no significant loss of staining intensity of the protein at 260kDa between experimental samples, however there was a significant reduction compared to sciatic nerve sample immediately snap-frozen. * indicates significance where $p < 0.05$ when compared to control, treated and AK295 treated, using ANOVA statistical test.

It was shown that the reduction of sodium channel staining after 3h of NHS incubation was the most significant compared to 0h (Figure 6.4B, χ^2 -test, $p < 0.001$), and therefore nerve was treated for 2.5h and extra-cellular recordings made for the last 30min.

6.2.4.2 Conduction of the sciatic nerve after 3h NHS incubation

The peak amplitudes of recorded CAP from sciatic nerve did not decrease significantly from the starting value over the course of the final 30min following 2.5h of NHS incubation (Figure 6.5A & B, 87.24% +/- 16% reduction from starting value, *paired t-test*, $p = 0.2$) compared to control (109% +/- 5.3%).

Nerves from both protocols were stained for Nav1.6 and the results between treated and control for 1h and 3h incubations compared. There was a significant loss of staining down to 54% and 53% positive NoR in treated nerve compared to control nerve for both the 1h and 3h incubations, respectively (Figure 6.5C, χ^2 -test, $p = 0.021$ and $p < 0.001$, respectively). The difference between tissue treated for 1h and 3h was not significant.

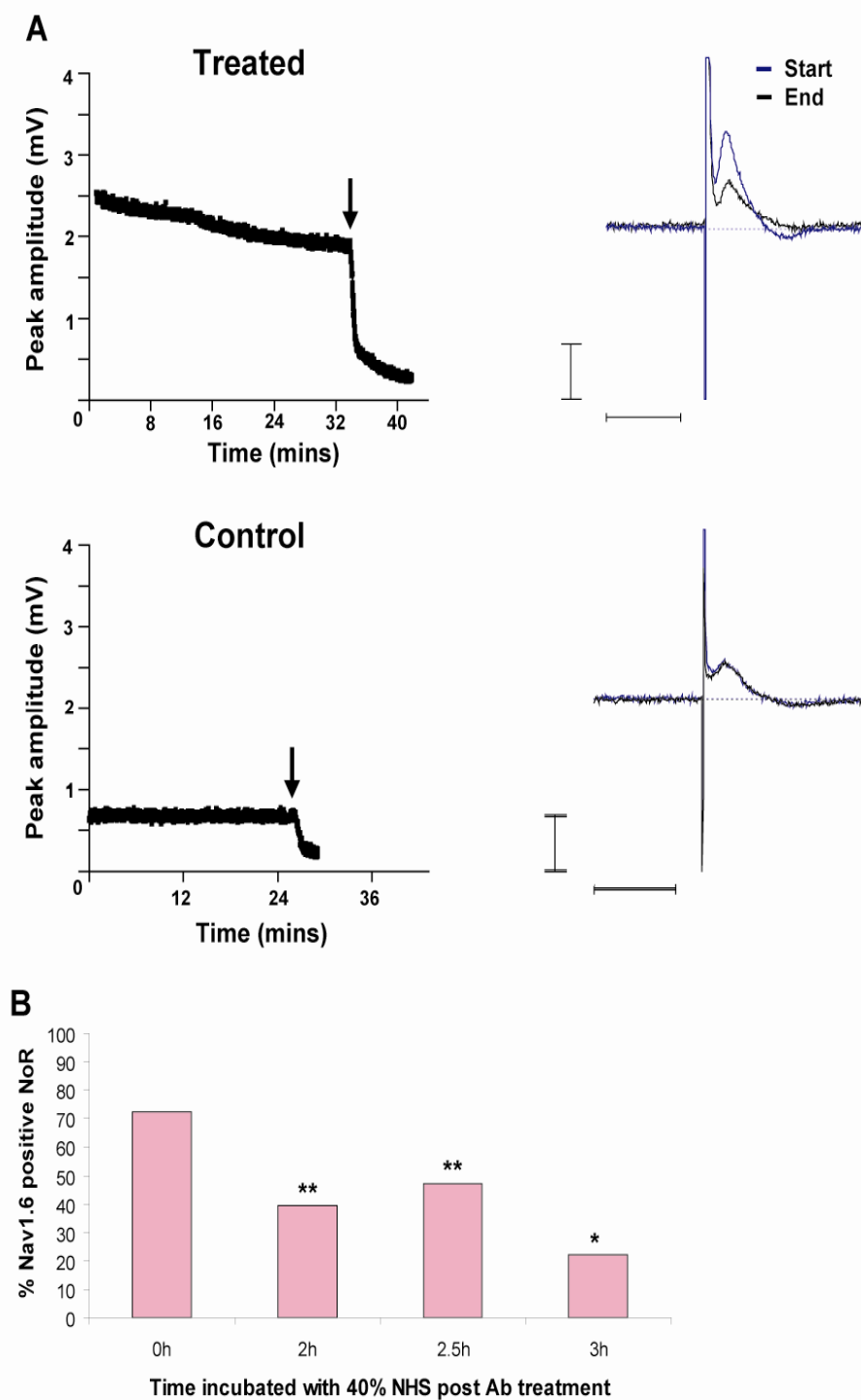


Figure 6.4: Sciatic nerve electrophysiological recordings and associated immunostaining.

A) Representative graphs of peak value of CAP over time (*left*) and overlay of single CAP traces from the beginning and end of the experiment (*right*) for sciatic nerve over the final half hour of a 1.5h injury model. Treated nerve shows a slight decline, which is significantly different to control ($p < 0.05$). Arrow indicates addition of $5\mu\text{M}$ TTX to ensure recordings are genuine. **B)** Graph showing loss of Nav1.6 staining over time in response to complement addition (0h) following antibody incubation. Loss of staining is most significant at 3h, therefore electrophysiological recordings were made to encompass these results. * indicates significance where $p < 0.001$ compared to control, while ** signifies significance where $p < 0.05$, using the Chi-squared test of independence. Note: the axes for all graphs are of different scales and are not comparable: vertical bar=1mV; horizontal bar=1ms.

6.2.4.3 Differential IgG deposition and injury at sensory and motor nerves

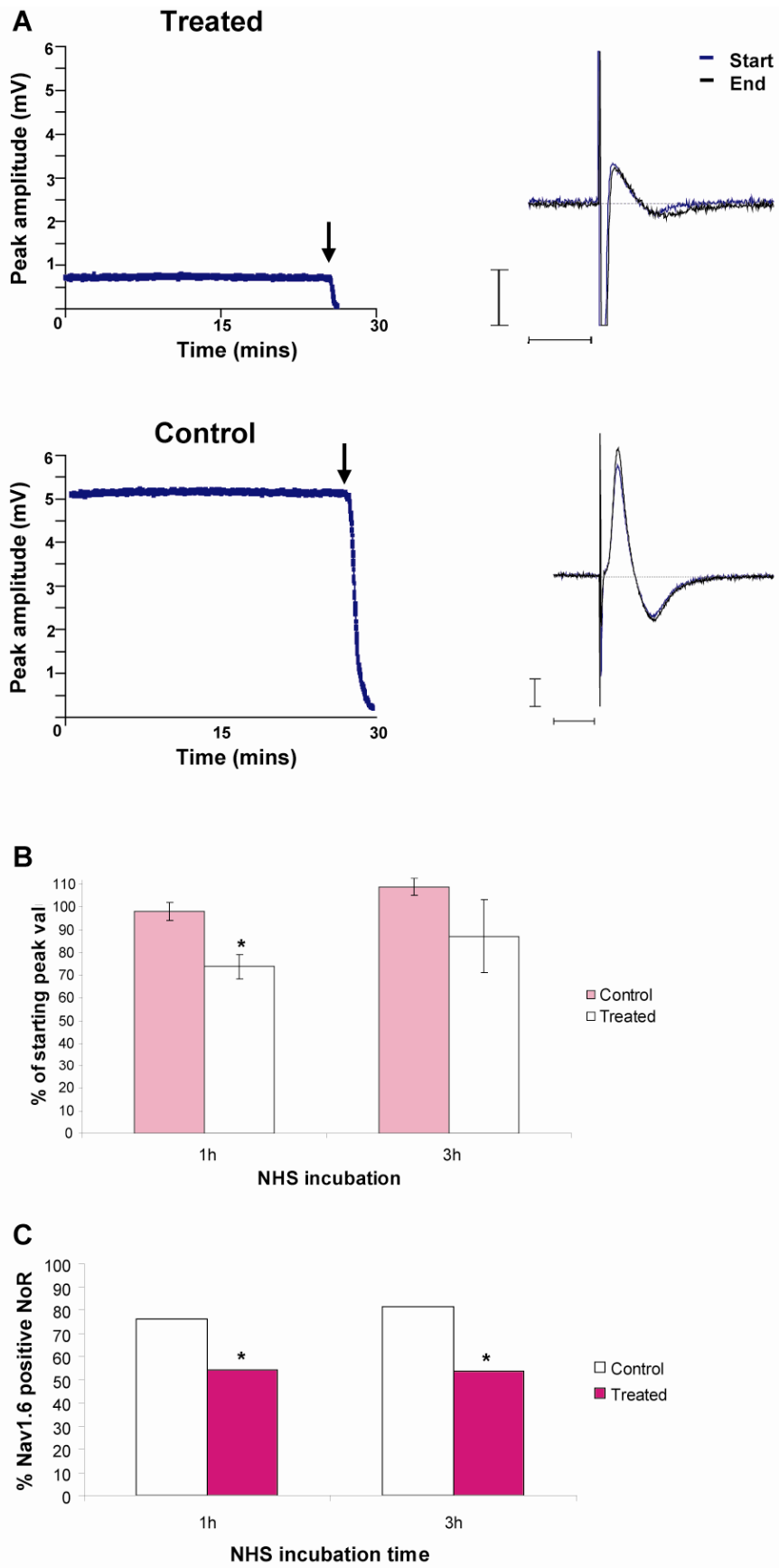
Immunostaining for sciatic nerve could be quite varied regarding IgG and MAC deposition. Initially it was speculated that this could be related to fibre diameter. However, as sciatic nerve is a mixed motor and sensory nerve, this could also explain the discrepancy. Therefore, IgG deposits at NoR of the purely motor phrenic and purely sensory sural nerve were compared.

The length of IgG deposition along the NoR was compared and the staining extended significantly further across phrenic nerve NoR compared to sural nerve (Figure 6.6, $p=0.0008$). The intensity of the staining between the two nerves on the other hand was not significantly altered ($p=0.38$).

IgG deposition at sural nerve was distinct from phrenic nerve NoR, as was the loss of Nav channel staining. Although IgG and MAC deposition can be associated with loss of Nav channel staining for phrenic nerve, at the sural nerve NoR the Nav channel staining remains intact even when coincident with MAC deposition (Figure 6.7A). The graph in Figure 6.7B exemplifies the maintenance of Nav1.6 channel staining after treatment in sural nerve, even though the percentage of NoR with MAC deposition is significantly greater than control (χ^2 -test, $p<0.001$).

Figure 6.5 (following page): Comparison of electrophysiological and immunohistochemical data from sciatic nerve treated for 1h or 3h.

A) Representative examples of sciatic nerve recordings after treatment for 3h with NHS (left panel) compared to control (right panel). Arrow indicates addition of 5 μ M tetrodotoxin to ensure recordings are genuine. B) Graph depicting the average peak of CAP as a percentage of the value from the start of recording from control and treated preparations at 1 and 3h. Although there was no significant difference there was a trend towards a decreasing CAP in treated nerve for both time-points. C) Immunostaining to Nav1.6 from both 1h and 3h groups showed a significant loss after treatment compared to control. * signifies significance where $p<0.05$ compared to control time-point counterpart, using the Chi-squared test of independence. Note: the axes for all graphs are of different scales and are not comparable: vertical bar=1mV; horizontal bar=1ms.



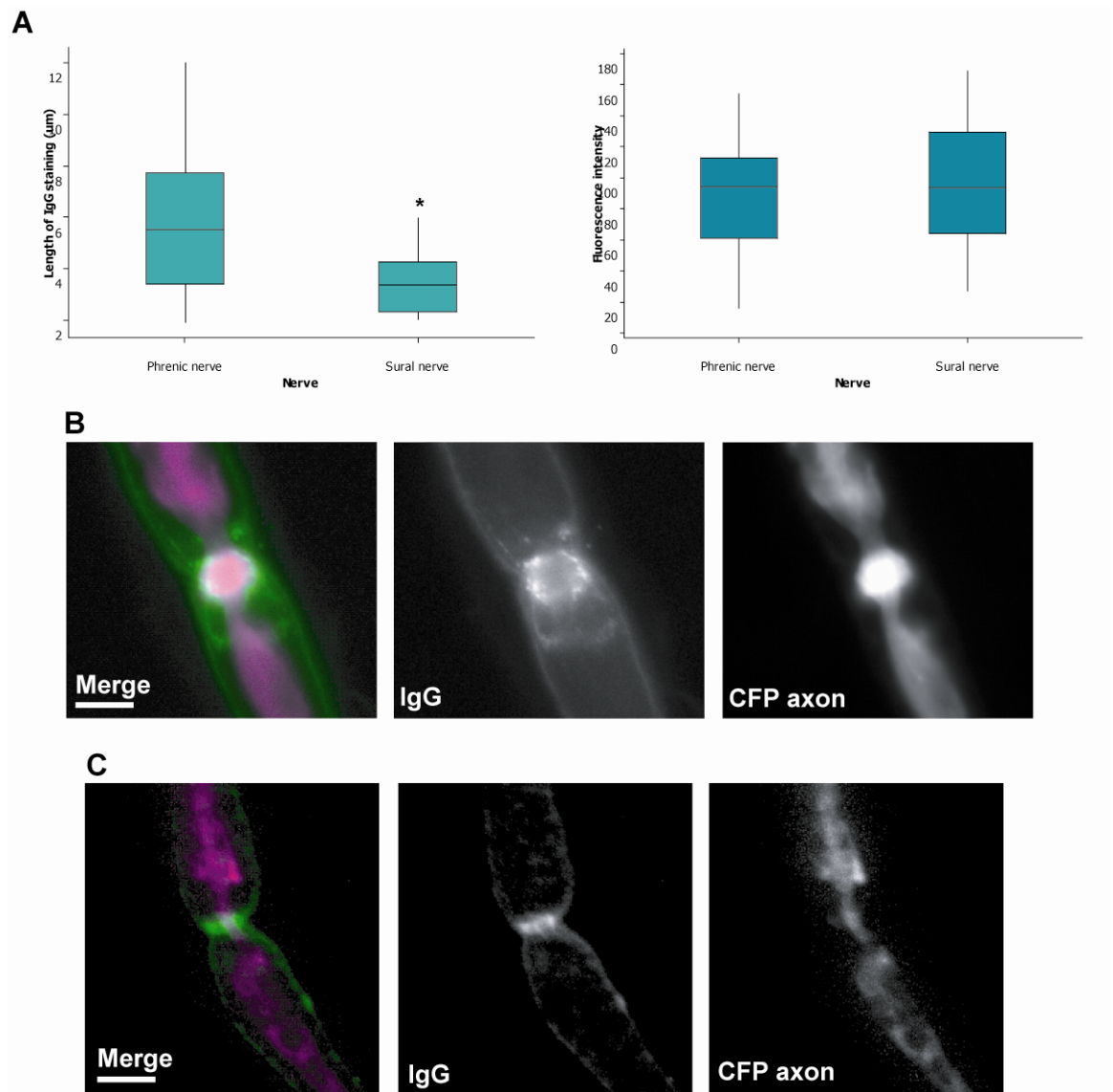


Figure 6.6: Comparison of IgG deposition between motor and sensory nerve NoR.

A) Length of IgG staining across the NoR was significantly greater for phrenic nerve compared to sural nerve. The same was not true for IgG intensity. Example of phrenic nerve (B) and sural nerve (C) IgG staining compared to CFP axon. * indicates significance where $p < 0.05$, scale bar = $5\mu\text{m}$.

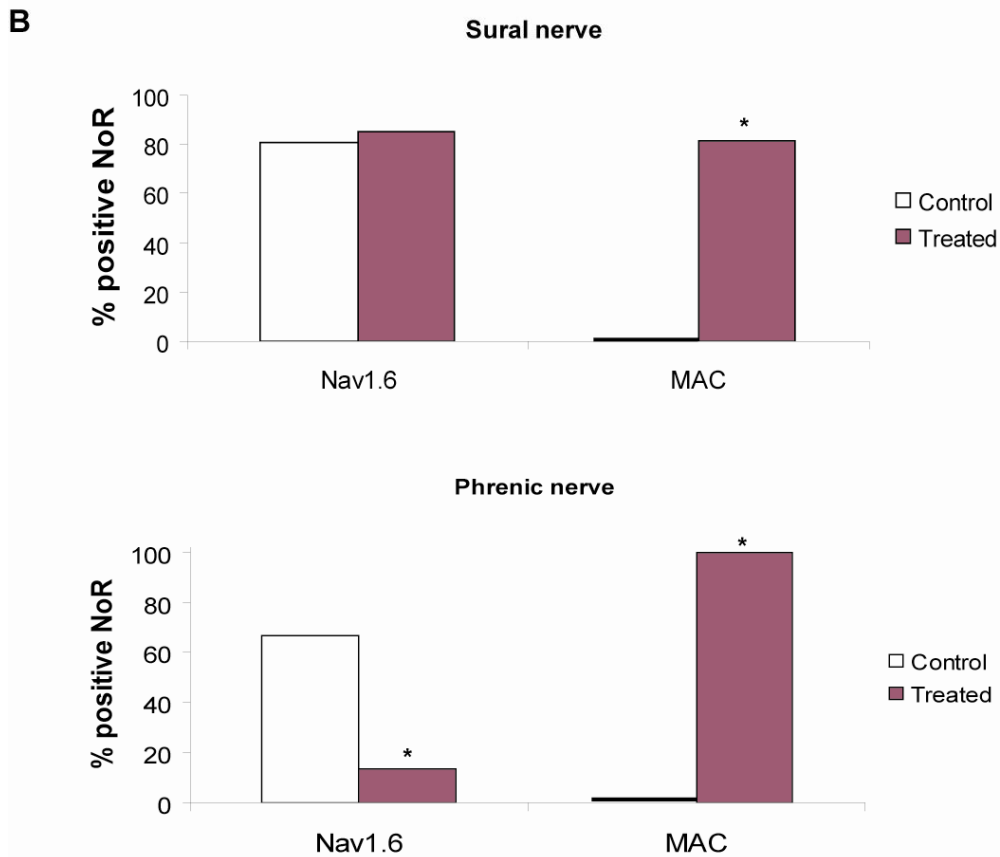
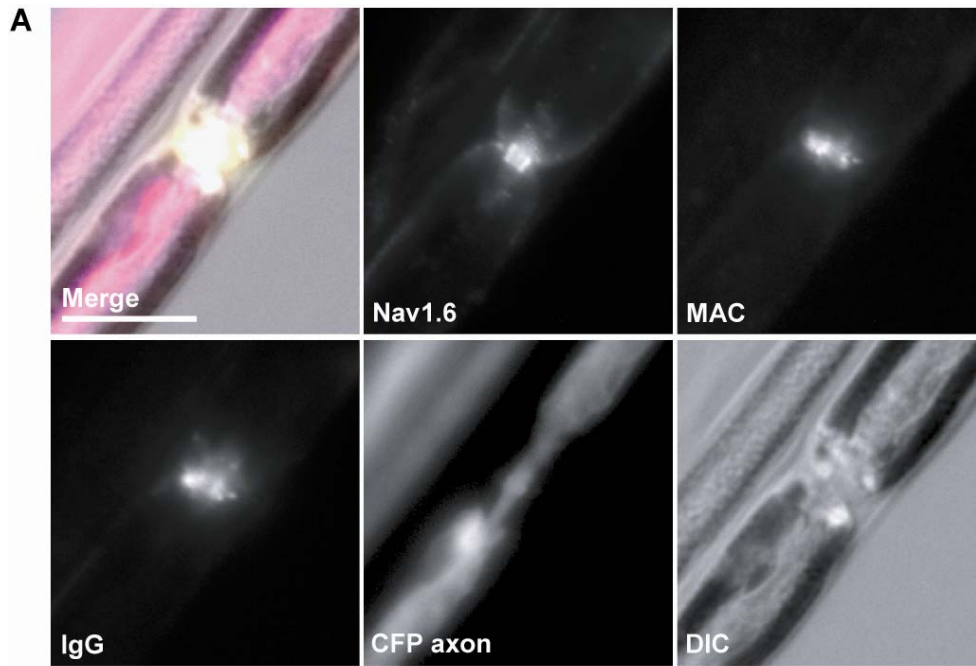


Figure 6.7: Comparison of Nav1.6 channel staining loss between motor and sensory nerve.

A) These images illustrate intact Nav1.6 channel staining at a sural nerve NoR, even though there is IgG and MAC deposition at this site. **B)** Graph depicts loss of Nav1.6 channel staining is only significant in treated phrenic nerve, while the percentage NoR with MAC deposition is significantly increased in both sural and phrenic nerve after treatment. * indicates significance where $p < 0.05$ compared to control, using the Chi-squared test of independence. Scale bar = $10\mu\text{m}$.

6.2.4.4 Effect of pathology on phrenic nerve versus sural nerve conduction

Unlike sciatic nerve, phrenic nerve and sural nerve could remain in the recording chamber and readings taken throughout the entire experiment on the direct addition of NHS to the middle chamber.

Phrenic nerve conduction was reduced by a 2h NHS incubation to an average of 40.53 +/- 10.7% of the starting peak value of CAP (Figure 6.8A & B). Where phrenic nerve would respond quite rapidly to NHS treatment, sural nerve often maintained a fairly steady CAP that would latterly begin to gradually decrease (Figure 6.8A & B). Due to this fact, although sural nerve CAP was only reduced on average to 76.3% +/- 9.6% of the starting peak value, this was not a significant difference compared to phrenic nerve due to experimental variation (*t-test*, $p=0.067$). An interesting observation nearing the end of the experiment was that all of the fibres appeared to 'fail' and no action potential was recorded. These records were omitted from the analysis of peak value as this would unfairly reduce the average. Furthermore, on occasion two peaks could be observed towards the conclusion of the experiment.

On treating phrenic nerve with the AK295 calpain inhibitor, there was no prevention of loss of current, and the peak value of CAP was reduced to 15% +/- 8.7% of the starting value, which was not significantly different compared to non-inhibitor treated phrenic nerve (Figure 6.8A & B, *t-test*, $p=0.298$).

Nav1.6 staining loss associated with electrophysiological results showed a significant reduction to 38.8% positive NoR in phrenic nerve compared to 64% Nav1.6 positive NoR in sural nerve (Figure 6.8C, *X²-test*, $p<0.001$). Phrenic nerve treated with AK295 also had significantly less Nav1.6 positive NoR compared to sural nerve (48.1%, *X²-test*, $p=0.008$). There was no significant rescue of Nav1.6 channel staining by AK295 under these experimental conditions ($p=0.11$).

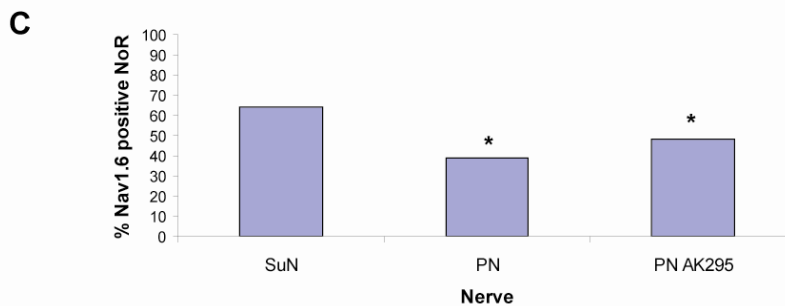
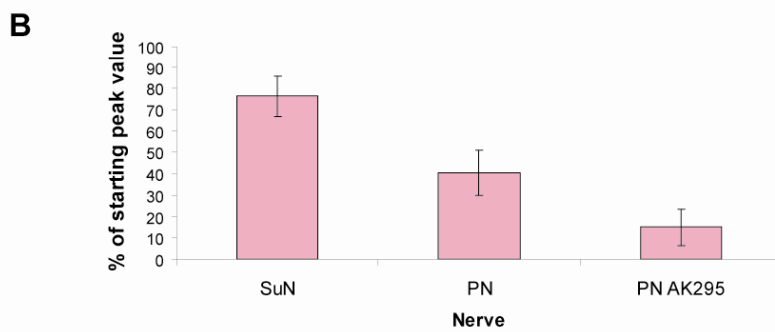
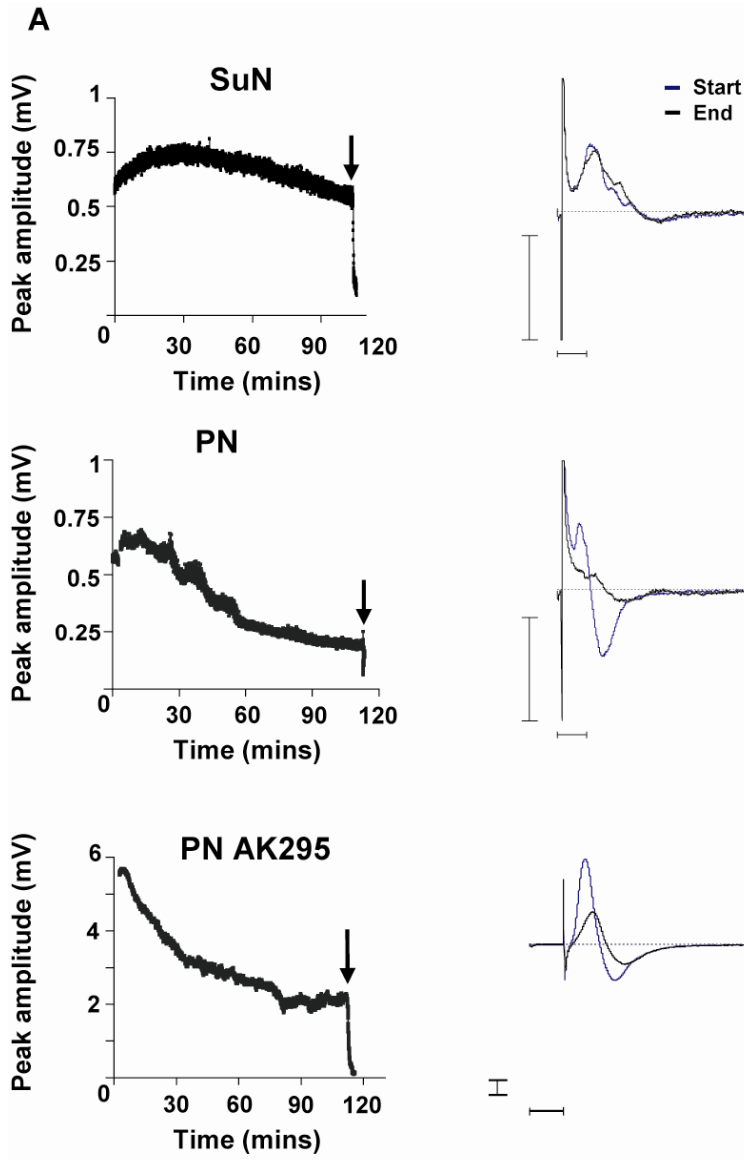


Figure 6.8 (previous page): Extracellular recordings from phrenic nerve and sural nerve treated with antibody and complement.

A) Left: Representative graphs plotting the peak amplitude of CAP over time demonstrates a rapid reduction for phrenic nerve compared to sural nerve. Arrows represent the addition of TTX to conclude the experiment. **Right:** Representative traces from the beginning (blue) and end (black) of the recording for each nerve. **B)** Data illustrating the reduction in peak CAP for each nerve as a percentage of the starting value. Although sural nerve showed a resilience to reduced conduction, experimental variability meant this was not significant compared to phrenic nerve. **C)** However, the loss of Nav1.6 staining at NoR was significantly reduced at phrenic nerve NoR compared to sural nerve. * signifies significance where $p < 0.05$ compared to sural nerve, using the Chi-squared test of independence. Note: the axes for all graphs are of different scales and are not comparable: vertical bar=1mV; horizontal bar=1ms.

6.2.4.5 Tetrodotoxin staining

It was intended that TTX used to end the experiment by binding the extracellular components of the pore and blocking ion flow, could be labelled to determine whether Na^+ channels were still intact extracellularly. A dilution series for the antibody to TTX was carried out, but even in control tissue staining appeared to traverse the entire width of the NoR including myelin which did not look like the Nav1.6 neat band. Unfortunately, the staining process was not reproducible and NoR were difficult to identify, likely due to a necessary dehydration step. Some examples are given in Figure 6.9.

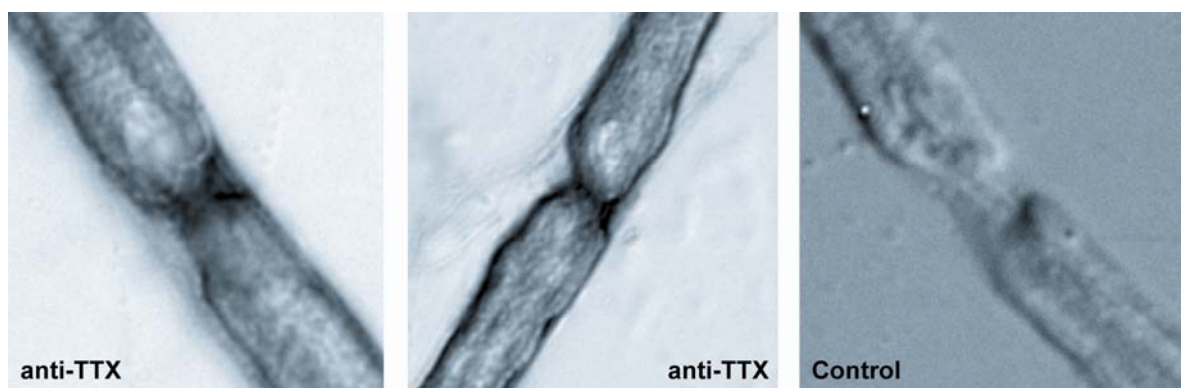


Figure 6.9: Tetrodotoxin staining of nerve.

Some example of nerves treated with TTX prior to labelling with an antibody targeted to the toxin shows indiscriminate labelling around the nodal region compared to control.

6.3 Discussion

Owing to the necessity of Nav channels for neurotransmission, it is important to ascertain what the fate of this channel is during a model of AMAN injury. In the rabbit model of AMAN, conduction failure at proximal sites was reported that coincided with disrupted Nav channel staining at the ventral root NoR (Susuki et al., 2007b). However, it was unclear from this study what precise mechanisms were occurring. It was the intention of the present study to make use of further antibodies to Nav channel, Western blot analysis and electrophysiology to shed some light on this conundrum.

Experiments using a pan sodium channel antibody against the cytoplasmic loop between domains III-IV of the alpha-subunit, showed that the loss of staining by this antibody mimicked that shown for an antibody targeting the II-III loop, i.e. anti-Nav1.6 antibody (Figures 4.5, 4.11). This result was perhaps fairly predictable from previous studies showing that all cytoplasmic loops could be cleaved by proteolytic enzymes injected intracellularly (Armstrong et al., 1973; Bergman et al. 1976; Eaton et al., 1978; Oxford et al., 1978; Rojas & Rudy 1976). Therefore I suspect that the cytoplasmic loops are cleaved non-specifically which may or may not result in the loss of staining, rather than the particular antigenic site of the antibody being cleaved. However, von Reyn *et al* (2009) propose that there are only two major calpain cleavage sites, located at loop I-II and II-III, of the Nav1.2 α -subunit (Figure 6.1A, white circles). The authors probed membrane surfaces with antibodies to fragments of the sodium channel and found that these were present and not internalised. This could be suggestive that the channel is still functional if it is still present in the membrane, which was the opinion of the work investigating cleavage of the cytoplasmic loops and loss only of the inactivation gate (Armstrong et al., 1973; Bergman et al., 1976; Eaton et al., 1978; Oxford et al., 1978; Rojas & Rudy 1976). The loss of pan-Nav channel staining observed in this study at a loop not suspected to be cleaved by calpain in the aforementioned study by von Reyn *et al* (2009), is contradictory (Figure 6.1A). Although they acknowledge that subtype cleavage may differ, it is also possible that the loss of staining occurring in the current study is controlled by a different mechanism.

There are many possibilities as to the loss of sodium channel immunolabelling. The ankyrin G binding site can be found on the linker between domains II-III (Lemaillet et al., 2003), which is also where the anti-Nav1.6 antibody binding site is located. Therefore it was initially suspected that the cause of channel staining loss could be down to a calpain cleavage of ankyrin G or its binding site, resulting in defective anchoring of the channel to the cytoskeleton and loss of clustering. As it is possible that all the cytoplasmic loops of the Nav channel could be calpain cleaved, the loss of association with ankyrin G may indeed play a role in the deficit of channel clustering. It would be beneficial to study even more antibodies to different regions of the channel in the future to determine particularly what sites are vulnerable.

Alternatively, the membrane is swollen and disrupted (shown by DIC, section 4.11, 4.12) and as only a small percentage of channels are likely to be labelled with antibody the loss of clustering may cause a significant reduction in fluorescent signal, but this does not exclude the possibility that channels are still present. Another possibility is that non-specific vesicular shedding of membrane that is intended to protect the membrane from MAC pores (Campbell & Morgan 1985; Morgan 1989) could also eliminate Nav channels located here. As the concentration of Nav channels is so great at the nodal gap, it is of my opinion that it is perhaps unlikely that all of the channels could be eliminated in this way, but maybe enough to affect immunostaining. The investigation into stages of Nav channel loss at early time-points presented here did sometimes show what looked like concentrated spots of staining. This could represent membrane vesicles being shed that contain Nav channels. However, Nav1.6 channel staining can be saved by AK295 application at the distal nerve when MAC pore formation still occurs, which perhaps nullifies this possibility. In the future it may be of interest to further study the formation of exosomes by way of co-localisation of Nav channel staining with vesicle markers.

There are two facts the prior immunohistochemical studies do not resolve:

1. Is the antibody still present and intact (excluding the cytoplasmic loops)?
2. Are the Nav channels still functional?

Western blotting for Nav channel was marred by many technical difficulties. The desire to label membranes for fodrin/ α -II spectrin to confirm calpain activation was hindered by its breakdown even in control samples. This could have been due to its ubiquitous distribution and its cleavage in other non-related tissue, such as myelin, which is found in excess in sciatic nerve. Incidentally, the use of β -actin as a loading control proved unsuccessful for its intended task, but did inadvertently detect calpain activity as actin is a calpain substrate.

From subsequent sciatic nerve studies it is not surprising that a great loss of sodium channels was not observed. It is regrettable that the Western blot analysis of Nav channel cleavage could not have been performed using phrenic nerve, but an excessive amount of tissue would be required. Equally, optic nerve would be an ideal candidate due to the low amount of tissue necessary, but a lesion could not be produced in this nerve. This was also the case for rat nerve, which was unfortunate as non-specific binding of the mouse anti-Nav channel antibody found in this study could have been reduced by using rat tissue. The studies that have demonstrated cleavage of Nav channels previously have used cells or brain homogenates which can express a great deal of these channels and thus make quantification more amenable (Iwata *et al.*, 2004; von Reyn *et al.*, 2009). However, I felt tissue would be a more appropriate method to test our model and to make direct correlations. Additionally, although Iwata *et al* (2004) and von Reyn *et al* (2009) demonstrate cleavage fragments of Nav channels by western blot, a functional output is not studied. This is important as although the channel may be cleaved, if this only occurs cytosolically it might be that only the inactivation gate is affected as shown in protease studies discussed above. Therefore, if Nav channels were damaged but still present, the changes that might be expected to occur would perhaps include loss of inactivation and possibly an increase in latency.

Consequently it was my intention to study the effect of injury on nerve conduction by extracellular recordings. Alterations to latency could not be studied as the stimulus artefact was too close and often merged with the rise of the CAP, which is attributable to the very short length of nerve undergoing recording. Therefore, the reduction to the peak of the CAP over time was recorded as a read-out of conduction failure. Electrophysiology was performed in parallel to immunohistochemistry to identify loss of conduction *and* loss of

staining since others who tried to show changes to conduction previously didn't concomitantly analyse Nav channel. Recordings were performed on the nerve trunk rather than intramuscular nerve bundles as the early loss of the nerve terminal activity by anti-ganglioside antibodies and complement (Bullens et al., 2000; Goodfellow et al., 2005; Goodyear et al. 1999; Halstead et al., 2004; O'Hanlon et al., 2001) precludes recording conduction from the more proximal nerve fibre to the synapse. This is unfortunate as the muscle and its nerve bundles present a more natural system. However, the number of NoR suffering Nav channel staining loss within the time-frame of my experiment only reached as far as small bundle NoR and differences in conduction between this short length of nerve would be incredibly difficult to measure. Additionally, if the stimulating electrode was placed further upstream, the vast number of intact NoR located here would interfere with the results.

As traces from all nerves could result in a massively varied size of CAP, no actual values were used. The phrenic nerve and sural nerve preparations were more favourable as no re-mounting was required. Remounting often affected the sciatic nerve recordings from start to finish resulting in the decision to only monitor the change in the final half an hour of the experiment.

First and foremost, my results are in agreement with those authors who described no effect on nerve conduction of anti-ganglioside antibodies alone (Harvey et al., 1995; Hirota et al. 1997; Paparounas et al., 1999). However, contrary to the results from the study by Paparounas *et al* (1999), I did find a mild reduction in conduction on the addition of a source of complement to sciatic nerve. As there were several adaptations to the model required to achieve this reduction, this may explain why it was previously not observed. It was unfortunate that the recordings for sciatic nerve could only be taken half an hour before the termination of the experiment and it was unknown what was occurring throughout the entire NHS incubation. The apparent levelling off of conduction block/sodium channel loss in sciatic nerve preparations could occur for several reasons. I suspect that due to the mixed nature of this nerve this partially resulted from the discrepancy between sensory and motor nerve susceptibility, and partially due to a penetration issue of the sciatic nerve, as it is possible that some fascicles may not have been adequately desheathed. Finally it is possible that the current is skipping injured NoR. This would probably

be a more plausible explanation at the distal nerve where the internodal distance is very short (~10 μ m) and the incidence of this phenomenon would be greater compared to a sciatic nerve with internodal length of about 1mm.

The difference in sensory and motor nerve susceptibility to loss of Nav1.6 channel staining mediated by anti-ganglioside antibody was somewhat unexpected. However, it mirrors the real-life situation where in AMAN patients only motor axons are targeted and injured. In the literature it is difficult to find a physical difference between the two nerve types, but in this study there seemed to be a moderate difference to the lateral spread of anti-GD1a antibody from the nodal gap. This in turn could affect MAC pore formation and the extent of the injury. MAC pore immunostaining always appears far more condensed in treated sural nerve, which would explain the delay in loss of Nav channel staining and conduction. In addition, CFP is usually maintained in injured sural nerve which is a good indicator of complement mediated injury (as shown by Eculizumab but not AK295 protection, chapter 5).

The lack of protection of conduction by AK295 is extremely indicative of another mechanism at work other than the calpain cleavage of Nav1.6 channels, especially as in the more proximal phrenic nerve, AK295 does not seem to as effectively protect staining of this channel compared to distal NoR. As images of treated nerve have shown a huge spread of MAC and antibody laterally from the nodal gap, and a massive swelling around the region in DIC, it is plausible that there is an osmotic imbalance causing the failure in conduction. If the channels were protected when the region regained a normal level of water and ion balance, this could potentially be of benefit therapeutically. Alternatively, disruption to the axo-glial junction, which is extremely detrimental to conduction (Bhat et al., 2001), could be more responsible for conduction failure than Nav1.6 channel cleavage/disruption.

Ultimately it would be very informative to identify whether channels are still present in the membrane after injury and possible cleavage. An extracellular marker would be ideal and it was hope that an antibody to Tetrodotoxin that binds the pore in this location (Narahashi et al., 1966) could be used to solve this problem. Unfortunately, there are several caveats with this method. TTX binds and diminishes conduction by blocking permeability of active Na⁺ ions (Nakamura

et al., 1965). In this study it would be unknown if binding was to intact Nav channels that are still conducting or also to those associated with loss of conduction. It was not possible to double stain for anti-Nav1.6 antibody and anti-TTX due to the protocols involved and thus inferences could only potentially be made regarding the above problem. Nav channels have been identified in plasma membrane post-cleavage in brain homogenates, but unfortunately their functionality was not examined (von Reyn et al., 2009). Combining the above electrophysiological techniques with this staining technique may help to determine the fate of the sodium channel in the future and further, whether the channel loss or another mechanism entirely is responsible for loss of conduction.

7 Conclusions

7.1 Permeability of peripheral nerve to circulating antibody

It is well documented that anti-ganglioside antibodies are associated with the various sub-types of GBS (Chiba et al. 1993;Ho et al., 1999;Illa et al., 1995;Ilyas et al., 1988;Kuwabara et al., 1998). It is therefore of importance to understand the binding patterns of these antibodies, and the effect of the permeability of the blood-nerve barrier on their binding. Therefore, the localisation and binding gradient of antibody was investigated in this study, as this is likely to be of consequence to region-specific injury.

GD3s^{-/-} mice engineered to over-express the a-series gangliosides (GM1, GD1a, GT1a) were utilised when determining the binding properties of anti-GD1a antibody to the GD1a ganglioside. It has previously been demonstrated in this transgenic mouse that GD1a is expressed on the axon at the terminal nerve at the neuromuscular junction (Goodfellow et al., 2005). Additionally, it has been shown in several studies that GD1a expression can be recognised by antibodies or toxins at the NoR of human and rodent nerve (De Angelis et al., 2001;Gong et al., 2002;Lugaresi et al. 1997;Sheikh et al., 1999a). In this work, GD1a expression was shown to spread laterally from the nodal gap and did not appear to be solely specific to the axon which suggests an expression of this ganglioside that is not exclusive to the axon as suggested by previous studies (De Angelis et al., 2001;Gong et al., 2002;Goodfellow et al., 2005). The lateral spread was more pronounced at proximal nerve fibre NoR, probably owing to the increase in calibre. Furthermore, there was a lesser degree of co-localisation of anti-GD1a antibody with the Schwann cell microvilli marker radixin, and a co-localisation with the paranodal loop marker MAG. This is perhaps not surprising as GD1a has been shown in axon *and* myelin fractions, albeit at a lower concentration in myelin (Ogawa-Goto et al., 1990;Ogawa-Goto et al., 1992). As anti-GD1a antibody titres have been associated with the axonal variant of GBS, it was perhaps presumed by many that this was the primary site of action. However, the localisation of this ganglioside to what appears to be the paranodal loops or

myelin adjacent to the nodal gap, could be indicative of a more general injury at the nodal region as a whole.

BNB permeability studies were performed using whole-mount muscle or nerve *ex vivo* preparations, while antibodies were passively transferred to study permeability *in vivo*. To illustrate the access and improved binding of antibody at NoR closest to the nerve terminal in intramuscular nerve bundles, these bundles were categorized into single fibres, small, medium and large bundles. At the distal intramuscular axons, the BNB is significantly more permeable closer to the terminal, which can be explained by the reduced number of layers in the perineurial sheath and its open end at the NMJ (Burkel 1967; Malmgren & Olsson 1980; Saito & Zacks 1969). The reduced level of antibody fluorescence intensity was confirmed to be caused by lack of permeability rather than reduced GD1a expression at NoR further upstream in sectioned diaphragm. Furthermore, it was established that permeability became an increasing issue in the proximal direction as phrenic nerve and sciatic nerve trunks exhibited no binding of antibody unless the sheath was removed.

In summary, this study has demonstrated a potential new site of GD1a expression, in addition to the axon, at the paranodal loops, and the BNB's role in creating a binding gradient to antibodies against this ganglioside. As the localisation of GD1a was performed using mice over-expressing this ganglioside it is possible that this is not a true representation of natural expression. Access to human nerve and the use of site-specific nodal markers could more clearly elucidate the specific location of GD1a in the future. In conclusion the general localisation to the NoR and the affect this antibody has to this region in association with complement is of utmost significance to understanding the pathology of AMAN and potential treatment.

7.2 Characterisation of antibody-mediated axonal injury

Reports of axonal degeneration, nodal disruption and nerve terminal damage in human post mortem tissue and animal models (Ang et al. 2001; Goodfellow et al., 2005; Greenshields et al., 2009; Griffin et al., 1996b; Hafer-Macko et al.,

1996;Halstead et al., 2004;Ho et al., 1997;O'Hanlon et al., 2001;Sheikh et al., 2004;Susuki et al., 2003;Susuki et al., 2007b;Yuki et al., 2001) led me to primarily investigate the injury caused by anti-GD1a antibody at the distal nerve in its entirety, before focusing on the NoR specifically.

The deposition of the terminal complement complex MAC, has previously been assessed in conjunction with nerve terminal injury in a mouse model of GBS (Goodfellow et al., 2005;Greenshields et al., 2009;Halstead et al., 2004;Halstead et al., 2005;O'Hanlon et al., 2001). In this study, MAC pore deposition was similarly co-localised with antibody at the distal NoR. This also followed the BNB permeability gradient-dependent binding effect demonstrated by anti-ganglioside antibody. In the previous mouse studies mentioned above, the axonal damage was analysed by measuring the loss of the cytoskeletal protein neurofilament. Therefore this and endogenous CFP of GD3/CFP mice were the first proteins studied in the distal axon after antibody and complement treatment to ascertain what processes were occurring.

The cross of a transgenic mouse that endogenously expresses CFP in the axons (Feng et al., 2000) with the GD3s^{-/-} (Kawai et al., 2001) to create the GD3/CFP mouse was of great value in this study for the identification of axons. Additionally the loss of CFP from axons after antibody-mediated complement-dependent injury was useful to the study of the disease process. Fluorescent mice have been utilised for many applications, but one of the key benefits is the ability to image axons over time (Beirowski et al., 2004;Kang et al., 2003;Lippincott-Schwartz & Patterson 2003;Zuo et al., 2004). It was hoped that this technique of multiple imaging could have been applied to acute injury paradigms in *ex vivo* tissue, and that the injury process, as measured by loss of CFP fluorescence, could be monitored in real-time. Unfortunately, bleaching was a prominent issue and the loss of CFP was not NoR specific as expected from the node-specific MAC pore deposition. It was equally difficult to assess precise loss of neurofilament staining along the distal axon using regular immunohistochemical procedures. While these experiments into distal axon injury were informative and showed a general disruption to the region, they require refinement.

As damage to the axon terminal had been shown in the mouse in response to anti-GD1a antibody previously (Goodfellow et al., 2005), it was of importance to determine if the injury recorded further upstream was a direct effect of terminal damage or due to injury at another site, which was expected to be the NoR. Use of the toxin α -latrotoxin that is specifically injurious to the terminal (Mallart & Haimann 1985), demonstrated that anti-GD1a antibody was causing injury elsewhere. This was shown by the maintenance of CFP along the axon in muscle treated with α -LTx compared to those treated with antibody and complement, and also the intact Nav channel staining at NoR upstream from the terminal after α -LTx treatment.

To study the effect of antibody and complement on NoR in greater detail, a battery of antibodies to proteins at this region were investigated at both distal and proximal fibres. Primarily the nodal gap ion channel Nav1.6 and the cytoskeletal protein ankyrin G were investigated. At the distal axon NoR, staining for these proteins could be described as present or absent. After treatment there was a significant reduction in the presence of both of these proteins. This was a similar case for the paranodal proteins Caspr and Neurofascin 155, although sometimes the staining for these proteins could also be described as disrupted rather than completely absent. Unusually, the Kv1.1 channel at the juxtaparanode showed no significant disruption or absence compared to control tissue, which led me to believe that the injury did not spread that far laterally, or at least not in the acute time-frame studied here. In the rabbit model of anti-GM1 mediated AMAN, Kv1.1 channel staining was only affected when the paranodes showed extreme disruption at advanced stages of injury (Susuki et al., 2007b). Due to the nature of the barrier function of the axo-glial junction, it is possible that if this is disrupted (which might be expected from the alteration and loss of Caspr and NFasc 155 staining) eventually Kv1.1 channels may translocate (Bhat et al., 2001). It is unfortunate that co-localisation of Kv1.1 channels with paranodal markers is not practical due to the loss of the latter under these circumstances. The Nav1.6 clusters may also be affected by a breakdown of the axo-glial junction as shown in mutant mice (Rasband et al., 1999; Sherman et al., 2005).

A further two proteins were studied at the phrenic nerve NoR. An antibody to the extracellular domain of the nodal gap transmembrane protein NrCAM

resembles Nav1.6 staining in control but after injury instead of its absence a spread of the protein distribution along what looks like the surface of the myelin sheath occurs. This was also true for the Schwann cell microvilli marker moesin. While it is unclear what is actually occurring, it is possible that mechanisms resulting in the loss of cytoskeletal ankyrin G and Nav1.6 do not affect NrCAM and moesin. However, as the staining is disrupted although present, it is indicative of a possible disorder to the region as a whole. This disorder is further represented by the unusual spread of IgG and MAC staining observed at phrenic nerve NoR. Schwann cell networks of the paranodal region have been associated with the sequestration of endocytic material (Gatzinsky et al., 1920). Therefore, this mechanism could play a role in the lateral spread of IgG and MAC reported in this study as it is unclear whether this is internal or external. This would require further examination.

In summary, anti-GD1a antibody-mediated complement dependent injury to the distal axon does indeed appear to be specifically targeted to the NoR rather than a result of injury to the terminal advancing up the axon. The loss of staining to nodal proteins is more severe at the nodal gap compared to the paranode, and the paranode compared to the juxtaparanode suggesting a lateral spread of disruption. The disruption to the non-axonal glial protein Neurofascin 155 is indicative of a disorder to the axo-glial junction which could potentially affect the entire region due to its important function as a barrier. Furthermore, the staining to extracellular domains of nodal gap proteins after treatment is not lost but equally does not display a normal staining pattern, which is also indicative of a general disruption to the area.

7.3 Complement and calpain mediated injury to distal axons

Complement activation has been associated with AMAN pathology related to immunohistochemical deposition (Hafer-Macko et al., 1996; Halstead et al., 2004; Susuki et al., 2007b; van Sorge et al., 2007), electrophysiological dysfunction (Arasaki et al., 1993; Arasaki et al., 1998; Santoro et al., 1992; Thomas et al., 1991), and prevention by complement inhibition (Halstead

et al., 2005;Halstead et al., 2008a;Halstead et al., 2008b;Phongsisay et al., 2008).

To examine the protection of the nodal proteins and CFP by complement inhibition, the complement inhibitor Eculizumab was utilised as this mAb has proven successful in the prevention of mouse nerve terminal injury (Halstead et al., 2008b). The effect of Eculizumab in this study was similarly successful. CFP and nodal protein staining was comparable to control tissue, which is indicative that complement deposition is an integral part of the injury pathway in response to anti-ganglioside antibody deposition. Testing of Eculizumab in our mouse model with human NHS is particularly relevant as it is an antibody to human complement product C5, so although it is tested in mouse, it is preventing the formation of human MAC.

As MAC pores are non-specific channels for ions and water, an influx of Ca^{2+} ions into the axon (and potentially the paranodal loops) at the NoR is likely to be triggered. This in turn could activate calpain, which if at high enough concentration could overwhelm the ability of the natural inhibitor calpastatin to prevent indiscriminate degradation of its various substrates such as neurofilament and ankyrin G, among others. Calpain activity has recently been identified as a potential mechanism of injury post-complement deposition at the mouse terminal in a model of GBS (O'Hanlon et al., 2003). Interestingly, in this study although neurofilament is protected by the calpain inhibitor calpeptin, the general ultrastructure is still heavily disturbed, which could represent a further mechanism of injury such as oedema caused by excessive influx of water. Two ways to examine the involvement of calpain in nodal injury are to measure calcium influx associated with complement deposition, and the prevention of protein loss by calpain inhibition.

Calcium influx, as measured by the calcium indicator Rhod 2-AM, occurred in response to anti-GD1a antibody and complement in PC12 cells, but unfortunately was difficult to establish in tissue. Consequently, the synthetic calpain inhibitor AK295 was used to examine the role of calpain in nodal protein loss. At the distal intramuscular fibre NoR, AK295 did indeed protect Nav1.6, ankyrin G and Caspr staining to a level comparable to control. However, the protection afforded to nerve trunk NoR protein staining was noticeably reduced. As IgG and MAC

deposition were shown to excessively spread outwith the region of the nodal gap along the myelin sheath, an exacerbated injury could be occurring at this site. Furthermore, the images of NoR captured in DIC showed a rather swollen, disrupted phenotype after treatment of the phrenic nerve. These two factors could suggest a much exaggerated injury that is caused by another mechanism and unable to be prevented by calpain inhibition as shown for the finer calibre fibre NoR. In addition, there is no change to NrCAM and moesin 'spread' staining with AK295 treatment, which further signifies the occurrence of another non-calpain related disturbance in the vicinity. It is unknown whether over time the axon could recover from this swelling/disruption and AK295 may still be beneficial, or if this is the critical point of pathology. Furthermore, the more excessive injury to proximal NoR compared to distal nerve NoR, could perhaps suggest that the further the damage progresses up the nerve the patient phenotype will be more severe and it is less likely intervention by calpain inhibition will be possible.

In conclusion, complement has a critical role in injury to the axon at the NoR after antibody deposition. Associated injury can be prevented by complement inhibition. As the attenuation of this pathway has shown positive results in the control of the disease process in a rabbit model of AMAN (Phongsisay et al., 2008), this method of intervention has potential for therapeutic management of disease in patients. Eculizumab is an excellent candidate as it is already known to be safe as it is used to treat patients with paroxysmal nocturnal hemoglobinuria where complement destroys the red blood cells resulting in anaemia (Hillmen et al., 2006). One major caveat of this study is that Eculizumab is added to NHS prior to addition to the tissue preparation. The results therefore do not exemplify the efficacy of the drug once injury has already been induced. It is likely that application of the drug during the course of injury would reduce the level of damage, and it would be of interest to investigate this in models in the future.

The results of the calpain inhibition experiments were slightly more ambiguous. It would appear that there is a discrepancy in protection between distal and proximal nerve NoR to antibody-mediated injury by the calpain inhibitor AK295. This could be explained by a divergent mechanism of injury in more proximal nerves. It is very possible that the phrenic nerve is more susceptible to injury in

this model as it has been unnaturally desheathed and under normal circumstances the sheath would provide appropriate protection. The ventral roots are known to have a more permeable BNB and thus the desheathed phrenic nerve could possibly reflect injury occurring at the root. It is entirely likely that calpain degradation of proteins is very destructive to the NoR, but it is probably not the only factor involved in the general breakdown of the area.

7.4 Fate of the sodium channel at NoR after injury

Sodium channels are essential to transmission of action potentials along the nerve. Therefore it is important to investigate the fate of this protein in the present experimental mouse model of AMAN, and whether there is a connection to conduction failure.

As loss of staining occurs for two antibodies raised against different sites of the sodium channel α -subunit, it is evident that both regions undergo cleavage by calpain. This is confirmed by the maintenance of staining at distal nerve NoR by the calpain inhibitor AK295. As this protection is not as effective at phrenic nerve NoR, it is likely that an additional mechanism of injury is occurring. This is further indicated by the lack of change to NrCAM and moesin staining spread between treated and calpain 'protected' tissue.

It is unclear whether sodium channels are essentially still present and merely missing their cytoplasmic loops, or if they are completely absent in treated phrenic nerve. The results from distal nerve are very suggestive that the sodium channel is still present at this location as calpain inhibition maintains the staining, even though MAC formation and water influx has still occurred. As far as I am aware this is the first study to demonstrate that Nav channel is a calpain substrate in *ex vivo* preparations that are very closely related to a natural situation. Nav channel has been shown to suffer cleavage due to calpain in *in vitro* brain homogenate (von Reyn et al, 2009), but even so only two cleavage sites were demonstrated which does not quite correspond to the present results where at least one other cleavage site in the third loop is likely to occur. It is unfortunate that Western blots representing cleavage fragments could not be

achieved in the present study, but perhaps the method could be improved upon in the future.

Electrophysiological analysis of nerve conduction showed a loss in conduction that was not prevented by AK295. It is of my opinion that there is a general disturbance to the area that quite possibly includes the break-down of the axo-glial junction and thus interferes with conduction by this route. Perineural recordings of the distal intramuscular bundles have been performed (described in detail in Appendix 1) and have shown a loss of sodium current in response to antibody and complement treatment at this region. Therefore in the future, performing these perineural recordings in the presence of AK295 may be very informative as to the potentially differing mechanisms between distal and proximal nerve injury and associated loss/protection of conduction.

The discrepancy between sensory and motor nerve Nav channel loss is akin to the scenario in AMAN where only motor axons are targeted. It has been well documented that ganglioside conformation in the membrane can play a role in antibody affinity and that different antibodies to seemingly the same ganglioside possess different binding properties (Gong et al., 2002; Lopez et al., 2008; Ogawa-Goto et al., 1990). It is possible that the particular anti-GD1a antibody used in this study displays a differential binding pattern in sensory compared to motor nerve and thus the pattern of injury is less severe initially in sural nerve.

To summarise these results, it has still not fully been elucidated what mechanisms are occurring to cause loss of Nav channel staining and conduction. The results are indicative that Nav channel undergoes calpain mediated proteolysis, which is probably the main or exclusive mechanism of disruption to staining at the distal NoR. At proximal nerve NoR, an ionic imbalance and axo-glial disorganisation are possible alternative routes of disruption to the region and its effects to staining and conduction cannot be readily resolved by calpain inhibition. Whether the transmembrane portion of the channel and its extracellular regions are still intact and/or functional is yet to be determined.

7.5 Future directions

There are several aspects of this work that would be interesting to develop in the future. The suggestions proposed in the previous text will be expanded upon, before exploring other potential directions.

1. **A more extensive study of GD1a localisation.** This should involve the co-localisation of GD1a antibody with several proteins in the nodal region in distal and proximal axons of the periphery. Also a more detailed exploration of differential anti-GD1a antibody binding between sensory and motor nerve would be useful to establish the source of diverse susceptibility of the two populations. An alternative more sensitive method to investigate specific ultrastructural GD1a localisation would be to use immunoelectron microscopy. It may be beneficial to investigate human tissue and if possible other anti-GD1a antibodies/toxins to establish how similar the binding in this study is to natural expression. Additionally, the treatment of various tissues with patient sera could more clearly demonstrate the binding patterns and effects of actual disease causing antibodies.

The alteration of the anti-GD1a antibody distribution in response to injury should also be further investigated. As this change is reflected by MAC deposition, it has been suggested that membrane shedding/vesiculation has a role to play in this process. It would therefore be convenient to investigate this further by utilising a recently developed transgenic mouse that only expresses gangliosides on the Thy1 promoter in the complex ganglioside null GalNAcT^{-/-} mouse strain. Not only would this establish definitively that GD1a is expressed axonally, but if it is found anywhere other than this location in this transgenic mouse, there is a mechanism of transferral of gangliosides occurring. This will be very enlightening to our understanding of the disease process. Some caution would be necessary though in interpreting the results as expression will only occur where the Thy1 promoter is active and this could lead to ectopic expression of GD1a that does not resemble natural circumstances.

Another avenue for investigation, is determining the exact difference between GM1 and GD1a deposition at the NoR. The disruption to the various nodal proteins may differ in response to an anti-GD1a and anti-GM1 antibody mediated injury which could correlate to differences in binding location around the region of the NoR. This may account for subtle phenotypic differences between AMAN patients.

- 2. Nav channel presence and function.** To ascertain whether sodium channel is still intact, aside from the cytoplasmic loops after injury, better antibodies to the extracellular domains are required. Alternatively the primary labelling of a toxin may be more successful. This may also be true of the method used by von Reyn *et al* (2009) to label membranes. Furthermore, the development of the Western blot to study fragmentation would be valuable. Nav channel, and even more specifically the Nav1.6 channel isoform, cleavage by calpain have never been demonstrated *in vivo* and therefore to provide this information *ex vivo* would be a step forward. Demonstration of cleavage in Western blot, protection by calpain inhibition and labelling of the intact remnants of channel would unequivocally prove that cleavage of the cytoplasmic loops is indeed occurring. Once this is established the results of the functional studies can be better evaluated. It may be easier to begin this line of investigation by cloning the Nav1.6 channel isoform into a ganglioside expressing cell line and determining the effect of anti-GD1a antibody and complement on channel cleavage at this level.

As alluded to above, perineural recordings would be indicative of what mechanisms are occurring at the distal intramuscular nerve bundle during injury. Appendix 1 details the specifics, but briefly, Na⁺ currents were reduced or absent in small and medium branches in response to antibody and complement treatment. If AK295 were applied to this system it would determine whether this calpain inhibitor could benefit the function of nerves attacked by complement. This would indicate the inhibitors relevance in a clinical setting.

- 3. Process of injury over time.** A more detailed investigation into the sequential loss of nodal proteins may elucidate if there is a lateral spread

of injury, or a general concurrent disruption at both the nodal gap and paranode/axo-glial junction. This could be achieved by studying the level of staining loss of all nodal markers at several time-points preceding the standard 3h NHS incubation, and subsequent to this time-point. If the axo-glial junction is indeed dismantled by the action of complement and calpain, this could be investigated by the progressive availability and staining of a protein that is masked under normal circumstances. For example, neurofascin 155 cannot be identified when antibody is applied directly to nerve without permeabilisation. However, if staining started to materialise after treatment it may be suggestive that the paranodal loops are becoming separated from the membrane. This is possible as this phenomenon has been shown ultrastructurally at ventral roots of the anti-GM1 mediated AMAN rabbit model (Susuki et al., 2007b).

Western blotting for fragment products of other nodal products could also enhance the model. Particularly, there is an antibody against the extracellular NF186 isoform and a pan antibody to both isoforms (Tait et al., 2000) that could be used to discriminate between cleavage or disruption of membrane. If the axonal portions of proteins are cleaved, the anti-NF186 antibody should detect a protein of a lower molecular weight than usual as the cytoplasmic tail will have been clipped. However, although NF155 staining is disrupted, there potentially should be no change to its molecular weight as it is not exposed to calpain.

- 4. Separation of calpain and oedema related pathological processes.** As it is possible that there are at least two injury mechanisms taking place in the phrenic nerve, it would be of great relevance to try and establish if they are equally detrimental. I propose that the two processes are calpain mediated cleavage of proteins, and MAC related influx of water resulting in an osmotic and ionic imbalance. To study the effect on conduction of excessive Ca^{2+} influx exclusively, the Ca^{2+} ion specific channel formed by ionomycin could be used to interpret what changes occur in response to calpain activation alone. Alternatively, proteolytic enzymes could be injected intraneurally and the response compared to that of suspected calpain cleavage. The increased influx of sodium ions, through the MAC pores in this study, could also play a role in injury as has been suggested

by previous authors in models of ischemia and EAN (Bechtold et al. 2005; Kapoor et al. 2003; Stys et al., 1992; Waxman et al. 1994). In these studies it has been shown that Nav channel blocking agents prevent axonal degradation. The suggested mechanism is that Nav channels are not fully inactivated, which leads to an influx of Na^+ and therefore Ca^{2+} due to the reverse operation of the Na^+ - Ca^{2+} exchanger. This potential mechanism could be further investigated by excluding Na^+ influx from the incubation medium, or by applying TTX. It is very possible that this mechanism does not have as prominent a role in the injury discussed in the present investigation as MAC pores alone allow the excessive movement and accumulation of unwanted ions.

5. ***In vivo* experiments and clinical relevance.** An *in vivo* model of the anti-GD1a antibody-mediated complement-dependent loss of nodal proteins is the next stage necessary to ensure the model translates to a real system. The attempts so far to create a mouse model are documented in Appendix 2. Previously a mouse model of AMAN was achieved only in a GD3s/CD59/DAF triple knock-out mouse. This is presumably due to the reduction in inhibition of MAC deposition due to absence of complement regulators causing an increased level of injury, as has been described before (Halstead et al., 2004). Alternatively, in a mouse model of EAN, CD59 inhibitor expression was shown to be increased (Vedeler et al. 1999), and perhaps as this is not possible in $\text{CD59}^{-/-}$ mice, injury is exacerbated. However, it is still a controversial issue whether mouse inhibitors can control human complement products. Furthermore, the expression of endogenous complement inhibitors is unclear, although recently CD59 was reported at the mouse NoR (Willison et al., 2008). It would be of interest to further elucidate the expression of complement inhibitors as this may be key to understanding the injury process. For instance, perhaps there is a higher expression at distal NoR compared to proximal sites and this alters susceptibility. Perhaps the sheath would normally offer the highest level of protection but when it is removed, the axons are more vulnerable. It is possible that this situation is similar to ventral roots that have a decreased level of protection by the BNB, and have been found to undergo injury in models of GBS. It would ultimately

be preferable if an *in vivo* model could be developed in the GD3s^{-/-} mouse without further manipulations to the complement inhibitors whose roles are not fully understood in this particular system. Another issue concerning the possible development of an *in vivo* mouse model, is the initial damage to nerve terminal. When this occurs, the diaphragm loses its innervation and thus the mouse will struggle to breathe and develop what can be described as a ‘wasp-like abdomen’. At this point the experiment must be terminated, but a great enough time may not have passed for the injury to progress to the NoR. This could possibly be overcome by the artificial ventilation of the mouse under terminal anaesthesia to prolong the experimental time without unnecessary suffering. The technique of intubating a mouse has already been developed to study the injury to the sternomastoid muscle of the neck (Feng et al., 2000), so should be easily transferred to this model.

If an *in vivo* model were developed where loss of staining was similar to that witnessed in *ex vivo* preparations, AK295 protection and efficacy could also be studied. One major concern of using a calpain inhibitor *in vivo* is the potential detrimental effect of preventing calpain activity in its normal signalling roles. However, prolonged intramuscular injection of leupeptin to inhibit calpain activity in monkeys appeared to have no adverse effects (Badalamente et al., 1989). Furthermore, an AK295 implant showed no undesirable side-effects in mice (Wang et al., 2004).

The clinical relevance of Eculizumab is not fully realised in the present study as this complement inhibitor is added prior to complement related damage. Therefore I think it would be helpful to assess the protective effects of this drug after the commencement of injury. It could well be the case that in patients it would only prevent the damage to NoR yet to be injured and thus the proposed model may not illustrate this protection. However, it may also prevent MAC deposition from reaching the threshold where it overwhelms the self-protective mechanisms and therefore there may be a noticeable alteration in susceptibility.

Finally, an *in vivo* model may overcome the problems encountered in acquiring quality examples of ultrastructural alterations after treatment.

This was unsuccessful in *ex vivo* nerve due to the extended length of time between removal from the body and fixation.

- 6. Correlation to real-life scenario.** Although much work to progress the understanding of GBS has been provided by mouse models exhibiting nerve terminal damage (Willison & Plomp 2008), this is not a recognised site of pathology in patients. It is possible that there is such a great deal of turnover of molecules at the nerve terminal due to neurotransmission, that the antibody binding to gangliosides can never accumulate to a high enough level to be pathogenic. The endocytosis and cycling of gangliosides is currently under investigation in this lab. However, the membrane cycling at NoR is less likely to be so fluid and thus it is an important step forward to begin elucidating the injury process at this sub-domain of the nerve. Autopsy tissue from fatal cases have shown degeneration and complement deposition at ventral root NoR (Griffin et al., 1996b; Hafer-Macko et al., 1996), and perhaps it would be beneficial to study this area in parallel to other regions of nerve such as the terminal and the distal nerve that are often omitted from analysis.

In conclusion, there are many experiments to be considered that could advance the results presented in this study. This acute *ex vivo* mouse model of AMAN represents the starting point from which the disruption observed by Susuki *et al* (2007) in the rabbit begins, and thus these studies together could provide a solid basis for the establishment of the disease processes occurring in human AMAN. The proposed mechanism of injury based upon the results of this research is depicted in Figure 7.1.

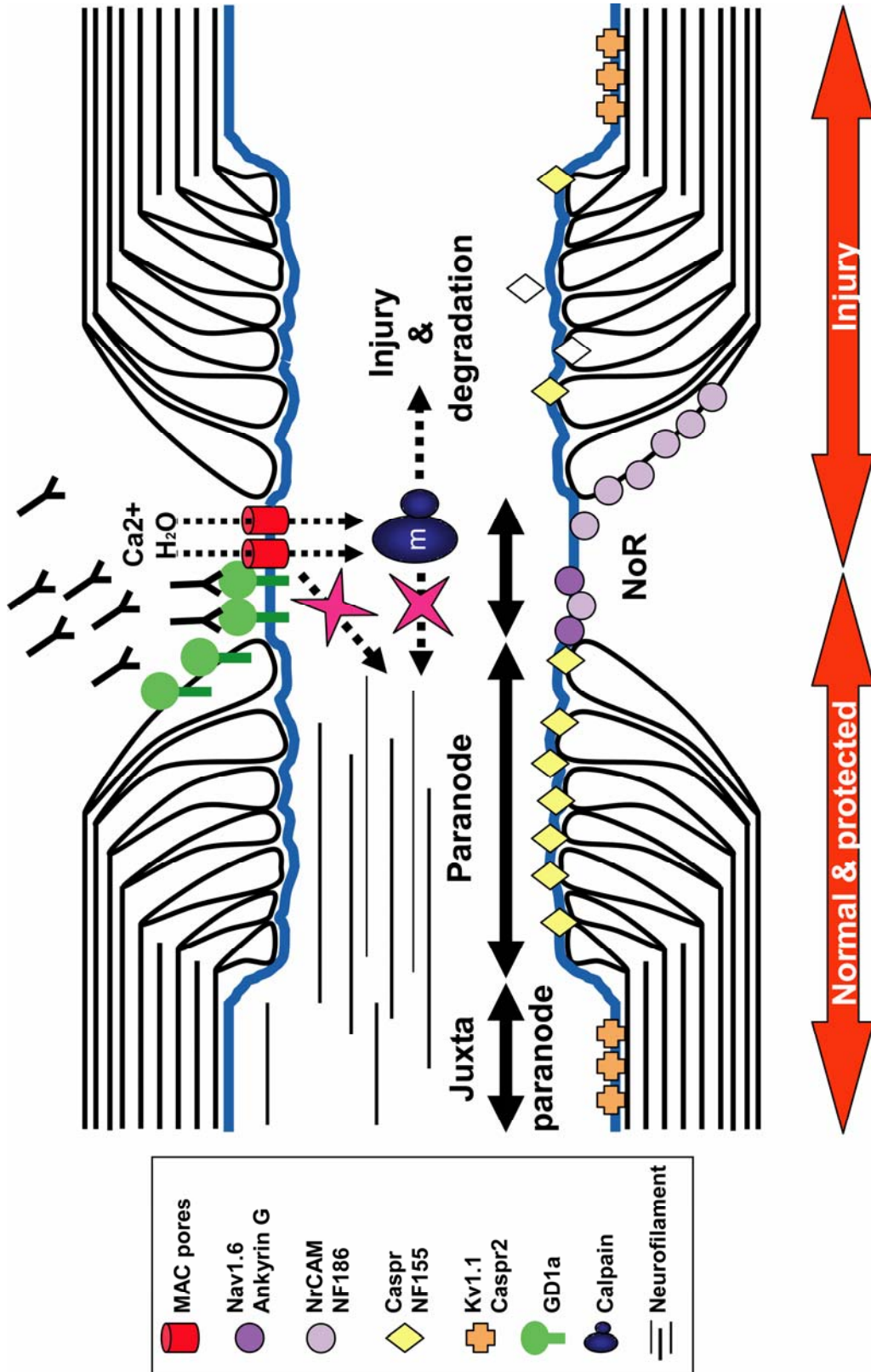


Figure 7.1: Schematic of suggested nodal injury mechanisms in response to anti-GD1a antibody and complement in the mouse nerve. The left hemi-node represents normal and inhibitor protected NoR, while the right hemi-node exemplifies damage. Red crosses through arrows represent prevention of disruption by complement and calpain inhibitors Eculizumab and AK295.

Appendix 1

Perineural Recordings

Introduction

In this study much of the analysis of nodal disruption was performed in intramuscular nerve bundles. Consequently, it was preferable that conduction studies were performed at this region to ascertain what the functional effect of immunostaining loss of many nodal proteins might be. Due to the damage at the nerve terminal and the fine calibre of distal axons, the action potential along these axons cannot be easily measured. Therefore the most appropriate electrophysiological recordings to investigate sodium ion movement at NoR of the distal axons are perineural recordings. These recordings can be used to measure the flow of currents within the perineurium of a nerve bundle as opposed to impaling and recording action potentials from individual axons. Unfortunately, it was not possible to learn this difficult technique in the available time-frame and thus I opted to measure conduction in nerve trunks by way of extracellular recordings, as discussed. However, latterly, it seemed rather important to acquire this information at the distal axons and consequently we enlisted the help of Dr Edward Rowan who performed the following experiments.

The TS muscle was dissected and the nerves isolated for stimulation. After incubation with antibody and complement as per previously described experimental procedures, recordings were made from terminals, small nerve bundles and large bundles. Representative traces for each bundle category from control and treated tissue are depicted in 2A. Quantification of currents were not performed as experimental variability of peak values did not make this feasible.

Results and Discussion

At all sites recorded in control tissue, there was a biphasic trace signifying the flow of a sodium and a potassium ion current. In treated tissue, the initial peak that signifies sodium current was completely ablated in small branches and

appeared of a lesser scale in larger bundles. The second peak that represents potassium ion current at the terminal was absent at all bundle categories. This terminal injury is confirmed by the ablation of MEPPs in treated muscle. The exclusive attenuation of the potassium current and not the sodium current by the terminal specific toxin α -LTx (Mallart & Haimann 1985), illustrates that the loss of the sodium current in this report is not an effect of terminal injury. These results are suggestive that the loss of immunostaining to Nav1.6 channel at distal NoR correlates well with loss of function. It is now imperative to determine whether this function can be protected by AK295 treatment. If this is the case, not only does this suggest AK295 could be of use clinically, but also that there is indeed another mechanism of injury occurring at proximal NoR as suspected.

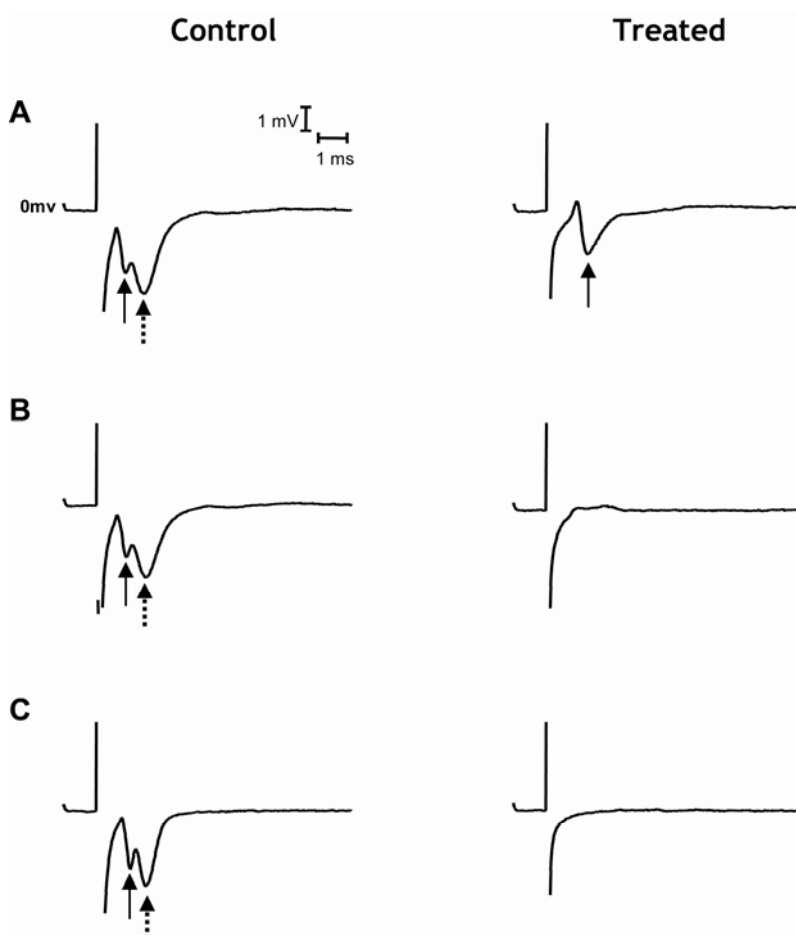


Figure A1: Perineural recordings from mouse intramuscular nerve bundles. Representative traces from large bundles (A), small bundles (B) and nerve terminals (C) are shown for control (left panel) and treated (right panel) intramuscular bundles of the mouse TS muscle. The solid arrow represents the sodium current and the broken arrow the potassium current. Both are present at all bundle categories in control tissue while only the sodium current can be detected in large bundles of treated tissue.

Appendix 2

In vivo mouse model

The established rabbit model of AMAN has been very informative regarding the progress in understanding the pathogenesis of this disease. However, issues with mouse tolerance to antibodies (see section 1.5.2.1) and lack of complement activation (Willison et al., 2008) have interfered with the development of a suitable mouse model. Genetic modifications have helped to overcome some of these issues.

In a previous unpublished study, a mouse lacking the CD59 and DAF complement regulators and over-expressing a-series gangliosides was used to create a successful disease phenotype in response to anti-GD1a antibody. The ability of mouse complement inhibitors to act on human complement is controversial and thus I sought to develop a model in the GD3s^{-/-} mouse alone.

Several injection protocols were piloted but none were successful (an example of some results are shown in Figure 2A). Complement injections were increased from 500µl to 1ml, and the agent hyaluronidase was added to improve dispersion of complement. A plethysmograph is an instrument for detecting changes in the breathing of an animal. As the diaphragm is the site of most obvious damage due to i.p. complement injection, it was hoped that whole-body plethysmography could be carried out to acquire a functional read-out of the damage done to the diaphragm and its effect on respiration. Unfortunately, when large volumes are injected into the peritoneum, this factor alone can have a detrimental effect on breathing. Motor functional tests such as rotarod seemed inappropriate as although antibody deposition can occur at leg muscles, complement is not activated at this location. Therefore it is the inability of the mouse to breathe rather than paralysis of the muscles that would affect performance. In the future I propose the following amendments to the current protocol:

- use of small (4 weeks of age), female mice
- multiple injections of complement over several days
- increased antibody concentration

- rather than performing behavioural tests, measure complement deposition at soleus muscle to ensure no effect on limb muscles

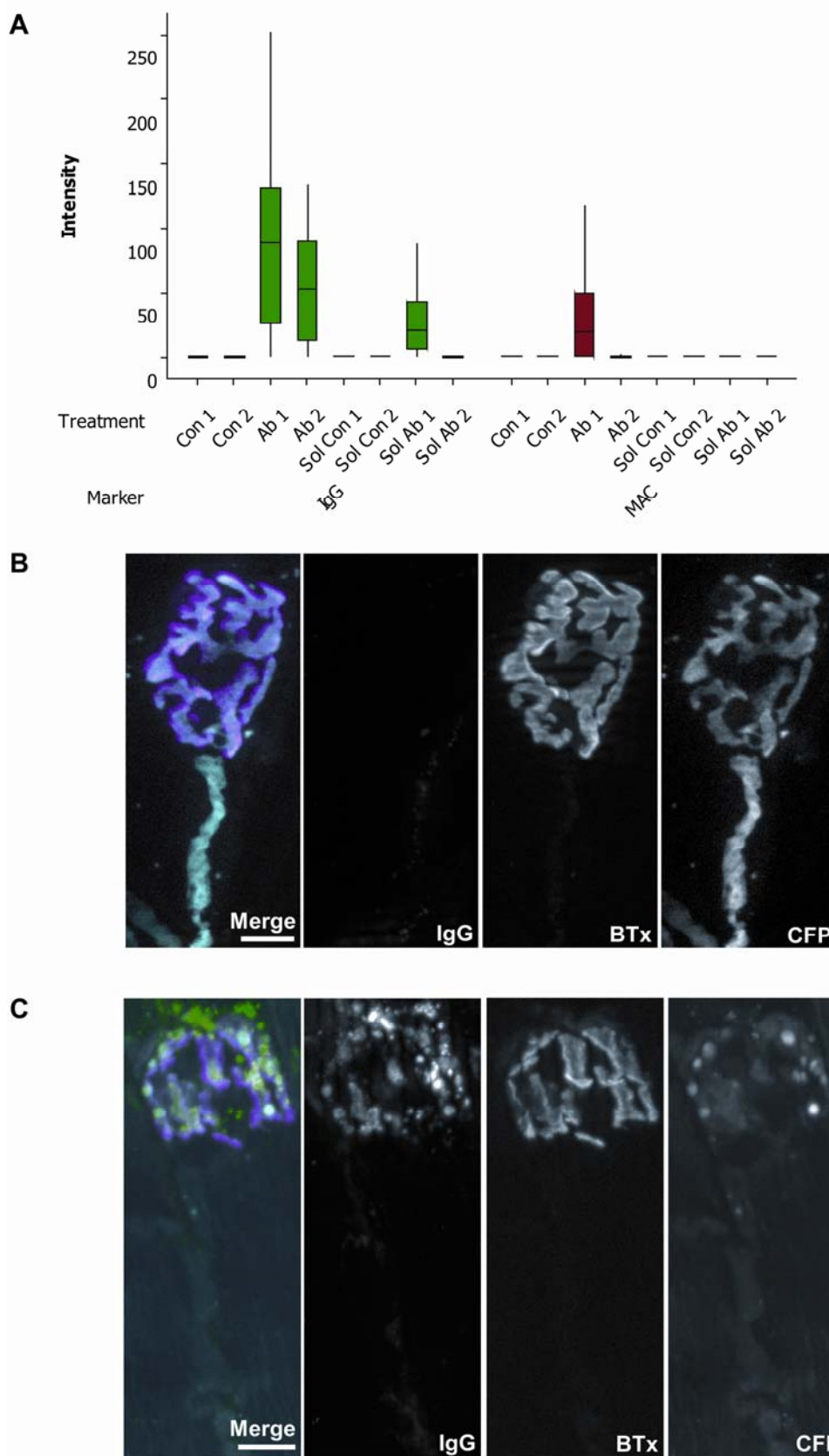


Figure A2 (previous page): *In vivo* IgG and MAC deposition at NMJ. A) Boxplots representing IgG (left) and MAC (right) deposition at NMJ of control and antibody treated mouse diaphragm and soleus muscle. IgG deposition was present at diaphragm of both treated animals (Ab1, Ab2), but only in the soleus of one (Ab1). MAC was present at the diaphragm of Ab1, unfortunately this did not coincide with Nav channel staining loss (data not shown). Examples of IgG and CFP at control (B) and treated (C) distal axons. Scale bar= 20µm.

List of Abstracts

McGonigal R, Halstead S.K., Willison H.W. 2008, "Predisposition of distal nodes of Ranvier to injury in a mouse model of Guillain Barré syndrome", *Folia Histochemica et Cytobiologica*. 46(2): S110

XIII International Congress of Histochemistry and Cytochemistry ICHC2008, Imaging of Cell Dynamics, 23rd-27th August 2008, Medical University of Gdansk, Poland

McGonigal R, Halstead S.K., Willison H.W. 2008, "Predisposition of distal nodes of Ranvier in intramuscular nerve to complement-mediated disruption in a mouse model of Guillain-Barré syndrome".

Young Neuroscientist's Day, 22nd October 2008, Cardiff University, Cardiff, UK.

References

- Ang, C. W., De Klerk, M. A., Endtz, H. P., Jacobs, B. C., Laman, J. D., van der Meche, F. G., & Van Doorn, P. A. 2001, "Guillain-Barre syndrome- and Miller Fisher syndrome-associated *Campylobacter jejuni* lipopolysaccharides induce anti-GM1 and anti-GQ1b Antibodies in rabbits", *Infection & Immunity*.69(4):2462-9.
- Arasaki, K., Kusunoki, S., Kudo, N., & Kanazawa, I. 1993, "Acute conduction block in vitro following exposure to antiganglioside sera", *Muscle & Nerve*.16(6):587-93.
- Arasaki, K., Kusunoki, S., Kudo, N., & Tamaki, M. 1998, "The pattern of antiganglioside antibody reactivities producing myelinated nerve conduction block in vitro", *Journal of the Neurological Sciences*.161(2):163-8.
- Armstrong, C. M., Bezanilla, F., & Rojas, E. 1973, "Destruction of sodium conductance inactivation in squid axons perfused with pronase", *Journal of General Physiology*.62(4):375-91.
- Arroyo, E. J., Xu, Y. T., Zhou, L., Messing, A., Peles, E., Chiu, S. Y., & Scherer, S. S. 1999, "Myelinating Schwann cells determine the internodal localization of Kv1.1, Kv1.2, Kvbeta2, and Caspr", *Journal of Neurocytology*.28(4-5):333-47, p. - May.
- Asbury, A. K. 1969, "The inflammatory lesion in idiopathic polyneuritis. Its role in pathogenesis", *Medicine*.48(3):173-215.
- Asbury, A. K. & Cornblath, D. R. 1990, "Assessment of current diagnostic criteria for Guillain-Barre syndrome.[see comment]. [Review] [13 refs]", *Annals of Neurology*.27 Suppl:S21-4.
- Aspinall, G. O., McDonald, A. G., & Pang, H. 1994, "Lipopolysaccharides of *Campylobacter jejuni* serotype O:19: structures of O antigen chains from the serostrain and two bacterial isolates from patients with the Guillain-Barre syndrome", *Biochemistry*.33(1):250-5.
- Aspinall, G. O., McDonald, A. G., Raju, T. S., Pang, H., Moran, A. P., & Penner, J. L. 1993, "Chemical structures of the core regions of *Campylobacter jejuni* serotypes O:1, O:4, O:23, and O:36 lipopolysaccharides.[erratum appears in Eur J Biochem. 1993 Sep 15;216(3):880; PMID: 8404908]", *European Journal of Biochemistry*.213(3):1017-27.
- Badalamente, M. A., Hurst, L. C., & Stracher, A. 1989, "Neuromuscular recovery using calcium protease inhibition after median nerve repair in primates", *Proceedings of the National Academy of Sciences of the United States of America*.86(15):5983-7.
- Barchi, R. L. 1983, "Protein components of the purified sodium channel from rat skeletal muscle sarcolemma", *Journal of Neurochemistry*.40(5):1377-85.

Bartus, R. T., Hayward, N. J., Elliott, P. J., Sawyer, S. D., Baker, K. L., Dean, R. L., Akiyama, A., Straub, J. A., Harbeson, S. L., & Li, Z. 1994, "Calpain inhibitor AK295 protects neurons from focal brain ischemia. Effects of postocclusion intra-arterial administration", *Stroke*.25(11):2265-70.

Bechtold, D. A., Yue, X., Evans, R. M., Davies, M., Gregson, N. A., & Smith, K. J. 2005, "Axonal protection in experimental autoimmune neuritis by the sodium channel blocking agent flecainide.[see comment]", *Brain*.128(Pt 1):18-28.

Becker, P. S., Schwartz, M. A., Morrow, J. S., & Lux, S. E. 1990, "Radiolabel-transfer cross-linking demonstrates that protein 4.1 binds to the N-terminal region of beta spectrin and to actin in binary interactions", *European Journal of Biochemistry*. no. 3, pp. 827-836.

Beirowski, B., Berek, L., Adalbert, R., Wagner, D., Grumme, D. S., Addicks, K., Ribchester, R. R., & Coleman, M. P. 2004, "Quantitative and qualitative analysis of Wallerian degeneration using restricted axonal labelling in YFP-H mice", *Journal of Neuroscience Methods*.134(1):23-35.

Bellen, H. J., Lu, Y., Beckstead, R., & Bhat, M. A. 1998, "Neurexin IV, caspr and paranodin--novel members of the neurexin family: encounters of axons and glia. [Review] [48 refs]", *Trends in Neurosciences*.21(10):444-9.

Bennett, V. & Baines, A. J. 2001, "Spectrin and ankyrin-based pathways: metazoan inventions for integrating cells into tissues. [Review] [457 refs]", *Physiological Reviews*.81(3):1353-92.

Bennett, V. & Lambert, S. 1999, "Physiological roles of axonal ankyrins in survival of premyelinated axons and localization of voltage-gated sodium channels. [Review] [94 refs]", *Journal of Neurocytology*.28(4-5):303-18, p. -May.

Berghs, S., Aggujaro, D., Dirkx, R., Jr., Maksimova, E., Stabach, P., Hermel, J. M., Zhang, J. P., Philbrick, W., Slepnev, V., Ort, T., & Solimena, M. 2000, "betaIV spectrin, a new spectrin localized at axon initial segments and nodes of ranvier in the central and peripheral nervous system", *Journal of Cell Biology*.151(5):985-1002.

Bergman, C., Dubois, J. M., Rojas, E., & Rathmayer, W. 1976, "Decreased rate of sodium conductance inactivation in the node of Ranvier induced by a polypeptide toxin from sea anemone", *Biochimica et Biophysica Acta*.455(1):173-84.

Bhat, M. A., Rios, J. C., Lu, Y., Garcia-Fresco, G. P., Ching, W., St Martin, M., Li, J., Einheber, S., Chesler, M., Rosenbluth, J., Salzer, J. L., & Bellen, H. J. 2001, "Axon-glia interactions and the domain organization of myelinated axons requires neurexin IV/Caspr/Paranodin", *Neuron*.30(2):369-83.

Boffey, J., Wagner, E. R., Goodyear, C. S., Bowes, T., Conner, J., Odaka, M., & Willison, H. J. 2002, "Analysis of ligand binding characteristics and variable region gene usage of murine antiganglioside antibodies. [Miscellaneous]", *Immunology - Supplement*, vol. 107 Supplement 1, pp. 45-46.

Boiko, T., Rasband, M. N., Levinson, S. R., Caldwell, J. H., Mandel, G., Trimmer, J. S., & Matthews, G. 2001, "Compact myelin dictates the differential targeting of two sodium channel isoforms in the same axon", *Neuron*.30(1):91-104.

Boivin, P., Galand, C., & Dhermy, D. 1990, "In vitro digestion of spectrin, protein 4.1 and ankyrin by erythrocyte calcium dependent neutral protease (calpain I)", *International Journal of Biochemistry*.22(12):1479-89.

Bowes, T., Wagner, E. R., Boffey, J., Nicholl, D., Cochrane, L., Benboubetra, M., Conner, J., Furukawa, K., Furukawa, K., & Willison, H. J. 2002, "Tolerance to self gangliosides is the major factor restricting the antibody response to lipopolysaccharide core oligosaccharides in Campylobacter jejuni strains associated with Guillain-Barre syndrome", *Infection & Immunity*.70(9):5008-18.

Boyle, M. E., Berglund, E. O., Murai, K. K., Weber, L., Peles, E., & Ranscht, B. 2001, "Contactin orchestrates assembly of the septate-like junctions at the paranode in myelinated peripheral nerve", *Neuron*.30(2):385-97.

Bullens, R. W., O'Hanlon, G. M., Goodyear, C. S., Molenaar, P. C., Conner, J., Willison, H. J., & Plomp, J. J. 2000, "Anti-GQ1b antibodies and evoked acetylcholine release at mouse motor endplates", *Muscle & Nerve*.23(7):1035-43.

Burgess, D. L., Kohrman, D. C., Galt, J., Plummer, N. W., Jones, J. M., Spear, B., & Meisler, M. H. 1995, "Mutation of a new sodium channel gene, Scn8a, in the mouse mutant 'motor endplate disease'", *Nature Genetics*.10(4):461-5.

Burkel, W. E. 1967, "The histological fine structure of perineurium", *Anatomical Record*.158(2):177-89.

Cajal, R. Y. 1928, *Degeneration and regeneration of the nervous system*. Oxford University Press, Oxford.

Caldwell, J. H., Schaller, K. L., Lasher, R. S., Peles, E., & Levinson, S. R. 2000, "Sodium channel Na(v)1.6 is localized at nodes of ranvier, dendrites, and synapses", *Proceedings of the National Academy of Sciences of the United States of America*.97(10):5616-20.

Campbell, A. K. & Morgan, B. P. 1985, "Monoclonal antibodies demonstrate protection of polymorphonuclear leukocytes against complement attack", *Nature*.317(6033):164-6, p. -18.

Caporale, C. M., Capasso, M., Luciani, M., Prencipe, V., Creati, B., Gandolfi, P., De Angelis, M. V., Di Muzio, A., Caporale, V., & Uncini, A. 2006, "Experimental axonopathy induced by immunization with Campylobacter jejuni lipopolysaccharide from a patient with Guillain-Barre syndrome", *Journal of Neuroimmunology*.174(1-2):12-20.

Carney, D. F., Hammer, C. H., & Shin, M. L. 1986, "Elimination of terminal complement complexes in the plasma membrane of nucleated cells: influence of extracellular Ca²⁺ and association with cellular Ca²⁺", *Journal of Immunology*.137(1):263-70.

- Castejon, M. S., Culver, D. G., & Glass, J. D. 1999, "Generation of spectrin breakdown products in peripheral nerves by addition of M-calpain", *Muscle & Nerve*.22(7):905-9.
- Catterall, W. A. 2000, "From ionic currents to molecular mechanisms: the structure and function of voltage-gated sodium channels. [Review] [120 refs]", *Neuron*.26(1):13-25.
- Chalfie, M., Tu, Y., Euskirchen, G., Ward, W. W., & Prasher, D. C. 1994, "Green fluorescent protein as a marker for gene expression", *Science*.263(5148):802-5.
- Chan, S. L. & Mattson, M. P. 1999, "Caspase and calpain substrates: roles in synaptic plasticity and cell death. [Review] [339 refs]", *Journal of Neuroscience Research*.58(1):167-90.
- Charles, P., Tait, S., Faivre-Sarrailh, C., Barbin, G., Gunn-Moore, F., Denisenko-Nehrbass, N., Guennoc, A. M., Girault, J. A., Brophy, P. J., & Lubetzki, C. 2002, "Neurofascin is a glial receptor for the paranodin/Caspr-contactin axonal complex at the axoglia junction", *Current Biology*.12(3):217-20.
- Chiavegatto, S., Sun, J., Nelson, R. J., & Schnaar, R. L. 2000, "A functional role for complex gangliosides: motor deficits in GM2/GD2 synthase knockout mice", *Experimental Neurology*.166(2):227-34.
- Chiba, A., Kusunoki, S., Obata, H., Machinami, R., & Kanazawa, I. 1993, "Serum anti-GQ1b IgG antibody is associated with ophthalmoplegia in Miller Fisher syndrome and Guillain-Barre syndrome: clinical and immunohistochemical studies", *Neurology*.43(10):1911-7.
- Chiba, A., Kusunoki, S., Obata, H., Machinami, R., & Kanazawa, I. 1997, "Ganglioside composition of the human cranial nerves, with special reference to pathophysiology of Miller Fisher syndrome", *Brain Research*.745(1-2):32-6.
- Chiba, A., Kusunoki, S., Shimizu, T., & Kanazawa, I. 1992, "Serum IgG antibody to ganglioside GQ1b is a possible marker of Miller Fisher syndrome", *Annals of Neurology*.31(6):677-9.
- Chiu, S. Y. 1980, "Asymmetry currents in the mammalian myelinated nerve", *Journal of Physiology*.309:499-519.
- Chiu, S. Y. & Ritchie, J. M. 1981, "Evidence for the presence of potassium channels in the paranodal region of acutely demyelinated mammalian single nerve fibres", *Journal of Physiology*.313:415-37.
- Chiu, S. Y. & Ritchie, J. M. 1984, "On the physiological role of internodal potassium channels and the security of conduction in myelinated nerve fibres", *Proceedings of the Royal Society of London. Series B, Containing Papers of a Biological Character*.220(1221):415-22.
- Chowdhury, D. & Arora, A. 2001, "Axonal Guillain-Barre syndrome: a critical review. [Review] [95 refs]", *Acta Neurologica Scandinavica*.103(5):267-77.

- Chrast, R., Verheijen, M. H., & Lemke, G. 2004, "Complement factors in adult peripheral nerve: a potential role in energy metabolism. [Review] [27 refs]", *Neurochemistry International*.45(2-3):353-9, p. -Aug.
- Crotty, P., Sangrey, T., & Levy, W. B. 2006, "Metabolic energy cost of action potential velocity", *Journal of Neurophysiology*.96(3):1237-46.
- Cuatrecasas, P. 1973, "Gangliosides and membrane receptors for cholera toxin", *Biochemistry*.12(18):3558-66.
- Cuerrier, D., Moldoveanu, T., & Davies, P. L. 2005, "Determination of peptide substrate specificity for mu-calpain by a peptide library-based approach: the importance of primed side interactions", *Journal of Biological Chemistry*.280(49):40632-41.
- Custer, A. W., Kazarinova-Noyes, K., Sakurai, T., Xu, X., Simon, W., Grumet, M., & Shrager, P. 2003, "The role of the ankyrin-binding protein NrCAM in node of Ranvier formation", *Journal of Neuroscience*.23(31):10032-9.
- Dailey, A. T., Avellino, A. M., Benthem, L., Silver, J., & Klot, M. 1998, "Complement depletion reduces macrophage infiltration and activation during Wallerian degeneration and axonal regeneration", *Journal of Neuroscience*.18(17):6713-22.
- Davies, A., Simmons, D. L., Hale, G., Harrison, R. A., Tighe, H., Lachmann, P. J., & Waldmann, H. 1989, "CD59, an LY-6-like protein expressed in human lymphoid cells, regulates the action of the complement membrane attack complex on homologous cells", *Journal of Experimental Medicine*.170(3):637-54.
- Davis, J. Q. & Bennett, V. 1994, "Ankyrin binding activity shared by the neurofascin/L1/NrCAM family of nervous system cell adhesion molecules", *Journal of Biological Chemistry*.269(44):27163-6.
- Davis, J. Q., Lambert, S., & Bennett, V. 1996, "Molecular composition of the node of Ranvier: identification of ankyrin-binding cell adhesion molecules neurofascin (mucin+/third FNIII domain-) and NrCAM at nodal axon segments", *Journal of Cell Biology*.135(5):1355-67.
- De Angelis, M. V., Di Muzio, A., Lupo, S., Gambi, D., Uncini, A., & Lugaresi, A. 2001, "Anti-GD1a antibodies from an acute motor axonal neuropathy patient selectively bind to motor nerve fiber nodes of Ranvier", *Journal of Neuroimmunology*.121(1-2):79-82.
- Denisenko-Nehrbass, N., Oguievetskaia, K., Goutebroze, L., Galvez, T., Yamakawa, H., Ohara, O., Carnaud, M., & Girault, J. A. 2003, "Protein 4.1B associates with both Caspr/paranodin and Caspr2 at paranodes and juxtaparanodes of myelinated fibres", *European Journal of Neuroscience*.17(2):411-6.
- Devaux, J. J., Kleopa, K. A., Cooper, E. C., & Scherer, S. S. 2004, "KCNQ2 is a nodal K⁺ channel", *Journal of Neuroscience*.24(5):1236-44.

- Dirks, P., Thomas, U., & Montag, D. 2006, "The cytoplasmic domain of NrCAM binds to PDZ domains of synapse-associated proteins SAP90/PSD95 and SAP97", *European Journal of Neuroscience*.24(1):25-31.
- Doctor, R. B., Bennett, V., & Mandel, L. J. 1993, "Degradation of spectrin and ankyrin in the ischemic rat kidney", *American Journal of Physiology*.264(4 Pt 1):C1003-13.
- Duchen, L. W., Gomez, S., & Queiroz, L. S. 1981, "The neuromuscular junction of the mouse after black widow spider venom", *Journal of Physiology*.316:279-91.
- Durand, M. C., Porcher, R., Orlikowski, D., Aboab, J., Devaux, C., Clair, B., Annane, D., Gaillard, J. L., Lofaso, F., Raphael, J. C., & Sharshar, T. 2006, "Clinical and electrophysiological predictors of respiratory failure in Guillain-Barre syndrome: a prospective study.[see comment]", *Lancet Neurology*.5(12):1021-8.
- Dzhashiashvili, Y., Zhang, Y., Galinska, J., Lam, I., Grumet, M., & Salzer, J. L. 2007, "Nodes of Ranvier and axon initial segments are ankyrin G-dependent domains that assemble by distinct mechanisms", *Journal of Cell Biology*.177(5):857-70.
- Eaton, D. C., Brodwick, M. S., Oxford, G. S., & Rudy, B. 1978, "Arginine-specific reagents remove sodium channel inactivation", *Nature*.271(5644):473-6.
- Einheber, S., Zanazzi, G., Ching, W., Scherer, S., Milner, T. A., Peles, E., & Salzer, J. L. 1997, "The axonal membrane protein Caspr, a homologue of neurexin IV, is a component of the septate-like paranodal junctions that assemble during myelination", *Journal of Cell Biology*.139(6):1495-506.
- Ellisman, M. H. 1979, "Molecular specializations of the axon membrane at nodes of Ranvier are not dependent upon myelination", *Journal of Neurocytology*.8(6):719-35.
- England, J. D., Levinson, S. R., & Shrager, P. 1996, "Immunocytochemical investigations of sodium channels along nodal and internodal portions of demyelinated axons. [Review] [51 refs]", *Microscopy Research & Technique*.34(5):445-51.
- Erne, B., Sansano, S., Frank, M., & Schaeren-Wiemers, N. 2002, "Rafts in adult peripheral nerve myelin contain major structural myelin proteins and myelin and lymphocyte protein (MAL) and CD59 as specific markers", *Journal of Neurochemistry*.82(3):550-62.
- Eshed, Y., Feinberg, K., Poliak, S., Sabanay, H., Sarig-Nadir, O., Spiegel, I., Bermingham, J. R., Jr., & Peles, E. 2005, "Gliomedin mediates Schwann cell-axon interaction and the molecular assembly of the nodes of Ranvier", *Neuron*.47(2):215-29.
- Feasby, T. E., Gilbert, J. J., Brown, W. F., Bolton, C. F., Hahn, A. F., Koopman, W. F., & Zochodne, D. W. 1986, "An acute axonal form of Guillain-Barre polyneuropathy", *Brain*.109 (Pt 6):1115-26.

- Feng, G., Mellor, R. H., Bernstein, M., Keller-Peck, C., Nguyen, Q. T., Wallace, M., Nerbonne, J. M., Lichtman, J. W., & Sanes, J. R. 2000, "Imaging neuronal subsets in transgenic mice expressing multiple spectral variants of GFP", *Neuron*.28(1):41-51.
- Fields, R. D. & Stevens-Graham, B. 2002, "New insights into neuron-glia communication. [Review] [95 refs]", *Science*.298(5593):556-62.
- Fisher, C. M. 1956, "An unusual variant of acute idiopathic polyneuritis (syndrome of ophthalmoplegia, ataxia and areflexia)", *New England Journal of Medicine*.255:57-65, vol. 255, pp. 57-65.
- Friede, R. L. & Samorajski, T. 1967, "Relation between the number of myelin lamellae and axon circumference in fibers of vagus and sciatic nerves of mice", *Journal of Comparative Neurology*.130(3):223-31.
- Fruttiger, M., Montag, D., Schachner, M., & Martini, R. 1995, "Crucial role for the myelin-associated glycoprotein in the maintenance of axon-myelin integrity", *European Journal of Neuroscience*.7(3):511-5.
- Fujita, T., Inoue, T., Ogawa, K., Iida, K., & Tamura, N. 1987, "The mechanism of action of decay-accelerating factor (DAF). DAF inhibits the assembly of C3 convertases by dissociating C2a and Bb", *Journal of Experimental Medicine*.166(5):1221-8.
- Ganser, A. L., Kirschner, D. A., & Willinger, M. 1983, "Ganglioside localization on myelinated nerve fibres by cholera toxin binding", *Journal of Neurocytology*.12(6):921-38.
- Garcia, K. D., Sprunger, L. K., Meisler, M. H., & Beam, K. G. 1998, "The sodium channel Scn8a is the major contributor to the postnatal developmental increase of sodium current density in spinal motoneurons", *Journal of Neuroscience*.18(14):5234-9.
- Garver, T. D., Ren, Q., Tuvia, S., & Bennett, V. 1997, "Tyrosine phosphorylation at a site highly conserved in the L1 family of cell adhesion molecules abolishes ankyrin binding and increases lateral mobility of neurofascin", *Journal of Cell Biology*.137(3):703-14.
- Gatzinsky, K. P., Persson, G. H., & Berthold, C. H. 1920, "Removal of retrogradely transported material from rat lumbosacral alpha-motor axons by paranodal axon-Schwann cell networks", *GLIA*. no. 2, pp. 115-126.
- Girault, J. A., Oguievetskaia, K., Carnaud, M., Denisenko-Nehrbass, N., & Goutebroze, L. 2003, "Transmembrane scaffolding proteins in the formation and stability of nodes of Ranvier", *Biology of the Cell*, vol. 95, pp. 447-452.
- Glass, J. D., Culver, D. G., Levey, A. I., & Nash, N. R. 2002, "Very early activation of m-calpain in peripheral nerve during Wallerian degeneration", *Journal of the Neurological Sciences*. no. 1-2, pp. 9-20.
- Goldin, A. L., Barchi, R. L., Caldwell, J. H., Hofmann, F., Howe, J. R., Hunter, J. C., Kallen, R. G., Mandel, G., Meisler, M. H., Netter, Y. B., Noda, M.,

- Tamkun, M. M., Waxman, S. G., Wood, J. N., & Catterall, W. A. 2000, "Nomenclature of voltage-gated sodium channels", *Neuron*.28(2):365-8.
- Goldin, A. L., Snutch, T., Lubbert, H., Dowsett, A., Marshall, J., Auld, V., Downey, W., Fritz, L. C., Lester, H. A., & Dunn, R. 1986, "Messenger RNA coding for only the alpha subunit of the rat brain Na channel is sufficient for expression of functional channels in *Xenopus oocytes*", *Proceedings of the National Academy of Sciences of the United States of America*.83(19):7503-7.
- Goll, D. E., Thompson, V. F., Li, H., Wei, W., & Cong, J. 2003, "The calpain system. [Review] [504 refs]", *Physiological Reviews*.83(3):731-801.
- Gollan, L., Sabanay, H., Poliak, S., Berglund, E. O., Ranscht, B., & Peles, E. 2002, "Retention of a cell adhesion complex at the paranodal junction requires the cytoplasmic region of Caspr", *Journal of Cell Biology*.157(7):1247-56.
- Gong, Y., Tagawa, Y., Lunn, M. P., Laroy, W., Heffer-Laue, M., Li, C. Y., Griffin, J. W., Schnaar, R. L., & Sheikh, K. A. 2002, "Localization of major gangliosides in the PNS: implications for immune neuropathies", *Brain*.125(Pt 11):2491-506.
- Goodenough, D. A., Goliger, J. A., & Paul, D. L. 1996, "Connexins, connexons, and intercellular communication. [Review] [216 refs]", *Annual Review of Biochemistry*.65:475-502.
- Goodfellow, J. A., Bowes, T., Sheikh, K., Odaka, M., Halstead, S. K., Humphreys, P. D., Wagner, E. R., Yuki, N., Furukawa, K., Furukawa, K., Plomp, J. J., & Willison, H. J. 2005, "Overexpression of GD1a ganglioside sensitizes motor nerve terminals to anti-GD1a antibody-mediated injury in a model of acute motor axonal neuropathy", *Journal of Neuroscience*.25(7):1620-8.
- Goodyear, C. S., O'Hanlon, G. M., Plomp, J. J., Wagner, E. R., Morrison, I., Veitch, J., Cochrane, L., Bullens, R. W., Molenaar, P. C., Conner, J., & Willison, H. J. 1999, "Monoclonal antibodies raised against Guillain-Barre syndrome-associated *Campylobacter jejuni* lipopolysaccharides react with neuronal gangliosides and paralyze muscle-nerve preparations.[erratum appears in J Clin Invest 1999 Dec;104(12):1771]", *Journal of Clinical Investigation*.104(6):697-708.
- Greenblatt, R. E., Blatt, Y., & Montal, M. 1986, "The structure of the voltage-sensitive sodium channel. Inferences derived from computer-aided analysis of the *Electrophorus electricus* channel primary structure", *FEBS Letters*. no. 2, pp. 125-134.
- Greenshields, K. N., Halstead, S. K., Zitman, F. M., Rinaldi, S., Brennan, K. M., O'Leary, C., Chamberlain, L. H., Easton, A., Roxburgh, J., Pediani, J., Furukawa, K., Furukawa, K., Goodyear, C. S., Plomp, J. J., & Willison, H. J. 2009, "The neuropathic potential of anti-GM1 autoantibodies is regulated by the local glycolipid environment in mice", *Journal of Clinical Investigation*.119(3):595-610.
- Griffin, J. W., Li, C. Y., Ho, T. W., Tian, M., Gao, C. Y., Xue, P., Mishu, B., Cornblath, D. R., Macko, C., McKhann, G. M., & Asbury, A. K. 1996a, "Pathology of the motor-sensory axonal Guillain-Barre syndrome.[see comment]", *Annals of Neurology*.39(1):17-28.

Griffin, J. W., Li, C. Y., Macko, C., Ho, T. W., Hsieh, S. T., Xue, P., Wang, F. A., Cornblath, D. R., McKhann, G. M., & Asbury, A. K. 1996b, "Early nodal changes in the acute motor axonal neuropathy pattern of the Guillain-Barre syndrome", *Journal of Neurocytology*.25(1):33-51.

Grumet, M. 1997, "Nr-CAM: a cell adhesion molecule with ligand and receptor functions. [Review] [42 refs]", *Cell & Tissue Research*.290(2):423-8.

Grumet, M., Mauro, V., Burgoon, M. P., Edelman, G. M., & Cunningham, B. A. 1991, "Structure of a new nervous system glycoprotein, Nr-CAM, and its relationship to subgroups of neural cell adhesion molecules", *Journal of Cell Biology*.113(6):1399-412.

GUROFF, G. 1964, "A neutral, calcium-activated proteinase from the soluble fraction of rat brain", *Journal of Biological Chemistry*.239:149-55.

Guy, H. R. & Seetharamulu, P. 1986, "Molecular model of the action potential sodium channel", *Proceedings of the National Academy of Sciences of the United States of America*.83(2):508-12.

Gyls, K. H., Fein, J. A., & Cole, G. M. 2002, "Caspase inhibition protects nerve terminals from in vitro degradation", *Neurochemical Research*.27(6):465-72.

Hadden, R. D., Cornblath, D. R., Hughes, R. A., Zielasek, J., Hartung, H. P., Toyka, K. V., & Swan, A. V. 1998, "Electrophysiological classification of Guillain-Barre syndrome: clinical associations and outcome. Plasma Exchange/Sandoglobulin Guillain-Barre Syndrome Trial Group", *Annals of Neurology*.44(5):780-8.

Hafer-Macko, C., Hsieh, S. T., Li, C. Y., Ho, T. W., Sheikh, K., Cornblath, D. R., McKhann, G. M., Asbury, A. K., & Griffin, J. W. 1996, "Acute motor axonal neuropathy: an antibody-mediated attack on axolemma", *Annals of Neurology*.40(4):635-44.

Halstead, S. K., Humphreys, P. D., Goodfellow, J. A., Wagner, E. R., Smith, R. A., & Willison, H. J. 2005, "Complement inhibition abrogates nerve terminal injury in Miller Fisher syndrome", *Annals of Neurology*.58(2):203-10.

Halstead, S. K., Humphreys, P. D., Zitman, F. M., Hamer, J., Plomp, J. J., & Willison, H. J. 2008a, "C5 inhibitor rEV576 protects against neural injury in an in vitro mouse model of Miller Fisher syndrome", *Journal of the Peripheral Nervous System*.13(3):228-35.

Halstead, S. K., O'Hanlon, G. M., Humphreys, P. D., Morrison, D. B., Morgan, B. P., Todd, A. J., Plomp, J. J., & Willison, H. J. 2004, "Anti-disialoside antibodies kill perisynaptic Schwann cells and damage motor nerve terminals via membrane attack complex in a murine model of neuropathy", *Brain*.127(Pt 9):2109-23.

Halstead, S. K., Zitman, F. M., Humphreys, P. D., Greenshields, K., Verschuuren, J. J., Jacobs, B. C., Rother, R. P., Plomp, J. J., & Willison, H. J. 2008b, "Eculizumab prevents anti-ganglioside antibody-mediated neuropathy in a murine model.[see comment]", *Brain*.131(Pt 5):1197-208.

- Harada, K., Fukuda, S., Kunimoto, M., & Yoshida, K. 1997, "Distribution of ankyrin isoforms and their proteolysis after ischemia and reperfusion in rat brain", *Journal of Neurochemistry*.69(1):371-6.
- Hartshorne, R. P. & Catterall, W. A. 1984, "The sodium channel from rat brain. Purification and subunit composition", *Journal of Biological Chemistry*.259(3):1667-75.
- Harvey, G. K., Toyka, K. V., Zielasek, J., Kiefer, R., Simonis, C., & Hartung, H. P. 1995, "Failure of anti-GM1 IgG or IgM to induce conduction block following intraneural transfer", *Muscle & Nerve*.18(4):388-94.
- Heinemann, S. H., Terlau, H., Stuhmer, W., Imoto, K., & Numa, S. 1992, "Calcium channel characteristics conferred on the sodium channel by single mutations", *Nature*.356(6368):441-3.
- Hildebrand, C., Remahl, S., Persson, H., & Bjartmar, C. 1993, "Myelinated nerve fibres in the CNS. [Review] [432 refs]", *Progress in Neurobiology*.40(3):319-84.
- Hillmen, P., Young, N. S., Schubert, J., Brodsky, R. A., Socie, G., Muus, P., Roth, A., Szer, J., Elebute, M. O., Nakamura, R., Browne, P., Risitano, A. M., Hill, A., Schrezenmeier, H., Fu, C. L., Maciejewski, J., Rollins, S. A., Mojciak, C. F., Rother, R. P., & Luzzatto, L. 2006, "The complement inhibitor eculizumab in paroxysmal nocturnal hemoglobinuria.[see comment]", *New England Journal of Medicine*.355(12):1233-43.
- Hirota, N., Kaji, R., Bostock, H., Shindo, K., Kawasaki, T., Mizutani, K., Oka, N., Kohara, N., Saida, T., & Kimura, J. 1997, "The physiological effect of anti-GM1 antibodies on saltatory conduction and transmembrane currents in single motor axons", *Brain*.120 (Pt 12):2159-69.
- Ho, T. W., Hsieh, S. T., Nachamkin, I., Willison, H. J., Sheikh, K., Kiehlbauch, J., Flanigan, K., McArthur, J. C., Cornblath, D. R., McKhann, G. M., & Griffin, J. W. 1997, "Motor nerve terminal degeneration provides a potential mechanism for rapid recovery in acute motor axonal neuropathy after *Campylobacter* infection.[see comment]", *Neurology*.48(3):717-24.
- Ho, T. W., Willison, H. J., Nachamkin, I., Li, C. Y., Veitch, J., Ung, H., Wang, G. R., Liu, R. C., Cornblath, D. R., Asbury, A. K., Griffin, J. W., & McKhann, G. M. 1999, "Anti-GD1a antibody is associated with axonal but not demyelinating forms of Guillain-Barre syndrome", *Annals of Neurology*.45(2):168-73.
- HODGKIN, A. L. & HUXLEY, A. F. 1952, "A quantitative description of membrane current and its application to conduction and excitation in nerve", *Journal of Physiology*.117(4):500-44.
- Horresh, I., Poliak, S., Grant, S., Bredt, D., Rasband, M. N., & Peles, E. 2008, "Multiple molecular interactions determine the clustering of Caspr2 and Kv1 channels in myelinated axons", *Journal of Neuroscience*.28(52):14213-22.
- Hsieh, S. T., Kidd, G. J., Crawford, T. O., Xu, Z., Lin, W. M., Trapp, B. D., Cleveland, D. W., & Griffin, J. W. 1994, "Regional modulation of neurofilament organization by myelination in normal axons", *Journal of Neuroscience*.14(11 Pt 1):6392-401.

- Huang, Y., Qiao, F., Abagyan, R., Hazard, S., & Tomlinson, S. 2006, "Defining the CD59-C9 binding interaction", *Journal of Biological Chemistry*.281(37):27398-404.
- Hughes, R. A. & Cornblath, D. R. 2005, "Guillain-Barre syndrome.[see comment]. [Review] [173 refs]", *Lancet*.366(9497):1653-66.
- HUXLEY, A. F. & Stampfli, R. 1949, "Evidence for saltatory conduction in peripheral myelinated nerve fibres", *Journal of Physiology*.108(3):315-39.
- Illa, I., Ortiz, N., Gallard, E., Juarez, C., Grau, J. M., & Dalakas, M. C. 1995, "Acute axonal Guillain-Barre syndrome with IgG antibodies against motor axons following parenteral gangliosides", *Annals of Neurology*.38(2):218-24.
- Ilyas, A. A., Willison, H. J., Quarles, R. H., Jungalwala, F. B., Cornblath, D. R., Trapp, B. D., Griffin, D. E., Griffin, J. W., & Mckhann, G. M. 1988, "Serum antibodies to gangliosides in Guillain-Barre syndrome", *Annals of Neurology*.23(5):440-7.
- Ishibashi, T., Ding, L., Ikenaka, K., Inoue, Y., Miyado, K., Mekada, E., & Baba, H. 2004, "Tetraspanin protein CD9 is a novel paranodal component regulating paranodal junctional formation", *Journal of Neuroscience*.24(1):96-102.
- Iwata, A., Stys, P. K., Wolf, J. A., Chen, X. H., Taylor, A. G., Meaney, D. F., & Smith, D. H. 2004, "Traumatic axonal injury induces proteolytic cleavage of the voltage-gated sodium channels modulated by tetrodotoxin and protease inhibitors", *Journal of Neuroscience*.24(19):4605-13.
- Jaros, E. & Jenkison, M. 1983, "Quantitative studies of the abnormal axon-Schwann cell relationship in the peripheral motor and sensory nerves of the dystrophic mouse", *Brain Research*.258(2):181-96.
- Jenkins, S. M. & Bennett, V. 2001, "Ankyrin-G coordinates assembly of the spectrin-based membrane skeleton, voltage-gated sodium channels, and L1 CAMs at Purkinje neuron initial segments", *Journal of Cell Biology*.155(5):739-46.
- Joe, E. H. & Angelides, K. 1992, "Clustering of voltage-dependent sodium channels on axons depends on Schwann cell contact", *Nature*.356(6367):333-5.
- Kamakura, K., Ishiura, S., Sugita, H., & Toyokura, Y. 1983, "Identification of Ca²⁺-activated neutral protease in the peripheral nerve and its effects on neurofilament degeneration", *Journal of Neurochemistry*.40(4):908-13.
- Kang, H., Tian, L., & Thompson, W. 2003, "Terminal Schwann cells guide the reinnervation of muscle after nerve injury. [Review] [60 refs]", *Journal of Neurocytology*.32(5-8):975-85, p. -Sep.
- Kaplan, M. R., Cho, M. H., Ullian, E. M., Isom, L. L., Levinson, S. R., & Barres, B. A. 2001, "Differential control of clustering of the sodium channels Na(v)1.2 and Na(v)1.6 at developing CNS nodes of Ranvier", *Neuron*.30(1):105-19.
- Kaplan, M. R., Meyer-Franke, A., Lambert, S., Bennett, V., Duncan, I. D., Levinson, S. R., & Barres, B. A. 1997, "Induction of sodium channel clustering by oligodendrocytes", *Nature*.386(6626):724-8.

- Kapoor, R., Davies, M., Blaker, P. A., Hall, S. M., & Smith, K. J. 2003, "Blockers of sodium and calcium entry protect axons from nitric oxide-mediated degeneration. [see comment]", *Annals of Neurology*.53(2):174-80.
- Kawai, H., Allende, M. L., Wada, R., Kono, M., Sango, K., Deng, C., Miyakawa, T., Crawley, J. N., Werth, N., Bierfreund, U., Sandhoff, K., & Proia, R. L. 2001, "Mice expressing only monosialoganglioside GM3 exhibit lethal audiogenic seizures", *Journal of Biological Chemistry*.276(10):6885-8.
- Kawashima, I., Nakamura, O., & Tai, T. 1992, "Antibody responses to ganglio-series gangliosides in different strains of inbred mice", *Molecular Immunology*.29(5):625-32.
- Kayyem, J. F., Roman, J. M., de la Rosa, E. J., Schwarz, U., & Dreyer, W. J. 1992, "Bravo/Nr-CAM is closely related to the cell adhesion molecules L1 and Ng-CAM and has a similar heterodimer structure", *Journal of Cell Biology*.118(5):1259-70.
- Kazarinova-Noyes, K., Malhotra, J. D., McEwen, D. P., Mattei, L. N., Berglund, E. O., Ranscht, B., Levinson, S. R., Schachner, M., Shrager, P., Isom, L. L., & Xiao, Z. C. 2001, "Contactin associates with Na⁺ channels and increases their functional expression", *Journal of Neuroscience*.21(19):7517-25.
- Khodorov, B. I. & Timin, E. N. 1975, "Nerve impulse propagation along nonuniform fibres. [Review] [93 refs]", *Progress in Biophysics & Molecular Biology*.30(2-3):145-84.
- Kim, E., Niethammer, M., Rothschild, A., Jan, Y. N., & Sheng, M. 1995, "Clustering of Shaker-type K⁺ channels by interaction with a family of membrane-associated guanylate kinases", *Nature*.378(6552):85-8.
- Kolter, T., Proia, R. L., & Sandhoff, K. 2002, "Combinatorial ganglioside biosynthesis. [Review] [73 refs]", *Journal of Biological Chemistry*.277(29):25859-62.
- Komada, M. & Soriano, P. 2002, "[Beta]IV-spectrin regulates sodium channel clustering through ankyrin-G at axon initial segments and nodes of Ranvier", *Journal of Cell Biology*.156(2):337-48.
- Kordeli, E. & Bennett, V. 1991, "Distinct ankyrin isoforms at neuron cell bodies and nodes of Ranvier resolved using erythrocyte ankyrin-deficient mice", *Journal of Cell Biology*.114(6):1243-59.
- Kordeli, E., Davis, J., Trapp, B., & Bennett, V. 1990, "An isoform of ankyrin is localized at nodes of Ranvier in myelinated axons of central and peripheral nerves", *Journal of Cell Biology*.110(4):1341-52.
- Kordeli, E., Lambert, S., & Bennett, V. 1995, "AnkyrinG. A new ankyrin gene with neural-specific isoforms localized at the axonal initial segment and node of Ranvier", *Journal of Biological Chemistry*.270(5):2352-9.
- Koski, C. L. 1990, "Characterization of complement-fixing antibodies to peripheral nerve myelin in Guillain-Barre syndrome. [Review] [15 refs]", *Annals of Neurology*.27 Suppl:S44-7.

- Koski, C. L., Ramm, L. E., Hammer, C. H., Mayer, M. M., & Shin, M. L. 1983, "Cytolysis of nucleated cells by complement: cell death displays multi-hit characteristics", *Proceedings of the National Academy of Sciences of the United States of America*.80(12):3816-20.
- Koszowski, A. G., Owens, G. C., & Levinson, S. R. 1998, "The effect of the mouse mutation claw paw on myelination and nodal frequency in sciatic nerves", *Journal of Neuroscience*.18(15):5859-68.
- Kotani, M., Ozawa, H., Kawashima, I., Ando, S., & Tai, T. 1992, "Generation of one set of monoclonal antibodies specific for a-pathway ganglio-series gangliosides", *Biochimica et Biophysica Acta*.1117(1):97-103.
- Kuwabara, S., Ogawara, K., Sung, J. Y., Mori, M., Kanai, K., Hattori, T., Yuki, N., Lin, C. S., Burke, D., & Bostock, H. 2002, "Differences in membrane properties of axonal and demyelinating Guillain-Barre syndromes", *Annals of Neurology*.52(2):180-7.
- Kuwabara, S., Yuki, N., Koga, M., Hattori, T., Matsuura, D., Miyake, M., & Noda, M. 1998, "IgG anti-GM1 antibody is associated with reversible conduction failure and axonal degeneration in Guillain-Barre syndrome", *Annals of Neurology*.44(2):202-8.
- Lai, H. C. & Jan, L. Y. 2006, "The distribution and targeting of neuronal voltage-gated ion channels. [Review] [207 refs]", *Nature Reviews Neuroscience*.7(7):548-62.
- Lambert, S., Davis, J. Q., & Bennett, V. 1997, "Morphogenesis of the node of Ranvier: co-clusters of ankyrin and ankyrin-binding integral proteins define early developmental intermediates", *Journal of Neuroscience*.17(18):7025-36.
- Lambert, S., Yu, H., Prchal, J. T., Lawler, J., Ruff, P., Speicher, D., Cheung, M. C., Kan, Y. W., & Palek, J. 1990, "cDNA sequence for human erythrocyte ankyrin", *Proceedings of the National Academy of Sciences of the United States of America*.87(5):1730-4.
- Landon, D. N. & Langley, O. K. 1971, "The local chemical environment of nodes of Ranvier: a study of cation binding", *Journal of Anatomy*.108(Pt 3):419-32.
- Ledeen, R. W. 1978, "Ganglioside structures and distribution: are they localized at the nerve ending?. [Review] [137 refs]", *Journal of Supramolecular Structure*.8(1):1-17.
- Lemaitre, G., Walker, B., & Lambert, S. 2003, "Identification of a conserved ankyrin-binding motif in the family of sodium channel alpha subunits", *Journal of Biological Chemistry*.278(30):27333-9.
- Leuchtag, H. R. 1994, "Long-range interactions, voltage sensitivity, and ion conduction in S4 segments of excitable channels", *Biophysical Journal*.66(1):217-24.
- Li, X., Lynn, B. D., Olson, C., Meier, C., Davidson, K. G., Yasumura, T., Rash, J. E., & Nagy, J. I. 2002, "Connexin29 expression, immunocytochemistry and

freeze-fracture replica immunogold labelling (FRIL) in sciatic nerve", *European Journal of Neuroscience*. 16(5):795-806.

Li, Z., Ortega-Vilain, A. C., Patil, G. S., Chu, D. L., Foreman, J. E., Eveleth, D. D., & Powers, J. C. 1996, "Novel peptidyl alpha-keto amide inhibitors of calpains and other cysteine proteases", *Journal of Medicinal Chemistry*. 39(20):4089-98.

Lippincott-Schwartz, J. & Patterson, G. H. 2003, "Development and use of fluorescent protein markers in living cells. [Review] [59 refs]", *Science*. 300(5616):87-91.

Liszewski, M. K., Post, T. W., & Atkinson, J. P. 1991, "Membrane cofactor protein (MCP or CD46): newest member of the regulators of complement activation gene cluster. [Review] [57 refs]", *Annual Review of Immunology*. 9:431-55.

Liu, Y., Wada, R., Kawai, H., Sango, K., Deng, C., Tai, T., McDonald, M. P., Araujo, K., Crawley, J. N., Bierfreund, U., Sandhoff, K., Suzuki, K., & Proia, R. L. 1999, "A genetic model of substrate deprivation therapy for a glycosphingolipid storage disorder.[see comment]", *Journal of Clinical Investigation*. 103(4):497-505.

Lonigro, A. & Devaux, J. J. 2009, "Disruption of neurofascin and gliomedin at nodes of Ranvier precedes demyelination in experimental allergic neuritis", *Brain*. 132(Pt 1):260-73.

Lopez, P. H., Zhang, G., Bianchet, M. A., Schnaar, R. L., & Sheikh, K. A. 2008, "Structural requirements of anti-GD1a antibodies determine their target specificity", *Brain*. 131(Pt 7):1926-39.

Lu, J. L., Sheikh, K. A., Wu, H. S., Zhang, J., Jiang, Z. F., Cornblath, D. R., McKhann, G. M., Asbury, A. K., Griffin, J. W., & Ho, T. W. 2000, "Physiologic-pathologic correlation in Guillain-Barre syndrome in children.[see comment]", *Neurology*. 54(1):33-9.

Lu, X., Rong, Y., & Baudry, M. 2000, "Calpain-mediated degradation of PSD-95 in developing and adult rat brain", *Neuroscience Letters*. 286(2):149-53.

Lugaresi, A., Ragno, M., Torrieri, F., Di Guglielmo, G., Fermani, P., & Uncini, A. 1997, "Acute motor axonal neuropathy with high titer IgG and IgA anti-GD1a antibodies following Campylobacter enteritis", *Journal of the Neurological Sciences*. 147(2):193-200.

Lunn, M. P., Johnson, L. A., Fromholt, S. E., Itonori, S., Huang, J., Vyas, A. A., Hildreth, J. E., Griffin, J. W., Schnaar, R. L., & Sheikh, K. A. 2000, "High-affinity anti-ganglioside IgG antibodies raised in complex ganglioside knockout mice: reexamination of GD1a immunolocalization", *Journal of Neurochemistry*. 75(1):404-12.

Lux, S. E., John, K. M., & Bennett, V. 1990, "Analysis of cDNA for human erythrocyte ankyrin indicates a repeated structure with homology to tissue-differentiation and cell-cycle control proteins", *Nature*. 344(6261):36-42.

- Malhotra, J. D., Kazen-Gillespie, K., Hortsch, M., & Isom, L. L. 2000, "Sodium channel beta subunits mediate homophilic cell adhesion and recruit ankyrin to points of cell-cell contact", *Journal of Biological Chemistry*.275(15):11383-8.
- Mallart, A. & Haimann, C. 1985, "Differential effects of alpha-latrotoxin on mouse nerve endings and fibers", *Muscle & Nerve*.8(2):151-7.
- Malmgren, L. T. & Olsson, Y. 1980, "Differences between the peripheral and the central nervous system in permeability to sodium fluorescein", *Journal of Comparative Neurology*. no. 1, pp. 103-107.
- McCardle, J. J., Angaut-Petit, D., Mallart, A., Bournaud, R., Faille, L., & Brigant, J. L. 1981, "Advantages of the triangularis sterni muscle of the mouse for investigations of synaptic phenomena", *Journal of Neuroscience Methods*, vol. 4, pp. 109-115.
- McKhann, G. M., Cornblath, D. R., Griffin, J. W., Ho, T. W., Li, C. Y., Jiang, Z., Wu, H. S., Zhaori, G., Liu, Y., & Jou, L. P. 1993, "Acute motor axonal neuropathy: a frequent cause of acute flaccid paralysis in China", *Annals of Neurology*.33(4):333-42.
- McPhee, J. C., Ragsdale, D. S., Scheuer, T., & Catterall, W. A. 1998, "A critical role for the S4-S5 intracellular loop in domain IV of the sodium channel alpha-subunit in fast inactivation", *Journal of Biological Chemistry*.273(2):1121-9.
- Meadows, L., Malhotra, J. D., Stetzer, A., Isom, L. L., & Ragsdale, D. S. 2001, "The intracellular segment of the sodium channel beta 1 subunit is required for its efficient association with the channel alpha subunit", *Journal of Neurochemistry*.76(6):1871-8.
- Melendez-Vasquez, C. V., Rios, J. C., Zanazzi, G., Lambert, S., Bretscher, A., & Salzer, J. L. 2001, "Nodes of Ranvier form in association with ezrin-radixin-moesin (ERM)-positive Schwann cell processes", *Proceedings of the National Academy of Sciences of the United States of America*.98(3):1235-40.
- Menegoz, M., Gaspar, P., Le Bert, M., Galvez, T., Burgaya, F., Palfrey, C., Ezan, P., Arnos, F., & Girault, J. A. 1997, "Paranodin, a glycoprotein of neuronal paranodal membranes", *Neuron*. no. 2, pp. 319-331.
- Meri, S., Morgan, B. P., Davies, A., Daniels, R. H., Olavesen, M. G., Waldmann, H., & Lachmann, P. J. 1990a, "Human protectin (CD59), an 18,000-20,000 MW complement lysis restricting factor, inhibits C5b-8 catalysed insertion of C9 into lipid bilayers", *Immunology*.71(1):1-9.
- Meri, S., Morgan, B. P., Wing, M., Jones, J., Davies, A., Podack, E., & Lachmann, P. J. 1990b, "Human protectin (CD59), an 18-20-kD homologous complement restriction factor, does not restrict perforin-mediated lysis", *Journal of Experimental Medicine*.172(1):367-70.
- Meri, S., Waldmann, H., & Lachmann, P. J. 1991, "Distribution of protectin (CD59), a complement membrane attack inhibitor, in normal human tissues", *Laboratory Investigation*.65(5):532-7.

- Mi, H., Deerinck, T. J., Ellisman, M. H., & Schwarz, T. L. 1995, "Differential distribution of closely related potassium channels in rat Schwann cells", *Journal of Neuroscience*. 15(5 Pt 2):3761-74.
- Michaely, P. & Bennett, V. 1995, "Mechanism for binding site diversity on ankyrin. Comparison of binding sites on ankyrin for neurofascin and the Cl⁻/HCO₃⁻ anion exchanger", *Journal of Biological Chemistry*. 270(52):31298-302.
- Miller, J. R., Patel, M. K., John, J. E., Mounsey, J. P., & Moorman, J. R. 2000, "Contributions of charged residues in a cytoplasmic linking region to Na channel gating", *Biochimica et Biophysica Acta*. 1509(1-2):275-91.
- Miller-Podraza, H., Bradley, R. M., & Fishman, P. H. 1982, "Biosynthesis and localization of gangliosides in cultured cells", *Biochemistry*. 21(14):3260-5.
- Moran, A. P., Annuk, H., & Prendergast, M. M. 2005, "Antibodies induced by ganglioside-mimicking *Campylobacter jejuni* lipooligosaccharides recognise epitopes at the nodes of Ranvier", *Journal of Neuroimmunology*. 165(1-2):179-85.
- Morgan, B. P. 1989, "Complement membrane attack on nucleated cells: resistance, recovery and non-lethal effects. [Review] [163 refs]", *Biochemical Journal*. 264(1):1-14.
- Morgan, B. P. 1999, "Regulation of the complement membrane attack pathway. [Review] [202 refs]", *Critical Reviews in Immunology*. no. 3, pp. 173-198.
- Morgan, B. P. 2000, "The complement system: an overview. [Review] [46 refs]", *Methods in Molecular Biology*. 150:1-13.
- Morgan, B. P. & Harris, C. L. 2003, "Complement therapeutics; history and current progress. [Review] [146 refs]", *Molecular Immunology*. 40(2-4):159-70.
- Morgan, B. P., Luzio, J. P., & Campbell, A. K. 1986, "Intracellular Ca²⁺ and cell injury: a paradoxical role of Ca²⁺ in complement membrane attack. [Review] [51 refs]", *Cell Calcium*. 7(5-6):399-411.
- Murachi, T. 1989, "Intracellular regulatory system involving calpain and calpastatin. [Review] [66 refs]", *Biochemistry International*. 18(2):263-94.
- Nakamura, Y., Nakajima, S., & Grundfest, H. 1965, "The action of tetrodotoxin on electrogenic components of squid giant axons", *Journal of General Physiology*. 48(6):975-96.
- Narahashi, T., Anderson, N. C., & Moore, J. W. 1966, "Tetrodotoxin does not block excitation from inside the nerve membrane", *Science*. 153(737):765-7.
- Neuen, E., Seitz, R. J., Langenbach, M., & Wechsler, W. 1987, "The leakage of serum proteins across the blood-nerve barrier in hereditary and inflammatory neuropathies. An immunohistochemical and morphometric study", *Acta Neuropathologica*. 73(1):53-61.
- Ninomiya, H. & Sims, P. J. 1992, "The human complement regulatory protein CD59 binds to the alpha-chain of C8 and to the "b" domain of C9", *Journal of Biological Chemistry*. 267(19):13675-80.

- Nishimoto, Y., Koga, M., Kamijo, M., Hirata, K., & Yuki, N. 2004, "Immunoglobulin improves a model of acute motor axonal neuropathy by preventing axonal degeneration", *Neurology*.62(11):1939-44.
- Noda, M., Ikeda, T., Suzuki, H., Takeshima, H., Takahashi, T., Kuno, M., & Numa, S. 1986, "Expression of functional sodium channels from cloned cDNA", *Nature*.322(6082):826-8, p. -Sep.
- Noda, M., Shimizu, S., Tanabe, T., Takai, T., Kayano, T., Ikeda, T., Takahashi, H., Nakayama, H., Kanaoka, Y., & Minamino, N. 1984a, "Primary structure of Electrophorus electricus sodium channel deduced from cDNA sequence", *Nature*.312(5990):121-7, p. -14.
- Noda, M., Shimizu, S., Tanabe, T., Takai, T., Kayano, T., Ikeda, T., Takahashi, H., Nakayama, H., Kanaoka, Y., & Minamino, N. 1984b, "Primary structure of Electrophorus electricus sodium channel deduced from cDNA sequence", *Nature*.312(5990):121-7, p. -14.
- Noda, M., Suzuki, H., Numa, S., & Stuhmer, W. 1989, "A single point mutation confers tetrodotoxin and saxitoxin insensitivity on the sodium channel II", *FEBS Letters*.259(1):213-6.
- O'Hanlon, G. M., Humphreys, P. D., Goldman, R. S., Halstead, S. K., Bullens, R. W., Plomp, J. J., Ushkaryov, Y., & Willison, H. J. 2003, "Calpain inhibitors protect against axonal degeneration in a model of anti-ganglioside antibody-mediated motor nerve terminal injury", *Brain*, vol. 126, no. Pt 11, pp. 2497-2509.
- O'Hanlon, G. M., Paterson, G. J., Wilson, G., Doyle, D., McHardie, P., & Willison, H. J. 1996, "Anti-GM1 ganglioside antibodies cloned from autoimmune neuropathy patients show diverse binding patterns in the rodent nervous system", *Journal of Neuropathology & Experimental Neurology*.55(2):184-95.
- O'Hanlon, G. M., Plomp, J. J., Chakrabarti, M., Morrison, I., Wagner, E. R., Goodyear, C. S., Yin, X., Trapp, B. D., Conner, J., Molenaar, P. C., Stewart, S., Rowan, E. G., & Willison, H. J. 2001, "Anti-GQ1b ganglioside antibodies mediate complement-dependent destruction of the motor nerve terminal", *Brain*.124(Pt 5):893-906.
- Ogawa, Y., Schafer, D. P., Horresh, I., Bar, V., Hales, K., Yang, Y., Susuki, K., Peles, E., Stankewich, M. C., & Rasband, M. N. 2006, "Spectrins and ankyrinB constitute a specialized paranodal cytoskeleton", *Journal of Neuroscience*.26(19):5230-9.
- Ogawa-Goto, K., Funamoto, N., Abe, T., & Nagashima, K. 1990, "Different ceramide compositions of gangliosides between human motor and sensory nerves", *Journal of Neurochemistry*.55(5):1486-93.
- Ogawa-Goto, K., Funamoto, N., Ohta, Y., Abe, T., & Nagashima, K. 1992, "Myelin gangliosides of human peripheral nervous system: an enrichment of GM1 in the motor nerve myelin isolated from cauda equina", *Journal of Neurochemistry*.59(5):1844-9.

- Okada, M., Itoh, M. M., Haraguchi, M., Okajima, T., Inoue, M., Oishi, H., Matsuda, Y., Iwamoto, T., Kawano, T., Fukumoto, S., Miyazaki, H., Furukawa, K., Aizawa, S., & Furukawa, K. 2002, "b-series Ganglioside deficiency exhibits no definite changes in the neurogenesis and the sensitivity to Fas-mediated apoptosis but impairs regeneration of the lesioned hypoglossal nerve", *Journal of Biological Chemistry*.277(3):1633-6.
- Oldfors, A. 1981, "Permeability of the perineurium of small nerve fascicles: an ultrastructural study using ferritin in rats", *Neuropathology & Applied Neurobiology*.7(3):183-94, p. -Jun.
- Olsson, Y. 1990, "Microenvironment of the peripheral nervous system under normal and pathological conditions. [Review] [326 refs]", *Critical Reviews in Neurobiology*.5(3):265-311.
- Olsson, Y. & Reese, T. S. 1971, "Permeability of vasa nervorum and perineurium in mouse sciatic nerve studied by fluorescence and electron microscopy", *Journal of Neuropathology & Experimental Neurology*.30(1):105-19.
- Ortiz, N., Sabate, M. M., Garcia, N., Santafe, M. M., Lanuza, M. A., Tomas, M., & Tomas, J. 2009, "Effect of anti-GM2 antibodies on rat sciatic nerve: electrophysiological and morphological study", *Journal of Neuroimmunology*. no. 1-2, pp. 61-69.
- Otto, E., Kunimoto, M., McLaughlin, T., & Bennett, V. 1991, "Isolation and characterization of cDNAs encoding human brain ankyrins reveal a family of alternatively spliced genes", *Journal of Cell Biology*.114(2):241-53.
- Oxford, G. S., Wu, C. H., & Narahashi, T. 1978, "Removal of sodium channel inactivation in squid giant axons by n-bromoacetamide", *Journal of General Physiology*.71(3):227-47.
- Pan, B., Fromholt, S. E., Hess, E. J., Crawford, T. O., Griffin, J. W., Sheikh, K. A., & Schnaar, R. L. 1995, "Myelin-associated glycoprotein and complementary axonal ligands, gangliosides, mediate axon stability in the CNS and PNS: neuropathology and behavioral deficits in single- and double-null mice", *Experimental Neurology*. no. 1, pp. 208-217.
- Paparounas, K., O'Hanlon, G. M., O'Leary, C. P., Rowan, E. G., & Willison, H. J. 1999, "Anti-ganglioside antibodies can bind peripheral nerve nodes of Ranvier and activate the complement cascade without inducing acute conduction block in vitro.[see comment]", *Brain*.122 (Pt 5):807-16.
- Pedraza, L., Huang, J. K., & Colman, D. R. 2001, "Organizing principles of the axoglial apparatus. [Review] [49 refs]", *Neuron*.30(2):335-44.
- Peles, E., Nativ, M., Lustig, M., Grumet, M., Schilling, J., Martinez, R., Plowman, G. D., & Schlessinger, J. 1997, "Identification of a novel contactin-associated transmembrane receptor with multiple domains implicated in protein-protein interactions", *EMBO Journal*.16(5):978-88.
- Peters, A., Palay, S. L., & Webster, H. 1991, *The fine structure of the nervous system: neurons and their supporting cells*, 3rd edn, Oxford University Press.

Phongsisay, V., Susuki, K., Matsuno, K., Yamahashi, T., Okamoto, S., Funakoshi, K., Hirata, K., Shinoda, M., & Yuki, N. 2008, "Complement inhibitor prevents disruption of sodium channel clusters in a rabbit model of Guillain-Barre syndrome", *Journal of Neuroimmunology*. no. 1-2, pp. 101-104.

Poliak, S., Gollan, L., Martinez, R., Custer, A., Einheber, S., Salzer, J. L., Trimmer, J. S., Shrager, P., & Peles, E. 1999, "Caspr2, a new member of the neurexin superfamily, is localized at the juxtaparanodes of myelinated axons and associates with K⁺ channels", *Neuron*.24(4):1037-47.

Poliak, S. & Peles, E. 2003, "The local differentiation of myelinated axons at nodes of Ranvier. [Review] [176 refs]", *Nature Reviews Neuroscience*.4(12):968-80.

Poliak, S., Salomon, D., Elhanany, H., Sabanay, H., Kiernan, B., Pevny, L., Stewart, C. L., Xu, X., Chiu, S. Y., Shrager, P., Furley, A. J., & Peles, E. 2003, "Juxtaparanodal clustering of Shaker-like K⁺ channels in myelinated axons depends on Caspr2 and TAG-1", *Journal of Cell Biology*.162(6):1149-60.

Porter, J. D., Goldstein, L. A., Kasarskis, E. J., Brueckner, J. K., & Spear, B. T. 1996, "The neuronal voltage-gated sodium channel, Scn8a, is essential for postnatal maturation of spinal, but not oculomotor, motor units", *Experimental Neurology*.139(2):328-34.

Prasher, D. C., Eckenrode, V. K., Ward, W. W., Prendergast, F. G., & Cormier, M. J. 1992, "Primary structure of the *Aequorea victoria* green-fluorescent protein", *Gene*.111(2):229-33.

Pusch, M., Noda, M., Stuhmer, W., Numa, S., & Conti, F. 1991, "Single point mutations of the sodium channel drastically reduce the pore permeability without preventing its gating", *European Biophysics Journal*. no. 3, pp. 127-133.

Putzu, G. A., Figarella-Branger, D., Bouvier-Labit, C., Liprandi, A., Bianco, N., & Pellissier, J. F. 2000, "Immunohistochemical localization of cytokines, C5b-9 and ICAM-1 in peripheral nerve of Guillain-Barre syndrome", *Journal of the Neurological Sciences*.174(1):16-21.

Quick, D. C., Kennedy, W. R., & Donaldson, L. 1979, "Dimensions of myelinated nerve fibers near the motor and sensory terminals in cat tenuissimus muscles", *Neuroscience*.4(8):1089-96.

Rasband, M. N., Park, E. W., Zhen, D., Arbuckle, M. I., Poliak, S., Peles, E., Grant, S. G., & Trimmer, J. S. 2002, "Clustering of neuronal potassium channels is independent of their interaction with PSD-95", *Journal of Cell Biology*.159(4):663-72.

Rasband, M. N., Peles, E., Trimmer, J. S., Levinson, S. R., Lux, S. E., & Shrager, P. 1999, "Dependence of nodal sodium channel clustering on paranodal axoglial contact in the developing CNS", *Journal of Neuroscience*. no. 17, pp. 7516-7528.

Ratcliffe, C. F., Westenbroek, R. E., Curtis, R., & Catterall, W. A. 2001, "Sodium channel beta1 and beta3 subunits associate with neurofascin through their extracellular immunoglobulin-like domain", *Journal of Cell Biology*.154(2):427-34.

- Reles, A. & Friede, R. L. 1991, "Axonal cytoskeleton at the nodes of Ranvier", *Journal of Neurocytology*. no. 6, pp. 450-458.
- Rhodes, K. J., Strassle, B. W., Monaghan, M. M., Bekele-Arcuri, Z., Matos, M. F., & Trimmer, J. S. 1997, "Association and colocalization of the Kvbeta1 and Kvbeta2 beta-subunits with Kv1 alpha-subunits in mammalian brain K⁺ channel complexes", *Journal of Neuroscience*. 17(21):8246-58.
- Rhodes, K. M. & Tattersfield, A. E. 1982, "Guillain-Barre syndrome associated with Campylobacter infection", *British Medical Journal Clinical Research Ed.* 285(6336):173-4.
- Rios, J. C., Melendez-Vasquez, C. V., Einheber, S., Lustig, M., Grumet, M., Hemperly, J., Peles, E., & Salzer, J. L. 2000, "Contactin-associated protein (Caspr) and contactin form a complex that is targeted to the paranodal junctions during myelination", *Journal of Neuroscience*. no. 22, pp. 8354-8364.
- Rios, J. C., Rubin, M., St Martin, M., Downey, R. T., Einheber, S., Rosenbluth, J., Levinson, S. R., Bhat, M., & Salzer, J. L. 2003, "Paranodal interactions regulate expression of sodium channel subtypes and provide a diffusion barrier for the node of Ranvier", *Journal of Neuroscience*. 23(18):7001-11.
- Ritchie, J. M. & Rogart, R. B. 1977, "Density of sodium channels in mammalian myelinated nerve fibers and nature of the axonal membrane under the myelin sheath", *Proceedings of the National Academy of Sciences of the United States of America*. 74(1):211-5.
- Roberts-Lewis, J. M., Savage, M. J., Marcy, V. R., Pinsker, L. R., & Siman, R. 1994, "Immunolocalization of calpain I-mediated spectrin degradation to vulnerable neurons in the ischemic gerbil brain", *Journal of Neuroscience*. 14(6):3934-44.
- Rojas, E. & Rudy, B. 1976, "Destruction of the sodium conductance inactivation by a specific protease in perfused nerve fibres from *Loligo*", *Journal of Physiology*. 262(2):501-31.
- Rollins, S. A. & Sims, P. J. 1990, "The complement-inhibitory activity of CD59 resides in its capacity to block incorporation of C9 into membrane C5b-9", *Journal of Immunology*. 144(9):3478-83.
- Rollins, S. A., Zhao, J., Ninomiya, H., & Sims, P. J. 1991, "Inhibition of homologous complement by CD59 is mediated by a species-selective recognition conferred through binding to C8 within C5b-8 or C9 within C5b-9", *Journal of Immunology*. 146(7):2345-51.
- Rosenbluth, J. 1976, "Intramembranous particle distribution at the node of Ranvier and adjacent axolemma in myelinated axons of the frog brain", *Journal of Neurocytology*. 5(6):731-45.
- Rosenthal, L. & Meldolesi, J. 1989, "Alpha-latrotoxin and related toxins. [Review] [78 refs]", *Pharmacology & Therapeutics*. 42(1):115-34.
- Saatman, K. E., Murai, H., Bartus, R. T., Smith, D. H., Hayward, N. J., Perri, B. R., & McIntosh, T. K. 1996, "Calpain inhibitor AK295 attenuates motor and

cognitive deficits following experimental brain injury in the rat", *Proceedings of the National Academy of Sciences of the United States of America*.93(8):3428-33.

Saido, T. C., Nagao, S., Shiramine, M., Tsukaguchi, M., Yoshizawa, T., Sorimachi, H., Ito, H., Tsuchiya, T., Kawashima, S., & Suzuki, K. 1994, "Distinct kinetics of subunit autolysis in mammalian m-calpain activation", *FEBS Letters*.346(2-3):263-7.

Saito, A. & Zacks, S. I. 1969, "Ultrastructure of Schwann and perineural sheaths at the mouse neuromuscular junction", *Anatomical Record*.164(4):379-90.

Saito, F., Moore, S. A., Barresi, R., Henry, M. D., Messing, A., Ross-Barta, S. E., Cohn, R. D., Williamson, R. A., Sluka, K. A., Sherman, D. L., Brophy, P. J., Schmelzer, J. D., Low, P. A., Wrabetz, L., Feltri, M. L., & Campbell, K. P. 2003, "Unique role of dystroglycan in peripheral nerve myelination, nodal structure, and sodium channel stabilization", *Neuron*.38(5):747-58.

Sakurai, T., Lustig, M., Nativ, M., Hemperly, J. J., Schlessinger, J., Peles, E., & Grumet, M. 1997, "Induction of neurite outgrowth through contactin and Nr-CAM by extracellular regions of glial receptor tyrosine phosphatase beta", *Journal of Cell Biology*.136(4):907-18.

Salzer, J. L. 1997, "Clustering sodium channels at the node of Ranvier: close encounters of the axon-glia kind. [Review] [24 refs]", *Neuron*.18(6):843-6.

Sanders, M. E., Koski, C. L., Robbins, D., Shin, M. L., Frank, M. M., & Joiner, K. A. 1986, "Activated terminal complement in cerebrospinal fluid in Guillain-Barre syndrome and multiple sclerosis", *Journal of Immunology*.136(12):4456-9.

Santoro, M., Uncini, A., Corbo, M., Staugaitis, S. M., Thomas, F. P., Hays, A. P., & Latov, N. 1992, "Experimental conduction block induced by serum from a patient with anti-GM1 antibodies", *Annals of Neurology*.31(4):385-90.

Sasaki, T., Kikuchi, T., Yumoto, N., Yoshimura, N., & Murachi, T. 1984, "Comparative specificity and kinetic studies on porcine calpain I and calpain II with naturally occurring peptides and synthetic fluorogenic substrates", *Journal of Biological Chemistry*.259(20):12489-94.

Sato, C., Ueno, Y., Asai, K., Takahashi, K., Sato, M., Engel, A., & Fujiyoshi, Y. 2001, "The voltage-sensitive sodium channel is a bell-shaped molecule with several cavities.[see comment]", *Nature*.409(6823):1047-51.

Schafer, D. P. & Rasband, M. N. 2006, "Glial regulation of the axonal membrane at nodes of Ranvier. [Review] [39 refs]", *Current Opinion in Neurobiology*.16(5):508-14.

Scherer, S. S. 1996, "Molecular specializations at nodes and paranodes in peripheral nerve. [Review] [102 refs]", *Microscopy Research & Technique*.34(5):452-61.

Scherer, S. S. & Arroyo, E. J. 2002, "Recent progress on the molecular organization of myelinated axons", *Journal of the Peripheral Nervous System*.7(1):1-12.

- Scherer, S. S., Xu, T., Crino, P., Arroyo, E. J., & Gutmann, D. H. 2001, "Ezrin, radixin, and moesin are components of Schwann cell microvilli", *Journal of Neuroscience Research*.65(2):150-64.
- Seitz, R. J., Heininger, K., Schwendemann, G., Toyka, K. V., & Wechsler, W. 1985, "The mouse blood-brain barrier and blood-nerve barrier for IgG: a tracer study by use of the avidin-biotin system", *Acta Neuropathologica*.68(1):15-21.
- Seitz, R. J., Reiners, K., Himmelmann, F., Heininger, K., Hartung, H., & Toyka, K. V. 2004, "The blood-nerve barrier in Wallerian degeneration: A sequential long-term study", *Muscle & Nerve*, vol. 12, no. 8, pp. 627-635.
- Shapiro, L., Doyle, J. P., Hensley, P., Colman, D. R., & Hendrickson, W. A. 1996, "Crystal structure of the extracellular domain from P0, the major structural protein of peripheral nerve myelin", *Neuron*.17(3):435-49.
- Sheikh, K. A., Deerinck, T. J., Ellisman, M. H., & Griffin, J. W. 1999a, "The distribution of ganglioside-like moieties in peripheral nerves", *Brain*.122 (Pt 3):449-60.
- Sheikh, K. A., Sun, J., Liu, Y., Kawai, H., Crawford, T. O., Proia, R. L., Griffin, J. W., & Schnaar, R. L. 1999b, "Mice lacking complex gangliosides develop Wallerian degeneration and myelination defects", *Proceedings of the National Academy of Sciences of the United States of America*.96(13):7532-7.
- Sheikh, K. A., Zhang, G., Gong, Y., Schnaar, R. L., & Griffin, J. W. 2004, "An anti-ganglioside antibody-secreting hybridoma induces neuropathy in mice", *Annals of Neurology*.56(2):228-39.
- Sherman, D. L., Tait, S., Melrose, S., Johnson, R., Zonta, B., Court FA, Macklin, W. B., Meek, S., Smith, A. J., Cottrell, D. F., & Brophy, P. J. 2005, "Neurofascins are required to establish axonal domains for saltatory conduction", *Neuron*.48(5):737-42.
- Simone, C. B. & Henkart, P. 1982, "Inhibition of marker influx into complement-treated resealed erythrocyte ghosts by anti-C5", *Journal of Immunology*.128(3):1168-75.
- Sonnino, S., Mauri, L., Chigorno, V., & Prinetti, A. 2007, "Gangliosides as components of lipid membrane domains.[erratum appears in *Glycobiology*. 2007 Oct;17(10):1030]. [Review] [172 refs]", *Glycobiology*.17(1):1R-13R.
- Srinivasan, J., Schachner, M., & Catterall, W. A. 1998, "Interaction of voltage-gated sodium channels with the extracellular matrix molecules tenascin-C and tenascin-R", *Proceedings of the National Academy of Sciences of the United States of America*.95(26):15753-7.
- Srinivasan, Y., Elmer, L., Davis, J., Bennett, V., & Angelides, K. 1988, "Ankyrin and spectrin associate with voltage-dependent sodium channels in brain", *Nature*.333(6169):177-80.
- Stahel, P. F., Flierl, M. A., Morgan, B. P., Persigehl, I., Stoll, C., Conrad, C., Touban, B. M., Smith, W. R., Beauchamp, K., Schmidt, O. I., Ertel, W., & Leinhase, I. 2009, "Absence of the complement regulatory molecule CD59a leads

to exacerbated neuropathology after traumatic brain injury in mice", *Journal of Neuroinflammation*.6:2.

Staub, G. C., Walton, K. M., Schnaar, R. L., Nichols, T., Baichwal, R., Sandberg, K., & Rogers, T. B. 1986, "Characterization of the binding and internalization of tetanus toxin in a neuroblastoma hybrid cell line", *Journal of Neuroscience*.6(5):1443-51.

Stuhmer, W., Conti, F., Suzuki, H., Wang, X. D., Noda, M., Yahagi, N., Kubo, H., & Numa, S. 1989, "Structural parts involved in activation and inactivation of the sodium channel", *Nature*.339(6226):597-603.

Stys, P. K., Waxman, S. G., & Ransom, B. R. 1992, "Ionic mechanisms of anoxic injury in mammalian CNS white matter: role of Na⁺ channels and Na⁺-Ca²⁺ exchanger", *Journal of Neuroscience*.12(2):430-9.

Susuki, K., Baba, H., Tohyama, K., Kanai, K., Kuwabara, S., Hirata, K., Furukawa, K., Furukawa, K., Rasband, M. N., & Yuki, N. 2007a, "Gangliosides contribute to stability of paranodal junctions and ion channel clusters in myelinated nerve fibers", *GLIA*.55(7):746-57.

Susuki, K., Nishimoto, Y., Koga, M., Nagashima, T., Mori, I., Hirata, K., & Yuki, N. 2004, "Various immunization protocols for an acute motor axonal neuropathy rabbit model compared", *Neuroscience Letters*.368(1):63-7.

Susuki, K., Nishimoto, Y., Yamada, M., Baba, M., Ueda, S., Hirata, K., & Yuki, N. 2003, "Acute motor axonal neuropathy rabbit model: immune attack on nerve root axons", *Annals of Neurology*.54(3):383-8.

Susuki, K., Rasband, M. N., Tohyama, K., Koibuchi, K., Okamoto, S., Funakoshi, K., Hirata, K., Baba, H., & Yuki, N. 2007b, "Anti-GM1 antibodies cause complement-mediated disruption of sodium channel clusters in peripheral motor nerve fibers", *Journal of Neuroscience*.27(15):3956-67.

Svennerholm, L. 1994, "Designation and schematic structure of gangliosides and allied glycosphingolipids", *Progress in Brain Research*.101:XI-XIV.

Tait, S., Gunn-Moore, F., Collinson, J. M., Huang, J., Lubetzki, C., Pedraza, L., Sherman, D. L., Colman, D. R., & Brophy, P. J. 2000, "An oligodendrocyte cell adhesion molecule at the site of assembly of the paranodal axo-glia junction.[see comment]", *Journal of Cell Biology*.150(3):657-66.

Takamiya, K., Yamamoto, A., Furukawa, K., Yamashiro, S., Shin, M., Okada, M., Fukumoto, S., Haraguchi, M., Takeda, N., Fujimura, K., Sakae, M., Kishikawa, M., Shiku, H., Furukawa, K., & Aizawa, S. 1996, "Mice with disrupted GM2/GD2 synthase gene lack complex gangliosides but exhibit only subtle defects in their nervous system", *Proceedings of the National Academy of Sciences of the United States of America*.93(20):10662-7.

Takigawa, T., Yasuda, H., Kikkawa, R., Shigeta, Y., Saida, T., & Kitasato, H. 1995, "Antibodies against GM1 ganglioside affect K⁺ and Na⁺ currents in isolated rat myelinated nerve fibers.[see comment]", *Annals of Neurology*.37(4):436-42.

- Tao-Cheng, J. H. & Rosenbluth, J. 1983, "Axolemmal differentiation in myelinated fibers of rat peripheral nerves", *Brain Research*.285(3):251-63.
- Terlau, H., Heinemann, S. H., Stuhmer, W., Pusch, M., Conti, F., Imoto, K., & Numa, S. 1991, "Mapping the site of block by tetrodotoxin and saxitoxin of sodium channel II", *FEBS Letters*.293(1-2):93-6.
- The Guillain-Barre Syndrome Study Group * 1985, "Plasmapheresis and acute Guillain-Barre syndrome. [Article]", *Neurology*, vol. 35, no. 8, pp. 1096-1104.
- Thomas, F. P., Trojaborg, W., Nagy, C., Santoro, M., Sadiq, S. A., Latov, N., & Hays, A. P. 1991, "Experimental autoimmune neuropathy with anti-GM1 antibodies and immunoglobulin deposits at the nodes of Ranvier", *Acta Neuropathologica*.82(5):378-83.
- Thomas, P. K. 1963, "The connective tissue of peripheral nerve: an electron microscope study", *Journal of Anatomy*.97:35-44.
- Thomas, P. K. & Jones, D. G. 1967, "The cellular response to nerve injury. II. Regeneration of the perineurium after nerve section", *Journal of Anatomy*.101(Pt 1):45-55.
- Thomas, T. C., Rollins, S. A., Rother, R. P., Giannoni, M. A., Hartman, S. L., Elliott, E. A., Nye, S. H., Matis, L. A., Squinto, S. P., & Evans, M. J. 1996, "Inhibition of complement activity by humanized anti-C5 antibody and single-chain Fv", *Molecular Immunology*.33(17-18):1389-401.
- Thompson, V. F., Lawson, K., & Goll, D. E. 2000, "Effect of mu-calpain on m-calpain", *Biochemical & Biophysical Research Communications*.267(2):495-9.
- Tompa, P., Buzder-Lantos, P., Tantos, A., Farkas, A., Szilagyi, A., Banoczi, Z., Hudecz, F., & Friedrich, P. 2004, "On the sequential determinants of calpain cleavage", *Journal of Biological Chemistry*.279(20):20775-85.
- Traka, M., Dupree, J. L., Popko, B., & Karagogeos, D. 2002, "The neuronal adhesion protein TAG-1 is expressed by Schwann cells and oligodendrocytes and is localized to the juxtaparanodal region of myelinated fibers", *Journal of Neuroscience*.22(8):3016-24.
- Traka, M., Goutebroze, L., Denisenko, N., Bessa, M., Nifli, A., Havaki, S., Iwakura, Y., Fukamauchi, F., Watanabe, K., Soliven, B., Girault, J. A., & Karagogeos, D. 2003, "Association of TAG-1 with Caspr2 is essential for the molecular organization of juxtaparanodal regions of myelinated fibers", *Journal of Cell Biology*.162(6):1161-72.
- Triggs, W. J., Cros, D., Gominak, S. C., Zuniga, G., Beric, A., Shahani, B. T., Ropper, A. H., & Roongta, S. M. 1992, "Motor nerve inexcitability in Guillain-Barre syndrome. The spectrum of distal conduction block and axonal degeneration", *Brain*.115 (Pt 5):1291-302.
- Turnberg, D. & Botto, M. 2003, "The regulation of the complement system: insights from genetically-engineered mice. [Review] [107 refs]", *Molecular Immunology*.40(2-4):145-53.

Tzoumaka, E., Tischler, A. C., Sangameswaran, L., Eglen, R. M., Hunter, J. C., & Novakovic, S. D. 2000, "Differential distribution of the tetrodotoxin-sensitive rPN4/NaCh6/Scn8a sodium channel in the nervous system", *Journal of Neuroscience Research*.60(1):37-44.

Uetz-von Allmen, E., Sturzenegger, M., Rieben, R., Rihs, F., Frauenfelder, A., & Nydegger, U. E. 1998, "Antiganglioside GM1 Antibodies and Their Complement Activating Capacity in Central and Peripheral Nervous System Disorders and in Controls", *Experimental Neurology*., vol. 39, no. 2, pp. 103-110.

Vabnick, I., Novakovic, S. D., Levinson, S. R., Schachner, M., & Shrager, P. 1996, "The clustering of axonal sodium channels during development of the peripheral nervous system", *Journal of Neuroscience*.16(16):4914-22.

Vabnick, I. & Shrager, P. 1998, "Ion channel redistribution and function during development of the myelinated axon. [Review] [90 refs]", *Journal of Neurobiology*.37(1):80-96.

Vabnick, I., Trimmer, J. S., Schwarz, T. L., Levinson, S. R., Risal, D., & Shrager, P. 1999, "Dynamic potassium channel distributions during axonal development prevent aberrant firing patterns", *Journal of Neuroscience*. no. 2, pp. 747-758.

van Sorge, N. M., Yuki, N., Jansen, M. D., Nishimoto, Y., Susuki, K., Wokke, J. H., van de Winkel, J. G., van den Berg, L. H., & van der Pol, W. L. 2007, "Leukocyte and complement activation by GM1-specific antibodies is associated with acute motor axonal neuropathy in rabbits", *Journal of Neuroimmunology*.182(1-2):116-23.

Vassilev, P. M., Scheuer, T., & Catterall, W. A. 1988, "Identification of an intracellular peptide segment involved in sodium channel inactivation", *Science*.241(4873):1658-61.

Vedeler, C. A., Conti, G., Fujioka, T., Scarpini, E., & Rostami, A. 1999, "The expression of CD59 in experimental allergic neuritis", *Journal of the Neurological Sciences*.165(2):154-9.

Virchow R 1854, "Uber das ausgebreitete Vorkommen einer dem Nervenmark analogen Substanz in den tierischen Geweben.", *Archives Pathological Anatomy*, vol. 6, pp. 562-572.

Volkmer, H., Leuschner, R., Zacharias, U., & Rathjen, F. G. 1996, "Neurofascin induces neurites by heterophilic interactions with axonal NrCAM while NrCAM requires F11 on the axonal surface to extend neurites", *Journal of Cell Biology*.135(4):1059-69.

von Reyn, C. R., Spaethling, J. M., Mesfin, M. N., Ma, M., Neumar, R. W., Smith, D. H., Siman, R., & Meaney, D. F. 2009, "Calpain mediates proteolysis of the voltage-gated sodium channel alpha-subunit", *Journal of Neuroscience*.29(33):10350-6.

Waksman, B. H. & Adams, R. D. Allergic neuritis: an aexperimental disease of rabbits induced by the injection of peripheral nervous tissue and adjuvants. *Journal of Experimental Medicine* 102, 213-255. 1955.
Ref Type: Generic

- Wang, H., Kunkel, D. D., Martin, T. M., Schwartzkroin, P. A., & Tempel, B. L. 1993, "Heteromultimeric K⁺ channels in terminal and juxtaparanodal regions of neurons", *Nature*.365(6441):75-9.
- Wang, M. S., Davis, A. A., Culver, D. G., Wang, Q., Powers, J. C., & Glass, J. D. 2004, "Calpain inhibition protects against Taxol-induced sensory neuropathy", *Brain*. 127(Pt 3):671-9.
- Waxman, S. G. 1978, *Physiology and pathobiology of axons* Raven, New York.
- Waxman, S. G. 1980, "Determinants of conduction velocity in myelinated nerve fibers", *Muscle & Nerve*.3(2):141-50, p. -Apr.
- Waxman, S. G. 1995, "Sodium channel blockade by antibodies: a new mechanism of neurological disease?[comment]", *Annals of Neurology*.37(4):421-3.
- Waxman, S. G., Black, J. A., Ransom, B. R., & Stys, P. K. 1994, "Anoxic injury of rat optic nerve: ultrastructural evidence for coupling between Na⁺ influx and Ca(2⁺)-mediated injury in myelinated CNS axons", *Brain Research*.644(2):197-204.
- Weerasuriya, A., Rapoport, S. I., & Taylor, R. E. 1980, "Perineurial permeability increases during Wallerian degeneration", *Brain Research*. no. 2, pp. 581-585.
- West, J. W., Patton, D. E., Scheuer, T., Wang, Y., Goldin, A. L., & Catterall, W. A. 1992, "A cluster of hydrophobic amino acid residues required for fast Na⁽⁺⁾-channel inactivation", *Proceedings of the National Academy of Sciences of the United States of America*.89(22):10910-4.
- Wiley-Livingston, C. & Ellisman, M. H. 1980, "Development of axonal membrane specializations defines nodes of Ranvier and precedes Schwann cell myelin elaboration", *Developmental Biology*.79(2):334-55.
- Willison, H. J., Halstead, S. K., Beveridge, E., Zitman, F. M., Greenshields, K. N., Morgan, B. P., & Plomp, J. J. 201, "The role of complement and complement regulators in mediating motor nerve terminal injury in murine models of Guillain-Barre syndrome. [Review] [57 refs]", *Journal of Neuroimmunology*. pp. 172-182.
- Willison, H. J., Halstead, S. K., Beveridge, E., Zitman, F. M., Greenshields, K. N., Morgan, B. P., & Plomp, J. J. 2008, "The role of complement and complement regulators in mediating motor nerve terminal injury in murine models of Guillain-Barre syndrome. [Review] [57 refs]", *Journal of Neuroimmunology*. pp. 172-182.
- Willison, H. J. & Plomp, J. J. 2008, "Anti-ganglioside antibodies and the presynaptic motor nerve terminal. [Review] [52 refs]", *Annals of the New York Academy of Sciences*. 1132:114-23.
- Willison, H. J. & Yuki, N. 2002, "Peripheral neuropathies and anti-glycolipid antibodies. [Review] [270 refs]", *Brain*.125(Pt 12):2591-625.

Wirguin, I., Suturkova-Milosevic, L., Briani, C., & Latov, N. 1995, "Keyhole limpet hemocyanin contains Gal(beta 1-3)-GalNAc determinants that are cross-reactive with the T antigen", *Cancer Immunology, Immunotherapy*.40(5):307-10.

Wood, S. J. & Slater, C. R. 1998, "beta-Spectrin is colocalized with both voltage-gated sodium channels and ankyrinG at the adult rat neuromuscular junction", *Journal of Cell Biology*.140(3):675-84.

Xiao, Z. C., Ragsdale, D. S., Malhotra, J. D., Mattei, L. N., Braun, P. E., Schachner, M., & Isom, L. L. 1999, "Tenascin-R is a functional modulator of sodium channel beta subunits", *Journal of Biological Chemistry*.274(37):26511-7.

Yoshida, K. & Harada, K. 1997, "Proteolysis of erythrocyte-type and brain-type ankyrins in rat heart after postischemic reperfusion", *Journal of Biochemistry*.122(2):279-85.

Yu, F. H. & Catterall, W. A. 2003, "Overview of the voltage-gated sodium channel family. [Review] [51 refs]", *Genome Biology*.4(3):207.

Yuki, N., Kuwabara, S., Koga, M., & Hirata, K. 1999, "Acute motor axonal neuropathy and acute motor-sensory axonal neuropathy share a common immunological profile", *Journal of the Neurological Sciences*.168(2):121-6.

Yuki, N., Yamada, M., Koga, M., Odaka, M., Susuki, K., Tagawa, Y., Ueda, S., Kasama, T., Ohnishi, A., Hayashi, S., Takahashi, H., Kamijo, M., & Hirata, K. 2001, "Animal model of axonal Guillain-Barre syndrome induced by sensitization with GM1 ganglioside.[see comment]", *Annals of Neurology*.49(6):712-20.

Yuki, N., Yoshino, H., Sato, S., Shinozawa, K., & Miyatake, T. 1992, "Severe acute axonal form of Guillain-Barre syndrome associated with IgG anti-GD1a antibodies", *Muscle & Nerve*.15(8):899-903.

Zhang, X. & Bennett, V. 1996, "Identification of O-linked N-acetylglucosamine modification of ankyrinG isoforms targeted to nodes of Ranvier", *Journal of Biological Chemistry*.271(49):31391-8.

Zhang, X., Davis, J. Q., Carpenter, S., & Bennett, V. 1998, "Structural requirements for association of neurofascin with ankyrin", *Journal of Biological Chemistry*.273(46):30785-94.

Zhou, D., Lambert, S., Malen, P. L., Carpenter, S., Boland, L. M., & Bennett, V. 1998a, "AnkyrinG is required for clustering of voltage-gated Na channels at axon initial segments and for normal action potential firing", *Journal of Cell Biology*.143(5):1295-304.

Zhou, L., Zhang, C. L., Messing, A., & Chiu, S. Y. 1998b, "Temperature-sensitive neuromuscular transmission in Kv1.1 null mice: role of potassium channels under the myelin sheath in young nerves", *Journal of Neuroscience*.18(18):7200-15.

Zhou, W. & Goldin, A. L. 2004, "Use-dependent potentiation of the Nav1.6 sodium channel", *Biophysical Journal*.87(6):3862-72.

Zuo, Y., Lubischer, J. L., Kang, H., Tian, L., Mikesch, M., Marks, A., Scofield, V. L., Maika, S., Newman, C., Krieg, P., & Thompson, W. J. 2004, "Fluorescent

proteins expressed in mouse transgenic lines mark subsets of glia, neurons, macrophages, and dendritic cells for vital examination", *Journal of Neuroscience*.24(49):10999-1009.